THE ROLE OF PHYTOHORMONES IN CONTROLLING HEAT STRESS RESPONSES DURING WHEAT ANTHER DEVELOPMENT

MATTHEW DALE, MBiol.

Thesis submitted to The University of Nottingham for the degree of Doctor of Philosophy

July 2021

Abstract

Cereal crops are highly vulnerable to heat stress. Pollen development is particularly susceptible to high temperatures, with prolonged periods of exposure resulting in male sterility and yield loss. With global temperatures set to rise, yield losses are predicted to increase, warranting further investigation into the role of phytohormones in controlling wheat reproductive development and responses to abiotic stress. Various phytohormones have important roles in regulating many aspects of plant development, in particular pollen development and are also implicated in regulating heat stress responses. This project aimed to investigate the role of phytohormones in wheat development and the heat stress response.

A stable heat stress assay was initially developed specific for hexaploid wheat var. Cadenza. It was found that conditions of 4 days at 33/26°C d/n 80% humidity was enough to induce a significant loss of grain set when the stress was applied at meiosis or unicellular pollen stages. Utilising this assay, an RNAseq and global hormone analysis was performed on accurately staged anthers after either control or heat stress conditions. The results reveal the complex interplay of phytohormones in controlling pollen development, the changes that occur in response to heat treatment and the genes underlying these changes in accumulation.

The reverse genetics approach of TILLING was used to identify gain-of-function mutants which are insensitive to auxin and ethylene in Cadenza. Auxin-insensitive Aux/IAA mutants showed partial male sterility and increased sensitivity to heat stress, in addition to striking defects in lateral roots, root hairs and agravitropism.

This project defines an optimised heat stress assay for Cadenza which can be applied to investigating the heat stress response using reverse genetics or endogenous application of hormones. It also demonstrates an application of TILLING as a method to dissect complex signalling pathways and determine their role in development and abiotic stress tolerance of hexaploid wheat.

Acknowledgements

I would first like to acknowledge my Rothamsted supervisors: Steve, Andy and Peter for their guidance and support throughout the PhD. Your knowledge, feedback and advice have been vital for my project. My thanks also go to the pollen group at the University of Nottingham, especially for my Nottingham supervisor Zoe Wilson for her helpful suggestions and advice.

I would also like mention our industrial collaborators, Plant Impact, for both their helpful input and financial support. Especially Steve, Matt and Jahmel for their practical help and advice.

I would also like to give thanks to our collaboration with the root group at the University of Nottingham, especially to Malcolm and Rahul, for allowing me to use some of their fantastic phenotyping facilities and bounce ideas off each other. I would also like to mention my examiners, Malcolm and Sigrid, who have always helped me look at the bigger picture and see the value of my work, as well as providing excellent ideas and practical advice.

A thank you also goes to the members of the plant architecture lab group for their support and advice, as well as making the lab a pleasant place to work, in particular Megan, Lucia and Matt C. I would also like to thank Iris for her amazing help as a placement student during the first year of my PhD. I must also mention that none of this work would be possible without the plant husbandry of the glasshouse staff and the fantastic images taken with the help of Kirstie and Hannah in bioimaging, and Graham in VCU.

I would also like to give a special thanks to my close friends Patrycja and Florian. Thank you for chats, coffees, days out and for sending me into uncontrollably laughter. Thank you to my housemates Dan, Cassie and Sandrine and to all the Rothamsted students and staff members who have made the last 4 years so enjoyable. Finally, I would like to say a thank you to my family. My mum, Elaine, dad, Howard, and sister, Eleanor, who have always supported me in my love for biology and science. Thanks for all the lovely walks, talks and moments; I would not be here if it wasn't for your encouragement and strength.

Contents Table

List of Figures

List of Tables

List of Abbreviations

ABA	Abscisic Acid
ANOVA	Analysis of Variance
bHLH	Basic Helix-loop-helix
BLAST	Basic Local Alignment Search Tool
bp	Base Pair
BR	Brassinosteroid
cDNA	Complementary DNA
CE	Controlled environment
cm	Centimetre
CK	Cytokinin
DE	Differentially expressed
DNA	Deoxyribonucleic acid
DW	Dry weight
EMS	Ethyl methanesulfonate
FLS	Flag Leaf Sheath
GA	Gibberellin
GO	Gene Ontology
IAA	Indole 3-Acetic Acid
IWGSC	International Wheat Genome Sequencing Consortium
JA	Jasmonic Acid
LRP	Lateral Root Primordia
LSD	Least Significant Difference
ml	Millilitre
mm	Millimetre
mM	Millimolar
NAA	1-Naphthaleneacetic acid
NS	Null Segregant
PCD	Programmed Cell Death
PCR	Polymerase Chain Reaction
PMC	Pollen Mother Cell
pmol	Pico mole
REML	Restricted Maximum Likelihood
RNA	Ribonucleic Acid
RNA-Seq	RNA-Sequencing
ROS	Reactive Oxygen Species
RT	Room Temperature
SA	Salicylic acid
SED	Standard error of differences
SNP	Single Nucleotide Polymorphism
SPL	Secondary Parietal Layer
TF	Transcription Factor
TILLING	Targeted Induced Local Lesions in Genomes
TP	Tricellular Pollen
VPD	Vapour Pressure Deficit
WT	Wild type
µg	Microgram
µl	Microlitre
µm	Micrometre
µM	Micromolar

Chapter 1: Introduction

1.1 Wheat: From a simple grass to a global staple

Wheat is one of the top three most important worldwide crops, along with rice and maize, contributing to around 19% of the global diet(Ray *et al.*, 2013). Most recent estimates predict that around 729,000,000 tonnes of wheat are produced worldwide every year (fao.org/foastat).

Originally cultivated in the fertile crescent of the Middle East around 10,000 years ago, wheat was grown as a mixture of diploid *T.urartu* (AA) (einkorn) and tetraploid *T.turgidum* (AABB) (emmer) wheats. *T.turgidum* (AABB) was formed through a hydridisation of diploid *Triticum Urartu* (AA) and *Aegilops speltoides* (BB) 500,000 years ago in what is today South Eastern Turkey(Heun *et al.*, 1997; Dubcovsky and Dvorak, 2007). 9,000 years ago saw the spontaneous hybridisation of *T.turgidum* and *T.tauschii* (DD) to form *T.aestivum* (AABBDD), or modern bread wheat in the Fertile Crescent(Mcfadden and Sears, 1946) (Figure 1.1). Wheats' significance in human evolution is evident, with cultivation of wheat spelling the dawn of the 'Neolithic Revolution', where traditionally nomadic hunter gatherer lifestyles transitioned to a sedentary agricultural lifestyle, often based on cereals.

Today, wheat is grown far more widely than rice or maize from 67 °N in northern Scandinavia and the Russian Arctic to 45°S on the Argentinian plains(Shewry, 2009). Consequently, wheat is exposed to a variety of environmental conditions across its range and has led to the cultivation of a diversity of different wheat varieties each with their own adaptations to their local environment.

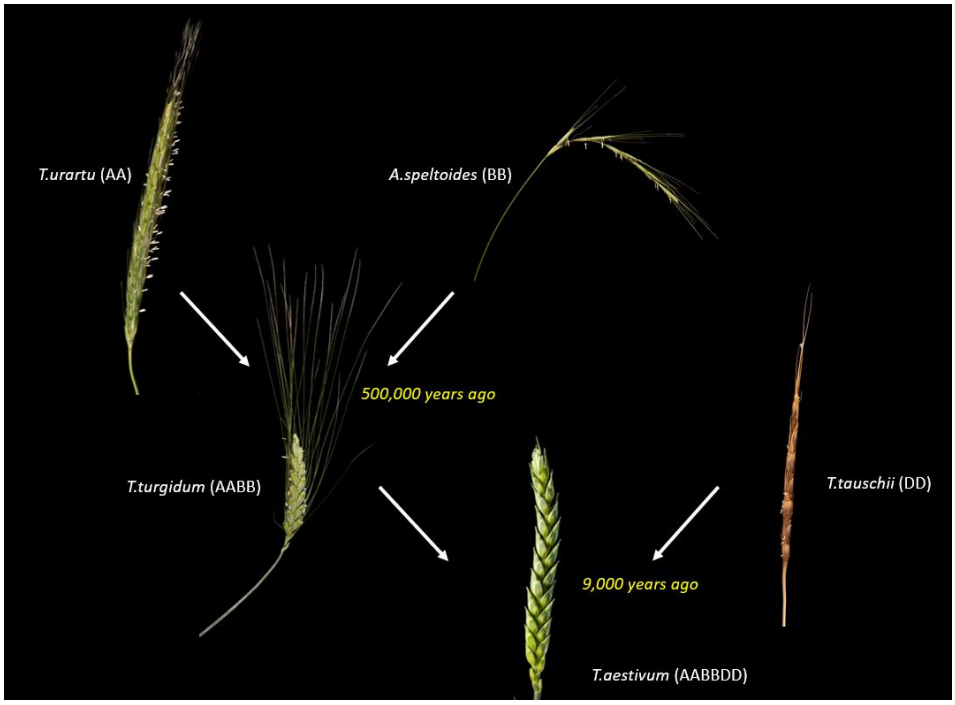

Figure 1.1*: The evolution of domesticated hexaploid wheat.*

Domestication initially began as a hybridisation between diploid Triticum Urartu (AA) and Aegilops speltoides (BB), forming tetraploid Triticum turgidum (AABB). This then led to the hybridisation of Triticum turgidum with Triticum tauschii (DD) to form modern bread wheat, or T.aestivum (AABBDD). Adapted from Shewry 2009.

Wheat production is increasing at a rate of 0.9% per year, far below the 2.4% rate of increase required to keep up with the rising world population (Ray *et al.*, 2013). Human population size is predicted to reach 9 billion by 2050; this ever increasing pressure on the world's food resources will raise global crop demand by 100-110% between 2005-2050(Tilman *et al.*, 2011). A sustainable method of raising yield is therefore required, one which does not rely on turning over more natural habitat to agricultural production(Ray *et al.*, 2013).

An additional complication to meeting global food demand is climate change. Climate change models have suggested that rising global temperatures have reduced the increase in yield gains more than would otherwise have been expected(Asseng *et al.*, 2014). Indeed a 1°C increase in world temperature is

expected to result in a loss of 6% in global food production(Asseng *et al.*, 2014). It has been estimated that rising global temperatures have resulted in a 50 megaton loss of yield from wheat, maize and barley per year since 1981, which equates to a global loss of $5 billion per year(Lobell and Field, 2007). Consequently, efforts should be made to ensure a sustainable increase in wheat yield, despite predictions for more adverse growth conditions. Therefore, better understanding into how wheat copes with adverse growth conditions is required to mitigate their impact on wheat production.

1.2 Impact of high temperature stress on wheat yield

Plants are sessile organisms that therefore cannot exhibit behavioural strategies to combat extremes in abiotic stress as animals can (Barnabás *et al.*, 2008). Commercial farming methods involve growing crops in large open fields which provide little protection from the elements and often have severe fluctuations in temperature throughout the day(Ferrez *et al.*, 2011). Heat stress is known to have a negative impact on cereal yield. Extreme heat causes various disruptions to cereal anatomy and biochemistry, such as oxidative damage, alteration of membrane fluidity, disrupted PSII function and denaturation/misfolding of proteins(Barnabás *et al.*, 2008).

Reproductive organs appear to be particularly sensitive to heat stress, having a lower ability to withstand prolonged periods of high temperatures (Barnabás *et al.*, 2008). Pollen development is especially vulnerable to heat stress, although plant female reproductive development is often considered to be more resilient. In barley, when the plants were exposed to less than three days of heat stress (30°C during the day and 25°C during the night) male fertility was retained(Sakata *et al.*, 2010). However, heat stress for longer than three days leads to a significant reduction in pollen viability and grain set(Sakata *et al.*, 2010). In wheat, studies have shown that moderate heat stress (30 – 35˚C) between meiosis of the pollen mother cells to the formation of young microspores leads to a significant loss of grain yield per spike (Figure 1.2) (Saini and Aspinall, 1982; Draeger and Moore, 2017). One study found that wheat exposed to 30°C for 3 days during this sensitive period lead

to 80% of florets containing abnormal anthers and reduced pollen viability(Saini and Aspinall, 1982).

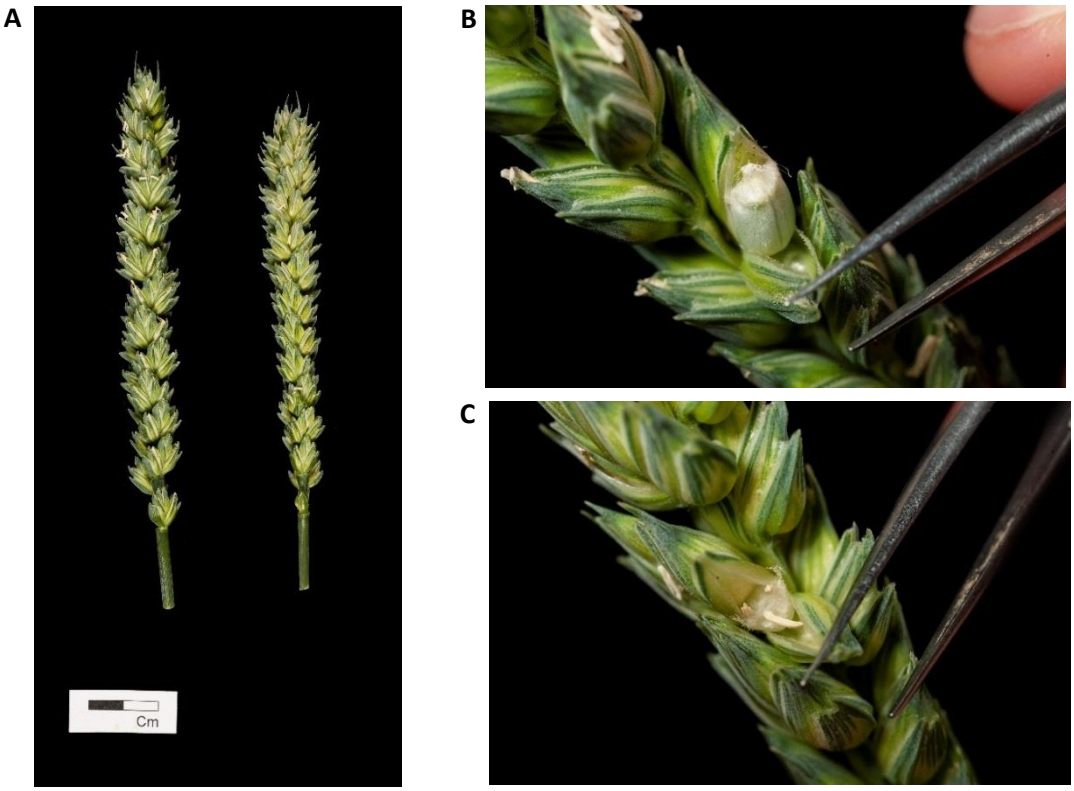

Figure 1.2: *Control and heat stressed wheat spikes.*

***A**: Left: Control spike. Right: Heat stressed for 4 days at 35/26°C day/night from meiosis.* ***B**: Control floret opened to reveal the developed seed at medium milk stage.* ***C**: Heat stressed floret of the same stage, opened to reveal the lack of seed and heat damaged anthers containing sterile pollen.*

1.3 The development of anthers and pollen

The development of fertile pollen requires the coordinative action of many different cell types in the anther. Pollen is the male reproductive gamete of seed plants and is formed in the floral organ called the anther. In summary, anther development begins with the specialisation of stamen primordia by the sporocyte and formation of anther tissues which support the generation of the male gametes. Sporogenous cells in the anther undergo meiosis to form a tetrad of four haploid microspores and after going through two further rounds of mitosis, the new tricellular pollen

accumulates starch and are eventually released from the anther as mature, haploid, tricellular pollen during anther dehiscence(Chaudhury, 1993).

In maize and barley (both closely related to wheat), anther development begins with the division of archesporial cells, which divide to form primary parietal cells and centralised cells form sporogenous cells. This results in a premature anther containing four maternal cell layers surrounding primary sporogenous cells(Kelliher and Walbot, 2011; Gomez and Wilson, 2012). The sporogenous cells (pollen mother cells – PMCs) then divide further to generate the meiocytes. The primary parietal cells divide to form the endothecium and secondary parietal cells, the secondary parietal cells subsequently divide again to form the middle layer and tapetum (Gomez *et al.*, 2015). This has set the basic anatomical format of the anther. Whereby the tapetum surrounds sporogenous cells forming a locule for the microspores/pollen to develop.

Within the locule, microsporogenesis occurs whereby sporogenous cells undergo meiosis to form a tetrad of four haploid microspores enclosed within a callose wall formed by the tapetum(Chaudhury, 1993). The callose wall then breaks down and haploid microspores are released into the anther locule. The microspores become progressively vacuolated and polarised(Gomez *et al.*, 2015). The microspores then go through one round to mitosis (mitosis I)(Owen and Makaroff, 1995). During mitosis I, the microspore asymmetrically divides to produce a generative and vegetative cell. The generative cell then goes through a further round of mitosis (mitosis II) to form two sperm cells. The two sperm cells enable the double fertilisation required to produce the endosperm and the embryo of the developing seed and the vegetative cell produces the pollen tube required to transfer the sperm to the ovule(Eady *et al.*, 1995). The final mature pollen is therefore tricellular (trinuclear). Once mature the anther filaments rapidly elongate and the flowers open and the pollen is released. The whole process is shown in figure 1.3.

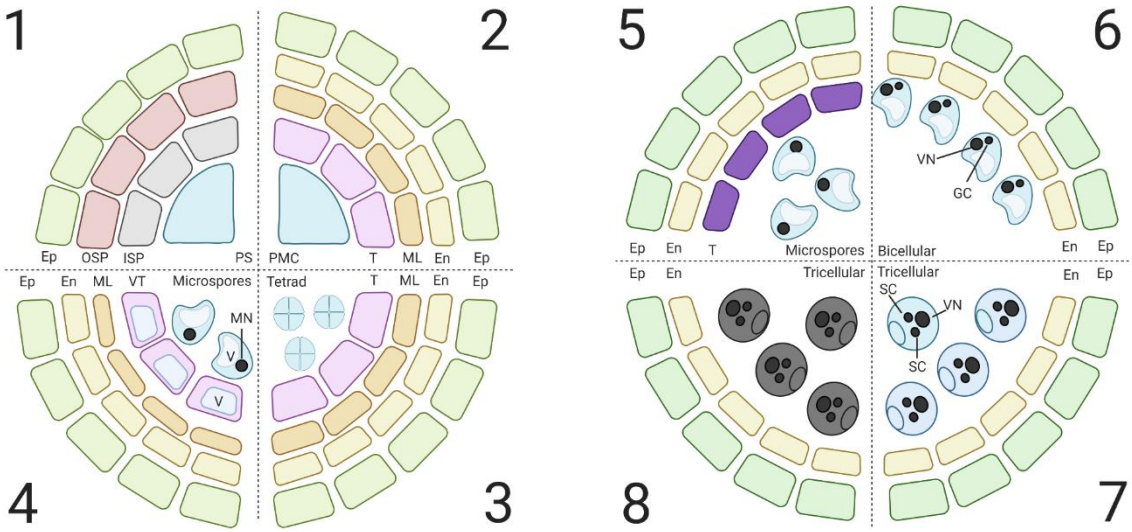

Figure 1.3: *Anther development in angiosperms.*

Anther development begins with the division of archesporial cells to form the primary parietal cells (PP) and primary sporogenous cells (PS). 1. PP cells divide to form an inner secondary parietal layer (ISP) and outer secondary parietal layer (OSP). 2. The OSP divides and differentiates to form the endothecium (En) and the ISP divides to form the tapetum (T) and middle layer (ML). Sporogenous cells have divided to form pollen mother cells (PMC). 3. PMCs undergo meiosis to for tetrads enclosed in a callose layer. 4. The breakdown of this layer results in the release of microspores into the anther locule. The tapetum also becomes vacuolated. 5. The ML begins to undergo crushing and the tapetum starts to degenerate. 6. Mitosis I occurs forming bicellular pollen and the tapetum has degraded/fragments remain. 7. Mitosis II occurs forming tricellular pollen. 8. Tricellular pollen begin to accumulate starch ready for dehiscence. V=Vacuole, MN=Microspore Nucleus, GC= Generative Cell, VN=Vegetative Nucleus and SC=Sperm Cell. Created with BioRender.com.

A key anther tissue in regulating pollen development is the tapetum. The tapetum is a layer of metabolically active cells immediately surrounding the developing pollen. These cells provide nutrients for the developing microspores and enzymes which are required for their release from the tetrad callose envelopes before undergoing degeneration via programmed cell death (PCD) (Figure 1.3)(Papini *et al.*, 1999; Wu and Cheung, 2000). The degradation of the tapetum is essential to ensure viable pollen, as when degrading it releases pollen wall forming compounds onto the developing pollen and is also required for dehiscence(Wu and Cheung, 2000; Parish

and Li, 2010). The timing of tapetal PCD is species dependent. In wheat and barley, it appears to occur during the vacuolated microspore stage and is complete by the bicellular stage(Mizelle *et al.*, 1989; Gomez and Wilson, 2012, 2014). Whereas in *Brachypodium* and rice tapetum degradation occurs earlier, at the tetrad stage and usually is still present (although greatly reduced in size) at bicellular stage(Zhang *et al.*, 2011).

Unique to the tapetal cells of grasses is the synthesis of electron-dense structures, Ubisch bodies. Ubisch bodies consist of sporopollenin, a stable polymer, which forms the exine walls of pollen grains and ensures its resilience to environmental damage(Heslop-Harrison, 1968; Quilichini *et al.*, 2015). In wheat, pre-Ubisch bodies are synthesised in the tapetum and then sporopollenin is deposited on top of this(El-ghazaly and Huysmans, 2001).

The final stage of pollen development is dehiscence. Dehiscence is when the anthers split and release the pollen from within the locule. This is initiated when the endothecium undergoes localised secondary thickening whereby the cells expand and deposition of ligno-cellulosic thickening occurs (Keijzer *et al.*, 1987). This is then followed by the breakdown of the septum and dehydration of the anther, causing stomium breakdown and release of the pollen as the anther splits(Keijzer *et al.*, 1987; Bonner and Dickinson, 1989; Anhthu *et al.*, 1999; Scott *et al.*, 2004).

1.4 Genetic regulation of reproductive development

Anther and pollen development are a remarkably complex and conserved processes in the angiosperms. It begins with stamen meristem specification and ends with release of viable tricellular pollen. Studies on dicot model *Arabidopsis thaliana* and monocot model rice have revealed the conserved regulatory pathways which ensure successful pollen development, with male sterile mutants are often found in orthologous genes(Gomez *et al.*, 2015). This collinearity between angiosperms means this knowledge can be translated to *Triticum aestivum* whose anther developmental pathway has been studied less extensively. Recent sequencing and annotation of the wheat genome allows a much faster pace of genomics research in wheat, whereby orthologous mutations can be brought forward for investigation,

especially with the recently available TILLING resources and optimised wheat gene editing technology.

1.4.1 Floral anatomy of wheat and genetic control

The reproductive physiology of wheat is typical of the grasses (Figure 1.4). The reproductive part of wheat is known as the spike. The spike, or ear, is the flower and grain baring part of the stem located at its tip. It consists of many spikelets, which themselves consist of glumes and a number of florets, which each contain the male and female reproductive organs. Each floret consists of the so called lemma and palea which surround and protect the reproductive organs(Whitford *et al.*, 2013). The lodicules, which are thought to be the equivalent of petals, are small scales at the base of the ovary which expand during anthesis, in doing so force apart the lemma and palea, thus opening the floret to ensure release of pollen(Heslop-Harrison and Heslop-Harrison, 1996).

Identities of floral organs of flowering plants are determined by an ABCE model of specification. Floral organs can be divided into sepals, petals, stamen and gynoecium, where each is specified by the overlapping expression of specific ABCE genes. In Arabidopsis, *APETALA1* (*AP1*) and *APETALA2* (*AP2*), are A function genes which determine sepal and petal identity. *APETALA3* (*AP3*)/*PISTILATA* is a B function gene which determines petal and stamen identity. *AGAMOUS* (*AG*) is a C function gene which determines stamen and carpel development and *SEPELLATA1*, *-2*, *-3* and *-4* are E function genes which are required for specifying all floral organs(Reviewed by H. Ma, 2005). A combination of B, C and E functions are required for assigning stamen identity. This system of floral development has been illustrated in figure 1.4.

This model of floral identity was based mostly on mutants of the model eudicot Arabidopsis. In cereals there have been found to be representatives of all A, B, C, E type genes(Reviewed by Ali et al., 2019). Therefore, it is thought that the model of floral development is conserved between monocots and dicots, despite clear differences in the flower morphology.

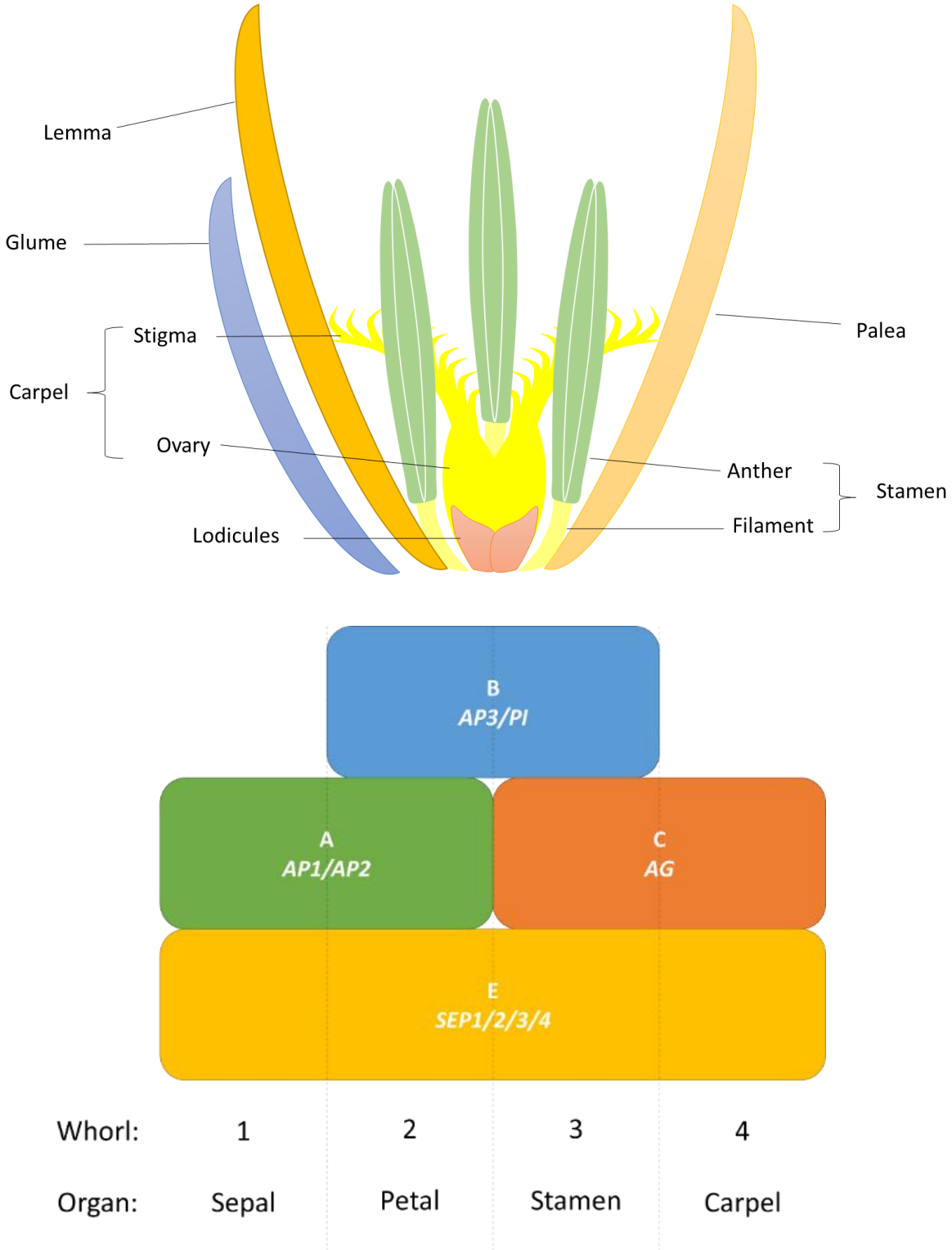

Figure 1.4: *Floral architecture of a wheat floret and the ABCE model of floral organ identity determination in Arabidopsis.*

Top: Diagram of wheat floret. Bottom: The 4 floral organs in eudicots: sepal, petal, stamen and carpel are all derived from the combined gene family expression of the ABCE genes in different whorls. A+E = sepals, A+B+E = Petals, B+C+E= stamen and C+E = carpels. Adapted from Ma, 2005.

1.4.2 Genetic regulation of anther and pollen development

Arabidopsis has proven to be a vital study species for more complex plants, such as rice and wheat. Forward genetic screens for male sterility in Arabidopsis have uncovered an array of genes regulating pollen and anther development. In general, reproductive development is highly conserved between the monocots and dicots. Many features of the physiological and the gene regulation network are highly conserved between model dicots Arabidopsis and monocot rice, as well as shared orthologous genes being found in other less well studied species (Gomez *et al.*, 2015).

The development of the tapetum (the cell layer immediately surrounding the development pollen) is a particularly well studied area, with an array of different proteins involved in determining its formation and timing it's PCD. Tapetal degradation is essential as it releases pollen wall forming compounds onto the developing pollen and is also required for dehiscence(Wu and Cheung, 2000; Parish and Li, 2010).

The formation of the tapetum has been linked to a number of genes. One such gene is *SPOROCYTLELESS* (*SPL*)/*NOZZLE*(*NZZ*) which is required for differentiation of sporogenous cells to become the tapetum in Arabidopsis (Schiefthaler *et al.*, 1999; Yang *et al.*, 1999). The Arabidopsis *EXCESS MALE SPOROCYTES1* (*EMS1*) and *TAPETUM DETERMINANT1* (*TPD1*) and the rice orthologues (*MULTIPLE SPOROCYTE* (*MSP1*) and *OsTDL1/MIL2*)) are involved in differentiation of meiocytes and tapetal cell identity, with mutants producing excess sporocytes and lacking a tapetum, resulting in male sterility(Canales *et al.*, 2002; Zhao *et al.*, 2002, 2008; Nonomura *et al.*, 2003; Yang *et al.*, 2003).

Arabidopsis *DYSFUNCTIONAL TAPETUM1* (*DYT1*) and the rice orthologue *UNDEVELOPED TAPETUM1* (*UDT1*) are both thought to be involved in progression of meiosis and tapetal development(Jung *et al.*, 2005; Feng *et al.*, 2012). Another basic helix-loop-helix (bHLH)-type transcription factor is *ABORTED MICROSPORES* (*AMS*) in Arabidopsis and its rice ortholog *TAPETUM DEGENERATION RETARDATION* (*TDR*), known to regulate tapetum biosynthesis of lipids and phenolic components

involved in pollen wall synthesis(Sorensen *et al.*, 2003; Xu *et al.*, 2010, 2014; Zhang *et al.*, 2011). As well as a number of leucine-rich repeat receptor-like protein kinases (LRR-RLKs), BAM1/2, SERK1/2 and MPK3-6 are involved in differentiation of parietal cells into the tapetum, middle cell and endothecium layer(Albrecht *et al.*, 2005; Colcombet *et al.*, 2005; Hord *et al.*, 2006, 2008). *MALE STERILITY1* (*MS1*) is a Plant Homeodomain (PHD)-finger transcription factor whose gene expression is positively regulated by AMS and is involved in formation of the pollen wall and tapetum PCD(Vizcay-Barrena and Wilson, 2006; Yang, Vizcay-Barrena, *et al.*, 2007). The Arabidopsis *ms1* mutant is male sterile, with degeneration of immature pollen occurring after microspore release due to lack of exine formation and the tapetum failing to go through PCD(Vizcay-Barrena and Wilson, 2006; Ito *et al.*, 2007). Mutants in orthologous genes in rice (*OsPTC*) and barley (*HvMS1*) show a similar phenotype, indicating this gene has conserved function(H. Li *et al.*, 2011; Gomez and Wilson, 2014).

In rice tapetum degradation is controlled by a regulatory cascade of genes controlled by the transcription factor *OsGAMYB*. OsGAMYB and OsUDT1 (UNDEVELOPED TAPETUM1) work together to increase the transcription of *OsTDR* (*TAPETUM DEGENERATION RETARDATION*) (Liu *et al.*, 2010). OsTDR forms a heterodimer with OsTIP2 (TDR INTERACTING PROTEIN2) and together they promote the expression of *OsEAT1* (*ETERNAL TAPETUM 1*) (Fu *et al.*, 2014). OsEAT1 then promotes the expression of aspartic proteases, OsAP25 and OsAP37, which subsequently lead to tapetum degradation(Niu *et al.*, 2013).

Along with controlling tapetum degradation. Numerous genes have also been found to play roles in pollen exine formation, another essential component in ensuring pollen viability. *RAFTIN* is a rice gene required for formation of Ubisch bodies and are expressed in both the tapetum and microspores(Wang *et al.*, 2003). *DEX1* and *NEF1* are two proteins required for pollen exine formation and sporopollenin transport in Arabidopsis (Ariizumi *et al.*, 2004; L. J. Ma *et al.*, 2013). GAMYB also functions in promoting the secretory function of the tapetum in order to form the pollen coat. GAMYB is known to promote the expression of lipid metabolism genes

cytochrome P450 hydroxylase (*CYP703A3*) and β-*ketoacyl-reductase* (*KAR*), both thought to be linked to sporopollenin formation(Aya *et al.*, 2009).

There has been growing interest in understanding pollen development pathways in crops, in particular wheat. Not only due to the sensitivity of pollen development to abiotic stress(Saini and Aspinall, 1982), but also there has been increased interest in the production of hybrid wheat owing to the progeny showing heterosis, or hybrid vigour, increasing yield by 3.5-15% in wheat (Longin *et al.*, 2012). Hybrid breeding involves the cross of two genetically distinct parents, which is a challenge in wheat as it is mostly self-pollinating(De Vries, 1971). This calls for increased investigation into the developmental and regulatory genes which are involved in pollen development to achieve more efficient hybrid production by forcing outcrossing. Specifically, by means of producing either male sterile lines and/or lines which are effective pollen donors, possessing traits such as high levels of flower opening, anther extrusion and successful dehiscence. In order to do this model species such as Arabidopsis and rice give clues as to orthologous genes which share the same function in the relatively conserved pathway of anther and pollen development.

1.5. The role of phytohormones in male reproductive development

Hormones have been implicated to play key roles in male reproductive development. Transcriptional and hormone studies have revealed the remarkable cell specific expression and accumulation of hormones in male reproductive tissues, alluding to the cruciality of these hormones in controlling reproductive development(Kobayashi *et al.*, 1988; Hua *et al.*, 1998; Cheng *et al.*, 2006; Feng *et al.*, 2006; Hirano *et al.*, 2008; Cecchetti *et al.*, 2013).

The generation and characterisation of mutants which are hormone deficient or hormone insensitive has provided important insights into the role of these hormones in key stages of male reproductive development: anther filament elongation, tapetum degradation and dehiscence (Figure 1.5). Rather than each hormone playing its own individual role there appears to be an overlap of function. GA and ethylene both positively promote filament elongation, tapetum degradation and dehiscence, whereas JA has so far only been found to promote filament

elongation and dehiscence. Auxin appears to positively promote filament elongation, but actively inhibits tapetum PCD and dehiscence and therefore is likely to be a key part of the regulation of these developmental processes. The tissue specific accumulation of these hormones appears crucial in determining changes in gene expression necessary to trigger tapetum PCD, filament elongation, pollen exine formation and dehiscence.

This section specifically focuses on auxin, JA, GA and ethylene, although it must be mentioned that other plant hormones, such as cytokinins and brassinosteroids, are also implicated to be involved in pollen development(Huang *et al.*, 2003; Ariizumi *et al.*, 2008). Transcriptional data and hormonal data of rice pollen reveals that auxin, JA, GA and ethylene all rapidly accumulate towards the end of unicellular stages of pollen development, reaching their peak during tricellular stage(Hirano *et al.*, 2008). Therefore, indicating that successful pollen development relies on the accumulation of all four of these plant hormones.

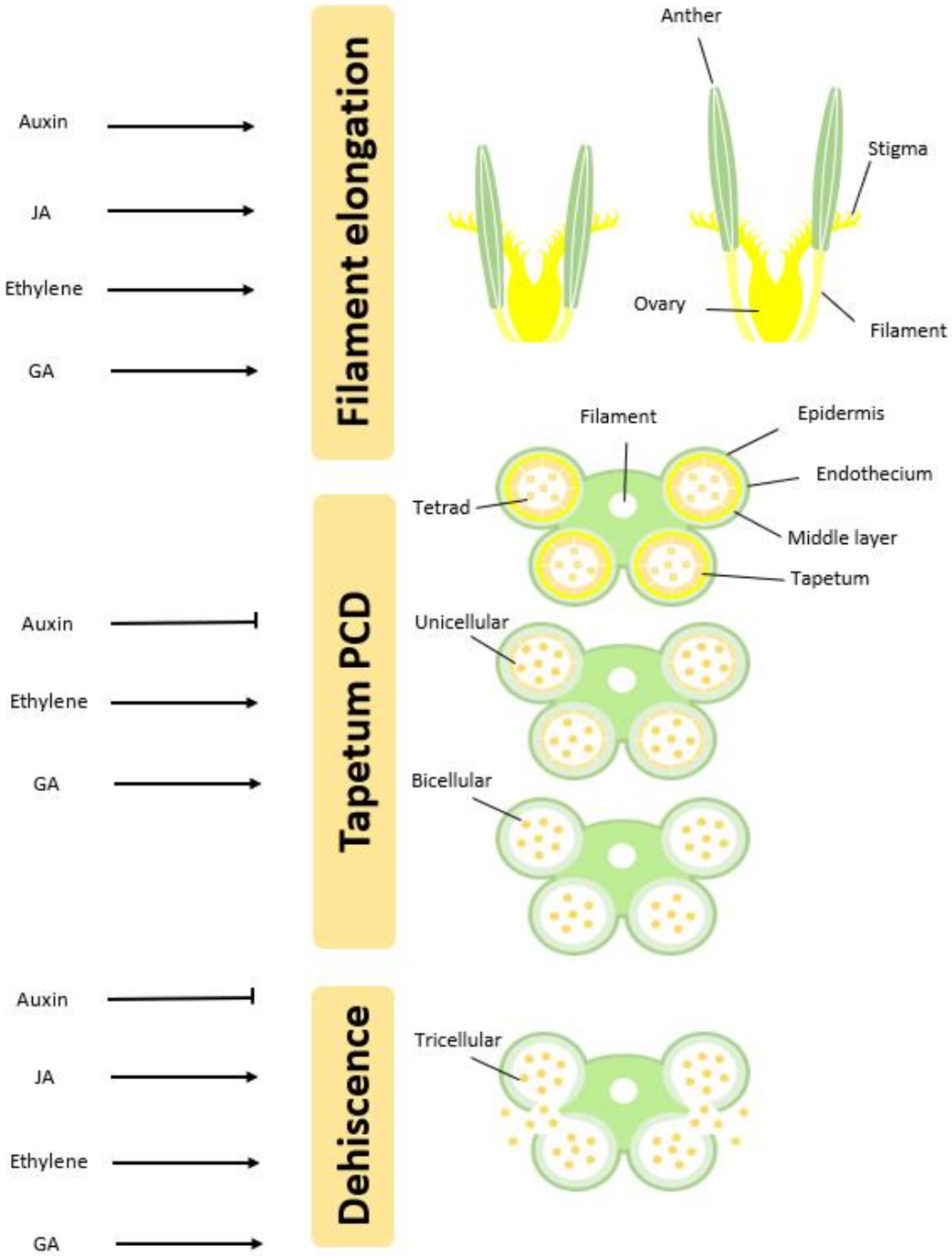

Figure 1.5: *The role of hormones in three key parts of angiosperm male reproductive development: tapetal PCD, filament elongation and dehiscence.*

Auxin, JA (Jasmonic Acid), ethylene and GA (Gibberellin) all promote the elongation of the anther filament. Ethylene and GA promote tapetal PCD, whereas auxin represses it. JA, ethylene and GA promotes dehiscence, whereas auxin represses it.

1.5.1 Auxin

Auxin is a plant hormone involved in controlling a plethora of different developmental activities. It is a key component of regulating vascular tissue formation, organogenesis, apical dominance, root formation and gravitropism. On a cellular level it is involved in division, enlargement and differentiation, which leads to these physiological changes(Mockaitis and Estelle, 2008). Auxin has also been identified to be an important hormone in controlling male reproductive development.

Mutants in auxin biosynthesis commonly confer phenotypes of accelerated anther dehiscence and reduced filament elongation. The auxin biosynthesis double mutant *yuc2 yuc6* successfully formed stamens, but their elongation was halted(Cheng *et al.*, 2006). Filament elongation was shown to be normal in quadruple auxin receptor mutant, *tir1 afb1 afb2 afb3*, until just before anthesis when filament elongation was reduced (Figure 1.6D)(Cecchetti *et al.*, 2008). Auxin signalling has been demonstrated to be crucially important in controlling the start of anther dehiscence by determining the timing of the lignification of the endothecium cell layer. Both the triple auxin receptor mutants *tir1 afb2 afb3* and quadruple mutants *tir1 afb1 afb2 afb3* showed earlier endothecium lignification and dehiscence (Figure 1.6E)(Cecchetti *et al.*, 2008). These studies therefore confirm that auxin plays a key role in preventing premature anther dehiscence and pollen maturation(Cecchetti *et al.*, 2008). It has therefore been suggested that auxin is important for controlling the timing of anther dehiscence, by preventing premature endothecium lignification. Timing is crucial, as it ensures that the pollen is released when the stigma is at its most receptive.

Auxin is thought to negatively regulate endothecium lignification via the transcription factor MYB26. MYB26 is downstream of JA and is involved in inducing stomium opening in Arabidopsis(Cecchetti *et al.*, 2013). The expression of JA biosynthesis genes *OPR3* and *DAD1* was found to be reduced after application of synthetic auxin 1-Naphthaleneacetic acid (NAA) and enhanced in auxin perception mutants in the flower buds(Cecchetti *et al.*, 2013). JA signalling is known to be an important part of inducing dehiscence (Chapter 1.5.2). This led to the theory that

auxin inhibits dehiscence by reducing the accumulation of JA. It was also found that MYB26 was reduced in expression on application of NAA and more highly expressed in the auxin perception mutant(Cecchetti *et al.*, 2013). MYB26 is known to be involved in endothecium secondary thickening, which is necessary for dehiscence(Yang, Xu, *et al.*, 2007).

Auxin is known to activate the expression of auxin response factors (ARFs). ARFs are transcription factors which control auxin responsive gene expression. Several ARFs have been demonstrated to be regulated by auxin and are an important downstream part of inducing filament elongation and inhibiting dehiscence. Mutant studies have shown that there was reduced filament elongation and delayed/absent dehiscence in double mutants *arf1 arf2* and *arf6 arf8* and single mutant *arf17* (Ellis *et al.*, 2005; Nagpal *et al.*, 2005; Xu *et al.*, 2019). Further downstream of this, expression of *MYB108* was found to at least be partially positively regulated by ARF17(Xu *et al.*, 2019). *myb108* was found to show a dehiscent phenotype and showed delayed endothecium lignification(Xu *et al.*, 2019).

ARF17 has also been identified to be involved in tapetum development, with *arf17* mutants showing an abnormally vacuolated tapetum and under developed callose walls surrounding the tetrad, ultimately leading to sterility(Wang *et al.*, 2017). The sterility has been attributed to an absence of primexine (the first part of the exine to be formed) and has been linked to the role of ARF17 in activating expression of *CALLOSE SYNTHASE5* (*CalS5*) which is involved in callose biosynthesis(Yang *et al.*, 2013).

Studies of the expression of auxin biosynthesis and responsive genes have located the key sites and stages of auxin-accumulation. In Arabidopsis, auxin induced reporter activity has been shown to occur in anthers towards the later stages of pollen development(Feng *et al.*, 2006). Expression of the auxin biosynthesis *YUC* genes, specifically *YUC6*, were shown to occur in both the stamen and the developing pollen(Cheng *et al.*, 2006). In rice pollen, the expression of one of these *YUC* genes, *YUCCA4*, seems to also occur predominantly in bicellular and tricellular pollen (Hirano *et al.*, 2008). In rice, expression of *YUCCA5* predominantly occurs in the tapetum during meiosis and tetrad stages, with a decline in expression at

unicellular sage(Hirano *et al.*, 2008). The transcriptional data was complimented with evidence of direct measurement of indole-3-acetic acid (IAA) concentration in the anther, which was found to peak just before tapetum degeneration and then declines again after this(Cecchetti *et al.*, 2013).

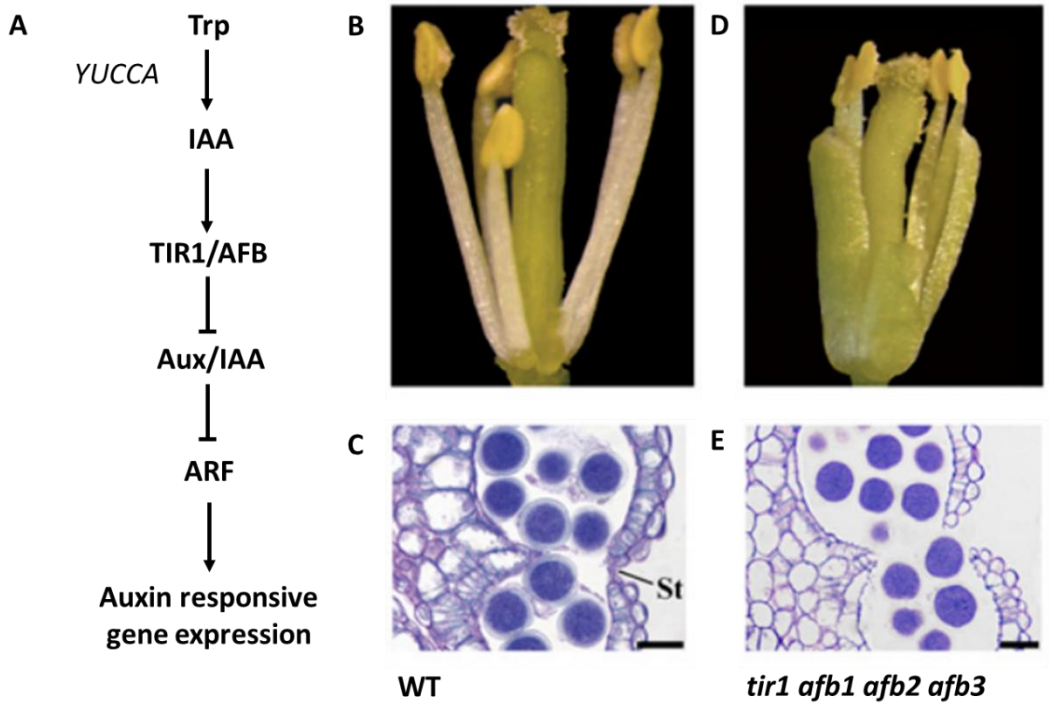

Figure 1.6: *The auxin signalling pathway and its role in male reproductive development.*

A. Simplified auxin signalling pathway. Tryptophan (TRP) is converted to IAA, by a number of enzymes including YUCCA. IAA targets the degradation of Aux/IAAs, by forming a complex with them and TIR1/ARF. This relieves their repression on Auxin Response Factors (ARFs). The ARFs then induce auxin responsive gene expression. Flower morphology and anther cross sections of Arabidopsis WT (B and C) and auxin signalling quadruple mutant tir1 afb1 afb2 afb3 (D and E). Photographs taken from (Cecchetti *et al.*, 2008). *St= stomium. Scale bar = 20 µM.*

1.5.2 Jasmonic Acid

Jasmonates (JAs) are plant hormones involved in a diversity of different functions. JA has been found to have important roles in abiotic/biotic stresses, germination, root growth and architecture, gravitropism, trichome formation and leaf senescence(Howe and Jander, 2008; Wasternack and Hause, 2013; Goossens *et al.*,

2016). Many studies have also confirmed their involvement in male reproductive development in both monocots and dicots.

JA is known to be crucial in stamen elongation, pollen maturation and dehiscence. The various JA signalling mutants which have been identified in Arabidopsis were found to show characteristic reduced stamen filament elongation, abolished pollen viability and a failure to complete dehiscence. This phenotype is evident in JA-deficient mutants which are defective in various JA biosynthesis enzymes: *anther dehiscence1* (*dad1*), *opr3, aos, fad3 fad7 fad8, dde2-2* and *lox3 lox4* double mutants(McConn and Browse, 1996; Sanders *et al.*, 2000; Stintzi and Browse, 2000; Ishiguro *et al.*, 2001; Park *et al.*, 2002; Von Malek *et al.*, 2002; Caldelari *et al.*, 2011). The male sterile phenotype of these mutants was completely rescued by exogenous application of JA (Sanders *et al.*, 2000; Stintzi and Browse, 2000; Park *et al.*, 2002; Von Malek *et al.*, 2002).

It is thought that JA is an important component of water transport, whereby it promotes transport of water from the anther locules, through the anther walls and finally into the filaments and petals(Ishiguro *et al.*, 2001). Ishiguro *et al.,* 2001 proposed that this could be due to JA increasing expression of genes involved in water transport, such as the H^+-sucrose transporter SUC1, which is known to occur in the anther and be involved in water removal(Stadler *et al.*, 1999). Increased water in the filament leads to increased cell size, which is responsible for the filament elongation. Desiccation of the locules is necessary in order to dehydrate and shrink the endothecium, thus resulting in it rupturing to release the pollen during dehiscence(Keijzer, 1987).

The downstream components of JA signalling on male reproductive development have been extensively investigated in Arabidopsis. JA functions via inducing degradation of JASMONATE-ZIM DOMAIN (JAZ) proteins which are repressors of JA signalling. JA does this by inducing their degradation via the SCF^{COI1} E3 ubiquitin ligase complex which ubiquitinates the proteins and targets them for degradation by the 26S proteasome (Figure 1.7A) (Thines *et al.*, 2007; Chung and Howe, 2009).

Mutated JAZ proteins which are resistant to degradation are JA-insensitive and have also been found to be male sterile (Thines *et al.*, 2007; Chung *et al.*, 2010; Huang *et al.*, 2017), therefore their degradation is essential for ensuring male fertility. Downstream of the JAZ proteins are transcription factors MYB21 and MYB24, which were found to interact with JAZ1, JAZ8 and JAZ11 proteins. The double mutant *myb21 myb24* showed defective pollen maturation, delayed anther dehiscence and reduced filament elongation (Figure 1.7C) (Song *et al.*, 2011). MYB21 and MYB24 are known to form complexes with MYC2, MYC3, MYC4, and MYC5. The bHLH quadruple mutants *myc2 myc3 myc4 myc5*, were also shown to have stamen development defects and have partial sterility(Qi *et al.*, 2015). Further downstream, expression of MYB108 has been found to be dependent on MYB21 and increased 100-fold 22 hours after JA treatment(Mandaokar and Browse, 2009). *myb108* mutant was found to show no defects in stamen elongation, but did show delayed dehiscence(Mandaokar and Browse, 2009). Interestingly, this shows an overlap in the JA and auxin regulation of dehiscence. With MYB108 expression also being induced by Auxin Response Factor 17 (ARF17)(Xu *et al.*, 2019). Mutants in ARFs demonstrate the complex interplay between auxin and JA signalling. Arabidopsis *arf6-2 arf8-3* double mutants showed reduced levels of JA accumulation in the flower buds, suggesting that ARF6 and ARF8 regulate genes involved in JA synthesis(Nagpal *et al.*, 2005). *LOX2* and *AOS* are genes in the JA biosynthesis pathway, both were found to be upregulated by auxin in Arabidopsis seedlings (Tiryaki and Staswick, 2002), both of these genes also contain auxin-responsive motifs which are possibly bound by ARFs to induce their expression. Nagpal *et al.,* 2005 found that both *LOX2* and *AOS* showed much lower levels of expression in the *arf6-2 arf8-3* double mutant.

As have been shown in Arabidopsis, in monocots it is also believed that JAs have a similar function in pollen development. Microarray analysis has revealed that JA biosynthesis genes are active in the tapetum of rice during all stages of tapetum development and in the microspore/pollen there appears to be preferential synthesis during the tricellular stage(Hirano *et al.*, 2008). Rice JA-deficient mutants *osjar1* and *cpm1/2*, were found to have impaired dehiscence, abnormal and

reduced filaments(Riemann *et al.*, 2013; Xiao *et al.*, 2014). The phenotype is also evident in rice signalling mutant *eg2-1D* (a mutant in *OsJAZ1*) and after overexpression of JAZ proteins that are resistant to JA-induced degradation (Cai *et al.*, 2014; Hori *et al.*, 2014).

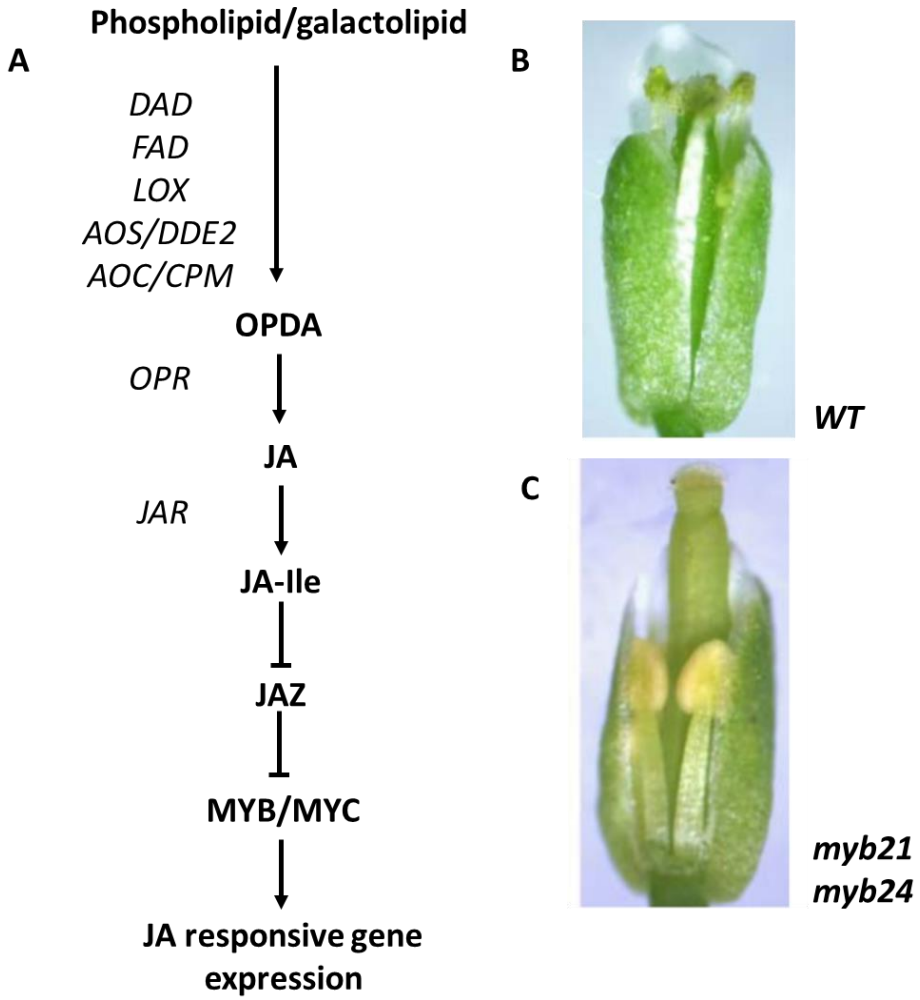

Figure 1.7: *The JA signalling pathway and male reproductive development.*

A. Simplified JA signalling pathway. JA is synthesised by a number a different enzymes. It is converted to bioactive JA-Ile by JAR. JA-Ile targets JAZ proteins for degradation, this allows the release of transcription factors, such as MYC2, which then induce JA mediated gene expression. Flower morphology of Arabidopsis WT. B. and JA signalling double mutant myb21 myb24. C. Photographs taken from(Song *et al.*, 2011).

1.5.3 Ethylene

Ethylene is a gaseous hormone which has been found to have roles in abiotic/biotic stress tolerance, germination, fruit ripening, senescence and abscission(Binder, 2020). Compared to JA, auxin and GA there is considerably less research into the role of ethylene in male reproductive development.

Mutants which are defective in ethylene signalling showed various levels of disrupted male reproductive development in a number of different plant species. Ethylene-insensitive tobacco plants (transformed with the mutant ethylene receptor etr1-1 from Arabidopsis) showed normal anther development, but delayed anther dehiscence(Rieu *et al.*, 2003). When WT tobacco plants were treated with ethylene they showed accelerated dehiscence and when exposed to the ethylene-perception inhibitor 1-methyl-cyclopropene (MCP) it resulted in delayed dehiscence(Rieu *et al.*, 2003). Overexpression of a mutated ethylene receptor unable to bind ethylene (*CmETR1/ H69A*) in *Nicotiana tabacum* led to a severe ethylene-insensitive phenotype, with the anthers showing reduced filament elongation and delayed degradation of the tapetum (Figure 1.8D/E)(Takada *et al.*, 2006). Suppression of another ethylene receptor, PhETR2, in petunia led to stomium degeneration and premature dehiscence before the pollen was ready for release, the pollen however was viable (Wang and Kumar, 2007). The evidence therefore suggests that ethylene plays a role in promoting filament elongation, tapetum degradation and dehiscence.

Expression analysis of key components of the ethylene signalling pathway also allude to ethylene's possible roles in anther and pollen development. In Arabidopsis expression of ethylene receptors *AtEIN4* and *AtERS2* reveal relatively high levels of expression in the stamen, tapetal and pollen cells(Hua *et al.*, 1998). In rice, ethylene biosynthesis genes, *OsACS6* and *OsACO2/3*, were found to show greatest expression during the later stages of pollen development and expression of these genes is also active within the tapetum(Hirano *et al.*, 2008).

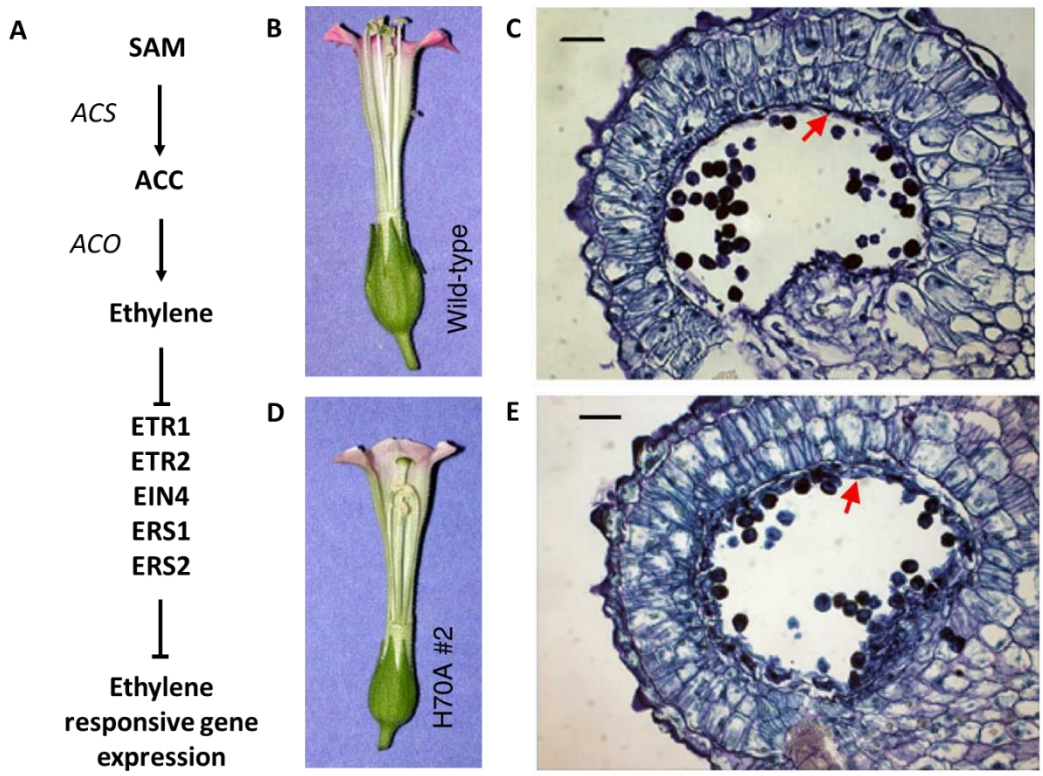

Figure 1.8: *The ethylene signalling pathway and its role in male reproductive development.*

A. Simplified ethylene signalling pathway. S-adenosyl-methionine (SAM) is converted to the ethylene precursor (1-Aminocyclopropane-1-carboxylic acid) ACC and then to ethylene by a number of different enzymes. Ethylene represses the action of ethylene receptors, which in the absence of ethylene repress ethylene responsive gene expression. Flower morphology and anther cross sections of tobacco WT (B and C) and ethylene insensitive mutant H70A#2 (D and E). Photographs taken from(Takada *et al.*, 2006).

1.5.4 Gibberellin

Gibberellins (GAs) are tetracyclic diterpenoid carboxylic acids which are found in certain species of bacteria, fungi and plants(Hedden and Thomas, 2012). Numerous different GAs have been discovered, but only a few have been identified as being bioactive: GA_1, GA_3, GA_4 and GA_7. Since their discovery GAs have been found to be important in controlling many aspects of development including seed germination, stem elongation, leaf expansion, floral development and trichome formation(Richards *et al.*, 2001).

GA have also been demonstrated to be an important hormone for controlling male reproductive development. In rice anthers there was found to be high concentrations of bioactive GAs in mature anthers(Kobayashi *et al.*, 1988; Hirano *et al.*, 2008). Different bioactive GAs appears to accumulate in different tissues, indicating their divergent roles in controlling plant development. Most notably, there was found to be an extremely high accumulation of GA_4 in mature anthers compared to the leaf blade and pistil in rice (Hirano *et al.*, 2008). In contrast, another bioactive GA, GA_1 predominantly accumulates in vegetative tissue of rice(Kobayashi *et al.*, 1989; Nakajima *et al.*, 1991; Hasegawa *et al.*, 1995; Hirano *et al.*, 2008).

Transcriptome analysis of anther tissue has revealed that there is extensive expression of GA related genes throughout tapetum development in Arabidopsis and rice(Hirano *et al.*, 2008; Hu *et al.*, 2008). Two key enzymes involved in the formation of bioactive GAs are GA 20-oxidase (GA20ox) and GA 3-oxidase (GA3ox), (Hedden and Phillips, 2000). The conversion of GA_{12} /GA_{53} to the immediate bioactive GA precursors GA_9/GA_{20} is catalysed by GA20ox. GA_9/GA_{20} are then converted to bioactive GAs, GA_4/GA_1 which is catalysed by GA3ox.

GA3ox3 and *GA3ox4* were both found to be only expressed in the anther of Arabidopsis, expression gradually increased from meiosis, reached its peak in all cell layers surrounding microspores just prior to mitosis and decreased with the tapetal PCD(Hu *et al.*, 2008). Expression of *GA3ox3* and *GA3ox4* in the microspores/pollen was also initially low until meiosis whereupon it gradually increased and continued even after the degradation of the tapetum and dehiscence(Hu *et al.*, 2008). In rice, *GA20ox3* and *GA3ox1* are most highly expressed in the microspores/pollen at bicellular and tricellular stages of pollen development and *GA20ox1/2* were most highly expressed at unicellular stage in the tapetum(Hirano *et al.*, 2008). It was therefore predicted that bioactive GAs increasingly accumulate towards the later stages of pollen development, specifically GA_4(Hirano *et al.*, 2008). In the anther filament, *GA3ox1* was found to show particularly high levels of expression(Mitchum *et al.*, 2006; Hu *et al.*, 2008).

Mutants of GA20ox and GA3ox, producing non-functional proteins, were found to have a deficiency of bioactive GAs(Hu *et al.*, 2008; Rieu *et al.*, 2008). The double mutant *ga3ox1 ga3ox3* showed reduced elongation of the stamen and a lack of dehiscence(Hu *et al.*, 2008). Likewise, double mutants of *ga20ox1 ga20ox2* were found to also have shorter filaments and the defective anther dehisce(Rieu *et al.*, 2008). GA deficient GA20ox triple mutant *ga20ox1 ga20ox2 ga20ox3-3* was found to show an even longer time to flower compared to the WT, defective tapetum degradation and shorter filaments (Figure 1.9D/E)(Plackett *et al.*, 2012). GA is known to be a positive regulator of stamen elongation, with Arabidopsis GA-deficient mutant *ga1-3* showing reduced cell length of the stamen rather than cell number(Cheng *et al.*, 2004).

The role of GA in anther development appears to be conserved in the monocots. Rice mutants which were defective in certain proteins of the GA biosynthesis and signalling pathway led to GA-deficiency (*oscps1-1*) and GA-insensitivity (*gamyb-2, gid1-4* and *gid2-5*). These mutants showed male fertility defects, having defects in tapetum degradation and a lack of Ubisch body accumulation in the tapetum. This led to the production of microspores which only contained a single layer of exine (as opposed to three layers), this lack of structural integrity led to the collapse of the defective microspore(Aya *et al.*, 2009). TUNEL (terminal deoxynucleotidyl transferase-mediated dUTP nick-end labelling) assays were used on the signalling mutants to detect fragmentation of DNA and therefore an indication of imminent PCD. *gamyb-2, gid1-4* and *oscps1-1* failed to show any tapetal cell signal and *gid2-5* only showed a faint signal in the tapetum(Aya *et al.*, 2009). The failure to complete dehiscence must in part be due to the failure for the tapetum to degrade(Wilson *et al.*, 2011). Treatment with GA_3 on GA-deficient mutants induced the programmed cell death of the tapetum and pollen viability was restored(Aya *et al.*, 2009), once again suggesting GA is key to this physiological process. GA was found to upregulate genes involved in lipid metabolism, among these include *CYP703A3* which is essential for sporopollenin biosynthesis(Aya *et al.*, 2009).

Along with GA deficient and GA-insensitive mutants showing male sterility, constitutive GA-response mutants also showed reduced pollen viability(Lanahan

and Ho, 1988; Ikeda *et al.*, 2001; Plackett *et al.*, 2014). This suggests that a constitutive GA response can also induce male sterility.

GAMYB is a transcription factor which is upregulated by GA in the aleurone of barley(Gubler *et al.*, 1995). It is a key facilitator of the signalling pathway which ultimately results in tapetal programmed cell death. In rice, *OsGAMYB* and *UNDEVELOPED TAPETUM1*(*OSUDT1*), independently regulate the expression of *TAPETUM DEGENERATION RETARDATION*(*OsTDR*)(Liu *et al.*, 2010). This begins the cascade of regulatory genes which eventually trigger the degradation of the tapetum. Loss-of-function mutants of *GAMYB* in rice were found to show impaired tapetal PCD and defective formation of pollen wall exine and Ubisch bodies. The non-degraded tapetum instead was found to expand into the lumen of the anther. A combination of all these defects led to male sterility (Kaneko *et al.*, 2004; Aya *et al.*, 2009; Liu *et al.*, 2010). The same phenotype of male sterility due to failed PCD and hypertrophy of the tapetum was found in double mutant *myb33myb65* in Arabidopsis(Millar and Gubler, 2005). Overexpression of *HvGAMYB* in barley led to normal development up to tricellular stage, after this the anthers failed to dehisce, this has been suggested to be due to a lack of pollen expansion in the lumen meaning there is less pressure on the stomium which remains intact. Along with failure to dehisce the pollen was found to be mostly sterile(Murray *et al.*, 2003).

DELLAs have also been found to be a key component of controlling anther and stamen development. DELLAs are negative regulators of the GA response. GA triggers GA responsive gene expression by targeting DELLAs for degradation by the proteasome, thus relieving them of the repressive nature of DELLAs (Reviewed by Harberd, Belfield and Yasumura, 2009). Arabidopsis DELLA proteins RGA, RGL1 and RGL2 have been found to repress petal, stamen and anther development(Cheng *et al.*, 2004; Tyler *et al.*, 2004). Excessive GA signalling, as a consequence of loss of DELLA activity was found to also result in male sterility in rice, barley and Arabidopsis Col-0 ecotype(M B Lanahan and Ho, 1988; A. Ikeda *et al.*, 2001; Plackett *et al.*, 2014). Defects in the Arabidopsis *rga-28 gai-td1* mutant were found to have post-meiotic developmental defects, these were restored by reintroduction of functional RGA DELLA(Plackett *et al.*, 2014).

It is also apparent that we cannot look at signalling pathways in isolation. As was found with auxin, JA also interacts with the GA signalling pathway. MYB21, MYB24, and MYB57 are components of both the GA and JA signalling pathway(Cheng *et al.*, 2009). Furthermore, GA was found to suppress DELLAs which then leads to a subsequent upregulation of *DAD1,* a key gene in JA biosynthesis(Cheng *et al.*, 2009). Therefore, an increase in GA accumulation, will subsequently lead to an increase in JA accumulation.

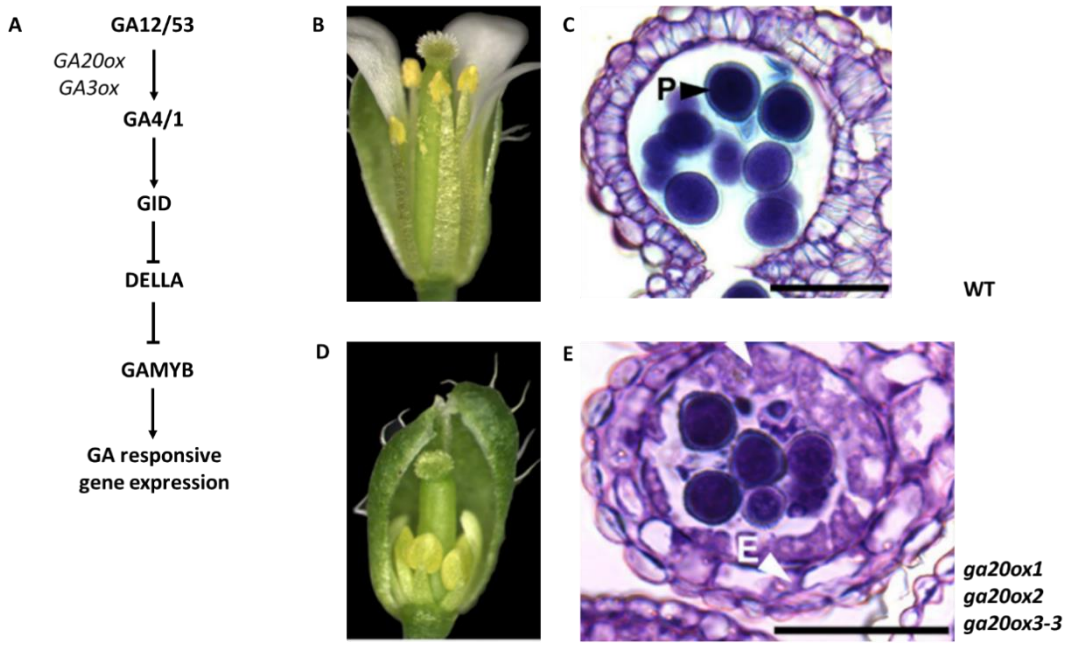

Figure 1.9: *The GA signalling pathway and its role in male reproductive development.*

A. Simplified GA signalling pathway. $GA_{4/1}$ are bioactive GAs. The soluble GA receptor, GID, then recognises the bioactive GAs and triggers the degradation of DELLA. This relieves the repression of DELLA on GAMYB. GAMYB binds to the promoters of GA responsive genes and induces their transcription. Flower morphology and anther cross sections of Arabidopsis WT (B and C) and GA deficient triple mutant ga20ox1 ga20ox2 ga20ox3-3 (D and E). Photographs taken from(Plackett *et al.*, 2012)*. P=pollen. E=endothecium. Scale bar = 50 µM.*

1.6 Impact of high temperature on anther and pollen development

As previously described, male reproductive development is more sensitive to heat stress than female reproductive development(Peet *et al.*, 1998; Oshino *et al.*, 2007; J. Xu *et al.*, 2017). In general the longer the heat treatment and higher the

temperatures the greater the reduction in seed set and pollen viability(Sato *et al.*, 2002).

The vulnerability to heat stress is pollen stage dependent, although the stage can be more or less vulnerable in different plant species. Meiosis is generally considered to be the most vulnerable stage of pollen development, although later stages of pollen germination and pollen tube growth are also sensitive to heat. In Arabidopsis, wheat, rice, barley and tomato meiosis and early microspore stage have been identified to be the most sensitive stage of heat stress(Iwahori, 1965; Saini *et al.*, 1984; Sakata *et al.*, 2000; Kim *et al.*, 2001; Endo *et al.*, 2009). Heat treatment during meiosis has led to two types of abnormal pollen development in wheat. The first is that the PMCs complete meiosis, but failed to orientate themselves around the anther lumen, due to premature tapetum degradation and consequently failed to complete mitosis I (Saini *et al.*, 1984). The second effect is where microspores complete the first round of mitosis I, but fail to go through mitosis II (Saini *et al.*, 1984). Both of these defective phenotypes were also observed in barley(Sakata *et al.*, 2000), resulting in reduced pollen viability.

The vulnerability to heat stress is due to premature degradation of the tapetum as found in, barley, rice, soybean and wheat(Saini *et al.*, 1984; Abiko *et al.*, 2005; Feng *et al.*, 2018). From meiosis to the release of microspores the tapetum is at its largest and most active, therefore its premature degradation during this highly active time makes these stages the most vulnerable to heat stress. Heat stress causes increased vacuolisation, swelling of mitochondria and irregularities with the endoplasmic reticulum of the tapetal cells (Ku *et al.*, 2003; Oshino *et al.*, 2007). Similar characteristics have been observed prior to tapetal PCD, with the mitochondria and cytoplasm becoming vacuolised, condensed chromatin and fragmented nuclei(Varnier *et al.*, 2005). These occur immediately prior to tapetal PCD. Therefore, heat stress is prematurely initiating the tapetal PCD, which would naturally occur later anyway. With the premature degradation of the tapetum comes defects in pollen exine, owing to its initial role in its formation (Djanaguiraman *et al.*, 2013; Harsant *et al.*, 2013; Prasad and Djanaguiraman, 2014).

High temperatures also caused a reduction in mitotic index of all cells within the anther, therefore resulting in lower proliferation of cells in barley(Oshino *et al.*, 2007). This is supported by findings of inhibited proliferation of DNA from mitochondria and chloroplasts in the first two days of heat treatment and eventually nuclei within 3 days in barley panicles(Oshino *et al.*, 2011). This indicates a disruption in cell differentiation and replication, both processes are needed for successful pollen development. Heat treatment prior to the formation of PMCs and tapetal cells was found to completely abolish the occurrence of either of these cells(Sakata *et al.*, 2000).

Another vulnerable period (although not to the same level of sensitivity as meiosis/early microspore stage) is anthesis(Jagadish *et al.*, 2010; Shi *et al.*, 2018). This phenomenon has particularly been observed in rice, which is actually its most sensitive stage to temperature stress. The primary cause of sterility has been attributed to fewer pollen grains being shed onto the stigma due to disrupted dehiscence(Matsui *et al.*, 1997, 2000; Prasad *et al.*, 2006; Jagadish *et al.*, 2010). There is also evidence of reduced germination rates of pollen at higher temperatures(Matsui *et al.*, 1997). The number of germinating pollen grains on the stigma and spikelet fertility has been shown to be highly correlated(Jagadish *et al.*, 2010). The disrupted dehiscence is thought to be due to increased stickiness of the pollen and smaller openings of the anther that restrict release of the pollen(Liu *et al.*, 2006). Prior to dehiscence there is an increase in the diameter of pollen grains. This is thought to be driving the opening of the anthers. High temperatures on the day of flowering are thought to reduce the swelling of the pollen and is therefore inhibits dehiscence(Matsui *et al.*, 2000, 2001). Dehiscence is also disrupted if high temperatures are exposed just before flowering, although there was found to be no difference in the swelling of pollen grain, therefore suggesting that the physical process of the anther splitting is directly impacted(Matsui *et al.*, 2000).

Although considerably less well studied, the pistil was also found to show vulnerability to heat stress in wheat. Successful stigma function is essential for ensuring fertilisation of the ovule. The stigma is required for capturing and hydrating the dehisced pollen, as well as guiding the elongation of the pollen tube

to the ovary(Harrison, 1979). After exposing wheat to 32/24°C day/night and withholding watering for 5 days from mid-unicellular stage, there was found to be desiccation of the stigma. This desiccation is thought to reduce the pollen capturing ability of the stigma(Prasad and Djanaguiraman, 2014; Fábián *et al.*, 2019). Heat stress was also found to induce morphological differences in the stigmas of heat stressed plants, with papilla cells showing fragmented nuclei and cytoplasm and the stylodia showing crushed cortical and transmitting cells (Fábián *et al.*, 2019). After heat stressing wheat at 30°C for three days from meiosis there was found to be a similar number of pollen grains which landed on the pistil, however there was a lower germination rate of pollen. Pollen tubes were also found to be shorter and did not grow in the direction of the ovary(Saini *et al.*, 1983). Cross sections of the ovaries were taken just prior to anthesis and a third were found to contain an abnormal nucellus or embryo sac, whereas the rest showed normal development(Saini *et al.*, 1983). This contrasts to findings by(Fábián *et al.*, 2019), which found no defects in the ovule or female gametophyte.

1.7 The role of phytohormones in heat stress tolerance

High temperatures disrupt a number of cellular processes which can lead to cell death. High temperatures are known to alter cell membrane fluidity and permeability(Alfonso *et al.*, 2001). The damage to the cells membranes and proteins can also result in oxidative stress, caused by a build-up of ROS(Reviewed by Pucciariello, Banti and Perata, 2012). Heat stress also leads to a reduction in photosynthetic activity. This has been attributed to disruption of PSII and rubisco activity, with heat stress being found to affect its function in wheat(Feng *et al.*, 2014). Plants are sessile organisms and therefore have to respond not by behavioural mechanisms, but by biochemical and growth responses to abiotic stress(Barnabás *et al.*, 2008).

Plants exhibit two types of thermotolerance: basal and acquired. Basal thermotolerance is the inherent ability to survive and acquired is an increase in thermotolerance after a period of acclimation. Acquired thermotolerance is induced when plants are exposed to non-lethal periods of high temperature prior to a later heat treatment(Kapoor *et al.*, 1990; Burke *et al.*, 2000; Hong *et al.*, 2003). This has

been linked to increased accumulation of heat shock protein (HSP) during the acclimation period in Arabidopsis(Burke *et al.*, 2000). HSPs act as molecular chaperones which both protect proteins from heat stress induced denaturation and also refold misfolded proteins(Boston *et al.*, 1996).

As was previously described (Chapter 1.3.2) male reproductive development is especially vulnerable to high temperatures. Fertile pollen relies on the coordinated accumulation of phytohormones which are required to regulate the processes of tapetal breakdown, mitosis, filament elongation and dehiscence. Many studies indicate that heat treatment disrupts ordinary development of anthers and pollen. This could be linked to disruptions in accumulation of different hormones (Figure 1.10).

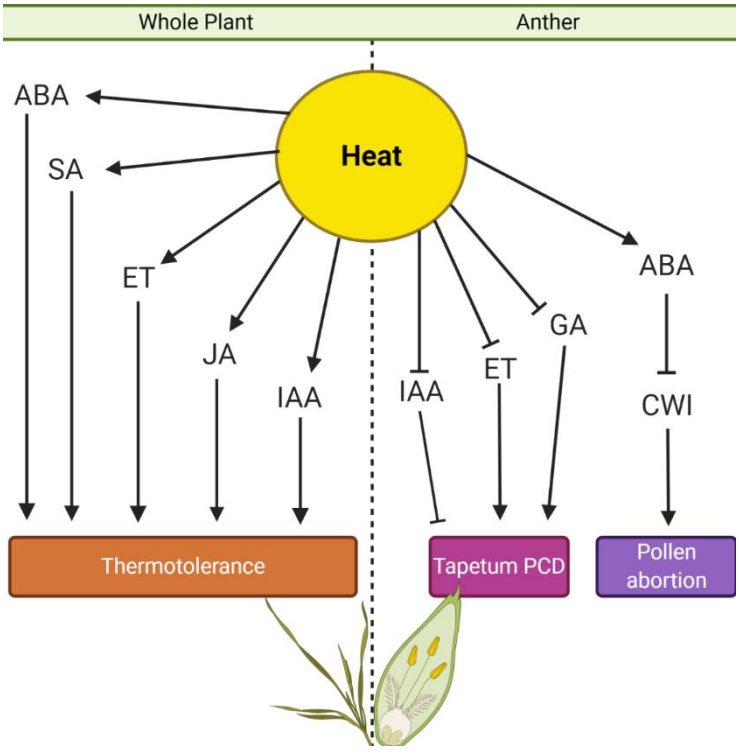

Figure 1.10: *The impact of heat stress on phytohormone accumulation in vegetative and anther tissue.*

IAA (Auxin), JA (Jasmonic acid), ET (Ethylene), SA (Salicylic acid), ABA (Abscisic acid), CWI (Cell Wall Invertase). PCD (Programmed Cell Death). Created with BioRender.com.

1.7.1 Vegetative tissue

In response to heat treatment there was found to be an upregulation of JA inducible genes and endogenous free JA in Arabidopsis (Clarke *et al.*, 2009). There was also found to be an increase in ethylene concentration in response to heat stress, that was induced as a result of JA and SA(Clarke *et al.*, 2009). Likewise, in seedlings there was found to be an upregulation of IAA in response to heat treatment(Gray *et al.*, 1998).

A number of hormones have been found to be involved in whole plant thermotolerance. Exogenous application of ABA, SA and ACC (the precursor of ethylene) has been shown to increase thermotolerance in Arabidopsis, specifically by reducing oxidative damage(Larkindale and Knight, 2002; Clarke *et al.*, 2004). Exogenous application of methyl jasmonates was also found to increase heat stress tolerance of Arabidopsis(Clarke *et al.*, 2009).

Seedlings defective in ethylene signalling were found to be defective in their basal thermotolerance in Arabidopsis(Larkindale *et al.*, 2005). Ethylene is thought to be more critical for basal thermotolerance, rather than acquired thermotolerance, with ethylene insensitive mutants *ein2* and *etr1* being defective in basal thermotolerance, although they still had the ability to acquire thermotolerance(Larkindale *et al.*, 2005). In contrast to this study, another study found that ethylene insensitive plants were less susceptible to heat stress(Clarke *et al.*, 2009), however lower temperatures and older plants were used.

ABA has been determined to be critical in acquired thermotolerance, with ABA biosynthesis mutants *aba1*, *aba2* and *aba3*, and ABA insensitive mutants *abi1* and *abi2* showing defective acquired thermotolerance(Larkindale *et al.*, 2005). The *cpr5-1* mutant in Arabidopsis was found to have constitutively active SA, JA and ethylene signalling and was found to have greater heat stress tolerance(Clarke *et al.*, 2009). Salicyclic acid (SA) has also been determined to be involved in thermotolerance. SA mutants which are deficient in SA and over-accumulate SA showed lower and higher thermotolerance respectively(Clarke *et al.*, 2004). Seedlings defective in SA signalling were also found to be defective in their basal thermotolerance(Larkindale *et al.*, 2005).

Evidence also points to the role of GA in heat stress tolerance. As previously discussed, GAMYB is a transcription factor downstream of GA. The expression of *GAMYB* is positively regulated by GA and is involved in initiating GA responsive signalling. Expression of all three of the *GAMYB* homoeologues increased in wheat seedling leaves in response to heat treatment(Wang *et al.*, 2012). GAMYB is regulated by controlled cleavage of miRNA miR159 on a post transcriptional level. In Arabidopsis, ABA has been found to induce accumulation of miR159, which in turn was found to induce transcriptional degradation of *AtMYB33* and *AtMYB101*, and result in ABA induced growth arrest during early seedling development(Reyes and Chua, 2007). The orthologous TamiR159 has been found to negatively regulate *TaGAMYB1* and *TaGAMYB2* in wheat, whereby it induces the cleavage of the transcripts. *TamiR159* was found to be downregulated after heat stress in wheat leaves (Xin *et al.*, 2010). *TaGAMYB1* was found to be upregulated after 2 hours of heat treatment in the leaves, with the heat sensitive variety Chinese Spring showing less of an upregulation compared to the heat tolerant variety. However, overexpression of *TamiR159* in rice led to increased heat sensitivity in rice(Wang *et al.*, 2012), as it causes greater GAMYB degradation and lower GA responsive signalling.

1.7.2 Anther and pollen development

Heat stress is marked by a reduction in the endogenous levels of auxin in the anthers of barley, resulting in male sterility. This was reversed by exogenous application of auxins, IAA/NAA(Sakata *et al.*, 2010). Likewise in rice, heat stress induced a reduction of IAA content of spikelets, and endogenous application of IAA also relieved pollen sterility as a result of heat stress(Sharma *et al.*, 2018). The reduction in endogenous auxin has been linked to a reduction in expression of IAA biosynthesis genes (*YUCCA*) in the stamens in response to heat treatment (Sakata *et al.*, 2010; Sharma *et al.*, 2018).

The IAA and GA content in rice anthers of both heat sensitive and heat tolerant varieties of rice were found to decrease in response to high temperatures, but most notably in the heat sensitive lines(Tang *et al.*, 2008). Samples of anthers were taken directly after the treatment. Indicating that sustained IAA and GA levels are

essential for mitigating the impact of heat stress. There was also found to be a significant increase in ABA content of anthers in both rice cultivars in response to the high temperatures, although less drastic in the heat tolerant cultivar(Tang *et al.*, 2008). As previously described in section 1.5 auxin and gibberellins are both crucial for ensuring normal pollen development. ABA is known to induce sterility in both rice and wheat and stresses of cold and drought lead to the accumulation of ABA in the anthers(Oliver *et al.*, 2007; Ji *et al.*, 2011). ABA has been found to repress the expression of cell wall invertase genes in the anther, *TaIVR1*, and *OSINV4*. These proteins are crucial to ensuring a supply of sugars to the tapetum and pollen grains(Oliver *et al.*, 2007; Ji *et al.*, 2011).

In tomato, pollen viability and germination was increased after treatment with ethephon, an ethylene releasing agent, and decreased when treated with AVG, an ethylene biosynthesis inhibitor(Firon *et al.*, 2012), therefore suggesting that ethylene decumulates as a result of heat stress and possibly this is contributing to male sterility. Studies have shown that tomato mutants which are ethylene insensitive showed greater adverse effects of heat stress on male fertility, having reduced pollen production and viability (Firon *et al.*, 2012).

1.8 Project aims and objectives

Extensive research has been completed on understanding the roles of hormones in male reproductive development and abiotic stress tolerance in Arabidopsis and rice. However, there is very little research focused on understanding the roles of these phytohormones in the abiotic stress tolerance of wheat, particularly during heat stress. This project will examine the roles of hormones and their signalling pathways in pollen development and heat stress tolerance in wheat and in doing so will address the following objectives:

<u>Establish a reliable heat stress assay for wheat var. Cadenza (Chapter 3)</u>

In order to establish a reliable heat stress assay, a non-destructive staging method of pollen development will be developed for our chosen wheat variety Cadenza. This will involve using the elongation of the flag leaf sheath (FLS) as an indication of anther developmental stage. Using this, a pollen stage specific heat stress assay will

be developed to determine which stages and temperatures are most vulnerable to heat treatment.

Identification of transcriptional and hormonal changes associated with heat stress during anther development in wheat (Chapter 4)

A global hormone analysis will be conducted on whole anthers taken from different stages of pollen development. Comparisons will be made between anthers exposed to either control or the optimised heat stress conditions.

RNAseq analysis will also be performed on replicates of these anther samples. From this, key genes involved in anther and pollen development of wheat will be identified, along with how heat stress interferes with their expression.

Generation of wheat hormone signalling mutants and characterisation of their general phenotype and response to heat treatment (Chapter 5/6)

Auxin and ethylene have both been identified to be important hormones in ensuring successful male reproductive development (Chapter 1.5), as well as promoting heat stress tolerance of vegetative and reproductive tissue (Chapters 1.6 and 1.7), in model plants. We sought to investigate if these same findings can be applied to wheat. Auxin and ethylene-insensitive gain-of-function mutants will be identified from the wheat TILLING population and the general phenotype of these mutants will be characterised, paying attention to grain set as an indication of fertility. Alterations in their heat stress tolerance will also be investigated by grain counts and measurements of pollen number/viability. It is expected that these mutants will show defects in male reproductive development and a reduced heat stress tolerance. As auxin-insensitive mutants have been shown to have highly divergent root phenotypes, a detailed investigation into the root phenotype of these auxin-insensitive wheat mutants will also be conducted.

Establish how exogenous application of hormones could be used to confer heat stress tolerance (Chapter 5)

Exogenous application of synthetic auxin, 1-Naphthaleneacetic acid (NAA) will be applied to wheat tillers before and during heat treatment to investigate whether it is able to mitigate the effect of heat stress on grain set.

In addressing these objectives pollen development and heat stress tolerance will be investigated on a biochemical, molecular and physiological level. Greater understanding of the signalling pathways responsible for regulating heat-induced disruption of pollen development will allow the development of chemical treatment strategies to mitigate this abiotic stress.

Chapter 2: Materials and Methods

2.1 Plant Material and Growth Conditions

Mature grains of wheat var. Cadenza were sterilised in 5% (v/v) bleach solution and washed 5x in ddH_2O before being germinated on sterile petri dishes with dampened filter paper. The plates were then placed at 4 °C for 3 days to imbibe and then transferred to light conditions to initiate germination. The seedlings were initially planted in growth trays to allow them to grow to 3 leaf stage, at which point they were then transferred to 13 cm diameter plastic pots and were grown in glasshouse conditions with a photoperiod of 16 hours using natural light from 400-1000 and supplemented with 500 $\mu molm^{-2}s^{-1}$ PAR from SON-T sodium lamps. The plants were irrigated twice daily, and the temperature is maintained at 18-20 °C day and 14-15 °C night. Rothamsted prescription mix compost (75% peat, 12% sterilised loam, 10% grit and 3% vermiculite) was used.

Plants grown under controlled environment growth conditions were either grown in Fitotron growth chambers (Weiss Gallenkamp, Weiss Technik, Loughborough, U.K.) or Conviron Adaptis cabinets (Conviron Europe ltd, Cambridgeshire, UK) as indicated. The conditions were maintained at 20 °C/ 15 °C for day/ night temperatures, with photoperiods of sixteen hours per day at 500 $\mu molm^{-2}s^{-1}$ PAR provided by tungsten fluorescent lamps. The plants were irrigated by hand regularly and the relative humidity was maintained at 65%/ 75% day/night in normal growth conditions. The plants were hand irrigated once a day and during heat stress experimentation they were irrigated carefully to soil water saturation every morning.

2.2 Genomic DNA Extractions

2.2.1 Tube DNA Extraction

Young leaf tissue was harvested and freeze dried in 2 ml eppendorf tubes and ground using 3mm steel ball bearings (Atlas Ball and Bearing Co Ltd, Walsall, UK) in a GenoGrinder (SPEX SamplePrep, Metuchen, New Jersey, U.S.A). 1 ml of PVP-extraction buffer (pH 9.5) was added to each sample and incubated at 65 °C for 1 hour. The extraction buffer contained 100mM Trizma base (Tris base), 1M

potassium chloride, 2% v/v 0.5M EDTA, 0.18mM polyvinylpyrrolidone (PVP-40) and 34.5mM sodium bisulphate. The pH was adjusted using 1M NaOH. The reagents were purchased from Sigma-Aldrich (St.Louis, Missouri, U.S.A.) 333 µl 5M potassium acetate (pH 5.8) was then added to each tube. The samples were centrifuged for 2 minutes at 13,000rpm to pellet tissue debris and 1 ml of cleared supernatant was transferred to fresh tubes. 500 µl of pre-chilled isopropanol was transferred into each tube, vortexed and incubated at RT for 10 minutes to precipitate the DNA. The samples were centrifuged for 10 minutes at 13,000 rpm and the supernatant discarded. The resultant pellet containing gDNA was washed in 500 µl of 70%(v/v) EtOH, spun to re-pellet and excess EtOH removed and the rest allowed to evaporate at RT. The gDNA was then resuspended in 200 µl of 10mM Tris.HCl (pH7.5), with added Pancreatic RNase A (100µg/ml). The solution was incubated at 50 °C for 1 hour, vortexing every 15 minutes. The concentrations were measured using a Nanodrop™ ND-1000 spectrophotometer (LabTech International Ltd, U.K.).

2.2.2 96-Well Plate DNA Extraction

Buffers were prepared as above. Leaf tissue was placed directly into 96-well plates. Solutions were transferred into the plate via a multidropper with differing volumes to the single tube extraction method. 600µl extraction buffer, 200µl of 5M potassium acetate, 165µl isopropanol, 500µl 70% ethanol and 200µL TER was used.

2.2.3 Polymerase Chain Reaction (PCR)

PCR was used for the genotyping of the TILLING mutants. HotShot Diamond^{TM} PCR Master Mix, Clent Life Science, York House, Stourbridge, U.K containing $MgCl_2$ (6 mM), Taq polymerase and dNTPs. Each 20 µl PCR reaction contained the following:

Reagent	Volume
HotShot Diamond^{TM} Mastermix	10µl
Distilled H_2O	7µl
Forward primer (10 µM)	0.5µl
Reverse primer (10 µM)	0.5µl
Template DNA (25 ng/µl)	2µl

PCR reactions were carried out in a C1000 Thermal Cycler (Bio-Rad Laboratories, Hercules, California, U.S.A) using the following conditions:

Step	Temperature	Time	Nom cycles
Initial denaturation	98°C	5 mins	1x
Denaturation	97°C	30s	30-40x
Annealing	55-70°C	30s	
Extension	72°C	1min/kb	
Final extension	72°C	6 mins	1x
Hold	4°C	~	

Graded PCRs were used to determine the optimum temperature to amplify the gene of interest and reduce the amount of non-specific amplification.

2.2.4 Agarose Gel Electrophoresis

Agarose gel electrophoresis was used to determine the size of the PCR product and the degree of non-specific amplification. Agarose gel was made using 1x TBE buffer (45 mM Tris-borate, 1 mM EDTA, pH 8.3) and 1% (w/v) agarose (Fischer Scientific, Loughborough, U.K). Ethidium bromide was added to a concentration of 0.5 µg/µl. 1kb GeneRuler^{TM} DNA ladder or 100 bp DNA ladder (Thermo Scientific, Hemel

Hempstead, U.K.) was loaded into the gel along with the PCR products to ascertain the size of the PCR product. The PCR reactions were mixed with 5x loading dye (Thermo Scientific, Hemel Hempstead, U.K.) to track the progression of the PCR product migration through the agarose gel. Electrophoresis was carried out at 80 mV for 90 minutes. Once completed the gel was visualised under UV light using a SynGene GelDoc imaging camera (Synoptics Ltd, Cambridge, U.K.).

2.2.5 PCR purification

PCR products were purified using the QIAquick PCR purification kit (QIAgen, Hilden, Germany) according to the manufacturer's instructions.

2.2.6 PCR Sequencing

15 µl of purified PCR product at a concentration of 5 ng/µl was sent pre-mixed with 2 µl of relevant forward or reverse primer (10 µM) to Eurofins Genomics (Wolverhampton, U.K.) for sequencing. Sequenced results were analysed using Geneious (v10.0.02, Biomatters Ltd, Auckland, New Zealand) where they were aligned with WT genomic sequences to identify SNPs. WT sequences were obtained from Ensembl Plant(https://plants.ensembl.org/Triticum_aestivum/Info/Index), which contains the latest iwgsc_refseqv1.0 wheat genome annotation.

2.2.7 Plate sequencing

15µl of unpurified PCR products were loading into 96-well PlateSeq Kit PCR (Eurofins Genomics, Luxembourg) and sequenced in bulk with primers (10 µM).

2.2.8 Primer Design

PCR primers were designed using Geneious (v. 8.1.3, BioMatters Ltd, Auckland, New Zealand). Homoeologue specific primers were designed to have a GC content of 40-60%, 18-24 bp in size, T_m of 58-62°C and homologue specific differences on the 3' end of the primer.

Table 2.1: *Primers used for PCR genotyping.*

Tilling line	Gene	Sequence (5'-3')	Length (bp)
1331/1247/1865	TraesCS1B02G127000	CTAGAGCCTGTCATATAA GAGTCCTTCCCAACTCAAC	704
1779/1445	TraesCS4A02G274300	TGATATGAGCCTGCTGTG GATTTCATGAGTTAGCATCC	553
0407	TraesCS4B02G039300	TAGGAACGGAGGGAGTACATAA AGCTCCCTCGTTTTGACACT	491
0139	TraesCS1B02G138100	CACCAACACCAACTCCTCCT GCAGAGCTTGTGTAGCCAG	475
1812	TraesCS5A02G378300	TGTGTGAGGGGGGAAAAGA GCCGATGGTGAAGGAGCTGAAC	447
1374	TraesCS5A02G382600	AGGGCAAGAAAATGATGT GCCGTCCATGCTCACCTTGACA	593
0161	TraesCS5B02G058500	AAGAAACCCATGCATCTGTG TGCTCACCTTGACGAACGCC	145
0188/1420	TraesCS5B02G381900	ACGTACACTGATAATGCAGCA ATGGTGAAGGAGCTGAACAT	386
1806	TraesCS5B02G446100	TCGTCGTCGACAGTGGCACT ATGAGGTCGCCGTCCTTGTCCT	418
1366	TraesCS5D02G388300	TGGCCAAATCTTATACGCTGAC CGTCATCCCCTGAGCCTGC	268
1305	TraesCS7A02G322000	TGTTGGCTTGTCTTTCACTG CCATGGTCTTCTTCTTCATAGC	205

2.3 RNA

2.3.1 RNA extraction

Anther samples were immediately harvested and frozen in liquid nitrogen before being transferred to -80°C for long term storage. The samples were then ground to a powder using 3mm steel ball bearings (Atlas Ball and Bearing Co Ltd, Walsall, UK)

in the GenoGrinder (SPEX SamplePrep, Metuchen, New Jersey, U.S.A). RNA was extracted using of the Monarch Total RNA Miniprep Kit (NEB, Ipswich, MA, USA). The frozen samples were treated with 500µl of 1x RNA protection reagent. The sample was immediately vortexed to homogenise it. The sample was then pelleted by centrifuging at 16000g for 2 mins. The supernatant was transferred to an RNase-free microfuge tube. 500µl of RNA lysis buffer was added and vortexed. The solution was then passed through a gDNA removal column to remove the gDNA by spinning for 30 secs. The RNA was then precipitated by adding 1ml of ethanol before being transferred over to an RNA purification column and the flow through discarded. A DNase step was conducted by firstly washing the column with 500µl of RNA wash buffer followed by adding 5µl DNase I and 75µl DNase I reaction buffer and incubating for 15 mins at RT. The RNA was then prepared for elution by washing with 500µl RNA priming buffer for 30 secs. The column was then washed 2x with 500µl of RNA wash buffer, the first time for 30 secs and the second for 2 mins. The RNA was then eluted by 50µl Nuclease-free water by centrifuging for 30 secs. The RNA was then stored at -80°C in long term storage.

2.3.2 Quantification of RNA concentration and quality

For RT PCR, the RNA was firstly checked using a Nanodrop™ ND-1000 spectrophotometer (LabTech International Ltd, U.K.) to measure the concentration, OD260/230 (carbohydrate contamination) and OD260/280 (protein contamination). The quality was then further checked by running the samples on agarose gel using RNA Gel 2x Loading Dye (Thermo Scientific, Waltham, MA, USA). The RNA samples were mixed with the loading dye and then denatured at 70°C for 10 mins, before being run on an agarose gel.

For RNAseq analysis the quantity and quality of the extracted RNA was tested using an Agilent Nano RNA Kit (Agilent, Santa Clara, California, USA) and Agilent 2100 Bioanalyzer (Agilent, Santa Clara, California, USA). The preparation followed the manufacturer's instructions.

2.3.3 RNAseq analysis

RNA was sent to Novogene (UK) Company Limited (Babraham Research Campus, Cambridge, UK) for RNA sequencing. The resultant raw fasta file received from

Novogene was processed using GALAXY and the free online tool https://3drnaseq.hutton.ac.uk/app_direct/3DRNAseq/. The raw fasta.q files were uploaded to GALAXY and mapped to the latest iwgsc_refseqv1.0 assembly for *Triticum aestivum* via the Salmon quant function. The resultant tabular files were uploaded to the 3drnaseq website and the data was analysed using a CPM cut-off of 1. A table of TPMs for each gene was produced and from this the means and SE were calculated.

Gene functions were analysed using the online resource Knetminer https://knetminer.com/Triticum_aestivum/. Gene Ontology (GO) enrichment analysis was performed using g:Profiler https://biit.cs.ut.ee/gprofiler/gost.

Heat maps were plotted using https://software.broadinstitute.org/morpheus/ from the raw TPM data of hormone biosynthesis/regulatory genes which were found to be significantly differentially expressed between control and heat treatments when grouping unicellular, bicellular and tricellular stages together for each treatment.

Orthologues of genes were found using Ensemble Plant BioMart Tool and in many cases checked using the BLAST function http://plants.ensembl.org/index.html. The expression profiles of these genes were plotted using the Z value.

2.4 Quantification of Phytohormone levels in Wheat Anthers

Phytohormones were quantified using an adapted protocol from(Šimura *et al.*, 2018). The hormone data was produced in collaboration with the Plant Laboratory of Growth Regulators, Palacký University, Olomouc, Czech Republic. Whole anther samples were collected and freeze dried for 4 days. The samples were then weighed. Collected anther material was homogenised in 1ml 60% acetonitrile and 10/20 µl of internal standard was added depending on the number of times the samples would be split. 4 silica beads were placed in each tube and the samples were homogenised in a Retsch MM400 bead mill at a frequency of 27/s for 5 minutes. The samples were then sonicated for a further 3 minutes and then rotated for 20 rotations/minute for 30 minutes at 4°C. The samples were then centrifuged in a Beckman Avanti 30 Centrifuge at 20,000 RPM, for 15 minutes at 4°C. The supernatant was removed and placed in a separate 2ml Eppendorf tube. The

samples were purified by being passed through RP polymer-based SPE Oasis HLB (hydrophilic-lipophilic-balanced) columns which allow targeted compounds to pass through the SPE column while retaining interfering compounds. The column was first activated using 100% MeOH followed by ddH_2O and then equilibrated using 100% ACN (1ml for 30mg HLB tube and 2 ml for 60mg HLB tube). After this the sample was passed through the column, followed by elution using 60% acetonitrile (ACN) and 30% ACN (500µl for 30mg HLB tube and 1ml for 60mg HLB tube). The samples were then evaporated using a nitrogen evaporator until completely dry and dissolved in 50µl 30% ACN, by vortexing and 5 minutes of sonification. The volume was then transferred to a 1.5ml centrifuge tube before being centrifuged for 5 mins at 8500rpm to remove any remaining debris. The samples can then be transferred to insert-equipped vials and centrifuged again for 10 minutes to bring down any remaining debris. The vials can then be stored at 4°C for a maximum of 1 day.

The samples could then be analysed using a triple quadrupole mass spectrometer Xevo® 581 TQ-S MS (Waters, Manchester, UK). Prior to the injection the samples should be spun down for 5 minutes to avoid any particulates. On the day of use 0.01% Formic Acid in ACN was used for Mobile Phase A and 0.01% Formic Acid in H_2O was used for Mobile Phase B. Different phytohormones have different retention times and produce a unique peak on the resultant chromatogram. The areas under each peak corresponded to the abundance of that particular phytohormone per sample. Dividing this abundance by the weight of the sample corresponds to the abundance of the hormone per weight of dry tissue.

In some instances, the resultant tissue concentration of a targeted compound was below the limit of detection (LOD). For statistical analysis the tissue samples were considered to be two thirds of the respective LODs(Šimura *et al.*, 2018).

2.5 Histological analysis

2.5.1 Fixation and embedding of tissue

Sectioning of wheat anthers was completed based on a method used on barley anthers (Gomez and Wilson, 2012). Whole anther, spikelet or spike tissue was infiltrated in a fixative (4% paraformaldehyde in PBS pH 7.2, 0.1% Triton X-100 and

0.1% Tween 20) overnight at 4°C. The tissue was then brought to RT and washed twice in PBS buffer for 30 mins/wash. The tissue was then dehydrated by an ethanol series: 30%, 50%, 70%, 90% and 2x 100% for 1 hour each. The dehydrated tissue was infiltrated with Technovit 7100 T218 TAAB resin dissolved in 1% (w/v) Hardener I (Solution A). This was applied in a concentration series of 2:1 (EtOH/Solution A), 1:1 (EtOH/Solution A) and 1:2 (EtOH/Solution A) for 1 hour each and finally 100% Solution A at 4°C. The tissue was then embedded in Solution B (Solution A and 9% v/v Hardener II) within gelatine capsules and allowed to harden overnight. Once fully hardened, warm water was used to remove the gelatine capsule.

For root sections a slightly different protocol was implemented. Freshly cut roots were infiltrated with a fixative (4% paraformaldehyde in PBS pH 7.2, 0.1% Triton X-100 and 0.1% Tween 20) for 2h at RT in rotation and then left overnight at 4°C. The samples were then washed 3x in 0.05M phosphate buffer for 30 mins/change. The tissue was then dehydrated by the ethanol series: 10%, 20%, 30%, 40%, 50%, 60%, 70% (4°C overnight), 80%, 90% and 2x100% for 1 hour at each concentration at RT. Infiltration of samples with LRWhite Resin (Agar Scientific, Stansted, U.K.) was also carried out by starting with a lower ratio of ethanol 100% : LR resin and slowly increasing the concentration of LR resin. The ratio followed the following 1:4, 3:2, 2:3 and 4:1 (v/v) for 1 hour followed by 100% LR white for 6 hours at 4°C. The samples were then placed in resin filled capsules and polymerised at 60 °C for 24 hours. The samples were left to cool before sectioning.

4 µM sections were cut using a glass knife in a Reichert-Jung Ultracut microtome (Leica, Wetzlar, Germany). Samples were mounted onto glass slide cover slips and dried on a warm plate. Before being stained the sections were inspected using an Olympus BH-2 light microscope (Olympus, Shinjuku, Japan).

2.5.2 Section staining and visualisation

For general staining a drop of Toluidine blue (0.05%) was placed on each section for 20-30 secs and rinsed with distilled water. The slides were then re-dried on the warm plate and mounted with a cover slip using DPX (Sigma-Aldrich, St.Louis, Missouri, U.S.A.). Digital images of fixed samples were captured using a Zeiss Axiophot light microscope (Zeiss, Jena, Germany) with a Retiga digital camera (Q-

Imaging, Surrey, Canada). MetaMorph ® (Molecular Devices (UK) Ltd, Wokingham, U.K.) software was used to process the images.

In order to visualise nuclei, DAPI staining was used. DAPI (4',6-diamidino-2-phenylindole), is a fluorescent stain which binds to A-T rich regions of DNA. A single drop of 1µg/ml DAPI was placed onto the sample and slides were mounted with a cover slip using DPX. Digital images of samples were captured using a Zeiss Axioimager Z2 microscope (Zeiss, Jena, Germany), using Zeiss ZEN 2010 software.

2.5.3 Iodine Staining of pollen

Mature pollen grains were stained using iodine to visualise the accumulation of starch within the mature pollen grain. The result is a darkened staining of pollen which has successfully accumulated starch and is fertile. A stain solution of 0.06M KI and 0.02M I_2 was applied to dissected anthers on a glass slide and the images were captured on a Zeiss Axiophot light microscope (Zeiss, Jena, Germany). Images were analysed on ImageJ where viable pollen was counted by eye and calculated as a percentage of total pollen.

2.5.4 Starch granule staining of root tip

Starch granule staining was completing using methods previously described(Y. Li *et al.*, 2011). In summary, root tips were fixed overnight at 4^{o}C with FAA (3.7% formaldehyde, 5% acetic acid, and 50% EtOH). Samples were then washed with 50% EtOH and stained with lugol solution (0.37% iodine, 0.71% potassium iodide) for 1 min and chloral hydrate solution (200% chloral hydrate in 1:1 glycerol and water) for 2 mins. Images were captured using the Zeiss Axio Imager 2 Light Microscope(Zeiss, Jena, Germany).

2.6 Flow Cytometer Measurements

An Ampha Z32 Impedance Flow Cytometer (Amphasys, Luzern, Switzerland) was used to determine the stage of the pollen, percentage viability and pollen number. Three anthers were collected in a 1.5ml Eppendorf and suspended in 0.75ml AF6 buffer and gently crushed with a micro pestle to release the pollen within, before

being passed through a 100µm filter to remove debris. 0.75ml of AF6 was then added to further dilute the sample.

Setup for hormone and RNAseq experiment:

The instrument was set up with the following settings specific for wheat pollen: triggering frequencies 2 MHz (percentage viability) and 12 MHz (pollen staging), modulation 5, amplification 5, demodulation 0, pump speed 60rpm and levels 0.15 viab. and 0.03 dev.

Setup for pollen counting and viability experiments:

An updated wheat pollen viability template was downloaded from the Amphasys website. The pollen viability template implemented the new autocalibration feature to ensure greater consistency between replicates. Pollen viability was measured at the beginning of tricellular stage of pollen development (18MHz frequency used to stage the pollen in this template) at a frequency of 2 MHz. The non-viable pollen was determined using a heat treatment to denature the pollen and determine the non-viable population.

An updated wheat pollen counting template was downloaded from the Amphasys website. For consistency of measuring pollen number, a 1ml aliquot of the homogenised anther and AF6 solution was taken.

2.7 Exploiting the TILLING population

A total of 2,735 TILLING lines have been produced using the EMS mutagen to create a reverse genetic resource to screen for mutations of interest(Krasileva *et al.*, 2017). TILLING mutants were found using the TILLING archive website http://www.wheat-tilling.com/. Annotations of mutants in each scaffold were analysed by converting the spreadsheets from the website into a gff file format (http://www.ensembl.org/info/website/upload/gff.html). This format was used to annotate the scaffold containing the gene of interest with the mutated SNPs in Geneious.

The M_4 TILLING lines were taken from the TILLING mutant archives of Dr Andrew Phillips, Rothamsted Research, Harpenden, U.K. The presence of the mutation was

confirmed by PCR sequencing (Section 2.2.3) using homoeologue specific primers (Section 2.2.9). The M_4 plants were germinated and backcrossed twice to WT Cadenza to remove 75% of other EMS induced mutations.

2.8 Optimised heat stress assay

Plants were initially grown in glasshouse conditions (Section 2.1). On reaching booting stage they were transferred into two conviron cabinets (Conviron Europe ltd, Cambridgeshire, UK): one for control and the other for heat stress (Section 2.1). Tillers were tagged at 9-13cm FLS extension, as this corresponds with the heat sensitive meiosis stage, and then exposed to 4 days of control (20/15°C day/night-65%/75% humidity) or heat treatment (33/26°C day/night - 80% humidity). Each plant was watered to saturation once a day during the heat treatment. This assay was optimised from findings in chapter 3. Once the heat treatment was completed the plants were transferred back to glasshouse conditions to allow the completion of pollen development and seed maturation. The grain set was then calculated. Seeds were only counted from the central 6 spikelets and only the outer florets (Section 3.3.4; Figure 3.7).

2.9 Exogenous application of NAA and heat stress tolerance

Spray treatments consisting of three different concentrations of NAA (0µM, 10µM and 100µM - 0.1% vol/vol Tween and 0.5% DMSO) were applied 1 day prior to meiosis and the subsequent first three days of the 4-day heat treatment (Section 2.8) starting at meiosis. 6ml was directly sprayed onto the elongating FLS and the flag leaf once a day. Upon finishing the heat treatment plants were moved back into standard GH conditions. Elongation rate of FLS from pre-meiosis to the end of the heat treatment (across a total of 5 days) was recorded. Time to reach meiosis of each selected tiller from the first spray treatment was also recorded and the subsequent grain set of the central 6 spikelets either side of the spike as described in chapter 3.

2.10 Root phenotyping

2.10.1 Quantification of lateral root number

Seeds were sterilised and imbibed for three days on damp filter paper at 4°C. They were then placed at room temperature in the light to allow elongation of the primary root to around 1cm. Seeds of equal rate of germination were then placed within a growth pouch system. Each pouch consisted of a sheet of germination paper (24x30cm; Anchor Paper Company, St Paul, MN, USA), covered with a black polythene film (75µm thick; Cransford Polythene Ltd, Suffolk, UK) to ensure the roots grow along the surface of the germination paper. The germination paper and film were grown vertically and were secured together using an acrylic rod (316x15x15mm; Acrylic Online, Hull, UK). A single seedling was placed in each pouch, 1cm from the top. The orientation was to point the roots downwards and the crease-side facing the germination paper. The germination paper was infiltrated used ¼ Hoagland's No.2 Basal Salt Mixture (Sigma-Aldrich, St.Louis, Missouri, U.S.A), adjusted to pH 6 using KOH. The plants were grown in controlled environment with a 16-hour photoperiod: 20°C/15°C day/night, with a light intensity of 400 µmole $m^{-2}s^{-1}$ PAR. After 10 days the polythene film was removed, and an image of the roots taken. Measurements of the length of the primary seminal roots were taken using ImageJ.

2.10.2 Impact of auxin on lateral root number

A 'cigar role' system was utilised with a protocol based on methods previously described(Zhu *et al.*, 2005; Bai *et al.*, 2013). Plants were initially germinated on filter paper as described before (Section 2.1), before 5 germinating seeds (one from each genotype) were placed randomly and uniformly 1cm from the top of 1 sheet of germination paper (25 x 38 cm Anchor paper company, St. Paul, MN, USA), before being carefully rolled together to secure it and placed vertically in a mesh of 2cmx2cm holes. The bases of rolls were placed in a tray of ¼ Hoagland's No.2 Basal Salt Mixture (Sigma-Aldrich, St.Louis, Missouri, U.S.A). The plants were grown in CE conditions at 21/16°C day/night and 16-hour photoperiod. Light was emitted from tungsten fluorescent lamps providing 500 µmol$m^{-2}s^{-1}$ PAR. After 7 days the nutrient solution was replaced with either fresh ¼ Hoagland's solution or ¼ Hoagland's

solution containing 5µM NAA. The plants were grown for additional 3 days before the paper rolls were opened and photos were taken by a Canon PowerShot G7 camera and the diameter, length and number of lateral roots were calculated using SmartRoot as a plugin of Image J.

2.10.3 Establishing auxin-insensitivity

Seeds were sterilised and imbibed for three days in darkness on damp filter paper at 4°C (Section 2.1). They were then placed at room temperature in the light for 1 day to initiate germination. The primary root was allowed to elongate to around 1cm in length before being placed 12.5 cm from the top of a 25x25cm square plate of 3% Phytagel (Sigma-Aldridge, St. Louis, Missouri, U.S.A.) medium and 4.6Mm $CaCl_2$. NAA (Sigma-Aldridge, St. Louis, Missouri, U.S.A.) was added at different concentrations: 0 µM, 10nM, 100nM and 1µM. To ensure roots grew in contact with the gel surface a layer of black plastic was placed across the lower half of the plate, covering the roots whilst allowing the shoot to grow normally. Plates were kept in darkness and placed vertically in controlled environment conditions of 21^{o}C/16^{o}C day/night. The seedlings were left to grow for 3 days before photographs were taken using a Canon PowerShot G7 camera. Measurements of the length of the primary seminal roots and shoots were taken using ImageJ and root hair images were taken using the Leica M205 FA Stereomicroscope. Measurements of only the primary seminal roots were taken due to *TaIaa18-Bb* often failing to produce more than 2 roots, compared to 5 roots being the standard for the other mutants and WT Cadenza.

2.10.4 Nodal root phenotyping

Seedlings were grown in cylindrical sand columns (Coelho Filho *et al.*, 2013). 6 sand and nutrient solution filled columns (45cm long and 15cm diameter) were placed in each tray containing nutrient solution. The nutrient solution consisted of 2.0 mM $Ca(NO_3)_2$, 1 mM KH_2PO_4, 4.0 mM KCl, 2.0 mM $MgSO_4$, 4.0 mM $CaCl_2.2H_2O$, with the following micronutrients: 60 µM Si, 50 µM B, 50 µM Fe, 15 µM Mn, 0.8 µM Zn, 0.3 µM Cu and 0.1 µM Mo. Seedlings were germinated on filter paper for 1 day before being transplanted into a 2cm deep hole and grown for 23 days. The plants were grown in controlled environment conditions of 22/18°C day/night, 14-hour

day, light level 450 µmole $m^{-2}s^{-1}$ PAR and 70/80% humidity day/night. The tillers for each plant were counted and dried at 80°C overnight and the dry weight determined. The complete root network was stored in 70% EtOH for further analysis. 5 of the longest nodal roots were taken from each plant and images were taken using WinRhizo (Regent Instruments, Quebec, Canada) and analysed using ImageJ, via the plugin SmartRoot.

2.10.5 Gravitropism measurements

Grains of Cadenza, *Talaa18-Bb, Talaa22-Bb, Talaa22-Bc* and *Talaa22-Db* were sterilised and imbibed for three days in darkness on damp filter paper at 4°C, before being played in the light and allowed to initiate germination for 1 day (Section 2.1). The seeds were then transferred to 3% Phytagel (Sigma-Aldridge, St. Louis, Missouri, U.S.A.) medium, prepared in the same way as previously described in section 2.10.2. Plates were kept in darkness and placed vertically in controlled environment conditions 21°C/16°C day/night for 1 day. Photographs were taken and the plates were then rotated 90° and roots were allowed to grow for 1 more day and further photographs were taken. The angle between the direction of gravity and the tip of the shoot and the primary seminal root was measured using ImageJ (Figure 2.1).

Figure 2.1: *Measurements of gravitropic response of primary seminal root and shoot.*

2-day old seedlings grown vertically for 1 day (left), prior to being rotated 90° and left for 1 more day (right). The angles of shoot and root (red) were taken against the direction of gravity (yellow arrow).

2.11 Ethylene response assays

30x15cm WYPALL L20 paper towel (Cromwell Ltd, UK) and black plastic were cut out soaked in 30ml of ddH_2O. Sterilised and imbibed seeds were placed 5cm from each other 1cm below the top of the role, leading to a total of 5 seeds per role. The roles were rolled up and placed in sterile glass tubes and a further 15ml of ddH_2O was added to ensure the roots never dried out. The plants were then placed in continuous light conditions at 21°C for two days. The roles were then re-opened and seeds which showed irregular germination were removed and subsequently re-rolled. The tubes were then placed in airtight 10L sized containers. One chamber was treated as the control and the other was injected with 300µl of ETOH (30µl L^{-1}). The plants were grown for a further 3 days in the same conditions before the length of the shoot and longest root were measured.

Chapter 3: The effect of heat stress on the reproductive development of Cadenza

3.1 Introduction

Wheat pollen development is sensitive to high temperatures(Saini *et al.*, 1984; Prasad and Djanaguiraman, 2014; Draeger and Moore, 2017) (Section 1.2). Multiple studies of different wheat varieties have described a range of different conditions that induce heat stress during reproductive development. Exposure to temperatures above 24˚C, for 5 days from the start of heading, led to a reduction in grain set in the Chinese wheat variety Chinese Spring. Floret fertility reduced from 84% at 24˚C to 0% at 35˚C. Grain set losses also increased with the duration of heat treatment(Prasad and Djanaguiraman, 2014).

Certain stages of pollen development are more sensitive to temperature extremes. Exposure to 36/26˚C day/night, 14-hour photoperiod and 85% humidity for 2/5 days showed a significant reduction in grain set and pollen viability especially when imposed during pollen development stages meiosis and tetrad(Prasad and Djanaguiraman, 2014). Similarly, another study on Chinese Spring found that temperatures of 30 and 35˚C for just 20 hours lead to an 18% and 100% reduction in grain number respectively(Draeger and Moore, 2017), indicating that short periods of heat stress at critical stages of pollen development are enough to trigger a loss of grain yield. In the Australian wheat var. Gabo, it was found that 3 days constantly at 30˚C from the onset of meiosis was enough to lead to a 68% reduction in grain set(Saini *et al.*, 1984).

As well as meiosis being a sensitive stage in heat stress tolerance, just a few days prior to anthesis also appears to be susceptible to heat. Studies found that 35˚C for one day before anthesis was enough to cause a 33% reduction in the grain set of the heat sensitive Australian wheat var. Janz(Talukder *et al.*, 2014). Although heat stressing a plant just prior to anthesis leads to a reduction in grain number, it was not found to result in a loss of pollen viability(Prasad and Djanaguiraman, 2014). This could be due to poor pollen germination rates and/or decreased rate of pollen tube growth. It is hypothesised that at these temperatures there is desiccation of

the style, causing it to fail to provide the directional stimuli required for successful pollen tube growth; therefore the ovules are not fertilised by the pollen(Prasad and Djanaguiraman, 2014).

The heat tolerance of wheat var. Cadenza has yet to be investigated. Cadenza is currently the chosen model hexaploid wheat variety because it was used in the development of an EMS induced TILLING population(Krasileva *et al.*, 2017). This population has provided a valuable genetic resource which can be applied to a reverse genetics' platform. Therefore, optimising a heat stress assay specific for this variety will allow the use of genetic approaches to understand heat stress response pathways and develop mitigating strategies to improve tolerance.

In developing a stage specific heat stress assay, it is necessary to determine both the most sensitive stage of pollen development to heat stress and the critical temperatures required to induce a reduction in grain yield. The majority of anther and pollen development in Cadenza occurs when the spike is concealed within the flag leaf sheath (FLS). Therefore, the only way to access the pollen and determine the stage is to destructively peel back the sheath to reveal the spike within. In order to see which stages of pollen development are most sensitive to heat stress a method of non-destructive staging of the anthers of Cadenza was developed. This was combined with the use of impedance flow cytometry as two methods to determine pollen stage(Heidmann *et al.*, 2016).

The non-destructive staging method looks in more detail at the so called Booting stage of the Zadoks scale of cereal development (Figure 3.1A)(Zadoks *et al.*, 1974). Booting begins at growth stage 41 (GS41), where the FLS begins to extend away from the node below. Within the FLS the spike develops and moves upward causing the FLS to swell with the growing reproductive tissue inside (GS45). Eventually the FLS begins to open (GS47), spelling the end of the booting stage and the beginning of Ear Emergence. The peduncle of the developing spike continues to elongate causing the spike to emerge beyond the FLS (GS55/61) (Figure 3.1B). The majority of the anther developmental stages occur during the booting period.

A

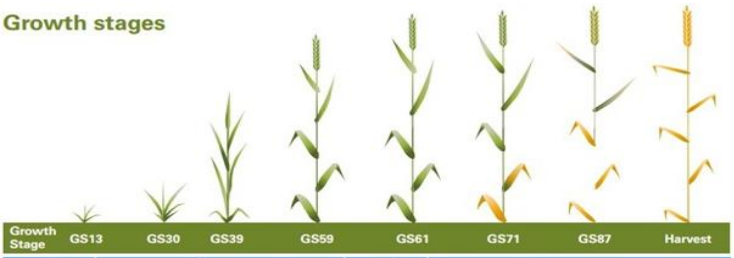

Growth Stage	Description of stage	Growth Stage	Description of stage
GS10-19	**Seedling Growth**		**Ear Emergence**
GS20-29	**Tillering**	GS51	First spikelet just visible above flag leaf ligule
GS30-	**Stem Elongation**	GS55	Half of ear emerged above flag leaf ligule
GS37	Flag leaf just visible	GS59	Ear completely emerged above flag leaf ligule
GS39	Flag leaf fully visible		**Flowering**
	Booting	GS61	Start of flowering
GS41	Flag leaf sheath extending	GS65	Flowering half way
GS42	Flag leaf sheath just visibly swollen	GS69	Flowering complete
GS45	Flag leaf sheath swollen	GS71-93	**Grain development**
GS47	Flag leaf sheath opening		

B

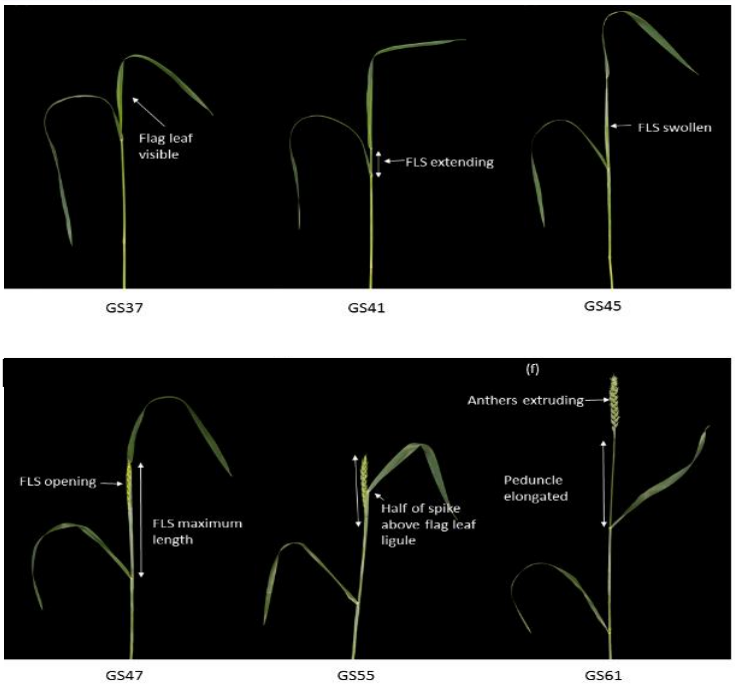

Figure 3.1: *The Zadoks scale of cereal development.*

A*: The Zadoks scale was developed as a method of dividing the phenological development of cereals into easily recognisable external morphological features*(Zadoks *et al.*, 1974). *Growth stages where male reproductive development is occurring are described in more detail. Adapted from ADHB (2015).* **B***: A detailed representation of GS37 -GS61. At GS37 the tip of the flag leaf begins to extend out of the stem. At GS41 the flag leaf sheath (FLS) begins to extend. At GS45 the FLS is swollen with the developing spike within. At GS47 the spike begins to extend out of the FLS, by the elongating peduncle. GS55 sees half the spike emerged from the FLS. GS61 corresponds to anthesis, by which the entire spike has emerged, and the peduncle has continued to extend beyond the FLS. Photographs taken of Cadenza tillers.* (Audley, 2016).

The length of the FLS and other parts of the developing wheat plant, have been shown to correlate with anther developmental stage in barley, wheat and rice(Satake and Harase, 1974; Oliver *et al.*, 2005; Ji *et al.*, 2010; Gomez and Wilson, 2012; Audley, 2016; Browne *et al.*, 2018; Fernández-Gómez *et al.*, 2020). There was found to be a positive correlation between spike length and anther stage of barley(Gomez and Wilson, 2012). Studies of 4 different varieties of wheat showed that all have positive correlations of auricle distance, anther length, anther width, spike length and spikelet length with anther developmental stage(Browne *et al.*, 2018).The elongation of the FLS has previously been used to infer the developmental stage of the anther in Cadenza(Audley, 2016; Fernández-Gómez *et al.*, 2020). It was necessary to confirm this staging method using the growth conditions under which the heat stress experiments will be performed.

Impedance flow cytometry is another rapid method of determining pollen stage and viability using fresh anther material. This provides a more rapid alternative to microscopy techniques of DAPI staining to determine pollen stage and iodine staging to determine viability. The Ampha Z32 Pollen Analyzer is a flow cytometer which can be used for pollen analysis. The Ampha Z32 Pollen Analyzer utilises a microfluidic chip which has an AC current passing through it. The pollen is suspended in a solution and passed through the chip. The chip measures change in the electrical resistance of the fluid when pollen passes through the electric field. The output is a phase amplitude dot-plot whereby the recorded phase can be used to determine viable vs non-viable pollen and the shift in amplitude can be used to determine the cell volume(Gawad *et al.*, 2001; Heidmann *et al.*, 2016). The resultant dot-plot shows patterns which are indicative of pollen viability and stage (Heidmann *et al.*, 2016). This study applied this new technology to staging the pollen once the spike was clear of the FLS and the FLS ceased to elongate. It was also used to determine pollen number and viability.

Using the described staging methods, a heat stress assay specific to Cadenza, based on pollen developmental stage was developed. The impact of heat stress on anther development was confirmed by microscopy and analysis of pollen viability and number using the Ampha Z32 Pollen Analyzer. This study provides a protocol which

can be applied to investigating the heat stress tolerance of different Cadenza genotypes and/or investigating the impact of exogenous application of chemicals which could either mitigate or reduce heat stress tolerance. Therefore, providing a vital resource for improving heat stress tolerance of wheat.

3.2 Materials and Methods

All growth conditions, sectioning techniques and pollen analysis are described in section 2.

3.3 Results

3.3.1 Anther development in Cadenza

An initial investigation into the anther development of hexaploid wheat var. Cadenza was necessary to confirm that Cadenza follows the classic stages of anther and pollen development as has previously been characterised in other plant species. Sectioning of developing anthers revealed that anther development in Cadenza follows the same developmental processes which are found in other monocots and dicots (Figure 3.2).

Anther development begins with the division of archesporial cells, which form primary parietal cells and centralised cells which form sporogenous cells(Kelliher and Walbot, 2011; Gomez and Wilson, 2012) (Figure 3.2A). The sporogenous cells divide further to form meiocytes and the primary parietal cells, which further divide to form the endothecium and secondary parietal cells (Figure 3.2B), the secondary parietal cells subsequently divide again to form the middle layer and tapetum (Gomez *et al.*, 2015) (Figure 3.2C). The meiocyte PMCs subsequently undergo meiosis to form a tetrad, this consists of 4 haploid microspores encapsulated in a callose wall, at this stage the tapetum is at its most prominent(Chaudhury, 1993) (Figure 3.2D). Following this the callose wall breaks down and the young microspores (unicellular pollen) are released into the lumen of the anther. The middle layer undergoes crushing and eventually degrades. The tapetum layer also starts to degenerate (Figure 3.2E). The microspores align themselves along the edge of the degrading tapetum, becoming vacuolated and polarised (Figure 3.2F). The commencement of the bicellular stages corresponds with polarised microspores undergoing the first round of mitosis (Figure 3.2G). The tricellular stage corresponds

with mitosis II and the accumulation of starch in the pollen. (Figure 3.2H and I). It must be noted that tapetum degradation occurs later in wheat, with tapetum degradation first starting to occur in the vacuolated microspore stage, whereas in rice and *Brachypodium* it begins to occur in the tetrad stage(Zhang *et al.*, 2011).

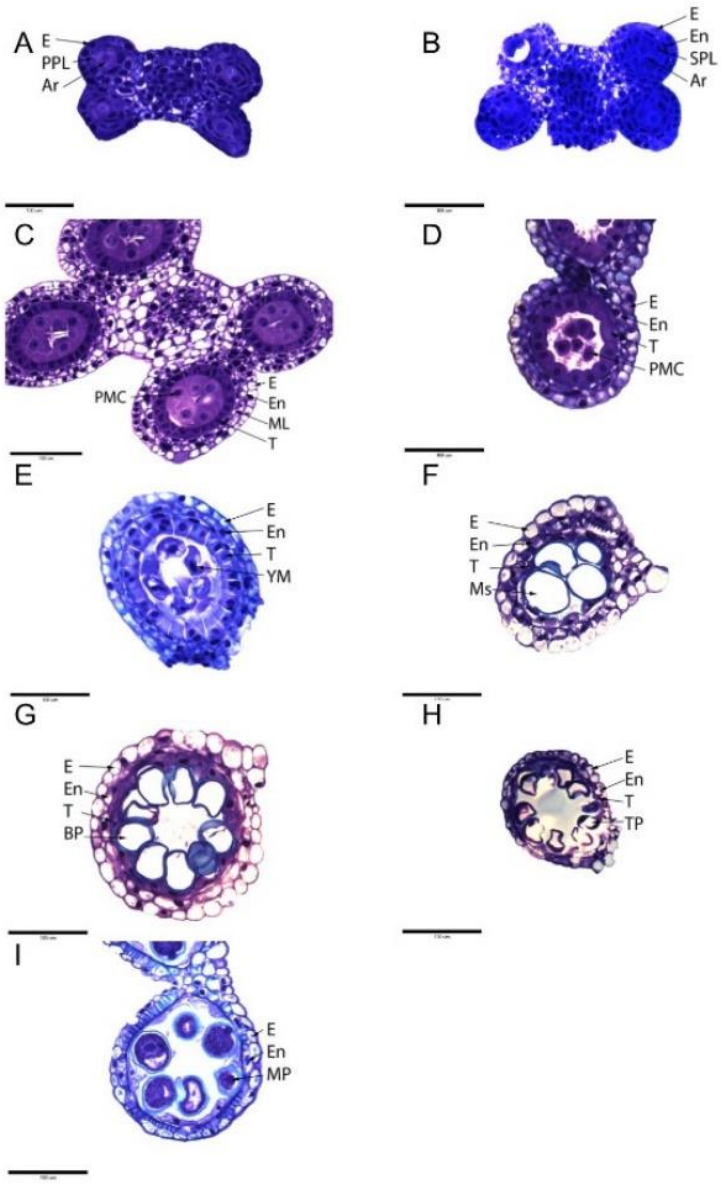

Figure 3.2: *Sections of anthers at different developmental stages stained with Toluidine blue.*

(A) Stage 1 archesporial (Ar) and primary parietal cells (PPL) are distinguishable and are surrounded by the epidermis (E). (B) At stage 2 archesporial cells are surrounded by three cell layers, consisting of secondary parietal cells (SPL), the endothecium and the epidermis. (C) At stage 3 PMCs are recognisable and the parietal cells differentiate into a tapetum (T) and middle layer (ML). (D) At stage 4 the PMCs undergo meiosis and the tapetum was very prominent. (E) At stage 5 the callose envelope of the tetrad releases young microspores (YM). Stage 6 is characterised by the alignment of the microspores to the degrading tapetum but is not shown in the figure. (F) At stage 7 the microspores (Ms) polarised and vacuolated. (G) At stage 8 the polarised microspores underwent the first round of mitosis, creating bicellular pollen (BP), which begins to develop a coat layer. (H) At stage 9 pollen mitosis II led to tricellular pollen (TP). Starch started to accumulate. (I) At stage 10 starch accumulation in mature pollen (MP) was complete. Scale bar = 100 µm.

3.3.2 A non-destructive method of staging pollen

The length of the FLS has been shown to correlate with anther development stage in wheat(Audley, 2016; Browne *et al.*, 2018; Fernández-Gómez *et al.*, 2020). We sought to investigate whether similar measurements in wheat var. Cadenza could be used to establish the stage of anther development.

Twenty-five Cadenza plants were grown from seed in Conviron Adaptis cabinets (Conviron Europe ltd, Cambridgeshire, UK) in normal conditions (Section 2.1). Tillers at GS37-47 were randomly selected and carefully dissected to reveal the developing spike within. Anther/spikelet/spike samples were taken, from the middle of the spike and from either of the outer two florets of each spikelet for consistency. Measurements of spike, peduncle and FLS length were taken (Figure 3.3). The samples were sectioned to determine the exact development stage of the anther following methods detailed in section 2.5.1/2.5.2(Gomez and Wilson, 2012). Statistical analysis and graphs were produced in RStudio software.

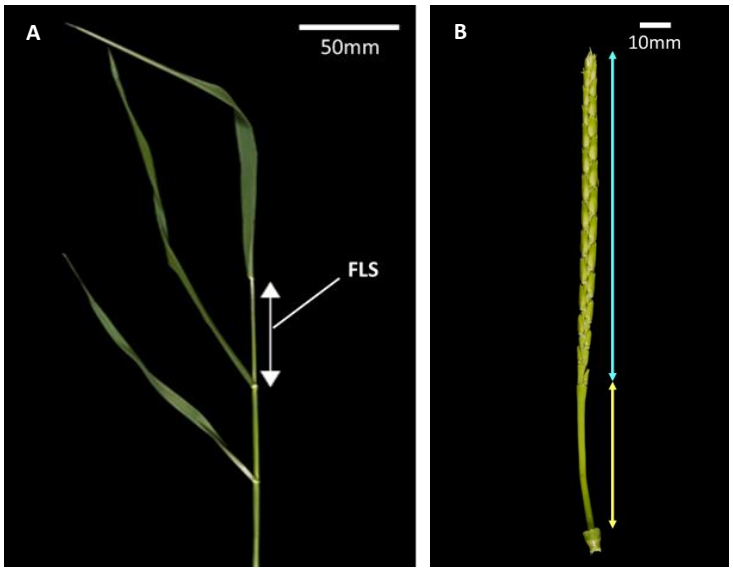

Figure 3.3: *Example measurements of flag leaf sheath (FLS), spike and peduncle.*

A: *The position of the flag leaf sheath (FLS) in wheat (white arrow). The FLS is the distance between the flag leaf (FL) and the next leaf below.* **B**: *Spike length (blue arrow) from the tip of the spike to the lowest spikelet and the peduncle length (yellow arrow) from the lowest spikelet to the first node.*

Elongation of the FLS was shown to positively correlate with anther stage (R^2= 0.8041, p<0.001, Figure 3.4A). Therefore, FLS length can be used as an effective form of non-destructive staging in Cadenza, as it already has in other cultivars of wheat and rice(Satake and Harase, 1974; Oliver *et al.*, 2005; Ji *et al.*, 2010; Browne *et al.*, 2018; Fernández-Gómez *et al.*, 2020). Browne *et al*., 2018 highlighted the importance of effective staging to be variety specific, as all 4 wheat varieties showed the same positive linear relationship as was found in this study, but the length of the FLS was different according to the variety. Cadenza has shown a longer FLS length compared to all 4 of the varieties, with meiosis corresponding to 9-13cm in Cadenza, but around 5cm in Halberd and around 0-2cm in Cranbrook, Young and Wyalkatchem(Browne *et al.*, 2018).

The elongation of the spike also corresponded to the anther/pollen developmental stage, following a positive linear correlation (R^2= 0.833; p<0.001, Figure 3.4B). Spike length has been shown to positively correlate with anther developmental stage in barley and other wheat cultivars: Halberd, Cranbrook, Young, and Wyalkatchem(Gomez and Wilson, 2012; Browne *et al.*, 2018). Once again studies highlight the difference in development between different varieties, showing that Cadenza spikes on average are longer than the other varieties, with 8cm corresponding to meiosis, whereas it was found that it varied between 2-4cm depending on the variety(Browne *et al.*, 2018). This highlights the importance of developing a variety specific pollen staging method. Gomez *et al*., 2020 used a combined approach of spike length and position within the pseudostem to accurately predict the stage of anther development of Cadenza. Spike length was found to show continuous growth from the beginning of anther development to the release of microspores, where the spike then ceased to grow(Fernández-Gómez *et al.*, 2020). Once the spike size stopped growing, the later stages of anther development were then determined based on spike position(Fernández-Gómez *et al.*, 2020). This study found different spike lengths correspond to different stages; for example we found around 8cm corresponds to meiosis, whereas they found that around 4.7-7.3cm corresponded to meiosis. This different result could be due to

different growing conditions. In this study they grew their plants in slightly lower temperatures 18/14°C (as opposed to 20/15°C), as well as using different pot sizes, compost and lamps(Fernández-Gómez *et al.*, 2020). This therefore highlights the importance of optimising staging for both the variety and the growth conditions. microspores/unicellular pollen.

Peduncle elongation and anther stage follow a non-linear relationship. Consequently, a Generalised Additive Model (GAM) was applied: R^2=0.586, p<0.001, Figure 3.4C. Little peduncle elongation occurs until around stage 5 of anther development, when it begins to elongate to a various amount dependent on the tiller (Figure 3.4C). There was, however, a high level of variability in the results and therefore it would not be recommended to use peduncle length as an estimate for anther stage in Cadenza.

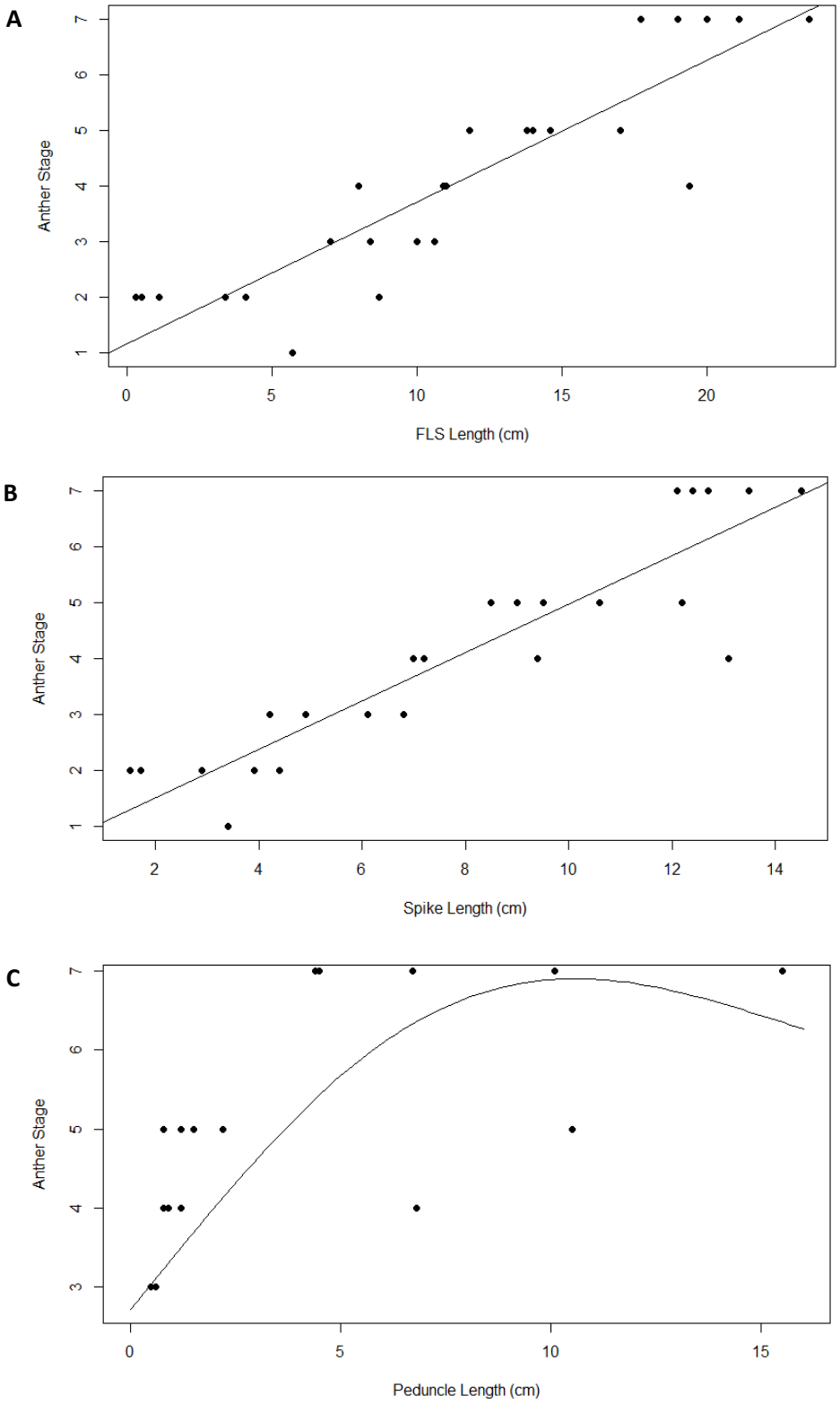

Figure 3.4: *The correlation between external physiology and anther development stage.*

A. *The FLS* ***B.*** *Spike and* ***C.*** *Peduncle length (cm) of 25 Cadenza tillers and the corresponding measured anther developmental stage and pollen developmental stage. Linear regression lines are shown for FLS length (R^2=0.8041) and spike length (R^2=0.833) and a GAM line was plotted for peduncle stage(R^2=0.586). p<0.001.*

3.3.3 Pollen development across the spike

In order to develop an effective stage specific heat stress assay, establishing the differences in pollen development stage across the length of the spike is essential to determining which stages are more sensitive to heat stress. Only florets which contain anthers that are known to be around the same stage of development should be included when establishing effects on fertility. In Cadenza different parts of the spike mature at different rates. It is important to investigate what position on the spike the florets will be at the same developmental stage and therefore can be reliably staged and analysed in a heat stress assay.

Three tillers were selected from glasshouse grown Cadenza at 5 different stages of spike emergence: spike still within the FLS, early spike emergence from FLS, late spike emergence from FLS, fully emerged spike and extending spike beyond the FLS. Three anthers from the same floret were taken from three florets at three different positions on the spike: top, middle and bottom, corresponding to spikelet positions 16-21, 6-15 and 1-5 respectively (Figure 3.5). The pollen developmental stage of the anthers was determined using the Ampha Z32 Pollen Analyzer (Amphasys, Luzern, Switzerland) (Section 2.6). The protocol for stage and viability determination of wheat pollen has already been optimised and is detailed on the Amphasys website. https://amphasys.com/wp-content/uploads/2019/02/Amphasys_Wheat_Pollen_Viability_Application_Note.pdf.

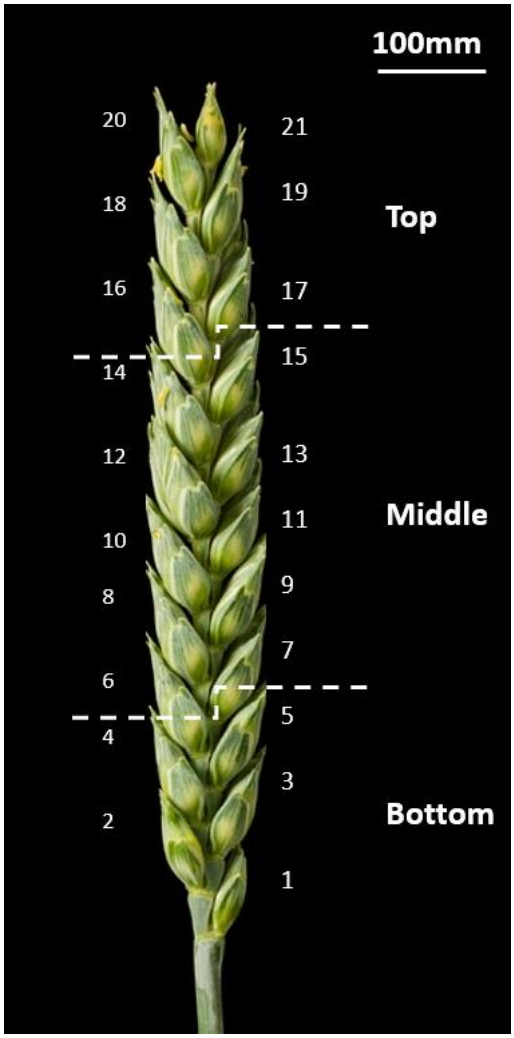

Figure 3.5: *Cadenza spike showing numbered spikelets.*

Spikelets were numbered from the lowest spikelet upward. Anthers were taken from the indicated positions: 16-21 (top), 6-15(middle) and 1-5(Bottom).

Table 3.1 indicates that often the middle and the top of the spike appears to be at the same pollen stage, whereas the bottom of the spike is sometimes at an earlier stage (Supplementary Figure 1 for flow cytometer measurements and spike photographs). This pattern of development is consistent throughout spike development. For staging consistently grain count measurements and pollen viability/number was taken from spikelets 6-17 in future heat stress assays.

Table 3.1: *Emergence of spike and corresponding developmental stage across different positions of the spike.*

15 tillers at different stages of development were investigated for their pollen development stage using Ampha Z32 Pollen Analyzer. Anthers were taken from florets 16-21 (Top), 6-15 (Middle) and 1-5 (Bottom) (Figure 3.5) of the spike. The stage of the majority of the pollen was recorded (Supplementary Figure 1).

Tiller	Tiller stage	Position on spike		
		Bottom	**Middle**	**Top**
1	Unmerged spike (12cm FLS)	Pre-microspore	Pre-microspore	Pre-microspore
2	Unmerged spike (14.8cm FLS)	Pre-microspore	Unicellular	Unicellular
3	Unmerged spike (17.8cm FLS)	Unicellular	Unicellular	Unicellular
4	About to emerge	Unicellular	Uni-Bicellular	Un-Bicellular
5	About to emerge	Unicellular	Unicellular	Uni-bicellular
6	About to emerge	Unicellular	Unicellular	Unicellular
7	Half emerged	Bicellular	Bicellular	Bicellular
8	Half emerged	Bicellular	Bicellular	Bicellular
9	Quarter emerged	Unicellular	Uni-Bicellular	Uni-Bicellular
10	Emerged	Bicellular	Tricellular	Tricellular
11	Emerged	Bicellular	Bi-Tricellular	Bi-Tricellular
12	Emerged	Bicellular	Bi-Tricellular	Bi-Tricellular
13	Extended 4.7cm	Bi-Tricellular	Tricellular	Tricellular
14	Extended 7.4 cm	Tricellular	Tricellular	Tricellular
15	Extended 6cm	Bi-Tricellular	Tricellular	Tricellular

3.3.4 Optimisation of heat stress assay

The tillers were selected prior to heat treatment and their pollen developmental stage was determined based on the length of the FLS and the degree of spike

emergence from the FLS. Based on this external morphology the tillers were assigned a pollen development stage: pre-meiosis, meiosis, unicellular, bicellular and tricellular stages (Figure 3.6). Pre-meiosis was assigned as 0-9cm FLS extension, 9-13cm corresponds with meiosis and 13cm-emergence corresponded with microspore (unicellular) stage. Mitosis I starts to occur as the spike emerges from the FLS, forming bicellular pollen, and mitosis II occurs just as the spike starts to completely emerge from the FLS, forming tricellular pollen. These observations closely follow that found in Cadenza from an earlier study(Fernández-Gómez *et al.*, 2020). The pollen remains tricellular until its release during dehiscence. The most vulnerable stages to heat stress were determined as those stages which showed the greatest reduction in grain set.

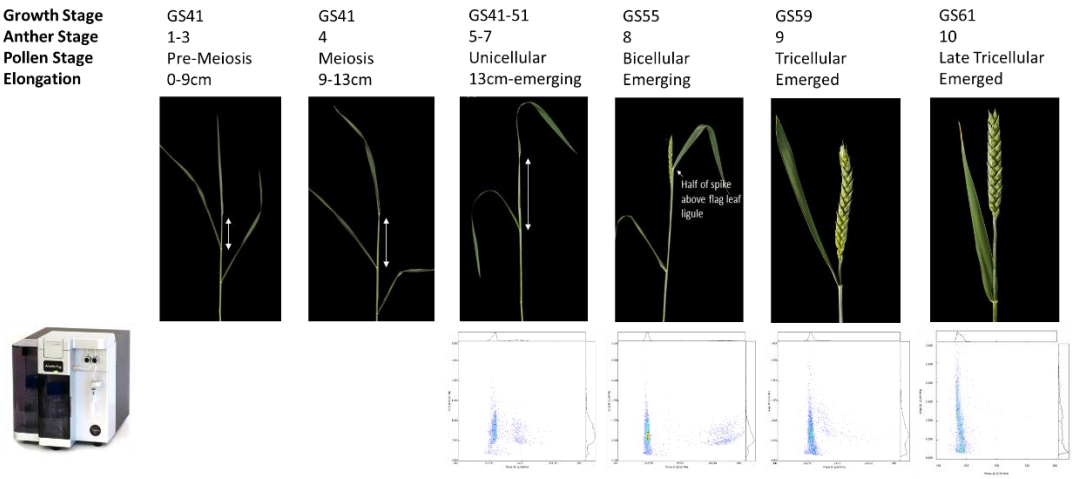

Figure 3.6: S*taging pollen in Cadenza.*

Anther stages 1-7 can be scored accurately using FLS length elongation. To broadly cover pollen development, pre-meiosis was assigned as 0-9cm FLS extension, 9-13cm corresponds with meiosis and 13cm-emergence corresponds with microspore (unicellular) stage. Bicellular stage corresponds with spike emergence from the FLS and tricellular stage occurs when the spike is completely emerged and extends beyond the FLS. Once the spike begins to emerge from the FLS the florets can be accessed and staged precisely using the Ampha Z32 Pollen Analyzer.

As wheat is a predominantly self-pollinating species any reduction in male fertility will have a direct impact on grain set, therefore grain counts can be a way to infer pollen viability. For consistency the top four spikelets were omitted and the grains were counted 6 spikelets down from either side of the spike from these top two (Figure 3.7A). The number of grains was then calculated as a percentage from a total of 24 florets.

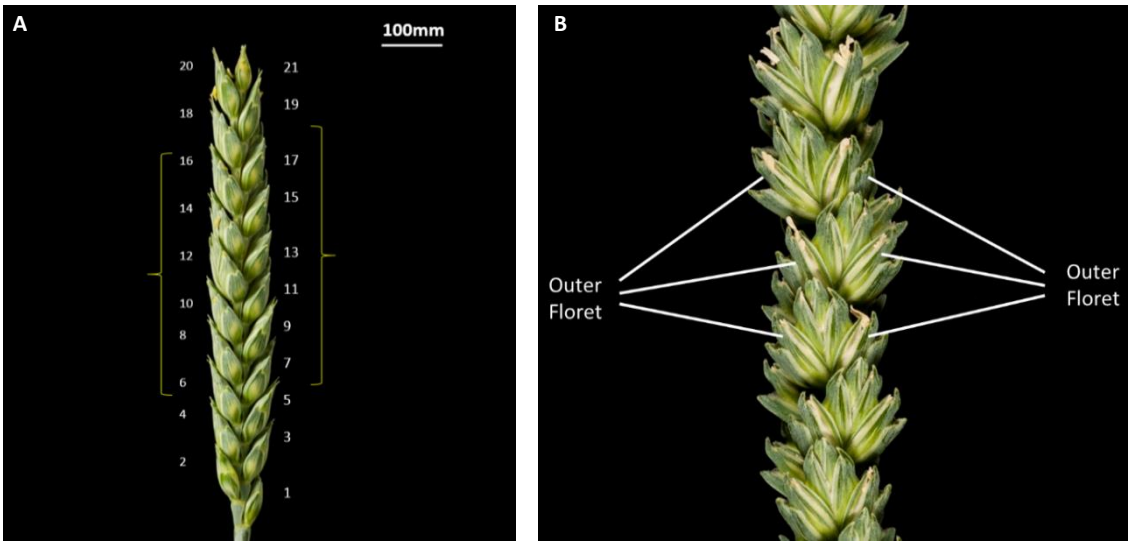

Figure 3.7: *Grain positions counted for quantification of the effect of heat stress.*

A: *Cadenza spike showing the positions of spikelets where grain numbers were counted. The top two rows of spikelets were omitted due to commonly lacking grain and the 6 spikelets were below this were included as they are at a similar stage of anther development. Positions 16/17, 12/13 and 6/7 indicate the top, middle and bottom where pollen viability and number were determined.* **B**: *The two outer florets of a wheat spikelet.*

Four different heat stress conditions were investigated: 1. 32/20˚C day/night 65-75% humidity (VPD = 1.67/ 0.59 kPa), 2. 32/26˚C d/n 80% (VPD = 0.95/ 0.67 kPa), 3. 33/26˚C d/n 80% (VPD = 1.00/ 0.67 kPa) and 4. 35/26˚C d/n 80% (VPD = 1.13/ 0.67 kPa) (Figure 3.8). Alterations in temperature day/night and humidity were used to develop a heat stress assay which specifically negatively impacts reproductive development and does not have any non-pollen specific affects.

For heat treatments 1 and 2, 60 plants were grown in glasshouse conditions until they entered the booting stage of development. On entering the booting stage 50 plants were randomly selected and placed across two Fitotron growth chambers.

For treatments 3 and 4, 30 plants were also grown in glasshouse conditions (Section 2.1) and 24 were selected and placed across two Conviron growth chambers. The plants were acclimated for around two weeks in the cabinets before inducing heat stress. During heat treatment the plants were exposed to 4 days at different temperatures depending on the treatment. The control plants were always kept at 20/15°C d/n 65/75% humidity (VPD 0.82 and 0.43 kPa respectively) during these 4 days. During heat treatment the plants were watered once a day until the soil was completely saturated. This ensured the plants were not droughted during the heat treatment, due to rapid evaporation and transpiration meaning the heat-treated plants required more replenishment of water to reach soil saturation. Soil saturation also ensured a similar level of soil moisture content between pots and treatments at the beginning of each day. After the heat treatment, the plants were transferred to glasshouse conditions of 18-20 °C/14-15°C day/night (Section 2.1) and allowed to set seed. For all light conditions see section 2.1. Once the tillers had set seed the presence or absence of grains in the outer two florets of each spikelet was noted and the position on the spike. For the analysis of the grain set from different heat treatments REML analysis was performed on the logit+1 transformed values in statistical handling software Genstat (v20, VSNI, Hemel Hempstead, U.K.).

There was found to be a highly significant interaction between temperature of treatment and pollen stage when heat stress was applied ($P<0.001$). 32/20˚C day/night for 4 days was not found to significantly induce a reduction in grain set across all stages of pollen development in Cadenza (Figure 3.8; Supplementary data Table 1). LSDs for comparing control and heat for pre-meiosis, meiosis, unicellular, bicellular and tricellular stages were 0.99, 1.01, 1, 0.991 and 0.999 respectively. In response to this, the night temperature was raised to 26**°**C and the humidity raised to 80% to counteract the cooling effects of transpiration(Chaves *et al.*, 2016). For this reason most studies have attempted to control and maintain their humidity to either 70%(Saini and Aspinall, 1982; Saini *et al.*, 1984), 75%(Draeger and Moore, 2017), or even 85%(Prasad and Djanaguiraman, 2014). However, this was once again not enough to induce a significant reduction in grain set at any of the stages of pollen development (Figure 3.8; Supplementary Table 1). LSDs for comparing

control and heat for pre-meiosis, meiosis, unicellular, bicellular and tricellular stages were 1.011, 1.027, 0.994, 0.99 and 0.993 respectively.

When daytime temperatures were increased to 35°C (35°C/26°C – 80% humidity) there was a significant reduction in grain set across all stages of pollen development (Figure 3.8; Supplementary Table 1). LSDs for comparing control and heat for pre-meiosis, meiosis, unicellular, bicellular and tricellular stages were 1.060, 1.063, 1.023, 1.023, 1.018 respectively. With reductions of grain set by 38% at pre-meiosis, 59% at meiosis, 84% at unicellular, 62% at bicellular and 65% at tricellular stage. Although this shows the limitations of Cadenza's heat stress tolerance, it does not show the subtleties in sensitivity of pollen development at different development stages. It is also possible that non pollen specific effects of heat stress are happening at these temperatures, possibly the heat is damaging the stigma so that successful fertilisation of the ovule cannot occur(Prasad and Djanaguiraman, 2014).

The daytime temperature was lowered to 33°C for the final treatment (33/26°C d/n-80% humidity). There was found to be a significant decrease in grain set when heat treatment began at meiosis and unicellular stages, whereas the stages of pre-meiosis, bicellular and tricellular stages were not significantly impacted by the heat treatment (Figure 3.8; Supplementary Table 1). There was found to be a reduction of grain set by 39% at meiosis and 80% at unicellular stages (LSD= 1.149 and 1.043 respectively). With a non-significant mean reduction of 22% grain set at pre-meiosis, 0.006% at bicellular and 0.04% at tricellular stages (LSD= 1.04, 1.04 and 1.008 respectively) (Figure 3.8; Supplementary Table 1). Many studies have linked the meiosis and early microspore stage as being the most sensitive stage to heat stress in plants. In this study meiosis and unicellular stage were seen to be the most sensitive to heat treatment, with the largest reduction in grain count. This has also been found in Arabidopsis, rice, cowpea and tomato, where late meiosis progressing onto early microspore stage was the most heat stress sensitive(Ahmed *et al.*, 1992; Kim *et al.*, 2001; Sato *et al.*, 2002; Endo *et al.*, 2009). Previous studies in hexaploid wheat also found that the transition from meiosis to early microspore stage is the most sensitive stage to heat stress(Saini *et al.*, 1984; Draeger and Moore, 2017).

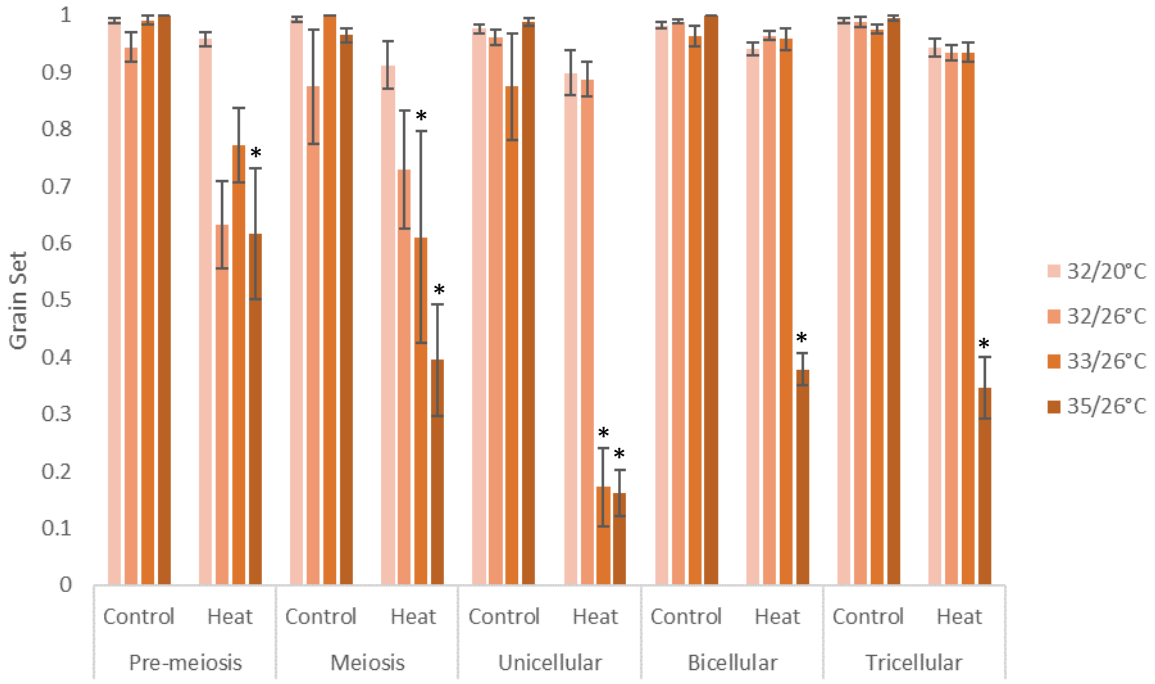

Figure 3.8: *The impact of different heat stress treatments at different pollen development stages on the grain set of Cadenza.*

*Grain set of the middle 6 spikelets of an ear when exposed to different heat treatments at different stages. +/- SE. Logit transformed values were used for statistical analysis (see Supplementary table 1). * indicates significantly different from control of same treatment (P<0.001). d.f = 396*

3.3.5 Effect of heat stress on pollen number and viability

The results of section 3.3.4 suggest that conditions of 33/26°C day/night and 35/26°C day/night (both for 4 days and at 80% humidity) were enough to induce a reduction in grain set (Figure 3.8). We decided to choose 33/26°C day/night as our heat treatment as it demonstrated pollen stage specific impacts on fertility.

Heat stress has been found to induce reductions in pollen viability in rice and barley(Sakata *et al.*, 2010; Feng *et al.*, 2018). To test the impact on male fertility in Cadenza wheat, tillers were selected which showed FLS lengths of 9-13cm (corresponding to pollen mother cell meiosis stage) and were subsequently either exposed to control conditions of 20/15°C day/night or heat stressed at 33/26°C

day/night at 80% humidity for 4 days (Section 2.8). Anther samples were then taken when the pollen had reached tricellular stage in order to ensure consistency. Analysis of pollen number and viability was conducted using the Ampha Z32 Pollen Analyzer (Section 2.6). Three anthers were taken from a single floret. Samples were taken from spikelet positions 16/17, 12/13 and 6/7, indicating the top, middle and bottom respectively, where pollen viability and number were determined (Figure 3.7A). This investigated the spatial effect of heat stress. Anther samples were only taken from either of the two outer florets of each spikelet. ANOVA analysis was performed on untransformed data, except for bottom pollen viability where a log e transformation was applied.

Analysis of pollen number and viability appears to show that the heat treatment has no significant impact on pollen number; P=0.431, 0.558 and 0.698 for top, middle and lower parts of the spike respectively (Table 3.2). However, heat stressed plants showed a significant reduction in pollen viability in the lower part of the middle 6 spikelets (P<0.001) with a 12.5% reduction in pollen viability. In contrast, anthers collected from the top and middle parts of the spike did not show a significant reduction in pollen viability (P=0.287 and 0.152 respectively), despite showing on average reductions of 7.1% and 9.7% respectively. However, when averaged across the spike there was found to be a significant reduction in pollen viability in the heat stressed plants (P=0.025). Control plants had on average 31.5% pollen viability, whereas heat stressed plants had 21.7% viability, 5% LSD is 8.38 at 14 d.f. Therefore, there was a significant reduction in pollen viability in response to heat stress across the length of the spike.

Table 3.2: *Effect of heat stress on pollen number and viability of Cadenza.*

*Tillers were selected at meiosis (FLS =9-13cm) and treated for 4 days in either control conditions of 20/15°C day/night or heat conditions of 33/26°C day/night. ANOVA output of anthers taken from the top, middle and lower parts of the spike, just after the completion of mitosis II. Pairwise comparisons were made between each genotype and treatment using 5% LSDs to determine the significance. Pollen viability of lower part of spike was Log e transformed to ensure normal distribution of data. Statistical analysis was performed on the transformed data of lower pollen viability, shown in brackets. * indicates significantly different from control treatment.*

Treatment	**Pollen viability (%)**			**Pollen number/ml**		
	Top	**Middle**	**Lower**	**Top**	**Middle**	**Lower**
Control 20/15°C	22.4	36.1	35.91(1.273)	4341	4248	4302
Heat 33/26°C	15.3	26.4	23.37(1.121)*	4067	4458	4439
P-value	0.287	0.152	<0.001	0.431	0.558	0.698
SED	6.39	6.41	0.0279	337.1	349.2	344.2
LSD (5%) (14 d.f)	13.72	13.74	0.0599	723.1	749.0	738.2

Figure 3.9 is a cross sectional image of anthers which have either been exposed to either control or heat stress conditions. The anthers were staged at late unicellular stage using the Ampha Z32 Pollen Analyzer. Anthers were then fixed and embedded, following methods detailed in section 2.5.1, and then sectioned longitudinally and stained with 0.05% Toluidine blue and 1µg/ml DAPI following methods detailed in section 2.5.2. Sections revealed that the tapetum is still present after both control and heat stress conditions. This indicates that at unicellular stage the heat stress assay does not result in a complete loss of the tapetum. Future experiments could take sections at bicellular stage, to investigate the state of the tapetum at this later stage of development after control or the heat treatment.

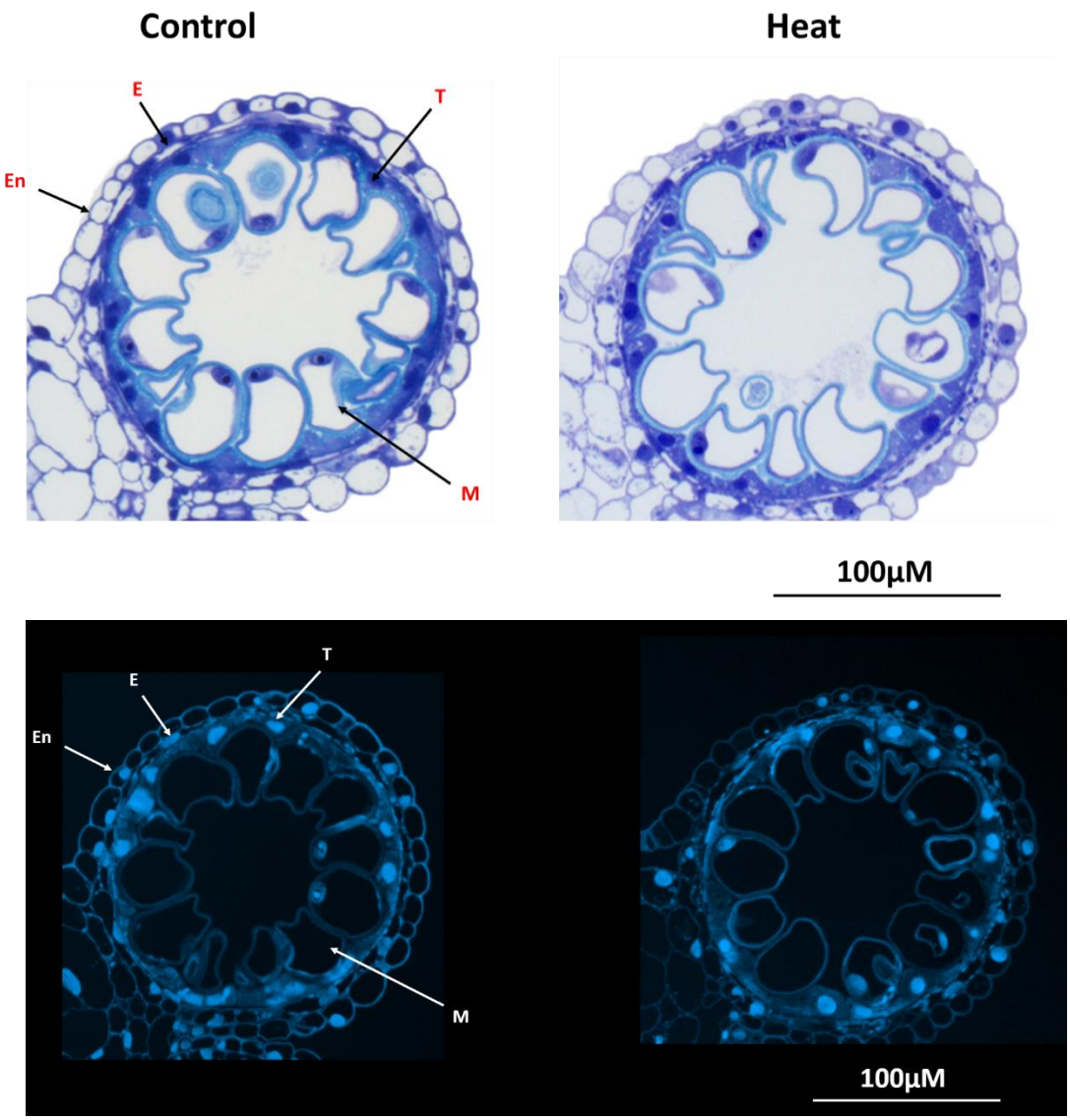

Figure 3.9: *Anther locules at late unicellular stage, taken after control conditions (left) or heat stress (right) conditions.*

Longitudinal cross sections were stained with toluidine blue (top) and DAPI (bottom). E=epidermis, En=endodermis, T=tapetum, M=microspores. Scale bar = 100µM.

3.4 Discussion

A large proportion of anther development occurs before the spike has emerged. From the initial stages of spike and anther development to late unicellular stage the spike is enclosed within the flag leaf sheath (Figure 3.1). Methods of staging anthers based on external physiology have been investigated in both barley and wheat (Gomez and Wilson, 2012; Browne *et al.*, 2018; Fernández-Gómez *et al.*, 2020). In

this study we firstly sought to investigate whether there are any correlations between external physiology and anther development stage in wheat var. Cadenza, as a method of rapidly estimating the anther/pollen stage. The FLS was deemed the best indicator as a non-destructive method of staging pollen, as it follows a clear positive linear relationship (Figure 3.4A). Knowing the anther development stage without having to invasively dissect the tiller prevents wastage and damage to the spike.

Using the FLS as an indicator of pollen stage, we successfully optimised a heat stress assay for wheat var. Cadenza, finding that it was most vulnerable to heat stress during meiosis and unicellular stages of development (Figure 3.8). This has been linked to a significant reduction in pollen viability rather than pollen number. Interestingly there was not a complete abolishment of viable pollen (Table 3.2).

3.4.1 The use of FLS length as a non-destructive method to stage pollen

In Cadenza, most anther development was found to occur within the flag leaf sheath. To accurately stage the developing anthers, would require dissecting out the spike and microscopy. This is time consuming and damaging to the plant. Instead we sought to develop a rapid and non-destructive method of accurately determining the anther and therefore pollen development stage.

The findings revealed that measurements of the spike and FLS length can be used to estimate the stage of the anthers and therefore the pollen in wheat var. Cadenza. There was found to be a positive linear correlation between anther stage and the length of the spike and FLS in Cadenza (Figure 3.4A/B). Both FLS and spike length have been shown to be effective forms of staging in other cultivars of wheat, rice and barley(Satake and Harase, 1974; Oliver *et al.*, 2005; Ji *et al.*, 2010; Gomez and Wilson, 2012; Browne *et al.*, 2018; Fernández-Gómez *et al.*, 2020).

In contrast, peduncle elongation and anther stage were found to follow a non-linear relationship (Figure 3.4C). There was, also a high level of variability in the results and therefore it would not be recommended to use peduncle length as an estimate for anther stage in Cadenza.

Both peduncle and spike length cannot be used as a non-destructive form of staging as prior to bicellular stage it would require dissecting the FLS. Therefore, in this study we used the length of the FLS to determine the anther and therefore pollen developmental stage prior to spike emergence.

Once the spike starts to emerge from the FLS the anthers are more easily accessible and therefore they can be staged using flow cytometry. The FLS no longer elongations so can no longer be used as an estimator of pollen stage. Emergence of the spike from the FLS corresponds to the progression from unicellular (microspore) stage to bicellular stage during mitosis I. Once the spike is completely clear of the FLS mitosis II occurs and the pollen becomes tricellular (Table 3.1; Supplementary Figure 1).

The stage of a spike was always determined by taking samples from a middle spikelet. However, different spikelets of a spike are likely to mature at different rates. Staging of anthers taken from different spikelets was used to determine the pollen development pattern across the length of the spike. Table 3.1 shows that in general the middle-top of the spike is at the same stage, with the lower part of the spike being at a slightly earlier stage. As a rule, we would ignore the first two rows of spikelets and consider the anthers from the two outer florets from the 6 rows of spikelets below this to be at the same pollen stage (Figure 3.7A).

The staging method developed gave us sufficient confidence to stage the development of the pollen based on the external development of the tiller. This was applied to investigate which stages of pollen development are most sensitive to heat stress in Cadenza based on the grain set of these 24 florets. Here we pinpoint the pollen stage to the level of the floret in order to even more accurately pinpoint the most sensitive stages to high temperatures.

3.4.2 The impact of heat stress on male fertility of Cadenza

Once we had established effective methods of staging Cadenza according to their tiller morphology, we applied this to developing an effective heat stress assay. This assay has the advantage of working on a tiller by tiller basis, therefore allowing a more accurate comparison of treatments than working on a whole plant basis. The

assay could be used for investigating how heat stress can be mitigated in different experimental conditions, such as exogenous application of plant hormones.

Initial conditions of 32/20˚C day/night for 4 days for treatment 1 were chosen based on previous studies indicating that 30/20˚C day/night for 3 days during meiosis led to a significant reduction in grain set in wheat cultivar Gabo(Saini and Aspinall, 1982; Saini *et al.*, 1984). Different studies used different heat stress conditions, taking into consideration duration of heat stress, day and night temperatures, humidity, watering regime and wheat variety. All of these factors will impact the severity of the heat treatment. There was found to be a strong linear negative correlation between duration of heat stress and floret fertility in wheat var. Chinese Spring, with complete sterility occurring after 30 days of 36/26°C day/night(Prasad and Djanaguiraman, 2014). However, most studies found heat stress between the temperatures 30-36˚C was enough to induce a significant reduction in grain set(Saini *et al.*, 1984; Prasad and Djanaguiraman, 2014; Talukder *et al.*, 2014; Draeger and Moore, 2017). In wheat variety Gabo, 3 days at 30°C day/night was sufficient to ensure a 68% loss of grain set when heat stress was applied during meiosis(Saini and Aspinall, 1982). Chinese spring appears to be more resilient than Gabo, with 36/26°C day/night during meiosis for 5 days resulting in just a 60% reduction in floret fertility(Prasad and Djanaguiraman, 2014). Clearly there is genetic component to heat stress tolerance as Chinese Spring which is missing chromosome 5D was found to be more sensitive to heat stress(Draeger and Moore, 2017).

We found that in order to achieve a significant reduction in grain set we had to raise the temperatures from the initial starting conditions of 32/20°C to 33/26°C 80% humidity for 4 days. In this assay we found that in Cadenza the most sensitive pollen stages of heat stress were pollen mother cell meiosis and unicellular stage (Figure 3.8). The use of the staging methods previously described (Figure 3.6) had the advantage over many other studies into the effect of heat stress on wheat by being pollen stage specific(Prasad and Djanaguiraman, 2014; Talukder *et al.*, 2014).

Heat stress induced sterility during meiosis/early microspore stage has been linked to premature degradation of the tapetum(Saini *et al.*, 1984; Ku *et al.*, 2003; Abiko *et*

al., 2005). The tapetum is essential as an energy and nutrient source for the developing microspores(Scott *et al.*, 2004). The tapetum also secretes enzymes which are essential for the release of microspores from the meiotic tetrad(Goldberg *et al.*, 1993). In wheat the tapetum is involved in the secretion of pre-Ubisch bodies, which is what sporopollenin is deposited onto (El-ghazaly and Huysmans, 2001). The tapetum naturally goes through programmed cell death. This degradation is required as it ensures release of molecular such as nutrient, proteins and lipids which are essential for pollen development (Parish and Li, 2010). It was found that Cadenza was sensitive to heat stress even until late unicellular stage. Suggesting the tapetum still has crucial roles in wheat pollen development until pollen mitosis I (Figure 3.8; Supplementary Figure 1).

Different studies investigating the impact of heat stress on the tapetum have identified the effect of heat stress on tapetal development. When barley was grown in continuous high temperatures for 5 days prior to the formation of the tapetum in the anther there was found to be no formation of the tapetal cells(Abiko *et al.*, 2005). Thermosensitive rice grown in continuous high temperatures showed successful formation of anthers, but abnormality began at the PMC stage, where tapetal cells because heavily vacuolated and at unicellular stage began to show signs of cytoplasmic degradation(Ku *et al.*, 2003). The result of this was a failure to accumulate sporopollenin on the surface of the pollen grains of the sterile pollen(Ku *et al.*, 2003). We found in our optimised heat stress assay that the tapetum was still present at unicellular stage in Cadenza in both control and heat stressed anthers (Figure 3.9). In control conditions, the tapetum was found to be present in snap bean (*Phaseolus vulgaris L.*) until bicellular stage, but was absent in heat treated plants(Suzuki *et al.*, 2001). We hypothesis that although premature tapetum breakdown is an important part of the impact of heat stress on pollen development, it is not the only contributor to low grain count. Future experiments should perform cross sections on wheat anthers at bicellular stage as a potentially better comparison for tapetal degradation.

To further investigate the impact of heat treatment on pollen development, measurements of pollen number and viability were taken from different parts of the

spike. Findings show that when looking at pollen number at tricellular stage, there was no significant effect of high temperatures during meiosis across the spike (Table 3.2). Potentially this could be due to pollen number being determined prior to meiosis and at this stage of pollen development the sterile pollen has not been aborted.

Heat stress has been linked to reductions of pollen viability in rice and barley(Sakata *et al.*, 2010; Feng *et al.*, 2018). Pollen viability was significantly reduced in the heat stressed plants by 9.8% ($P=0.025$). Surprisingly, pollen viability remained unaffected at the top and middle parts of the spike, whereas there was a strong significant drop ($P<0.001$) in pollen viability towards the lower part of the central 6 spikelets (Table 3.2). From the top to the lower part of the central 6 spikelets there is a gradient in reduction in pollen viability, with the top showing 7.1%, middle at 9.7% and the lower part a 12.5% reduction. Consequently, a reduction in pollen viability rather than number has been attributed to the significant reductions in grain count when heat stress is induced at meiosis.

Heat stress has also been known to reduced pollen tube growth in the stigma of wheat (Saini *et al.*, 1983). Heat treatment has been observed to desiccate the stigma and style, reducing pollen grains ability to adhere to the stigma leading to reduced ability to capture the pollen(Prasad and Djanaguiraman, 2014). Future studies could examine the stigma at anthesis and also measure the pollen germination rate, as other contributing factors to heat stress induced loss of grain set.

3.5 Conclusion

Using non-destructive methods of staging we were able to show that the wheat var. Cadenza is most sensitive to high temperatures during meiosis and unicellular stages of pollen development. Pre-meiosis, bicellular and tricellular pollen stages proved to be more resistant to heat stress. Temperatures of 33/26°C day/night 80% humidity for 4 days were required to induce a reduction in grain set at these two critical stages. 33°C and above appears to be the critical temperature for Cadenza, with lower daytime temperature of 32°C having no significant effect on grain count.

However, an increase in daytime temperature by 2°C to 35°C was enough to induce a dramatic reduction in grain set at all stages of pollen development. Demonstrating how sensitive wheat pollen development is to even slight changes in daytime temperature. The reductions in grain set have been linked at least partially to a significant reduction in pollen viability, but not pollen number.

Chapter 4: Transcriptional and hormonal changes that occur in the anther in response to heat stress

4.1 Introduction

Pollen development is thought to be a highly conserved process in higher plants(Gomez *et al.*, 2015). It is regulated by the coordination of different phytohormones which trigger signalling cascades that regulate anther development. This is required to ensure correct progression of anther development to result in fertile pollen. For self-pollinating plants, such as wheat, synchronisation of pollen development with the pistil development is especially important to ensure successful fertilisation of the ovules.

Mutants which are deficient or insensitive to plant hormones often show developmental defects in male reproductive development, specifically filament elongation, tapetal PCD and dehiscence. An Arabidopsis mutant which is defective in the auxin biosynthesis enzymes, *yuc2yuc6*, was found to show reduced anther filament elongation (Cheng *et al.*, 2006). Triple auxin receptor mutants *tir1 afb2 afb3* and quadruple *tir1 afb1 afb2 afb3*, lacking the ability to detect auxin, showed reduced filament elongation and earlier dehiscence(Cecchetti *et al.*, 2008). Arabidopsis mutants which are deficient in JA have been found to show reduced filament elongation, delayed/absent dehiscence and reduced pollen viability (McConn and Browse, 1996; Sanders *et al.*, 2000; Stintzi and Browse, 2000; Ishiguro *et al.*, 2001; Park *et al.*, 2002; Von Malek *et al.*, 2002; Caldelari *et al.*, 2011). Similarly, a number of mutants which are defective in JA signal transduction have also been shown to have male developmental defects. For example, the double mutant *myb21 myb24*, is defective and showed three defects of defective pollen maturation, delayed anther dehiscence and reduced filament elongation(Song *et al.*, 2011). Arabidopsis GA biosynthesis mutants which are defective in enzymes involved in forming bioactive GAs, *ga3ox1 ga3ox3* and *ga20ox1 ga20ox2* double mutants, were also found to show reduced filament elongation and disrupted dehiscence(Hu *et al.*, 2008; Rieu *et al.*, 2008). GA-insensitive rice mutants *gamyb-2, gid1-4* and *gid2-5* also showed defects in tapetal degradation and pollen exine formation(Aya *et al.*, 2009). Ethylene insensitive *Nicotiana tabacum* showed

reduced filament elongation, delayed tapetal degradation and delayed dehiscence(Rieu *et al.*, 2003; Takada *et al.*, 2005). Ethylene insensitive *Nicotiana tabacum* and *Chrysanthemum morifolium* were both found to have lower pollen production and viability(Takada *et al.*, 2005, 2006; Ishimaru *et al.*, 2006; Shinoyama *et al.*, 2012).

Taken together we can infer that anther filament elongation, tapetal PCD and dehiscence is positively promoted by GA and ethylene, whereas as far as we know JA only promotes filament elongation and dehiscence. This potentially explains why all three of these hormones were found to accumulate towards the later stages of pollen development. Auxin in contrast inhibits tapetal PCD and dehiscence and has been suggested to be crucial in preventing premature anther dehiscence and pollen maturation(Cecchetti *et al.*, 2008).

Clearly, hormones are required to ensure normal anther and pollen development. Transcriptional data in rice pollen/tapetal cells, coupled with direct measurements of hormone accumulation in mature anthers indicates the coordinated accumulation of GA, auxin, JA and ethylene towards the later bicellular and tricellular stages of pollen development (Hirano *et al.*, 2008). The accumulation patterns match their functional profile.

Heat stress has been linked with disrupting key hormone signalling pathways which regulate normal anther development, leading to male sterility (Ozga *et al.*, 2017). Endogenous levels of IAA in anthers were found to decrease in response to heat in barley and rice(Tang *et al.*, 2008; Sakata *et al.*, 2010). Indeed exogenous application of IAA/NAA prior to and during heat stress led to a recovery of pollen viability and consequently grain set(Sakata *et al.*, 2010). Ethylene has also been implicated to be involved in heat stress tolerance. *Never ripe* (*Nr*) tomato mutants which are ethylene-insensitive were found to be more sensitive to heat stress, with fewer and reduced viability of pollen compared to the WT(Firon *et al.*, 2012). Viability and germination of pollen also increased when WT plants were previously exposed to ethylene before heat treatment and decreased when exposed to an ethylene biosynthesis inhibitor(Firon *et al.*, 2012). GA content was found to decrease in response to heat stress in rice anthers(Tang *et al.*, 2008). Heat stress was also found

to induce accumulation of ABA in rice anthers(Tang *et al.*, 2008). More heat tolerant lines of rice were found to retain a higher level of GA and a lower level of ABA(Tang *et al.*, 2008). Following on from these studies, we sought to investigate the impact of heat stress on the hormone profile of wheat anthers.

Reproductive development is thought to be highly conserved in monocots and dicots(Gomez *et al.*, 2015). Forward genetic screens for pollen sterility have pinpointed genes which are involved in formation of the tapetum as crucial for ensuring the correct development of pollen (Section 1.4). The tapetum provides both nutrients for the developing microspores and enzymes which are required for their release from the tetrad callose envelopes after they have undergone meiosis(Papini *et al.*, 1999; Wu and Cheung, 2000). The formation of the tapetum is regulated by a cascade of genes including: *SPL/NZZ*, *EMS1*, *TPD1*, *DYT1*, *AMS*, *BAM1/2*, *SERK1/2* and *MPK3-6* in Arabidopsis, and *MSP1*, *TDL1* and *UDT1* in rice (Yang *et al.*, 2003; Schiefthaler *et al.*, 1999; Yang *et al.*, 1999; Canales *et al.*, 2002; Zhao *et al.*, 2002, 2008; Nonomura *et al.*, 2003; Albrecht *et al.*, 2005; Colcombet *et al.*, 2005; Jung *et al.*, 2005; Hord *et al.*, 2006, 2008; Feng *et al.*, 2012) (See section 1.4.2 for more detail). The biosynthesis of lipids and phenolic components involved in pollen wall synthesis in the tapetum is determined by AMS in Arabidopsis and TDR (its orthologue) in rice(Sorensen *et al.*, 2003; Xu *et al.*, 2010, 2014; Zhang *et al.*, 2011). Also critical to formation of viable pollen is the programmed cell death (PCD) of the tapetum at the correct stage. Directly downstream of AMS, MS1 in Arabidopsis, its rice orthologue OsPTC and HvMS1 in barley are all involved in initiating PCD(Vizcay-Barrena and Wilson, 2006; Ito *et al.*, 2007; H. Li *et al.*, 2011; Gomez and Wilson, 2014). Other transcription factors have been identified in rice as being involved in controlling tapetal PCD, OsTDR, OsUDT1 and OsGAMYB(Kaneko *et al.*, 2004; Jung *et al.*, 2005; Li *et al.*, 2006). Pollen exine formation is also critical for ensuring viable pollen, with DEX1 and NEF1 being involved in exine formation and sporopollenin transport(Ariizumi *et al.*, 2004; L. J. Ma *et al.*, 2013).

In addition to these key regulatory genes, a number of other genes are involved in controlling anther development. Microarray data of Arabidopsis anthers has demonstrated a number of stage specific expression of genes during anther

development (Pearce *et al.*, 2015). At meiosis, a number of tapetum specific genes were highly expressed, including genes associated with sporopollenin biosynthesis and exine formation. At mitosis I, genes associated with pollen exine formation, lipid biosynthesis and lipid transfer were highly expressed. Genes involved in pollen exine formation and sugar transport were found to increase in expression at the bicellular stage and at mitosis II genes involved in cell wall modification, sugar transport and microtube/filament movement were preferentially expressed(Pearce *et al.*, 2015).

The role of hormones and various signalling components behind anther and pollen development has been well studied in Arabidopsis and rice. However, little research has been done on the signalling components and the transcriptome of wheat anthers. One study determined differential gene expression using whole floret data from wheat spikes at anthesis treated with various different hormones(Qi *et al.*, 2019). Another study confirmed the expression of the wheat orthologue of *GAMYB* (*TaGAMYB*) in the anthers, with all three of the homoeologues being expressed(Wang *et al.*, 2012). Ramírez-González *et al.,* 2018 took a diversity of wheat tissues and published their transcriptome. This study did quantify data from the anthers, but only during anthesis. In addition, they quantified spikelet and whole spike data, however the exact stage of the anther was not determined.

In order to deduce the key hormones which are directly involved in anther and pollen development in wheat a complete hormone profile of wheat anthers grown in both control and heat stress conditions at different development stages was conducted. A hormonomics approach was used to determine the hormone profile in precisely staged whole wheat anthers. This data was supplemented with RNAseq analysis of these samples to identify the key genes involved in regulating pollen development, hormone accumulation/deaccumulation and downstream signalling responses. RNAseq and hormonomics was also applied to whole anthers which had experienced heat treatment during meiosis. The samples of control and heat were compared to investigate the impact of heat treatment on the hormone composition and transcriptional profile. Taken together these findings will improve our understanding of the hormone signalling pathways involved in anther development

and the heat stress response in wheat. The resultant data could be applied to identify genetic targets and chemical strategies to improve heat stress tolerance in wheat.

4.2 Materials and Methods

All experimental details are described in section 2.

4.3 Results

4.3.1 Determination of phytohormone levels during anther development

Anther development is associated with complex changes in hormone accumulation(Hirano *et al.*, 2008). An initial experiment was conducted to ascertain the changes in phytohormone accumulation of the whole wheat anther according to pollen developmental stage under optimal growth conditions (20/15°C day/night).

25 plants were grown in glasshouse conditions until they reached the booting stage. The plants were then transferred into Fitotron growth chambers to ensure consistent climatic conditions when sampling which could otherwise impact the hormone profiles (section 2.1). 5 plants were randomly selected to collect samples from each stage of development: meiosis, unicellular, bicellular, tricellular and late tricellular (just before anthesis). These are the main key stages of pollen development. Meiosis was determined using a flag leaf sheath length of 9-13cm and other stages were determined using a combination of external phenotyping and an Ampha Z32 Impedance Flow Cytometer (Amphasys, Luzern, Switzerland). Anther samples used for staging were taken from either of the central spikelets two outer florets. Once the stage was correctly determined, anthers were harvested only from the middle part of the ear and two outer florets of each spikelet to ensure anthers were at the same stage. This follows the same central 6 spikelets used to count grain set, as these were determined to be the same stage of pollen development (Chapter 3; Figure 3.7A). The samples were instantly frozen in liquid nitrogen and transferred to -80°C for storage. Anthers were always collected within the first three hours of the photoperiod to minimise the impact of circadian effects. The samples were freeze dried and hormones were extracted using the method detailed in section 2.4.

The compounds shown are JA (Jasmonic Acid), JA-Ile (Jasmonoyl-Isoleucine), IAA (Indoleacetic acid), iP (isopentenyladenine), tZ (trans-zeatin), DHZ (dihydrozeatin), CZ (cis-zeatin), CK (cytokinin) ribosides, ABA (Abscisic acid), SA (Salicylic acid) and $GA_{1/4}$ (Gibberellin$_{1/4}$). ANOVA analysis was performed using GenStat (v18, VSNI, Hemel Hempstead, U.K.). Bar charts were plotted using GraphPad Prism Software (San Diego, California, USA).

Jasmonic Acid:

JA and the conjugated form of JA, JA-Ile, were measured. JA-Ile was determined to be the bioactive JA(Fonseca *et al.*, 2009).In rice, transcriptional data of developing pollen indicated that there is a higher expression of JA biosynthesis genes in the pollen towards the later stages of pollen development and expression occurs throughout the tapetums lifecycle. Therefore suggesting an accumulation of JA towards the later stages (Hirano *et al.*, 2008). In wheat, hormone accumulation from carefully staged whole anthers showed a significant accumulation of JA ($P<0.001$, SED = 38.7, LSD =81) and JA-Ile ($P<0.001$, SED = 1145.7, LSD = 2389.9) from meiosis, peaking at bicellular stage, following by a slower deaccumulation at the tricellular stage (Figure 4.1). Both JA and JA-Ile follow a close accumulation pattern in the anther. From meiosis to bicellular stage, there was a 35-fold increase in JA accumulation and 530-fold increase in JA-Ile accumulation.

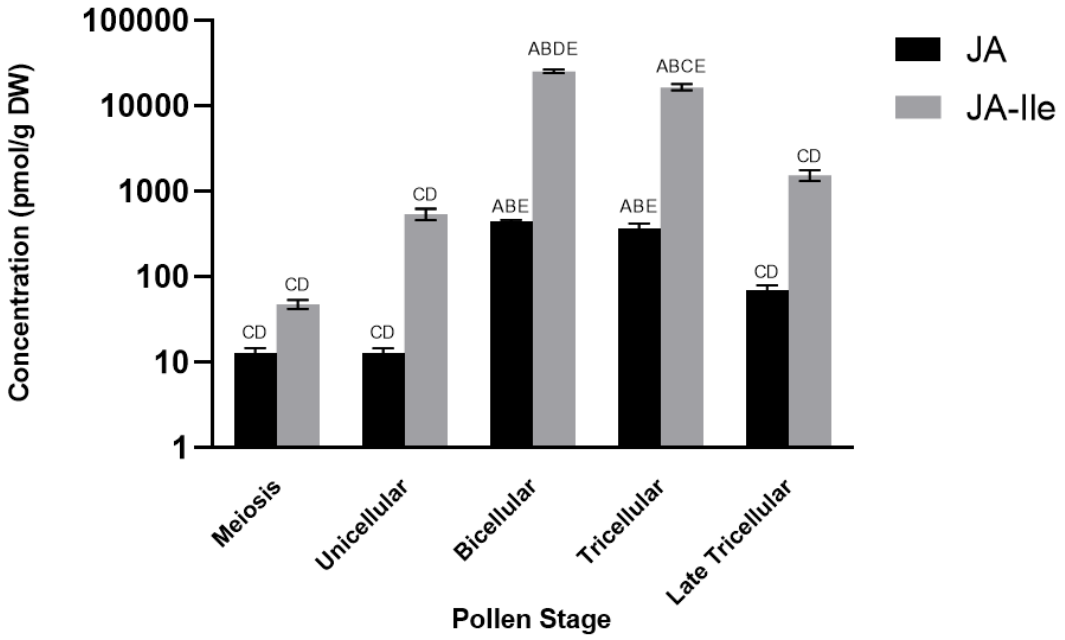

Figure 4.1: *Jasmonate accumulation across successive stages of anther development.*

Changes in JA (Jasmonic acid) and JA-Ile (JA-isoleucine) concentration in wheat anthers during meiosis, unicellular, bicellular, tricellular and late tricellular stages. Bars are the ANOVA output of 4-5 biological replicates taken for each stage. +/- 1 SE. LSD(5%)=81 (19 d.f) and 2389.9 (20 d.f) for JA and JA-Ile respectively. P<0.001. Significantly different from: A = Meiosis, B = Unicellular, C = Bicellular, D =Tricellular and E = Late Tricellular stages.

Auxin:

IAA (Indole-3-acetic acid) is the main naturally occurring bioactive auxin in plants(Reviewed by Korasick, Enders and Strader, 2013). IAA was the only bioactive form measured in this study. Other forms were either precursors or IAA conjugates and catabolites. Direct measurements of IAA accumulation in Arabidopsis anthers found that IAA accumulates most highly just before tapetum degradation and decreases in concentration after this(Cecchetti *et al.*, 2013). IAA showed an accumulation from meiosis to bicellular and tricellular stage and significantly declines at the late tricellular stage ($P<0.001$, SED = 1349.5, LSD = 2815.0) (Figure

4.2). From meiosis to the bicellular stage there was found to be a 70-fold increase in IAA accumulation.

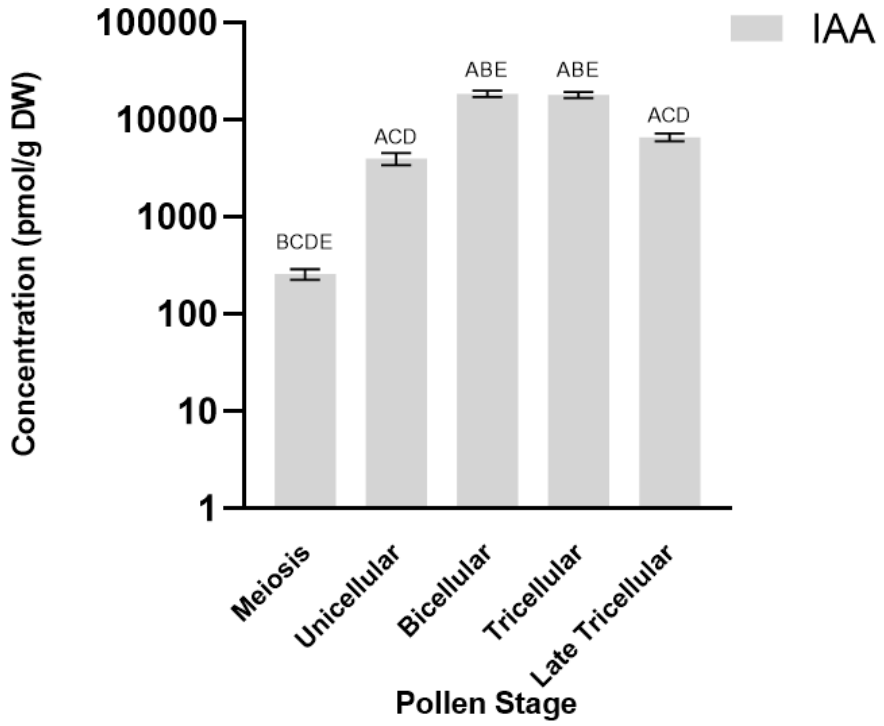

Figure 4.2: *Auxin accumulation across successive stages of anther development.*

Changes in IAA (Indole-3-acetic acid) concentration in wheat anthers during meiosis, unicellular, bicellular, tricellular and late tricellular stages. Bars are the ANOVA output of 4-5 biological replicates taken for each stage. +/- 1 SE. LSD(5%)=2815.0 (20 d.f). P<0.001. Significantly different from: A = Meiosis, B = Unicellular, C = Bicellular, D =Tricellular and E = Late Tricellular stages.

Cytokinin:

Cytokinins (CKs) were predicted to decrease in accumulation in microspores/pollen towards the later stages of their development (Hirano *et al.*, 2008). We took direct measurements of CKs, measuring both the precursor and bioactive forms. There are many bioactive forms which have different degrees of bioactivity. iP and tZ are the two most bioactive forms of CK in plants, followed by less bioactive forms DHZ and CZ (Spíchal *et al.*, 2004; Lomin *et al.*, 2011; Kuderová *et al.*, 2015). Both iP and CZ were found to accumulate from meiosis to bicellular stage (8-fold and 7.5-fold increase respectively) and then decline until late tricellular stages (ip=P<0.001,

SED=67.5, LSD=140.8; CZ: P<0.001, SED=28.15, LSD=58.72)(Figure 4.3). DHZ was only found to accumulate at bicellular stage and remained below the limit of detection (LOD) at other stages. tZ was found at lower concentrations than both iP and CZ and accumulated most highly at unicellular stage (tZ: P<0.001, SED=1.015, LSD=2.118). The CK ribosides can also be considered to be active forms of CK, as they have been found to bind to the poplar CK receptors(Jaworek *et al.*, 2020). The total CK ribosides were calculated as a sum of *trans*-zeatin riboside, *cis*-zeatin riboside, dihydrozeatin riboside and isopentenyladenine riboside. The total CK ribosides were found to accumulate from meiosis to unicellular/bicellular stage by around 11-fold, before declining at tricellular and late tricellular stage (CK Ribosides: P<0.001, SED=31.28, LSD=65.26). Taken together it appears that bioactive cytokinins accumulate from meiosis to bicellular stage and then decline towards the later stages.

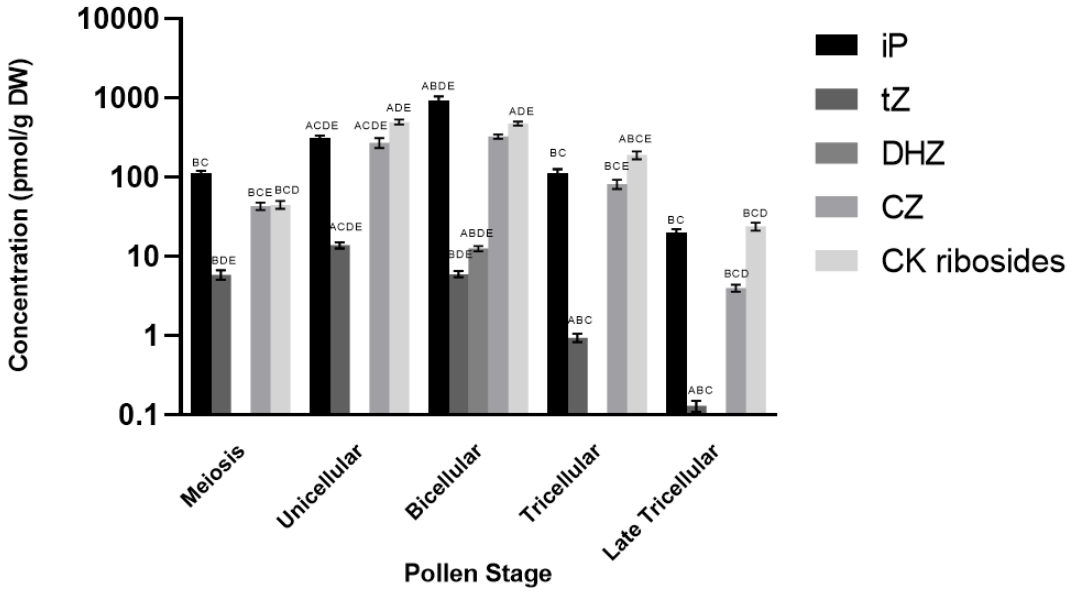

Figure 4.3: *Cytokinin accumulation across successive stages of anther development.*

Changes in bioactive Cytokinins: iP (isopentenyladenine) and tZ (trans-zeatin), DHZ (dihydrozeatin), CZ (cis-zeatin) and total CK ribosides concentration in wheat anthers during meiosis, unicellular, bicellular, tricellular and late tricellular stages. Bars are the ANOVA output of 4-5 biological replicates taken for each stage. +/- 1 SE. LSD(5%): iP = 140.8 (20 d.f), tZ = 2.118 (20 d.f), CZ = 58.72 (20 d.f) and total CK ribosides 65.26 (20 d.f). P<0.001. Significantly different from: A = Meiosis, B = Unicellular, C = Bicellular, D =Tricellular and E = Late Tricellular stages.

ABA and SA:

In rice the accumulation pattern of ABA (Abscisic acid) in microspores/pollen was hard to predict from microarray data, however it was suggested that there is a deaccumulation in the tapetum prior to PCD(Hirano *et al.*, 2008). The highest levels of ABA ($P<0.001$, SED=30.78, LSD=64.42) and SA (Salicylic Acid) ($P<0.001$, SED=159.0, LSD=332.7) were found at meiosis with reduced levels at later developmental stages (Figure 4.4). Deaccumulation was most rapid for SA, which showed a 4-fold decrease from meiosis to the unicellular stage.

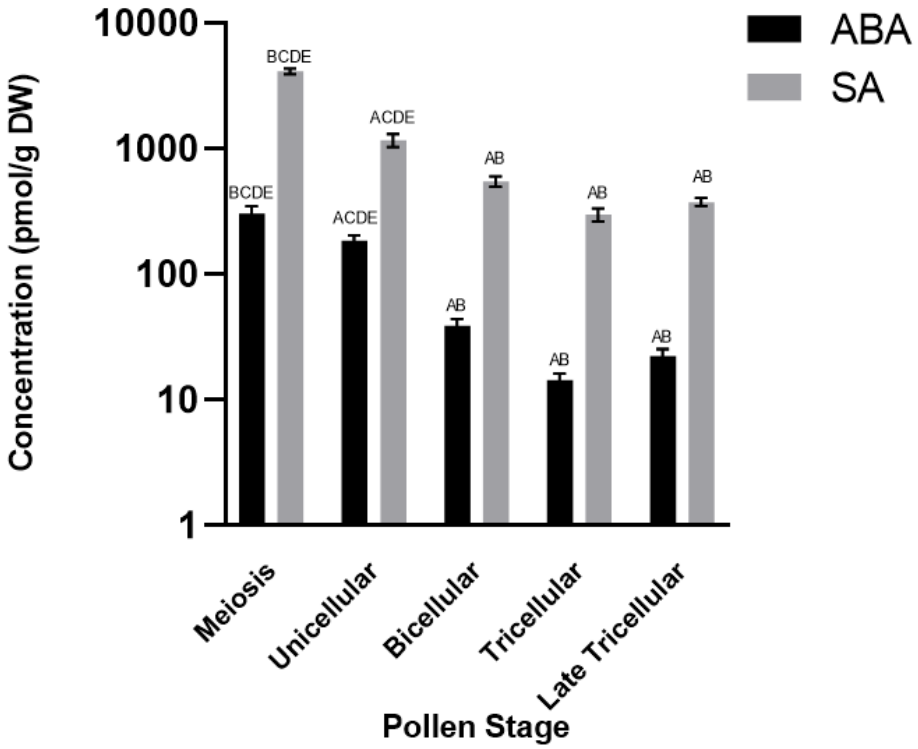

Figure 4.4: *ABA and SA accumulation across successive stages of anther development.*

Changes in ABA (Abscisic acid) and SA (Salicylic acid) concentration in wheat anthers during meiosis, unicellular, bicellular, tricellular and late tricellular stages. Bars are the ANOVA output of 4-5 biological replicates taken for each stage. +/- 1 SE. LSD(5%)=64.42 (19 d.f) and 332.7 (19 d.f) for ABA and SA respectively. P<0.001. Significantly different from: A = Meiosis, B = Unicellular, C = Bicellular, D =Tricellular and E = Late Tricellular stages.

Gibberellin:

Transcriptional data of rice pollen indicates that there is an accumulation of GA in microspores/pollen towards the later stages of pollen development (Hirano *et al.*, 2008). We found that GA_1 (a bioactive form of GA), was under the detection limit at all stages of pollen development. GA_1 was also not detected in whole rice anthers taken at mature tricellular stage(Hirano *et al.*, 2008). Another bioactive form of GA, GA_4, was found to accumulate somewhat at the unicellular stage, however, it was below the detection limit at the other stages of development (Figure 4.5). GA_4 was found to accumulate to a much higher level in the mature rice anther compared to GA_1 suggesting that GA_4 is predominantly used in the floral organs(Hirano *et al.*, 2008). Our results suggest this also applies to wheat. The accumulation of the other bioactive forms of GA: GA_3 and GA_7, were not established.

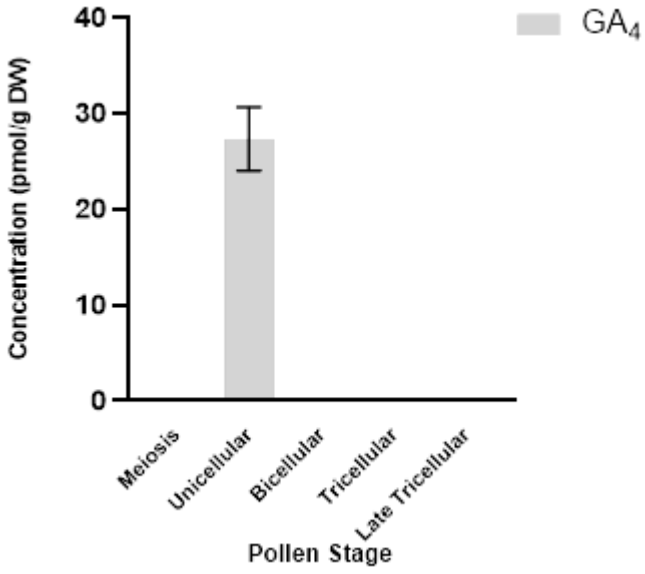

Figure 4.5: *Gibberellin accumulation across successive stages of anther development.*

Changes in bioactive GA_4 concentration in wheat anthers during meiosis, unicellular, bicellular, tricellular and late tricellular stages. Bars are the ANOVA output of 4-5 biological replicates taken for each stage. +/- 1 SE.

Brassinosteroid:

Finally, the accumulation of brassinosteroids was also investigated. Brassinosteroids are a group of phytohormones which widely occur in the plant kingdom (Bajguz and Tretyn, 2003). Transcriptional data of rice pollen showed no clear trend in the expression of BR synthesis genes, therefore making it difficult to predict a trend of accumulation (Hirano *et al.*, 2008). In this study, eight brassinosteroids were investigated: brassinolide, 24-*epi*brassinolide, homobrassinolide, 28-*nor*brassinolide, dolichosterone, homodolichosterone, dolicholide and homodolicholide. Only dolicholide was found to accumulate to low levels at bicellular and tricellular stages. Consequently, the results have not been presented. The results are likely due to the chemical properties of BRs making them difficult to ionize and therefore difficult to be investigated with LG-MS.

4.3.2 Changes in the hormone profile of wheat anthers in normal and heat stress conditions

Heat stress is known to induce changes in hormone accumulation in anthers of barley and rice(Tang *et al.*, 2008; Sakata *et al.*, 2010). We sought to conduct a second experiment investigating the impact of heat stress on phytohormone accumulation in wheat anthers. This is a repeat of the initial experiment, but as well as the control treatment we also performed a heat stress experiment running parallel. In this study we directly measured hormone accumulation according to pollen stage rather than running a time course. Heat treatment increases the rate of anther development in wheat (Section 5.3.8; Table 5.8). Therefore, if samples were collected as part of a time-course we would not be directly comparing anthers at the same stage of pollen development. The same compounds were measured as described in the previous hormone profiling experiment, however brassinosteroids were not measured due to difficulties measuring them in the initial experiment (Section 4.3.1). REML analysis was performed using GenStat (v18, VSNI, Hemel Hempstead, U.K.).

As previously found different stages of pollen development show large differences in hormone profiles (Section 4.3.1). To make sure we are directly comparing the effect of heat treatment, we collected samples which were staged using the Ampha Z32 Impedance Flow Cytometer (Amphasys, Luzern, Switzerland).

Along with measuring hormone accumulation, RNAseq analysis was also performed. This meant we could identify candidate genes involved in pollen development, as well as in the heat stress response, including those that may be responsible for the observed changes in hormone accumulation.

A graphical summary of the experiment design is shown in figure 4.6. Plants were grown in glasshouse conditions before being moved to Conviron cabinets (see section 2.1) where they were initially acclimated for 1 week in standard growth conditions (20/15°C day/night). Half the plants were then exposed to either control (20/15°C day/night) or heat stress conditions by increasing the temperature to 33/26°C day/night 80% humidity and watering to saturation 1x/day. The treatment lasted for 4 days, before being returned back to control growth conditions (20/15°C

day/night). This follows the conditions for the heat stress assay optimised for wheat var. Cadenza (see chapter 3). Meiosis and unicellular stage were both determined to be the stages most sensitive to heat stress (Chapter 3), however for consistency we only heat-treated tillers at meiosis stage, Meiosis stage was determined based on the length of the flag leaf sheath being 9-13cm. Whole anthers were taken at meiosis (prior to heat treatment), followed by unicellular, bicellular and tricellular stages after being exposed either to control or heat stress conditions.

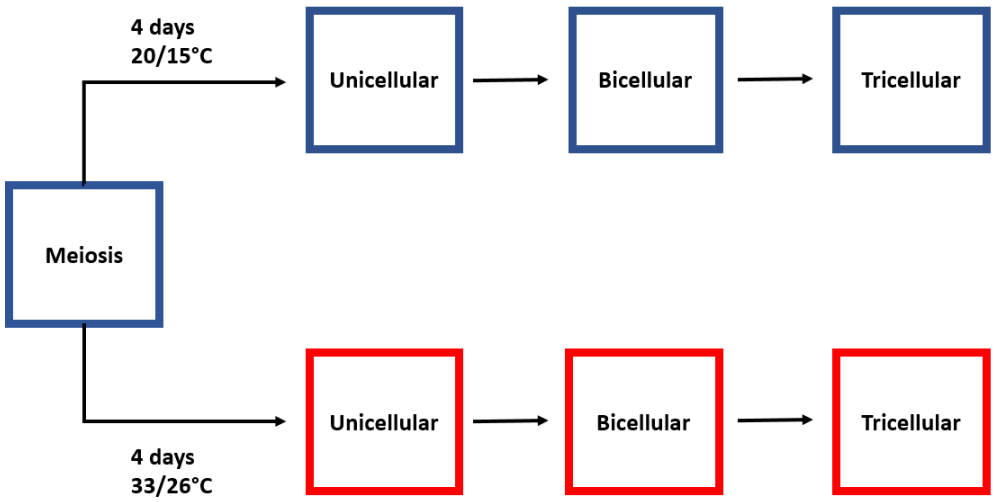

Figure 4.6: *Structure of the heat stress experiment.*

Whole anther samples were taken at meiosis, unicellular, bicellular and tricellular stages of pollen development. Tillers were tagged at meiosis stage (9-13cm FLS extension) before either being exposed to control or heat stress conditions. Control treatment: 4 days at 20/15°C day/night. Heat treatment: 4 days at 33/26°C day/night. Anthers were accurately staged using the Ampha Z32 Impedance Flow Cytometer.

Jasmonic Acid:

In control conditions there was found to be an accumulation of both JA and JA-Ile towards the later stages, this shows a similar pattern as that found in the initial experiment (Figure 4.1). The effect of heat stress on jasmonic acid accumulation was evident (Figure 4.7). There was a significant effect of stage and treatment, with a 5-fold accumulation of JA after heat stress at the unicellular stage ($P<0.001$, 5% LSD=468). There was also a significant increase in the concentration of the bioactive JA-Ile after heat stress with a 20-fold accumulation at the unicellular stage ($P<0.001$, 5% LSD=2726). This accumulation has been determined to be stage specific, as there was found to be no significant difference in JA or JA-Ile accumulation as a result of the prior heat treatment at bicellular and tricellular stages.

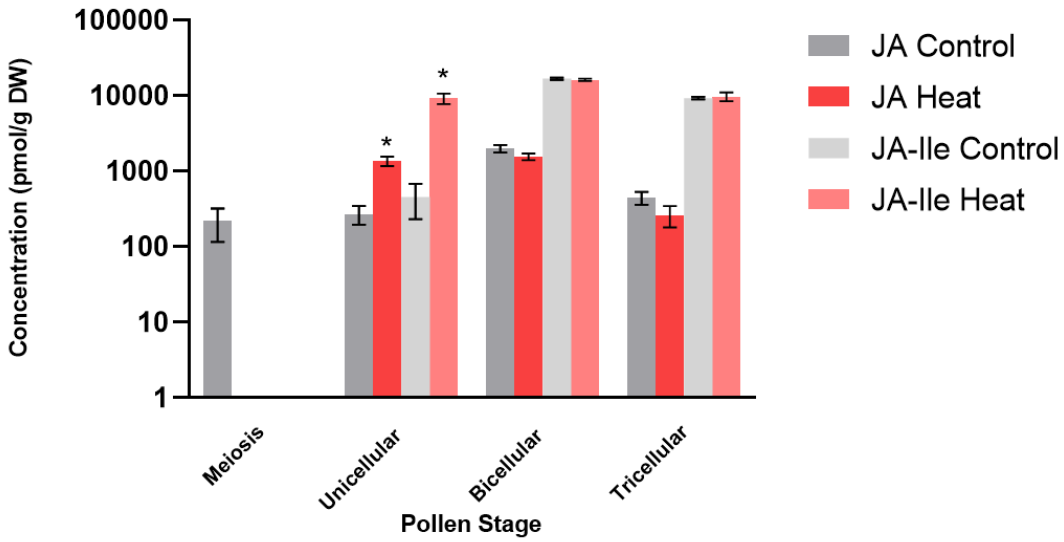

Figure 4.7: *Jasmonate accumulation in response to heat treatment.*

*Changes in JA (Jasmonic acid) and JA-Ile (JA-isoleucine) concentration in wheat anthers during meiosis, unicellular, bicellular, tricellular and late tricellular stages in response to heat treatment. Bars are the REML output of 4-5 biological replicates taken for each stage. +/- 1 SE. Max LSD(5%)=496.3 (27 d.f) and 2891 (27 d.f) for JA and JA-Ile respectively. *Significantly different from control treatment of the same pollen stage. P<0.001.*

Auxin:

In control conditions the accumulation of IAA follows a similar pattern as that found in the initial experiment (Figure 4.2). In response to heat treatment there was found to be a reduction in IAA content in rice and barley(Tang *et al.*, 2008; Sakata *et al.*, 2010). In contrast we found a 2.7-fold increase in IAA content in response to heat treatment at unicellular stage, although this was not found to be significant (Figure 4.8). After control or heat treatment, bicellular and tricellular stages of pollen development showed similar levels of IAA accumulation.

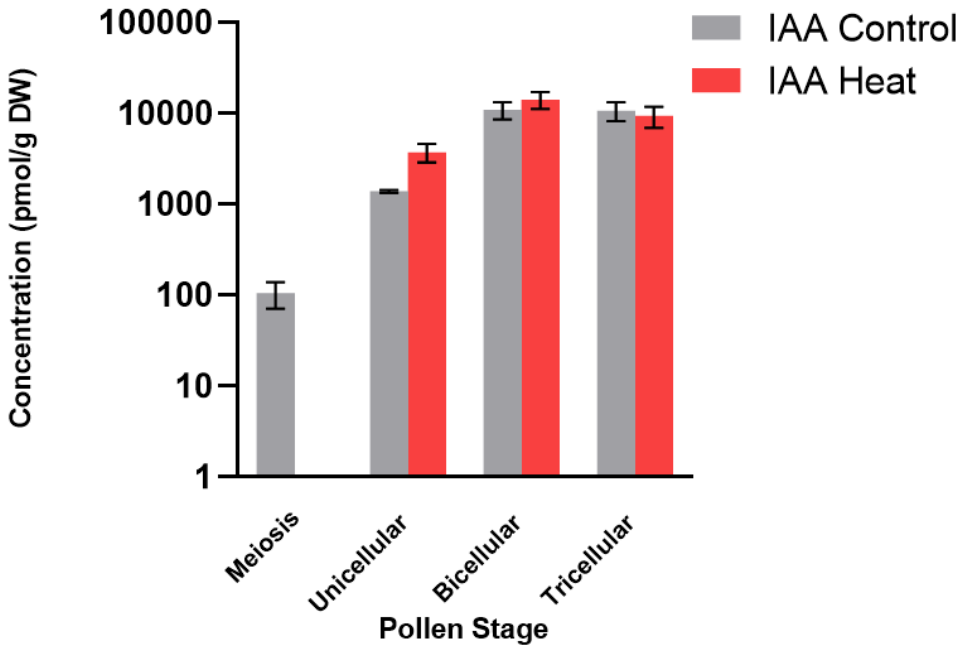

Figure 4.8: *Auxin accumulation in response to heat treatment.*

Changes in IAA (Indole-3-acetic acid) concentration in wheat anthers during meiosis, unicellular, bicellular, tricellular and late tricellular stages in response to heat treatment. Bars are the REML output of 4-5 biological replicates taken for each stage. +/- 1 SE. Max LSD(5%)=6781 (27 d.f). P=0.571.

Cytokinin:

There was found to be a similar pattern of accumulation of bioactive CKs in the control treatment, as was originally found in the initial experiment (Figure 4.3). Overall, in response to heat treatment there was found to be a deaccumulation of bioactive CKs (Figure 4.9). The bioactive CKs, iP and cZ, were found to show a

significant reduction in accumulation of CK at bicellular heat stage of pollen development compared to the control; showing a 73% and 41% decrease respectively (P=0.005, 5% LSD=207.9; P=0.178 5% LSD=130.4). There was also found to be a significant deaccumulation of tZ and cZ at unicellular stage; showing a 67% and 39% loss respectively (P=0.003, 5% LSD=1.488; P=0.178 5% LSD=130.4). DHZ was not detected in the anthers across all stages and treatments, unlike in the initial experiment. CK ribosides were not found to be significantly impacted by heat treatment (P=0.426; Max 5% LSD=427.3).

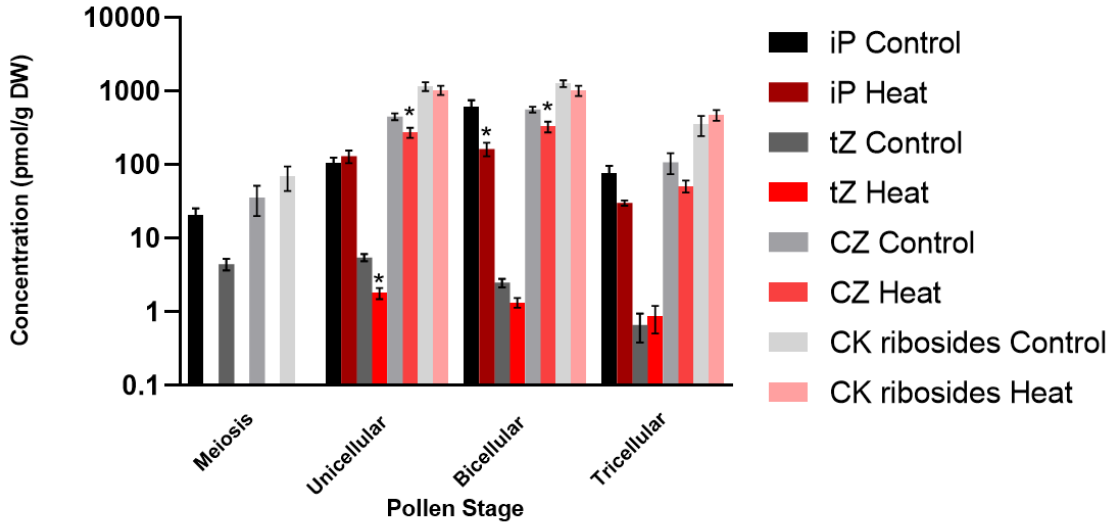

Figure 4.9: *Cytokinin accumulation in response to heat treatment.*

*Changes in bioactive Cytokinins: iP (isopentenyladenine) and tZ (trans-zeatin), CZ (cis-zeatin) and total CK ribosides concentration in wheat anthers during meiosis, unicellular, bicellular, tricellular and late tricellular stages in response to heat. Bars are the REML output of 4-5 biological replicates taken for each stage. +/- 1 SE. Max LSD(5%): iP = 220.5 (27 d.f), tZ = 1.578 (27 d.f), CZ = 138.3 (27 d.f) and total CK ribosides 427.3 (27 d.f). *Significantly different from control treatment of the same pollen stage. P=0.005, 0.003, 0.178 and 0.426 respectively.*

ABA and SA:

In the control conditions there was found to be a similar pattern of deaccumulation of ABA and SA from the earlier stages to the later stages (Figure 4.4). There were no significant interactions between stage and treatment for SA and ABA (P=9.814, Max 5% LSD=3962; P=0.577; Max 5% LSD=68.06 respectively) (Figure 4.10). This is in contrast to previous findings which showed that heat stress induces an accumulation of ABA in rice(Tang *et al.*, 2008).

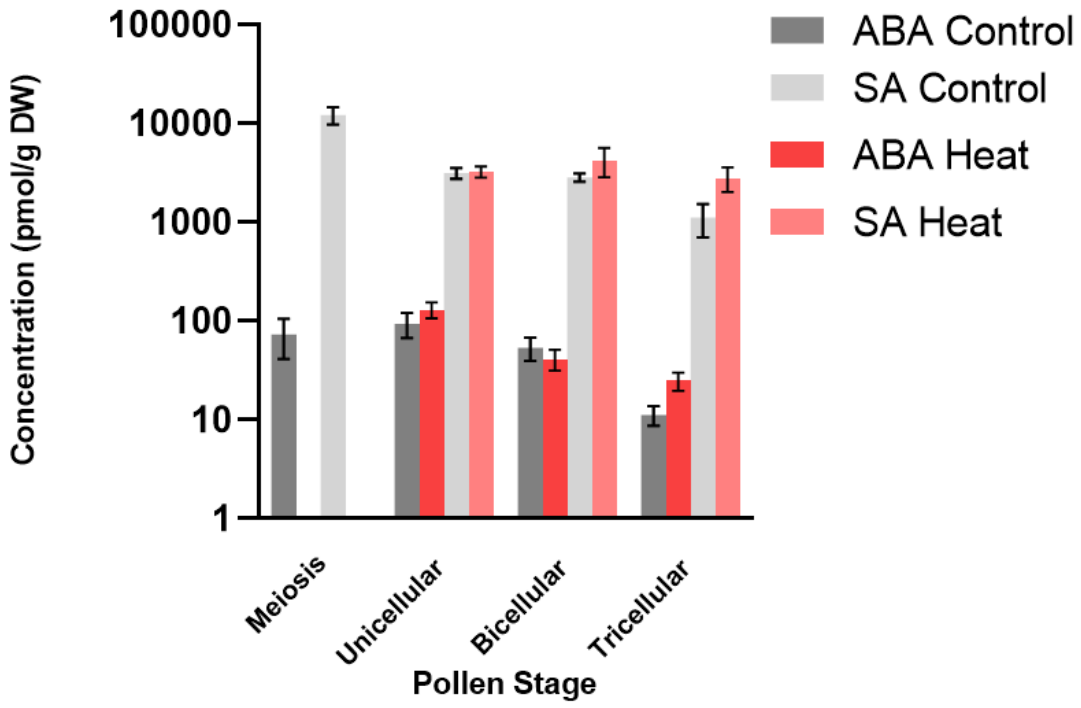

Figure 4.10: *ABA and SA accumulation in response to heat treatment.*

Changes in ABA (Abscisic acid) and SA (Salicylic acid) concentration in wheat anthers during meiosis, unicellular, bicellular, tricellular and late tricellular stages in response to heat treatment. Bars are the REML output of 4-5 biological replicates taken for each stage. +/- 1 SE. Max LSD(5%)=68.06 (27 d.f) and 3962 (27 d.f). P=0.557 and 0.814 for ABA and SA respectively.

Gibberellin

Due to low levels of GA detection, GA specific analysis was determined using the extracted samples of the heat stress experiment. This was completed using a protocol adapted from methods already described by (Urbanová *et al.*, 2013). There

was found to be a small amount of accumulation of GA_1, compared to the initial experiment which showed that across all stages it was below the limit of detection. GA_3 is another bioactive gibberellin which was also measured; it was found to accumulate to the greatest level at meiosis. GA_4 was found to accumulate from meiosis to its maximum at unicellular stage, before progressively decreasing to tricellular stage. In contrast, in the initial experiment GA_4 was found to only accumulate at unicellular stage (Figure 4.5), however these later findings show its accumulation peaked at meiosis stage. The disparity in the results does not overlook the fact that these are remarkably low levels of GA_4 found compared to previous studies on mature rice anthers(Hirano *et al.*, 2008). Indeed, similar findings have previously been found in wheat anthers. In preliminary GC-MS data there were found to be high levels of GA_4 in wheat anthers, the same methods of LC-MS used in our study found no GA_4 detected from anthers at 10 and 15cm FLS length extension (corresponding with meiosis and early microspore stage respectively) (Audley, 2016). This suggests an issue with the protocol.

There was found to be a significant reduction in GA_1 content at the bicellular stage after heat stress (P=0.026, 5% LSD = 0.995). There was also found to be a significant reduction in GA_4 content at unicellular stage after heat stress (P=0.106, 5% LSD = 0.8904). This reflects findings that rice anthers show a reduction in GA content in response to heat treatment(Tang *et al.*, 2008).

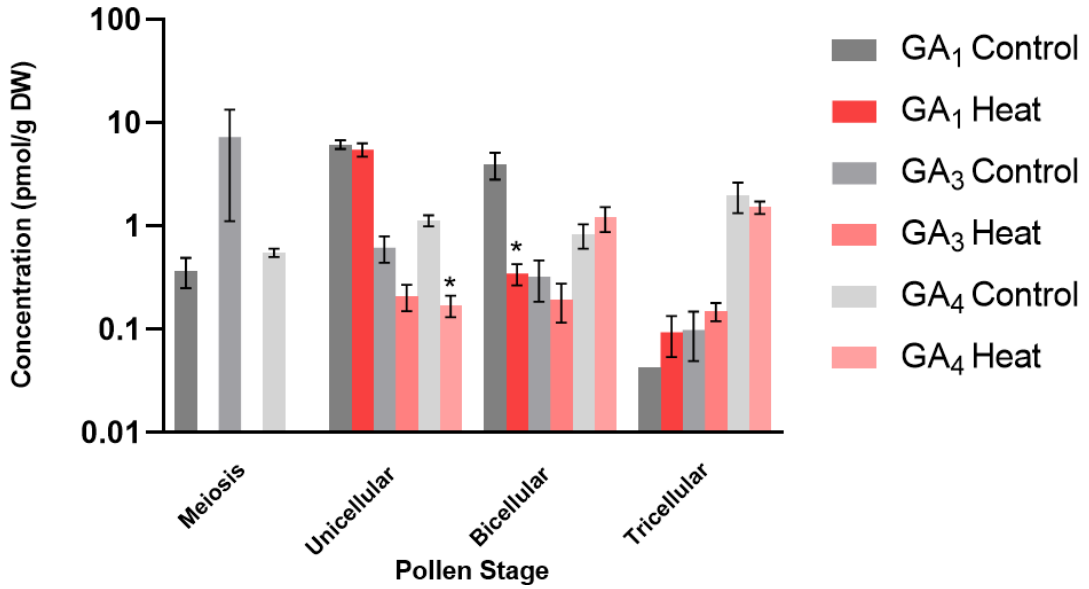

Figure 4.11: *Gibberellin accumulation in response to heat treatment.*

Changes in $GA_{1/3/4}$ concentration in wheat anthers during meiosis, unicellular, bicellular, tricellular and late tricellular stages in response to heat treatment. Bars are the REML output of 4-5 biological replicates taken for each stage. +/- 1 SE. Max LSD(5%)= 0.995 (27 d.f), 8.145 (27 d.f) and 0.9444 (27 d.f) for GA_1, GA_3 and GA_4 respectively.

**Significantly different from control treatment of the same pollen stage. P=0.026, 0.996 and 0.106 respectively.*

4.3.3 Changes in the gene expression profile of wheat anthers in response to heat stress

Alongside measurements of hormone accumulation, the transcriptome of the whole anthers was also measured using RNAseq. Anther samples were harvested and their RNA extracted, quantified and analysed according to methods detailed in section 2.3.

A full transcriptional profiling of the anthers coupled with the hormone data will allow the identification of potentially key genes involved in pollen development and how their expression changes in response to heat stress. It may also allow the identification of genetic components controlling hormone metabolism, which underlie the changes observed in the hormone profiling experiments. 4 biological replicates were used for each treatment and stage combination.

A cluster analysis was performed on the transcriptional data to identify clusters of genes which are differentially expressed according to pollen stage and temperature treatment. We were interested to identify DE genes which are indicative of certain pollen development stages. This has already been established in Arabidopsis on whole buds(Pearce *et al.*, 2015), but so far not in wheat anthers. Pollen stage specific clusters relevant to meiosis, unicellular, bicellular and tricellular stage in control conditions are shown in Figure 4.12. Cluster 1 indicates meiosis specific genes, cluster 10 specific for unicellular genes, cluster 15 corresponds with bicellular specific genes and cluster 16 corresponds with tricellular specific genes. Cluster 16 contains genes which are highly expressed at tricellular stage in both the control and heat treatment, however as previously shown there are fewer differences in differential expression at tricellular stage. Clusters 10 and 15 did not show any expression specific to the heat treatment. Cluster 1 contain 1386 DE genes, cluster 10 contains 2280, cluster 15 contains 1087 genes and cluster 16 contains 2441 genes.

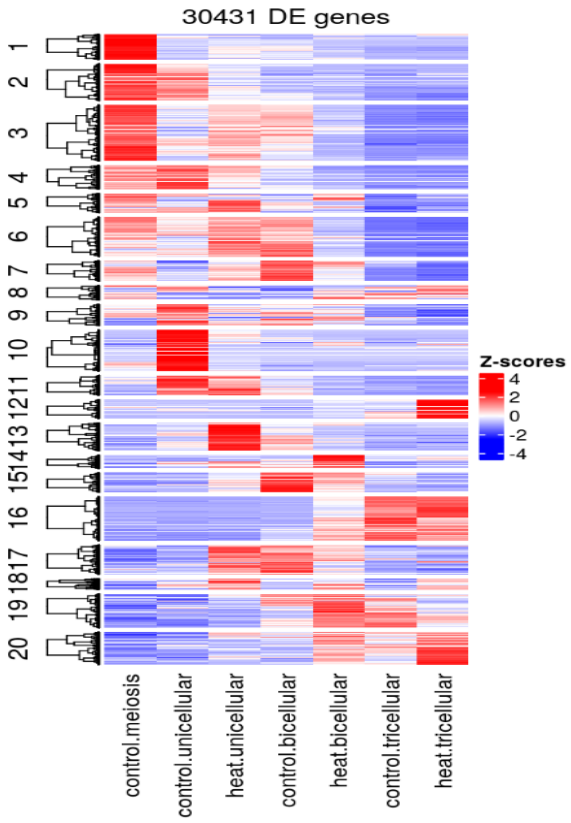

Figure 4.12: *Heat map showing the results of cluster analysis.*

20 clusters identified corresponding to the different stages and treatments. The colours correspond to the Z-score of the DE genes. Based on 4 biological replicates of anther tissue for each treatment and stage combination.

Gene Ontology (GO) enrichment analysis was conducted using the list of cluster specific genes identified. Each gene is assigned its so-called GO term. GO terms are assigned to genes as a way to predict function. GO analysis translates this list of gene functions into something more easily interpreted, owing to the numbers of DE genes. It identifies GO terms which are overrepresented. GO analysis of the clusters specific to certain pollen development stages have found genes indicative of certain stages of development in Arabidopsis (Pearce *et al.*, 2015).

GO analysis was performed on each cluster, as previously discussed, using the g:Profile tool https://biit.cs.ut.ee/gprofiler/gost. The most common corresponding GO terms for each cluster are shown in figure 4.13. Cluster 1 commonly contains genes involved in chromosome remodelling, DNA replication, chromosome segregation, these are indicative of the meiosis stage. Cluster 10 contains genes characteristic for the unicellular stage, such as those involved in pollen wall

assembly and sporopollenin biosynthesis. In cluster 15, corresponding with bicellular stage, genes involved in transmembrane transport were the most commonly expressed. Cluster 16 corresponds with tricellular stage and there was found to be extensive expression of genes involved in polysaccharide formation, consistent with starch accumulation prior to dehiscence.

A

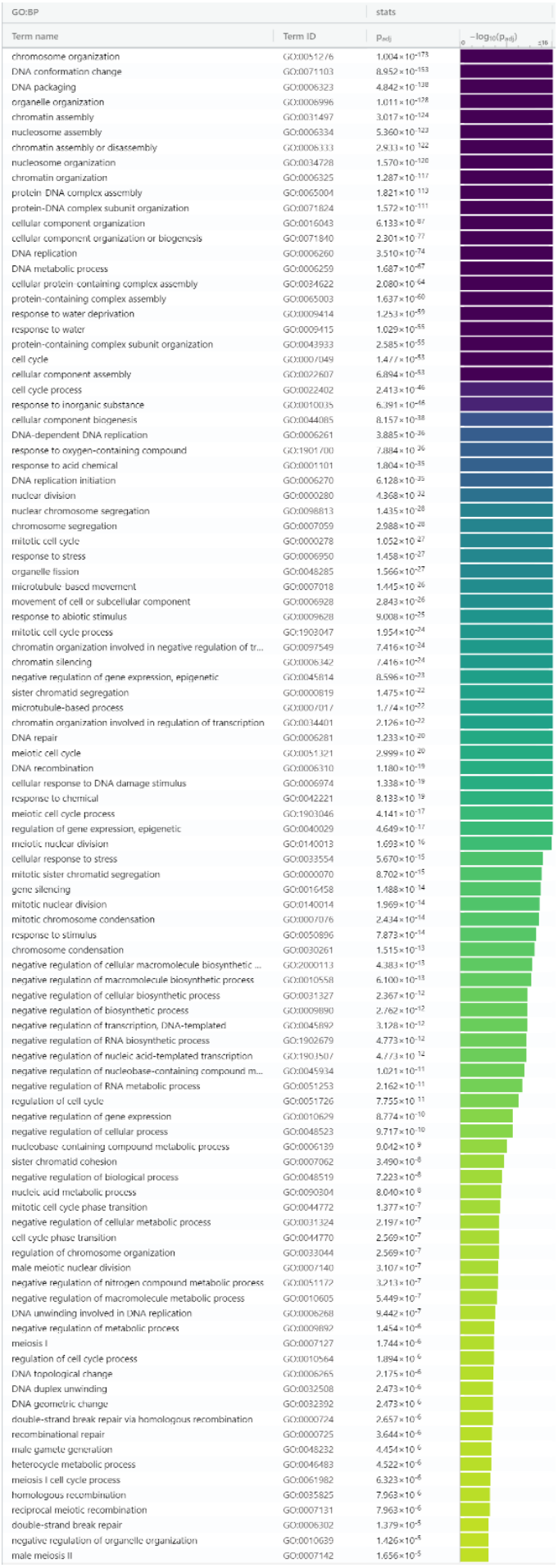

GO:BP		stats	
Term name	Term ID	p_{adj}	$-\log_{10}(p_{adj})$
chromosome organization	GO:0051276	1.004×10^{-173}	
DNA conformation change	GO:0071103	8.952×10^{-153}	
DNA packaging	GO:0006323	4.842×10^{-138}	
organelle organization	GO:0006996	1.011×10^{-128}	
chromatin assembly	GO:0031497	3.017×10^{-124}	
nucleosome assembly	GO:0006334	5.360×10^{-123}	
chromatin assembly or disassembly	GO:0006333	2.933×10^{-122}	
nucleosome organization	GO:0034728	1.570×10^{-120}	
chromatin organization	GO:0006325	1.287×10^{-117}	
protein-DNA complex assembly	GO:0065004	1.821×10^{-113}	
protein-DNA complex subunit organization	GO:0071824	1.572×10^{-111}	
cellular component organization	GO:0016043	6.133×10^{-87}	
cellular component organization or biogenesis	GO:0071840	2.301×10^{-77}	
DNA replication	GO:0006260	3.510×10^{-74}	
DNA metabolic process	GO:0006259	1.687×10^{-67}	
cellular protein-containing complex assembly	GO:0034622	2.080×10^{-64}	
protein-containing complex assembly	GO:0065003	1.637×10^{-60}	
response to water deprivation	GO:0009414	1.253×10^{-59}	
response to water	GO:0009415	1.029×10^{-55}	
protein-containing complex subunit organization	GO:0043933	2.585×10^{-55}	
cell cycle	GO:0007049	1.477×10^{-53}	
cellular component assembly	GO:0022607	6.894×10^{-53}	
cell cycle process	GO:0022402	2.413×10^{-46}	
response to inorganic substance	GO:0010035	6.391×10^{-46}	
cellular component biogenesis	GO:0044085	8.157×10^{-38}	
DNA-dependent DNA replication	GO:0006261	3.885×10^{-36}	
response to oxygen-containing compound	GO:1901700	7.884×10^{-36}	
response to acid chemical	GO:0001101	1.804×10^{-35}	
DNA replication initiation	GO:0006270	6.128×10^{-35}	
nuclear division	GO:0000280	4.368×10^{-32}	
nuclear chromosome segregation	GO:0098813	1.435×10^{-28}	
chromosome segregation	GO:0007059	2.988×10^{-28}	
mitotic cell cycle	GO:0000278	1.052×10^{-27}	
response to stress	GO:0006950	1.458×10^{-27}	
organelle fission	GO:0048285	1.566×10^{-27}	
microtubule-based movement	GO:0007018	1.445×10^{-26}	
movement of cell or subcellular component	GO:0006928	2.843×10^{-26}	
response to abiotic stimulus	GO:0009628	9.008×10^{-25}	
mitotic cell cycle process	GO:1903047	1.954×10^{-24}	
chromatin organization involved in negative regulation of tr...	GO:0097549	7.416×10^{-24}	
chromatin silencing	GO:0006342	7.416×10^{-24}	
negative regulation of gene expression, epigenetic	GO:0045814	8.596×10^{-23}	
sister chromatid segregation	GO:0000819	1.475×10^{-22}	
microtubule-based process	GO:0007017	1.774×10^{-22}	
chromatin organization involved in regulation of transcription	GO:0034401	2.126×10^{-22}	
DNA repair	GO:0006281	1.233×10^{-20}	
meiotic cell cycle	GO:0051321	2.999×10^{-20}	
DNA recombination	GO:0006310	1.180×10^{-19}	
cellular response to DNA damage stimulus	GO:0006974	1.338×10^{-19}	
response to chemical	GO:0042221	8.133×10^{-19}	
meiotic cell cycle process	GO:1903046	4.141×10^{-17}	
regulation of gene expression, epigenetic	GO:0040029	4.649×10^{-17}	
meiotic nuclear division	GO:0140013	1.693×10^{-16}	
cellular response to stress	GO:0033554	5.670×10^{-15}	
mitotic sister chromatid segregation	GO:0000070	8.702×10^{-15}	
gene silencing	GO:0016458	1.488×10^{-14}	
mitotic nuclear division	GO:0140014	1.969×10^{-14}	
mitotic chromosome condensation	GO:0007076	2.434×10^{-14}	
response to stimulus	GO:0050896	7.873×10^{-14}	
chromosome condensation	GO:0030261	1.515×10^{-13}	
negative regulation of cellular macromolecule biosynthetic ...	GO:2000113	4.383×10^{-13}	
negative regulation of macromolecule biosynthetic process	GO:0010558	6.100×10^{-13}	
negative regulation of cellular biosynthetic process	GO:0031327	2.367×10^{-12}	
negative regulation of biosynthetic process	GO:0009890	2.762×10^{-12}	
negative regulation of transcription, DNA-templated	GO:0045892	3.128×10^{-12}	
negative regulation of RNA biosynthetic process	GO:1902679	4.773×10^{-12}	
negative regulation of nucleic acid-templated transcription	GO:1903507	4.773×10^{-12}	
negative regulation of nucleobase-containing compound m...	GO:0045934	1.021×10^{-11}	
negative regulation of RNA metabolic process	GO:0051253	2.162×10^{-11}	
regulation of cell cycle	GO:0051726	7.755×10^{-11}	
negative regulation of gene expression	GO:0010629	8.774×10^{-10}	
negative regulation of cellular process	GO:0048523	9.717×10^{-10}	
nucleobase-containing compound metabolic process	GO:0006139	9.042×10^{-9}	
sister chromatid cohesion	GO:0007062	3.490×10^{-8}	
negative regulation of biological process	GO:0048519	7.223×10^{-8}	
nucleic acid metabolic process	GO:0090304	8.040×10^{-8}	
mitotic cell cycle phase transition	GO:0044772	1.377×10^{-7}	
negative regulation of cellular metabolic process	GO:0031324	2.197×10^{-7}	
cell cycle phase transition	GO:0044770	2.569×10^{-7}	
regulation of chromosome organization	GO:0033044	2.569×10^{-7}	
male meiotic nuclear division	GO:0007140	3.107×10^{-7}	
negative regulation of nitrogen compound metabolic process	GO:0051172	3.213×10^{-7}	
negative regulation of macromolecule metabolic process	GO:0010605	5.449×10^{-7}	
DNA unwinding involved in DNA replication	GO:0006268	9.442×10^{-7}	
negative regulation of metabolic process	GO:0009892	1.454×10^{-6}	
meiosis I	GO:0007127	1.744×10^{-6}	
regulation of cell cycle process	GO:0010564	1.894×10^{-6}	
DNA topological change	GO:0006265	2.175×10^{-6}	
DNA duplex unwinding	GO:0032508	2.473×10^{-6}	
DNA geometric change	GO:0032392	2.473×10^{-6}	
double-strand break repair via homologous recombination	GO:0000724	2.657×10^{-6}	
recombinational repair	GO:0000725	3.644×10^{-6}	
male gamete generation	GO:0048232	4.454×10^{-6}	
heterocycle metabolic process	GO:0046483	4.522×10^{-6}	
meiosis I cell cycle process	GO:0061982	6.323×10^{-6}	
homologous recombination	GO:0035825	7.963×10^{-6}	
reciprocal meiotic recombination	GO:0007131	7.963×10^{-6}	
double-strand break repair	GO:0006302	1.379×10^{-5}	
negative regulation of organelle organization	GO:0010639	1.426×10^{-5}	
male meiosis II	GO:0007142	1.656×10^{-5}	

Term name	Term ID	p_{adj}	$-\log_{10}(p_{adj})$
monovalent inorganic cation transport	GO:0015672	6.566×10^{-9}	
ATP metabolic process	GO:0046034	2.446×10^{-8}	
proton transmembrane transport	GO:1902600	9.663×10^{-8}	
cation transmembrane transport	GO:0098655	4.600×10^{-7}	
ATP synthesis coupled proton transport	GO:0015986	1.349×10^{-6}	
energy coupled proton transport, down electrochemical gra...	GO:0015985	1.349×10^{-6}	
ATP biosynthetic process	GO:0006754	1.486×10^{-6}	
cellular component assembly involved in morphogenesis	GO:0010927	1.820×10^{-6}	
inorganic cation transmembrane transport	GO:0098662	2.004×10^{-6}	
purine ribonucleoside triphosphate biosynthetic process	GO:0009206	5.880×10^{-6}	
purine nucleoside triphosphate biosynthetic process	GO:0009145	5.880×10^{-6}	
purine ribonucleoside triphosphate metabolic process	GO:0009205	5.880×10^{-6}	
purine nucleoside triphosphate metabolic process	GO:0009144	6.414×10^{-6}	
inorganic ion transmembrane transport	GO:0098660	1.124×10^{-5}	
pollen wall assembly	GO:0010208	1.854×10^{-5}	
polyamine metabolic process	GO:0006595	2.254×10^{-5}	
ribonucleoside triphosphate biosynthetic process	GO:0009201	3.799×10^{-5}	
ribonucleoside triphosphate metabolic process	GO:0009199	3.799×10^{-5}	
ion transmembrane transport	GO:0034220	4.019×10^{-5}	
nucleoside triphosphate biosynthetic process	GO:0009142	4.096×10^{-5}	
polyamine biosynthetic process	GO:0006596	1.012×10^{-4}	
carbohydrate transport	GO:0008643	1.080×10^{-4}	
cation transport	GO:0006812	3.296×10^{-4}	
nucleoside triphosphate metabolic process	GO:0009141	3.673×10^{-4}	
photorespiration	GO:0009853	3.882×10^{-4}	
purine-containing compound biosynthetic process	GO:0072522	7.768×10^{-4}	
purine ribonucleotide biosynthetic process	GO:0009152	1.178×10^{-3}	
photosynthesis	GO:0015979	1.202×10^{-3}	
purine ribonucleotide metabolic process	GO:0009150	1.479×10^{-3}	
pollen exine formation	GO:0010584	2.221×10^{-3}	
purine nucleotide biosynthetic process	GO:0006164	2.563×10^{-3}	
spermidine metabolic process	GO:0008216	2.610×10^{-3}	
purine-containing compound metabolic process	GO:0072521	2.951×10^{-3}	
purine nucleotide metabolic process	GO:0006163	3.334×10^{-3}	
sporopollenin biosynthetic process	GO:0080110	3.382×10^{-3}	
ion transport	GO:0006811	4.256×10^{-3}	
ribonucleotide metabolic process	GO:0009259	4.424×10^{-3}	
ribose phosphate metabolic process	GO:0019693	4.911×10^{-3}	
ribonucleotide biosynthetic process	GO:0009260	5.293×10^{-3}	
ribose phosphate biosynthetic process	GO:0046390	6.084×10^{-3}	
fatty acid derivative biosynthetic process	GO:1901570	7.621×10^{-3}	
response to molecule of fungal origin	GO:0002238	9.485×10^{-3}	
anatomical structure formation involved in morphogenesis	GO:0048646	1.103×10^{-2}	
amine biosynthetic process	GO:0009309	1.323×10^{-2}	
cellular biogenic amine biosynthetic process	GO:0042401	1.323×10^{-2}	
cellular aldehyde metabolic process	GO:0006081	1.655×10^{-2}	
nucleotide biosynthetic process	GO:0009165	1.990×10^{-2}	
nucleoside phosphate biosynthetic process	GO:1901293	2.139×10^{-2}	
long-chain fatty acid metabolic process	GO:0001676	2.733×10^{-2}	
nucleotide metabolic process	GO:0009117	2.918×10^{-2}	
generation of precursor metabolites and energy	GO:0006091	2.925×10^{-2}	
respiratory electron transport chain	GO:0022904	3.395×10^{-2}	
spermidine biosynthetic process	GO:0008295	3.607×10^{-2}	
fatty acid derivative metabolic process	GO:1901568	3.607×10^{-2}	
nucleoside phosphate metabolic process	GO:0006753	3.717×10^{-2}	
cellular biogenic amine metabolic process	GO:0006576	4.475×10^{-2}	

C

Term name	Term ID	p_{adj}	$-\log_{10}(p_{adj})$
transmembrane transport	GO:0055085	2.576×10^{-18}	
transport	GO:0006810	6.829×10^{-11}	
establishment of localization	GO:0051234	9.367×10^{-11}	
localization	GO:0051179	2.053×10^{-10}	
ion transmembrane transport	GO:0034220	1.662×10^{-5}	
pyridoxal phosphate metabolic process	GO:0042822	2.200×10^{-5}	
pyridoxal phosphate biosynthetic process	GO:0042823	2.200×10^{-5}	
organonitrogen compound biosynthetic process	GO:1901566	2.514×10^{-5}	
cation transmembrane transport	GO:0098655	9.712×10^{-5}	
aldehyde biosynthetic process	GO:0046184	1.506×10^{-4}	
vitamin B6 metabolic process	GO:0042816	3.219×10^{-4}	
vitamin B6 biosynthetic process	GO:0042819	3.219×10^{-4}	
ion transport	GO:0006811	6.143×10^{-4}	
inorganic cation transmembrane transport	GO:0098662	1.286×10^{-3}	
inorganic ion transmembrane transport	GO:0098660	3.578×10^{-3}	
pyridine-containing compound biosynthetic process	GO:0072525	4.270×10^{-3}	
pyridine-containing compound metabolic process	GO:0072524	4.270×10^{-3}	
cation transport	GO:0006812	6.851×10^{-3}	
cellular amino acid biosynthetic process	GO:0008652	7.978×10^{-3}	
urea transmembrane transport	GO:0071918	1.841×10^{-2}	
one carbon compound transport	GO:0019755	1.841×10^{-2}	
urea transport	GO:0015840	1.841×10^{-2}	
monovalent inorganic cation transport	GO:0015672	3.612×10^{-2}	
proton transmembrane transport	GO:1902600	3.869×10^{-2}	
coenzyme metabolic process	GO:0006732	4.441×10^{-2}	
indolalkylamine biosynthetic process	GO:0046219	4.451×10^{-2}	
tryptophan biosynthetic process	GO:0000162	4.451×10^{-2}	

D

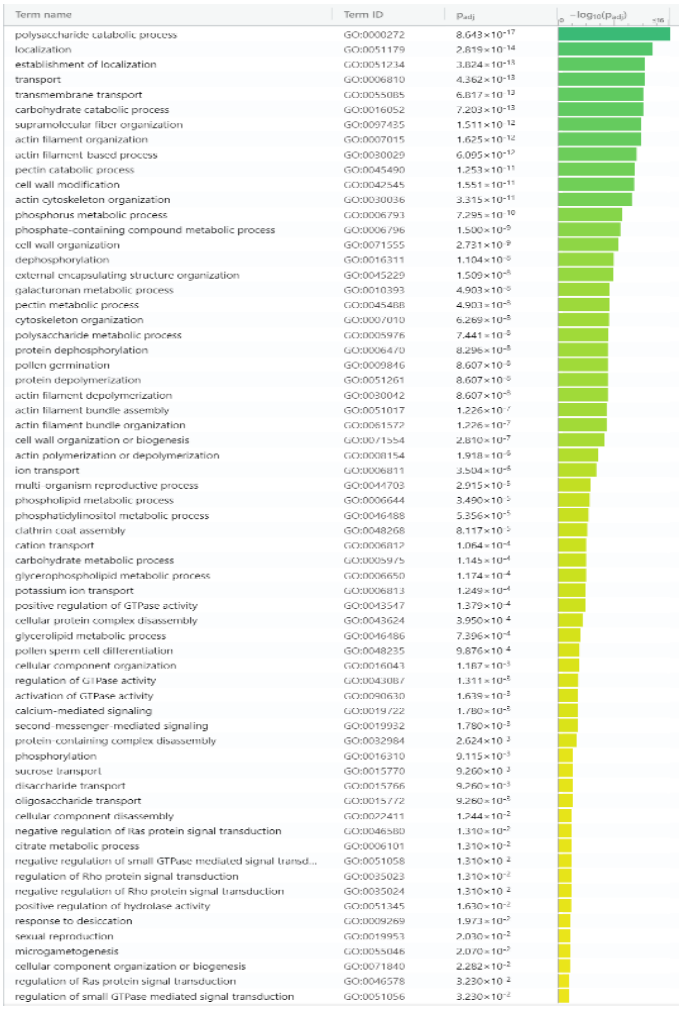

Term name	Term ID	p_{adj}
polysaccharide catabolic process	GO:0000272	8.643×10^{-17}
localization	GO:0051179	2.619×10^{-14}
establishment of localization	GO:0051234	3.824×10^{-13}
transport	GO:0006810	4.362×10^{-13}
transmembrane transport	GO:0055085	6.817×10^{-13}
carbohydrate catabolic process	GO:0016052	7.203×10^{-13}
supramolecular fiber organization	GO:0097435	1.511×10^{-12}
actin filament organization	GO:0007015	1.625×10^{-12}
actin filament based process	GO:0030029	6.095×10^{-12}
pectin catabolic process	GO:0045490	1.253×10^{-11}
cell wall modification	GO:0042545	1.551×10^{-11}
actin cytoskeleton organization	GO:0030036	3.315×10^{-11}
phosphorus metabolic process	GO:0006793	7.295×10^{-10}
phosphate-containing compound metabolic process	GO:0006796	1.500×10^{-9}
cell wall organization	GO:0071555	2.731×10^{-9}
dephosphorylation	GO:0016311	1.104×10^{-8}
external encapsulating structure organization	GO:0045229	1.509×10^{-8}
galacturonan metabolic process	GO:0010393	4.903×10^{-8}
pectin metabolic process	GO:0045488	4.903×10^{-8}
cytoskeleton organization	GO:0007010	6.269×10^{-8}
polysaccharide metabolic process	GO:0005976	7.441×10^{-8}
protein dephosphorylation	GO:0006470	8.296×10^{-8}
pollen germination	GO:0009846	8.607×10^{-8}
protein depolymerization	GO:0051261	8.607×10^{-8}
actin filament depolymerization	GO:0030042	8.607×10^{-8}
actin filament bundle assembly	GO:0051017	1.226×10^{-7}
actin filament bundle organization	GO:0061572	1.226×10^{-7}
cell wall organization or biogenesis	GO:0071554	2.810×10^{-7}
actin polymerization or depolymerization	GO:0008154	1.918×10^{-6}
ion transport	GO:0006811	3.504×10^{-6}
multi-organism reproductive process	GO:0044703	2.915×10^{-5}
phospholipid metabolic process	GO:0006644	3.490×10^{-5}
phosphatidylinositol metabolic process	GO:0046488	5.356×10^{-5}
clathrin coat assembly	GO:0048268	8.117×10^{-5}
cation transport	GO:0006812	1.064×10^{-4}
carbohydrate metabolic process	GO:0005975	1.145×10^{-4}
glycerophospholipid metabolic process	GO:0006650	1.174×10^{-4}
potassium ion transport	GO:0006813	1.249×10^{-4}
positive regulation of GTPase activity	GO:0043547	1.379×10^{-4}
cellular protein complex disassembly	GO:0043624	3.950×10^{-4}
glycerolipid metabolic process	GO:0046486	7.396×10^{-4}
pollen sperm cell differentiation	GO:0048235	9.876×10^{-4}
cellular component organization	GO:0016043	1.187×10^{-3}
regulation of GTPase activity	GO:0043087	1.311×10^{-3}
activation of GTPase activity	GO:0090630	1.639×10^{-3}
calcium-mediated signaling	GO:0019722	1.780×10^{-3}
second-messenger-mediated signaling	GO:0019932	1.780×10^{-3}
protein-containing complex disassembly	GO:0032984	2.624×10^{-3}
phosphorylation	GO:0016310	9.115×10^{-3}
sucrose transport	GO:0015770	9.260×10^{-3}
disaccharide transport	GO:0015766	9.260×10^{-3}
oligosaccharide transport	GO:0015772	9.260×10^{-3}
cellular component disassembly	GO:0022411	1.244×10^{-2}
negative regulation of Ras protein signal transduction	GO:0046580	1.310×10^{-2}
citrate metabolic process	GO:0006101	1.310×10^{-2}
negative regulation of small GTPase mediated signal transd...	GO:0051058	1.310×10^{-2}
regulation of Rho protein signal transduction	GO:0035023	1.310×10^{-2}
negative regulation of Rho protein signal transduction	GO:0035024	1.310×10^{-2}
positive regulation of hydrolase activity	GO:0051345	1.630×10^{-2}
response to desiccation	GO:0009269	1.973×10^{-2}
sexual reproduction	GO:0019953	2.030×10^{-2}
microgametogenesis	GO:0055046	2.070×10^{-2}
cellular component organization or biogenesis	GO:0071840	2.282×10^{-2}
regulation of Ras protein signal transduction	GO:0046578	3.230×10^{-2}
regulation of small GTPase mediated signal transduction	GO:0051056	3.230×10^{-2}

Figure 4.13: *GO enrichment analysis of pollen stage related clusters.*

A: *clusters 1 (meiosis),* **B**: *cluster 10 (unicellular),* **C**: *cluster 15 (bicellular) and* **D**: *cluster 16 (tricellular) shows GO terms of genes which are highly expressed in anthers at these pollen developmental stages.*

Comparisons were made between expressed genes at control and heat treatments at unicellular, bicellular and tricellular stages, as well as an overall comparison between control and heat treatments including all stages. The result was a calculation of the number of significantly differentially expressed (DE) genes and transcripts. The cut off P-value for significance was 0.01. This was calculated as a log2 fold change (log2FC).

In total there were 107,891 raw genes. Of these 66,764 were found to be expressed in the anther (CPM cut-off of 1), with 1 minimum sample to CPM cut-off.

Comparisons were made at unicellular, bicellular and tricellular stages, as well as comparing all regardless of stage. All comparisons showed a high number of genes which are differentially expressed (Table 4.1). Unicellular and bicellular stages showed the greatest number of differentially expressed genes between both treatments, showing 15118 and 16680 DE genes respectively, with tricellular stage showing 4498 DE genes. Unicellular stage also showed the highest number of DE transcripts at 17162, closely followed by bicellular stage at 13692. It appears that unicellular stage was most transcriptionally affected by heat stress, with progressively fewer differences as pollen development progressed.

Table 4.1: *A comparisons of the changes in gene expression in response to heat stress when directly comparing within the same stage separately and all stages (unicellular, bicellular and tricellular stage) together.*

DE (differentially expressed) gene/transcripts are when there was found to be a significant log_2 fold change in gene/transcript abundance between the control and heat stress treatment (t-test, $p < 0.01$ and $L_2FC \geq 0.5$).

Pollen stage	DE genes	DE transcripts
Unicellular	15118	17162
Bicellular	16680	13692
Tricellular	4498	2899
All stages	8382	7035

The top 10 up- and down-regulated genes, which compares control and heat stressed plants, are shown in table 4.2. Comparisons were made between unicellular, bicellular, tricellular stages and when comparing all three stages of pollen development. Most of these genes are of unknown function and their predicted function is based on their BLAST2GO description. A number of genes which are likely to be dehydrins are upregulated in the heat treatment: *TraesCS3D02G390200* at unicellular stage and *TraesCS3D02G390200* across all stages. Dehydrins are hydrophilic proteins which are thought to serve a number of roles related to stress tolerance, including reducing oxidative stress and preventing

protein denaturation(Reviewed by Liu *et al.*, 2017). Increased expression of various dehydrins in response to cold stress was reported in wheat and barley (Kosová *et al.*, 2011) and therefore this could be a general response to abiotic stress.

Many downregulated genes encode putative pectinesterases. *TraesCS2A02G344200, TraesCS2D02G322500, TraesCS2D02G523700* and *TraesCS2B02G341700* are all predicted to be pectinesterases and are downregulated in response to heat stress at bicellular stage. Pectinesterases are involved in modifying plant cell walls. Their reduction in expression could be a direct result of the earlier heat treatment. Pectinesterases have been found to be highly expressed during the later stages of pollen development in rice(Wang *et al.*, 2020). Arabidopsis pectin methylesterase mutants, *atppme1* and *BoPMEI1*, both showed growth retardation of their pollen tube(Tian *et al.*, 2006; Zhang *et al.*, 2010). *BoPMEI1* was found to be specifically expressed mostly in mature pollen and in germinating pollen(Zhang *et al.*, 2010). Their function is key in determining pollen tube growth as the apical pollen tube is constituted primarily of pectin(Ferguson *et al.*, 1998). The results suggest that the heat stressed pollen could be less capable of germinating and potentially will have defects in pollen tube elongation.

Table 4.2: *The top 10 up and downregulated genes when comparing control and heat treatments across individual stages (unicellular, bicellular and tricellular) and all stages.*

For each gene, the log2 fold change (FC) and p-value are shown along, with the Blast2Go description and knetminer gene name.

Stage	Expression	iwgsc_refseqv1.0	adj.pval	log2FC	BLAST2GO description	Knetminer gene name
Unicellular	Upregulated	*TraesCS1B02G349600*	2.40E-10	12.18	rRNA N-glycosidase	
		TraesCS3D02G390200	1.41E-10	11.78	Dehydrin	
		TraesCS4D02G118000	4.08E-10	11.09	Lipid transfer protein	
		TraesCS7B02G285300	1.14E-05	11.02	Carbonic anhydrase	*ATACA8*
		TraesCS7A02G382600	1.02E-07	11.01	Carbonic anhydrase	*ACA7*
		TraesCS2A02G400400	4.42E-10	10.83	Cytochrome P450 family protein	
		TraesCS1D02G115400	3.88E-10	10.63	Receptor protein kinase, putative	
		TraesCS2D02G342200	4.37E-08	10.60	Short-chain dehydrogenase/reductase 3	*KCR1*
		TraesCS7D02G379000	1.25E-06	10.36	Carbonic anhydrase	*ACA7*
		TraesCS1B02G292200	7.96E-08	10.27	Glycerol-3-phosphate acyltransferase	*GPAT5*
	Downregulated	*TraesCS2A02G004500*	3.17E-04	-10.82	Cytochrome P450 family protein, expressed	
		TraesCS1A02G310000	7.92E-05	-10.83	BURP domain protein RD22	
		TraesCS5D02G398300	5.12E-06	-11.00	Beta-glucosidase	
		TraesCS7B02G393200	1.76E-07	-11.05	WAT1-related protein	
		TraesCS1D02G268200	5.95E-05	-11.12	Queuine tRNA-ribosyltransferase	
		TraesCS2D02G089000	3.64E-11	-11.35	Short-chain dehydrogenase/reductase family protein	*SDR2A*
		TraesCS2D02G088900	1.34E-10	-12.48	Short-chain dehydrogenase/reductase family protein	*SDR2A*
		TraesCSU02G012200	9.59E-08	-12.52		
		TraesCS2B02G591900	2.82E-04	-12.72	Beta-glucosidase	
		TraesCS3B02G442100	4.39E-04	-13.09	Aldose 1-epimerase	
Bicellular	Upregulated	*TraesCS3D02G105500*	1.09E-04	7.42	Fasciclin-like arabinogalactan protein	*FLA11*
		TraesCS2B02G075700	1.51E-04	7.50	Proline-rich protein, putative, expressed	
		TraesCS5A02G401100	4.35E-04	7.63	N-acetyltransferase, putative, expressed	*HLS1*
		TraesCS2D02G414800	3.24E-03	7.68	Oleosin	
		TraesCS1D02G317700	5.50E-05	7.77	Peroxidase	*PER2*
		TraesCS5B02G364200	1.08E-04	7.90	Cytochrome P450 family protein, expressed	
		TraesCSU02G182700	2.53E-03	8.57		
		TraesCS6D02G092200	4.81E-04	8.68	Proline-rich protein	

		TraesCS6A02G103600	2.81E-03	8.74	Proline-rich protein	
		TraesCS6B02G473500	7.83E-06	9.72	Pentatricopeptide repeat-containing protein	
	Downregulated	*TraesCS2A02G344200*	2.84E-09	-14.84	Pectinesterase	*VGDH2*
		TraesCS6D02G153500	3.15E-07	-14.56	Pectin lyase-like superfamily protein, putative	
		TraesCS2D02G322500	1.44E-08	-14.38	Pectinesterase	*VGDH2*
		TraesCS6B02G192300	6.82E-09	-14.37	Pectin lyase-like superfamily protein	
		TraesCS2D02G523700	1.74E-09	-14.33	Pectinesterase	*VGDH2*
		TraesCS2B02G341700	6.47E-09	-14.32	Pectinesterase	*PME5*
		TraesCS7B02G304400	1.56E-08	-14.08	Pectin lyase-like superfamily protein	
		TraesCS6A02G159000	1.61E-08	-13.99	Pectin lyase-like superfamily protein	
		TraesCS7A02G405000	6.00E-08	-13.72	Pectin lyase-like superfamily protein, putative	
		TraesCS7D02G399000	9.92E-10	-13.67	Pectin lyase-like superfamily protein, putative	
Tricellular	**Upregulated**	*TraesCS1B02G207600*	5.34E-04	3.70	Replication factor C subunit, putative	
		TraesCS4D02G061900	4.91E-03	3.81	Sugar transporter family protein	
		TraesCS2A02G340700	7.07E-03	3.83	Sugar transporter, putative	
		TraesCS3B02G252600	1.66E-03	3.97	ATP-dependent RNA helicase	*STRS2*
		TraesCS5B02G277000	2.92E-03	3.99	Receptor-like kinase	
		TraesCS6D02G255900	4.98E-04	4.02	Protein MIZU-KUSSEI 1	
		TraesCS6A02G258000	2.60E-03	4.08	transcription repressor	
		TraesCS4A02G004400	4.63E-03	4.10	Metal transporter, putative	
		TraesCS7A02G388700	6.19E-03	4.19	GDSL esterase/lipase	
		TraesCS6B02G030800	6.02E-03	4.85	Hydroxycinnamoyl-CoA shikimate/quinate hydroxycinnamoyltransferase	*SHT*
	Downregulated	*TraesCS7A02G070500*	4.06E-04	-9.89	Avr9/Cf-9 rapidly elicited protein	
		TraesCS5D02G360600	2.92E-03	-9.44	11S globulin seed storage protein 2	
		TraesCS7D02G065700	8.32E-03	-9.19	Avr9/Cf-9 rapidly elicited protein	
		TraesCS5A02G537900	7.52E-06	-8.08	Serine/threonine-protein kinase	
		TraesCS2A02G424100	4.83E-04	-7.94	F-box family protein	
		TraesCS7D02G067400	7.30E-03	-7.85	Avr9/Cf-9 rapidly elicited protein	
		TraesCS5A02G537800	1.11E-07	-7.81	Serine/threonine-protein kinase	
		TraesCS6D02G063100	4.17E-05	-7.41	Cytochrome P450	
		TraesCS7A02G200200	4.39E-03	-7.32	Potassium channel	*SKOR*
		TraesCS3A02G061600	1.75E-04	-7.24	Cytochrome P450	
Uni/Bi/Tricellular	**Upregulated**	*TraesCS2D02G314500*	3.58E-03	3.75	Aspartic proteinase nepenthesin-1	
		TraesCS4D02G118000	6.13E-04	3.81	Lipid transfer protein	
		TraesCS3D02G390200	6.13E-04	3.86	Dehydrin	

	TraesCS1B02G349600	9.72E-05	3.88	rRNA N-glycosidase	
	TraesCS2D02G272200	7.98E-05	3.88	4-coumarate--CoA ligase family protein	*4CLL1*
	TraesCS2A02G316600	9.49E-03	4.02	Aspartic proteinase nepenthesin-1	
	TraesCS2D02G342200	7.54E-04	4.16	Short-chain dehydrogenase/reductase 3	*KCR1*
	TraesCS4A02G195500	2.34E-03	4.30	Lipid transfer protein	
	TraesCS2A02G321300	2.75E-04	4.31	Short-chain dehydrogenase/reductase 3	*KCR1*
	TraesCS4B02G119700	1.83E-05	4.48	Lipid transfer protein	
Downregulated	*TraesCS1B02G481400*	1.24E-05	-5.47	O-methyltransferase-like protein	*ASMT*
	TraesCS2D02G126100	6.59E-09	-5.38	Cellulose synthase, putative	*CSLD4*
	TraesCSU02G246000	1.14E-06	-5.34		*ASMT*
	TraesCS6B02G192300	5.38E-06	-5.19	Pectin lyase-like superfamily protein	
	TraesCS2A02G344200	4.62E-06	-5.17	Pectinesterase	*VGDH2*
	TraesCS3D02G061900	2.37E-04	-5.02	Cytochrome P450	
	TraesCS2B02G341700	1.11E-05	-5.00	Pectinesterase	*PME5*
	TraesCS7D02G399000	1.26E-06	-4.97	Pectin lyase-like superfamily protein, putative	
	TraesCS6B02G029200	1.42E-05	-4.96	gamma carbonic anhydrase-like 2	
	TraesCS7B02G304400	2.66E-05	-4.88	Pectin lyase-like superfamily protein	

4.3.4 Changes in expression of key genes involved in hormone synthesis/degradation

Transcriptional data from rice anthers showed the remarkably complex expression of genes involved in hormone biosynthesis/degradation and the downstream targets of hormone signalling(Hirano *et al.*, 2008). Using the RNAseq data we sought to identify the expression of orthologous genes in wheat anthers in control and after heat stress conditions. This new dataset will prove a valuable resource in understanding the key genes involved in the anther development of wheat. By comparing the control samples to the heat-treated sample, we can draw conclusions as to which genes change their expression in accordance with the heat treatment. These genes could give molecular explanations for the changes in hormone accumulation observed in section 4.3.2, and also suggest possible causes of sterility.

A complete list of wheat orthologues of known hormone signalling, synthesis and deactivation genes was investigated for changes in response to heat stress (Supplementary Table 2). The wheat orthologues of biosynthesis and degradation

genes were found through orthologue searches of rice genes taken from(Hirano *et al.*, 2008). These genes were searched for in the list of 8382 DE genes which were found to be differentially expressed in control/heat treatment when grouping together unicellular, bicellular and tricellular stages (t test, $p < 0.01$ and $L_2FC \geq 0.5$). The mean raw TPM for each of the treatments was plotted in a heatmap.

Auxin:

Wheat orthologues of IAA biosynthesis and downstream signalling genes were found from the those identified in rice (Supplementary Table 2)(Hirano *et al.*, 2008). IAA biosynthesis is thought to originate from chorismate, which is then converted to tryptophan (Trp), followed by conversion to a number of IAA precursors, and finally it is converted to bioactive IAA (Figure 4.4)(Reviewed by Korasick, Enders and Strader, 2013). Each step of the pathway is catalysed by different enzymes, some known and some unknown. The wheat orthologues of the IAA biosynthesis gene *YUCCA6* (involved in the process of converting tryptamine to the IAA (Zhao *et al.*, 2001)) were found to be upregulated at the unicellular stage in heat stressed plants(Figure 4.4). The wheat orthologues of rice *Nitrilase* (*NIT*) genes involved in converting the IAA precursor, IAN (indole-3-acetonitrile), to IAA(Normanly *et al.*, 1997)) were upregulated at both the heat bicellular and tricellular stages. Taken together the transcriptional data suggests that heat is leading to upregulation of the IAA biosynthesis pathway.

Downstream of IAA, the expression of several wheat Aux/IAAs is increased by the heat treatment (Figure 4.14). Aux/IAAs repress the expression of auxin responsive genes(Ulmasov *et al.*, 1997), but they are degraded in the presence of auxin(Gray *et al.*, 2001; Dos Santos Maraschin *et al.*, 2009). Wheat orthologues of *IAA1/6/13* were found to be significantly upregulated after heat treatment. This could be due to the slight, but not significant accumulation of auxin observed (Figure 4.7). Increase in Aux/IAA expression could be in response to negative feedback of increased degradation of the IAA proteins in response to increased auxin. Downstream of this, the Auxin Response Factors (ARFs) do not appear to show consistent expression,

some showing greater expression and some showing lower expression after heat treatment. Therefore, making it difficult to draw a conclusion from this.

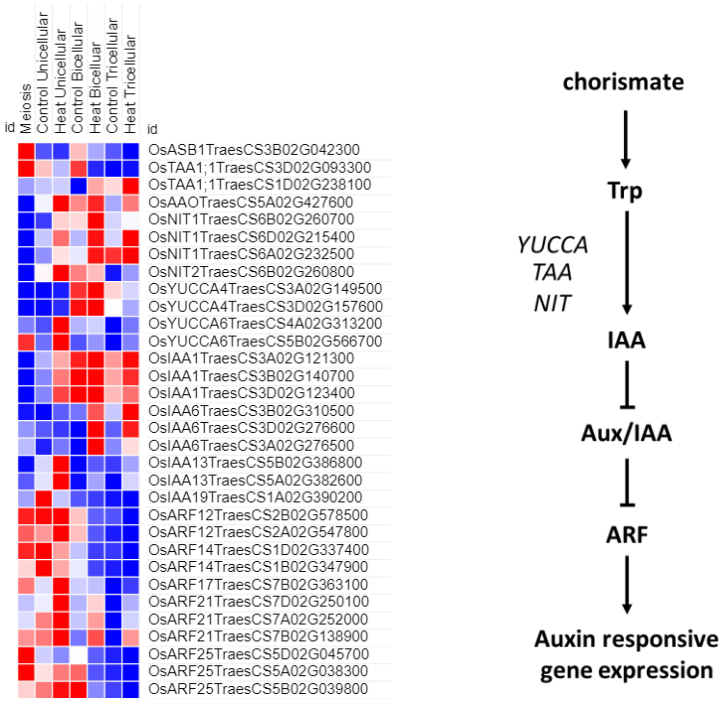

Figure 4.14: *Expression profile of anthers showing wheat orthologues of genes involved in auxin synthesis and signalling whose expression was significantly impacted by heat treatment.*

Anther samples were initially taken at meiosis stage (FLS 9-13cm), followed by unicellular, bicellular and tricellular stages after being exposed to either control conditions (4 days 20/15°C day/night) or heat stress conditions (4 days 33/26°C day/night) from meiosis stage. Samples were staged using the Ampha Z32 Pollen Analyzer. The heat map shows the average raw TPM. Each box represents the mean of 4 biological replicates.

<u>Jasmonic Acid:</u>

JA biosynthesis is initiated by the release of α-linolenic acid from the chloroplast membrane by lipases, such as *DAD1* (Ishiguro *et al.*, 2001). It is then transformed into OPDA (another precursor of JA) by a series of enzymes: AOS, AOC, LOX (Bell *et al.*, 1995; Maucher *et al.*, 2000; Ziegler *et al.*, 2000). OPDA is then converted to JA by a number of different enzymes, including OPDA reductase (OPR), acyl-CoA oxidase (ACX) and then via a series of β–oxidations by a number of different

enzymes, one being the multifunctional protein AIM1(Reviewed by Wasternack and Hause, 2013).

In the hormone analysis we found a significantly greater accumulation of JA and JA-Ile at unicellular stage after heat treatment (Figure 4.7). This has been hypothesised to be due to upregulation of JA biosynthesis genes in the anthers.

Allene oxide cyclase (AOC) is an enzyme which is involved in converting allene oxide to 12-oxo-phytodienoic acid (OPDA), a precursor of JA(Ziegler *et al.*, 1997, 2000). The rice AOC gene has a very high level of similarity to all three of the wheat homoeologues: *TraesCS6A02G334800*: 91.6% ID, *TraesCS6B02G365200*: 90.7% ID and *TraesCS6D02G314300*: 91.3% ID to the peptide sequence of the rice orthologue. There was only 1 orthologue found in wheat (Supplementary Table 2). All three of the wheat homoeologues were found to be upregulated at unicellular heat stage (Figure 4.15).

AIM1 is a 3-hydroxyacyl-CoA dehydrogenase involved in β-oxidation, known to be involved in biosynthesis of JA and SA(Richmond and Bleecker, 1999; L. Xu *et al.*, 2017). AIM1 is represented by a single gene in rice, but BLAST searches of the peptide sequence in the wheat genome reveals that it clusters closely with two wheat genes, each with three homoeologues on each of the wheat sub-genomes (Supplementary Table 2). Three homoeologues across the two genes were found to be upregulated at unicellular stage after heat treatment: *TraesCS6B02G153900, TraesCS6D02G116200 and TraesCS3D02G077200. TraesCS6B02G153900* has 88.8%ID, *TraesCS6D02G116200* has 88.4 % ID and *TraesCS3D02G077200* has 88% ID to the peptide sequence of the rice orthologue. The high level of similarity suggests that they have conserved function.

Other JA biosynthesis genes such as *DAD1;3, LOX2;5, OPR7* and *OPCL1* genes are upregulated by the heat treatment only at the tricellular stage (Figure 4.4).

JAR1 is an enzyme involved in conjugating JA to bioactive JA-Ile(Staswick *et al.*, 2002). There was found to be only one orthologue of rice *JAR1* in the wheat genome, and one homoeologue on every sub-genome (Supplementary Table 2). Compared to the rice JAR1 peptide sequence, TraesCS1A02G425100 has 87.4 %ID,

TraesCS1B02G459500 has 88.4 %ID and TraesCS1D02G434100 has 88.1 %ID. There was found to be an increase in expression of B and D homoeologues (but not the A homoeologue).

Downstream of the JA signalling pathways are JAZ proteins. JAZ proteins are active repressors of JA responsive genes expression. In the presence of JA-Ile, JAZ proteins are recognised by the SCFCOI1 complex and targeted for degradation by the 26S proteasome. Their degradation allows the release of transcription factors, such as *MYC2*, which positively bind to JA-responsive elements of promoters leading to activation of JA-mediated expression(Reviewed by Wasternack and Hause, 2013). Wheat orthologues of rice *JAZ1/3/5/7* along with all three of the orthologues of rice *OsMYC2* showed higher expression at tricellular stage after heat treatment.

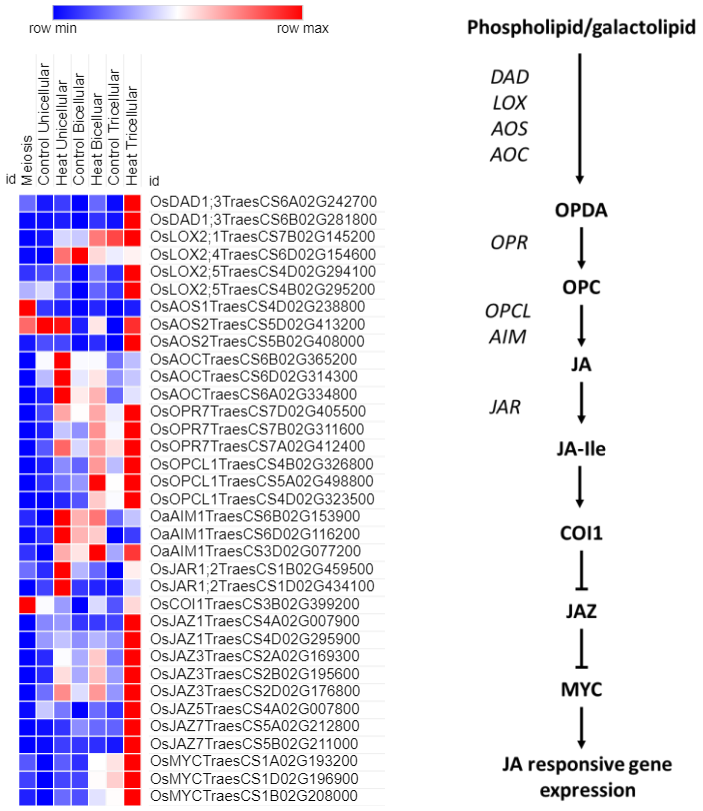

Figure 4.15: *Expression profile of anthers showing wheat orthologues of genes involved in JA synthesis and signalling whose expression was significantly impacted by heat treatment.*

Anther samples were collected as described in figure 4.14. The heat map shows the average raw TPM. Each box represents the mean of 4 biological replicates.

Ethylene:

In rice, ethylene biosynthesis is initiated by the conversion of S-adenosyl-methionine (SAM) to Amino-cyclopropane-1-carboxylic acid (ACC) by ACC synthetase (ACS). ACC is then converted to ethylene by ACC oxidase (ACO) (Reviewed by Rzewuski and Sauter, 2008). The wheat orthologue of rice *ACS2* was found to be highly upregulated at the heat bicellular stage on all three of its homoeologues (Figure 4.16). A number of *ACO* genes also appear to have a higher expression after heat treatment. These genes are ACOs which cluster closest to rice *OsACO1* (*Os09g0451400*) and *OsACO3* (*Os09g0451000*) (Supplementary Table 2).

Taken together this suggests that the ethylene biosynthetic pathway is upregulated by heat.

An accumulation of ethylene leads to inactivation of ethylene receptors, which relieves the suppression of *ETHYLENE INSENSITIVE2* (*EIN2*). EIN2 activates EIN3 which initiates expression of ethylene responsive genes(Chao *et al.*, 1997; Solano *et al.*, 1998; Alonso *et al.*, 2003; Binder, 2020). All three of the homoeologues of the wheat orthologue of rice ethylene responsive receptor *ETR1;2* (later renamed *OsERS2*- See Section 6.3.1) were upregulated at the bicellular stage after heat treatment (Figure 4.16). In Arabidopsis leaf tissue, expression of *ETR1* and *EIN4* were not found to be upregulated by ethylene, whereas *ERS1*, *ERS2* and *ETR2* were found to be upregulated(Hua *et al.*, 1998). *OsERS2* is phylogenetically closest to Arabidopsis *ERS2* (Figure 6.4), therefore suggesting that this increase in expression in response to heat could be due to an accumulation of ethylene. Further downstream, few wheat members of the wheat EIN3 family were upregulated at the bicellular heat stage (Figure 4.16). Overall, the expression suggests high expression of ethylene signalling components at bicellular stage after heat treatment.

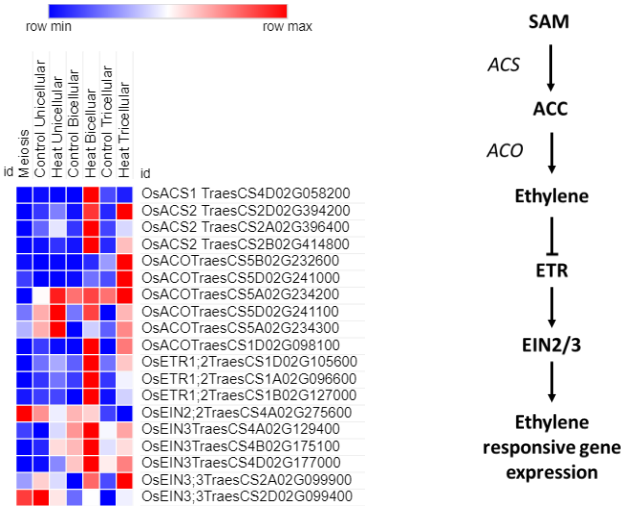

Figure 4.16: *Expression profile of anthers showing wheat orthologues of genes involved in ethylene synthesis and signalling whose expression was significantly impacted by heat treatment.*

Anther samples were collected as described in figure 4.14. The heat map shows the average raw TPM. Each box represents the mean of 4 biological replicates.

Gibberellin:

GA_1, GA_3, GA_4 and GA_7 are the bioactive form of gibberellin in higher plants. There has been observed to be a huge accumulation of GA_4 in particular in mature anthers of rice(Hirano *et al.*, 2008). Therefore, we could consider GA_4 to be the main bioactive gibberellin active in the anther. Indeed, GA_4 appears to be the most dominant bioactive GA in wheat anthers towards the later stages of pollen development (Figure 4.11).

GA transcriptional activity appears to occur in response to heat mostly at the tricellular stage. There was found to be a high level of expression of *GA20ox2/4*, especially at the tricellular stage of the heat-treated plants (Figure 4.17). GA20ox catalyses the conversion of $GA_{12}/_{53}$ to precursors of bioactive forms of GA ($GA_9/_{20}$). $GA_9/_{20}$ are then converted to GA_4 and GA_1 respectively by the action of GA3ox(Hedden and Phillips, 2000). There was also found to be higher levels of expression of the GA receptor GID1 at the tricellular heat stage too, suggesting a greater GA response(Ueguchi-Tanaka *et al.*, 2005). The presence of GA allows GID1 to interact with DELLAs (a negative regulator of GA responsive expression), which subsequently leads to the degradation of DELLA through the SCF^{GID2} complex, therefore relieving repression of GA responsive gene expression(Ikeda *et al.*, 2001; Sasaki *et al.*, 2003).

Along with findings indicating an accumulation of bioactive GAs and their signalling it must be noted that there also appears to be an increase in expression of the deactivating enzymes (Figure 4.17). EUI is a GA deactivating enzyme which was discovered in rice as a cytochrome P450 monooxygenase which showed abnormal final internode elongation as a result of increased accumulation of bioactive gibberellins(Zhu *et al.*, 2006). 5 homologues were identified in rice (EUI and EUIL1-4)(Hirano *et al.*, 2008). In wheat there was found to be a direct orthologue of both *EUI* and *EUIL1*, with *EUIL1* showing increased heat responsive gene expression across all three of its homoeologues, especially showing greater expression at heat tricellular stage. Rice *EUI* clusters closely with 5 wheat genes and of these 5 three show significant heat responsive gene expression, especially at bicellular heat stage.

All considering it is difficult to draw a conclusion from the expression data and the direction measurements of GA accumulation. Most expression changes are occurring at tricellular stages, whereas we found no significant effect of heat treatment at tricellular stage from the bioactive GAs (Figure 4.11).

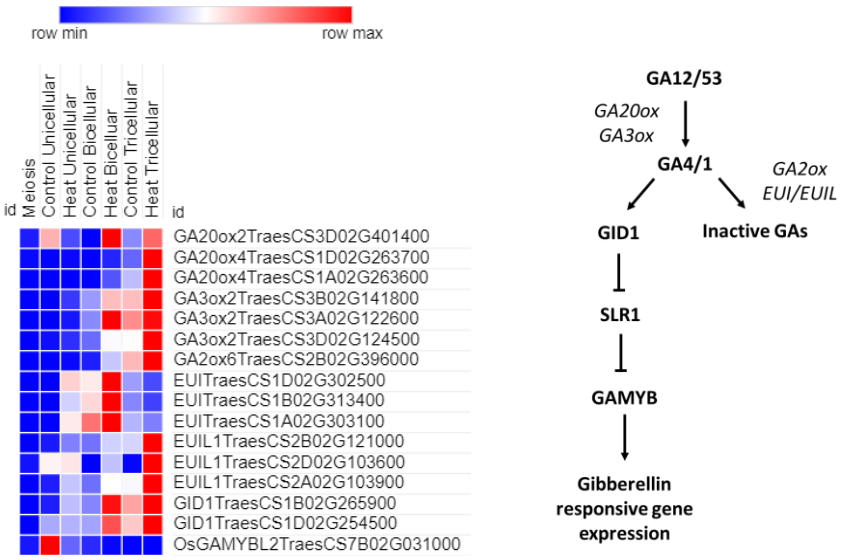

Figure 4.17: *Expression profile of anthers showing wheat orthologues of genes involved in gibberellin synthesis and signalling whose expression was significantly impacted by heat treatment.*

Anther samples were collected as described in figure 4.14. The heat map shows the average raw TPM. Each box represents the mean of 4 biological replicates.

ABA:

NCED (9-cis-epoxycarotenoid dioxygenase) is a rate limiting enzyme involved in the synthesis of xanthoxin (XHT), a precursor of ABA(Schwartz *et al.*, 1997). In response to heat treatment, the tricellular stage shows the highest expression of *NCED2,* however only the B homoeologue is upregulated.

Downstream of ABA is Phospholipase D alpha (PLDα), SAPK, VP1 and bZIP which positively regulate ABA signalling and phosphatase 2C (PP2C) proteins which negatively regulates ABA signalling(Hirano *et al.*, 2008). Many of the wheat orthologues of these genes show greater expression levels after heat treatment (Figure 4.18). However, the contrasting roles of these genes make it difficult to draw

a conclusion from the data. This and the fact that there was found to be no significant effect of heat treatment on ABA accumulation.

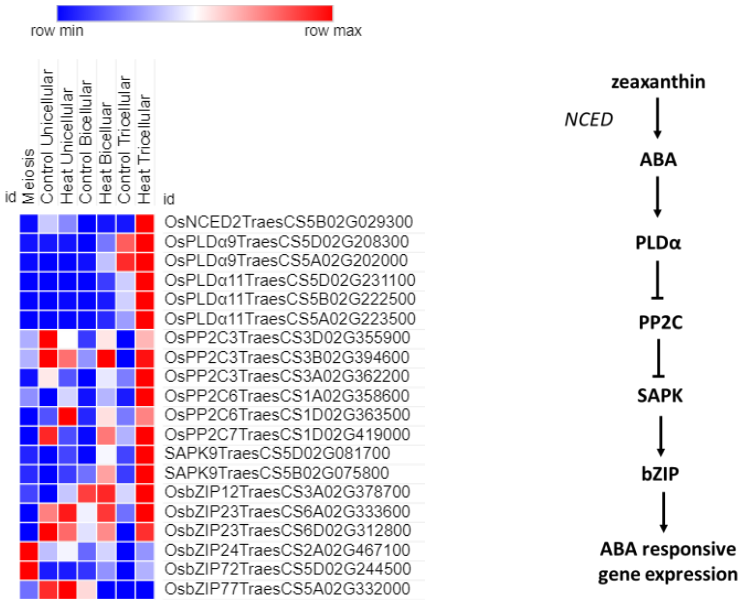

Figure 4.18: *Expression profile of anthers showing wheat orthologues of genes involved in ABA synthesis and signalling whose expression was significantly impacted by heat treatment.*

Anther samples were collected as described in figure 4.14. The heat map shows the average raw TPM. Each box represents the mean of 4 biological replicates.

Cytokinin:

We investigated the expression of the wheat orthologues of the rice adenosine phosphate-isopentenyltransferase (IPT) genes, which are key enzymes involved in cytokinin (CK) biosynthesis(Sakakibara, 2006). In total we found 12 orthologues of rice *OsIPT1/2/4/5/7/8* in wheat (Supplementary Table 2). Only one was found to show a significant change in expression in response to heat treatment, with a higher expression at unicellular stage in response to heat (Figure 4.19).

CK inactivation enzymes, cytokinin oxidases/dehydrogenase (CKX)(Schmülling *et al.*, 2003), seem to be more highly expressed in heat-treated anthers at the unicellular (CKX1) and tricellular stages (CKX5/9) (Figure 4.19) consistent with a deaccumulation of bioactive CKs in response to heat (Figure 4.9).

Perception of CK begins with the interactions between CK and histidine kinase (HK) receptors which then transfer a phosphate group to a downstream histidine phosphotransfer protein (HP) and then to A/B type response regulators (RRs) which induce CK responsive gene expression. B-type RRs promote the transcription of A-type RRs, which in turn inhibit the pathway(Reviewed by Ito and Kurata, 2006). Some of these have been identified to be significantly impacted by heat stress. Five HP orthologues have been identified in rice, named OsHP1-5 respectively(Ito and Kurata, 2006). One of the wheat orthologues of HP1 and HP2 was found to show the highest expression at unicellular stage after control treatment. A conclusion is however difficult to be drawn from this owing to an orthologue of HP4 being most highly expressed at unicellular stage after heat treatment. The wheat orthologue of the rice, *OsRR20*, had two homoeologues on the A and B genome which showed preferential expression at unicellular heat stage of pollen development (Figure 4.4). Therefore, suggesting an induction of CK responsive gene expression at these stages.

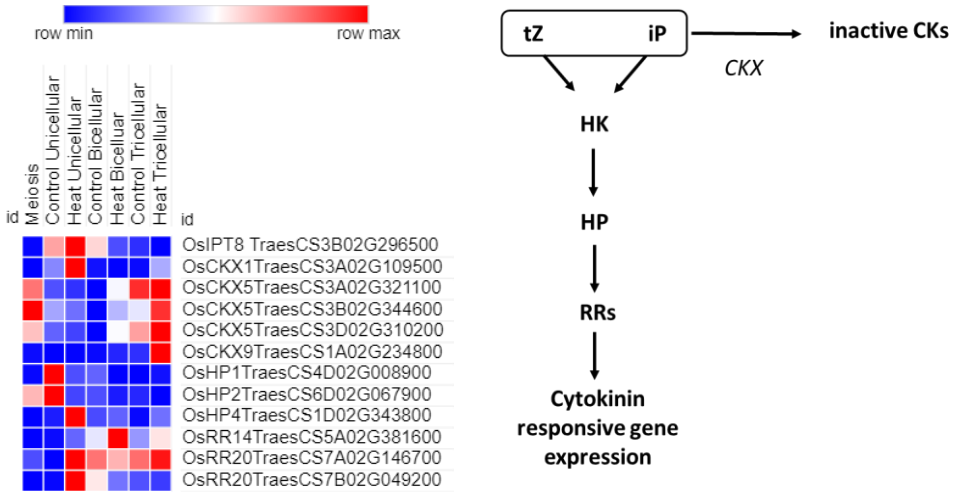

Figure 4.19: *Expression profile of anthers showing wheat orthologues of genes involved in cytokinin synthesis and signalling whose expression was significantly impacted by heat treatment.*

Anther samples were collected as described in figure 4.14. The heat map shows the average raw TPM. Each box represents the mean of 4 biological replicates.

4.3.5 Changes in expression of key male reproductive development genes in response to pollen stage and heat

A number of different genes have been identified to be crucial in ensuring normal anther and pollen development (Figure 4.20). Mutations have resulted in male sterility in many model plant species. Most of these proteins are thought to be centred around controlling tapetal PCD and sporopollenin/ubisch body formation.

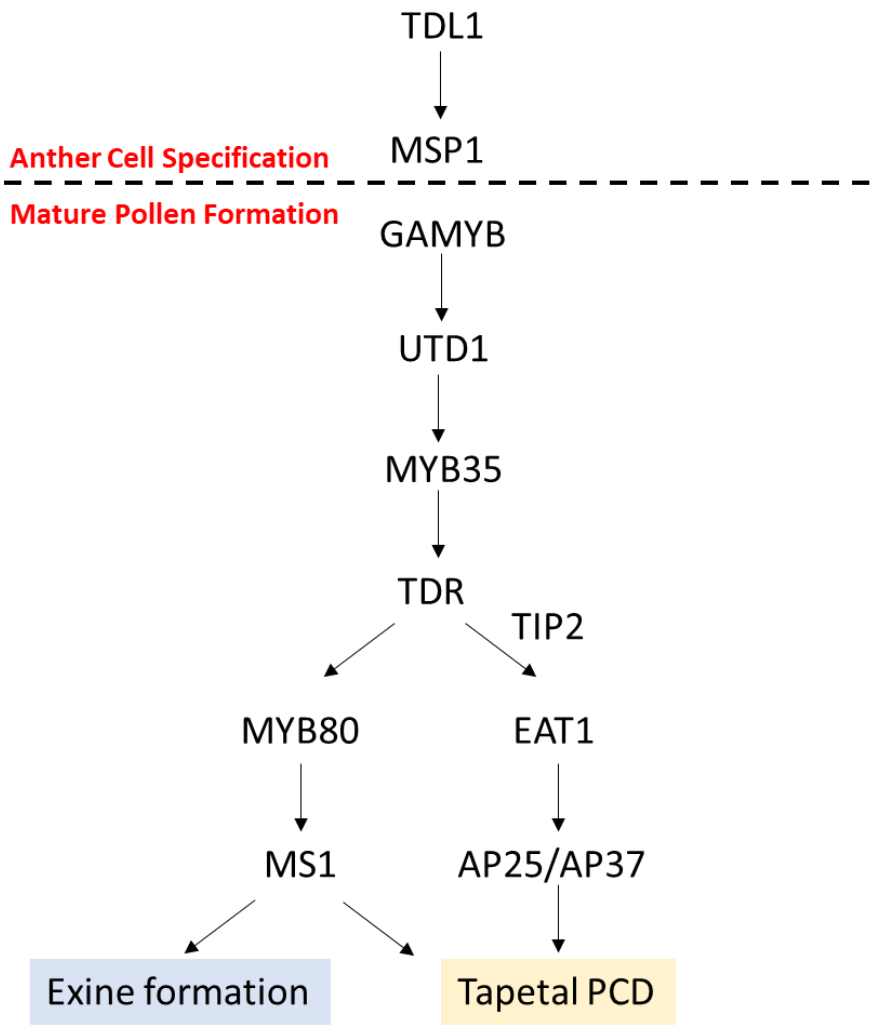

Figure 4.20: *Key genes involved in anther development and ensuring viable pollen formation.*

This figure highlights key components of the signalling cascade involved in pollen exine formation and tapetal PCD, two key processes required for viable pollen formation. Predicted based on orthologue analysis between rice and wheat. Figure adapted from(Gomez *et al.*, 2015).

The anther and pollen development pathway is considered to be highly conserved between monocots and dicots(Gomez *et al.*, 2015). Taking the key genes which have been identified in Arabidopsis and rice I identified orthologues in the wheat genome using Ensemble Plant https://plants.ensembl.org/index.html. Their expression profiles in anthers at different developmental stages and in response to heat treatment were then determined from the RNAseq data.

Rice genes *MULTIPLE SPOROCYTE* (*MSP1*) and *OsTDL1/MIL2* are involved in differentiation of meiocytes and tapetal cell identity, with mutants producing excess sporocytes and lacking a tapetum, resulting in male sterility(Nonomura *et al.*, 2003; Zhao *et al.*, 2008). The two proteins have been found to interact with each other, with OsTDL1 binding to the LR domain of MSP1(Zhao *et al.*, 2008). The RNAseq data indicate that the highest expression of orthologues of these genes in wheat is during meiosis stage, as expected owing to the function of these genes in tapetal development (Figure 4.21).

The degradation of the tapetum is essential to ensure viable pollen. In the process of degradation, the tapetum releases pollen wall forming compounds onto the developing pollen. Degradation is also required for successful dehiscence(Wu and Cheung, 2000; Parish and Li, 2010). Tapetum degradation has been found to be controlled by a cascade of regulatory genes. In rice, OsGAMYB facilitates the action of UNDEVELOPED TAPETUM1(OsUDT1), which increases the expression of *TAPETUM DEGENERATION RETARDATION* (*OsTDR*)(Liu *et al.*, 2010). *TDR INTERACTING PROTEIN2* (*OsTIP2*) is involved in specification of anther cell walls and promotes expression of *OsTDR*. OsTIP2 also forms a heterodimer with OsTDR and binds to the promoter of *ETERNAL TAPETUM 1*(*OsEAT1*), leading to the promotion of its expression(Fu *et al.*, 2014). OsEAT1 is a bHLH transcription factor which binds to OsTDR and promotes the expression of aspartic protease genes, *OsAP25* and *OsAP37*, which subsequently promote tapetum PCD(Niu *et al.*, 2013). In addition to these genes, *TAPETAL DEVELOPMENT and FUNCTION* (*TDF1/MYB35*) and *MYB80* encode transciption factors which have been found to be essential regulators of tapetum development and function in *Arabidopsis*(Zhang *et al.*, 2007; Zhu *et al.*, 2008).

MALE STERILITY1 (*MS1*), was discovered to be involved in pollen wall formation and tapetal PCD in Arabidopsis and has functionally similar genes in rice and barley (*OsPTC* and *HvMS1* respectively) (Vizcay-Barrena and Wilson, 2006; Yang, Vizcay-Barrena, *et al.*, 2007; H. Li *et al.*, 2011; Gomez and Wilson, 2014). An *Ms1* knockout has already been identified in bread wheat, however it is not an orthologue of the Arabidopsis *Ms1* gene. *TaMs1* was determined to be crucial for sporopllenin biosynthesis/transport and consequently pollen exine formation(Tucker *et al.*, 2017). When mutated by TILLING or Crispr/CAS it resulted in a male sterile phenotype in wheat(Tucker *et al.*, 2017; Okada *et al.*, 2019). *TraesCS4B02G017900* was identified as the *Ms1* gene from the latest wheat annotation. It was found to contain a homoeologue on the A-genome, but not on the D-genome, unlike what has previously been found(Tucker *et al.*, 2017). There was however a similar gene on the B-genome which we have included in schematic. *TraesCS4B02G017900* shows much greater expression than the other two genes, showing its peak of expression at meiosis stage (Figure 4.21). This is also what was previously found with pre-meiosis and meiosis being the stages with the greatest expression of *Ms1*(Tucker *et al.*, 2017).

Orthologues of these genes were found in the wheat genome. Each contained a homoeologue on each of the three wheat sub-genomes. *TDR* has undergone a duplication, leading to a total of 2 paralogues, each with 3 homoeologues. The majority of these tapetum degradation genes are highly expressed at the unicellular stage, in the control samples, but also interestingly at the meiosis stage (Figure 4.21). Indeed many of these genes show a shared expression pattern similar to that observed in their rice orthologues. Many of these genes were found to be expressed most highly during the earlier stages of pollen development. Using the online resource of RiceAntherNet (https://www.cpib.ac.uk/anther/riceindex.html) we were able to visualise the expression profiles of each rice gene from pre-meiosis to mature pollen. Many of these genes showed preferential expression towards the earlier stages of pollen development, as was observed in the wheat orthologues (Figure 4.21). RiceAntherNet was developed by generating the expression profiles of 5 collated experiments of rice anthers(Lin *et al.*, 2017). Using the online resource

we found that *OsTIP2*(*Os01g0293100*), *OsMSP1*(*Os01g0917500*), *OsTDR*(*Os02g0120500*), *OsEAT1*(*Os04g0599300*), *OsUTD1*(*Os07g0549600*) and *OsMYB35*(*Os03g0296000*) all clearly demonstrated higher expression towards the earlier stages of pollen development and decreased towards the later stages. A similar expression pattern is evident from their wheat orthologues (Figure 4.21).

RAFTIN is a rice gene required for the formation of Ubisch bodies and is expressed in both the tapetum and microspores(Wang *et al.*, 2003). The orthologues of these in wheat were very highly expressed, with tpms exceeding 5000 in *RAFTIN1-A* at the unicellular stage after heat treatment and the bicellular stage in the control. The expression of all three of the homoeologues was higher at unicellular stage in response to heat, but lower at bicellular stage in response to heat. This result suggests that expression of these genes was being turned on earlier as a result of the heat treatment.

DEX1 and *NEF1* are required for pollen exine formation and sporopollenin transport(Ariizumi *et al.*, 2004; L. J. Ma *et al.*, 2013). Their wheat orthologues were found to be most highly expressed during meiosis, although also showing high levels of expression at unicellular heat and bicellular control stages of pollen development. Once again suggesting that the expression of these genes is being switched on earlier as a result of the heat treatment.

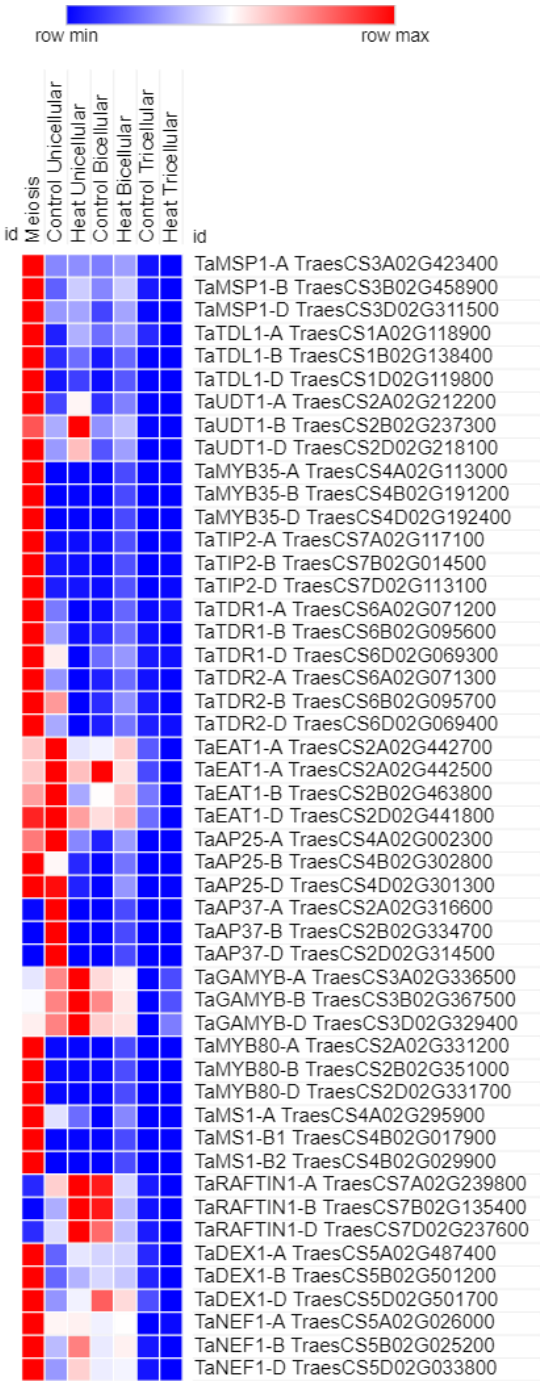

Figure 4.21: *Expression profile of anthers showing wheat orthologues of genes involved in tapetum formation/degradation and pollen exine formation.*

Anther samples were initially taken at meiosis stage (FLS 9-13cm), followed by unicellular, bicellular and tricellular stages after being exposed to either control conditions (4 days 20/15°C day/night) or heat stress conditions (4 days 33/26°C day/night) from meiosis stage. Samples were staged using the Ampha Z32 Pollen Analyzer. The heat map shows the Z-values. Each box represents the mean of 4 biological replicates.

4.4 Discussion

A combination of global hormone and transcriptional analysis has identified changes in hormone accumulation and gene expression of wheat anthers across different stages of pollen development. In summary, we found that wheat anthers accumulate IAA, JA and CK at bicellular and tricellular stages of pollen development (Figure 4.22). In contrast there was found to be a reduced concentration of SA and ABA from meiosis to late tricellular stage.

This study extended from work in rice, which investigated tissue specific microarray analysis of microspores/pollen and the tapetum at different stages of pollen development(Hirano *et al.*, 2008). In contrast we took measurements of the whole anthers, using methods of RNAseq and hormonomics. Hirano *et al.,* 2008 predicted from pollen microarray data that there would be an accumulation of JA, auxin, ethylene and GA towards tricellular stage and a deaccumulation of CK past tetrad stage. There are clearly some differences in what was predicted in rice pollen and what we found in whole wheat anthers. We hypothesis that these differences are likely due to whole anther data taken for this study and the Hirano data being based on the transcriptome rather than direct measurements of the hormones.

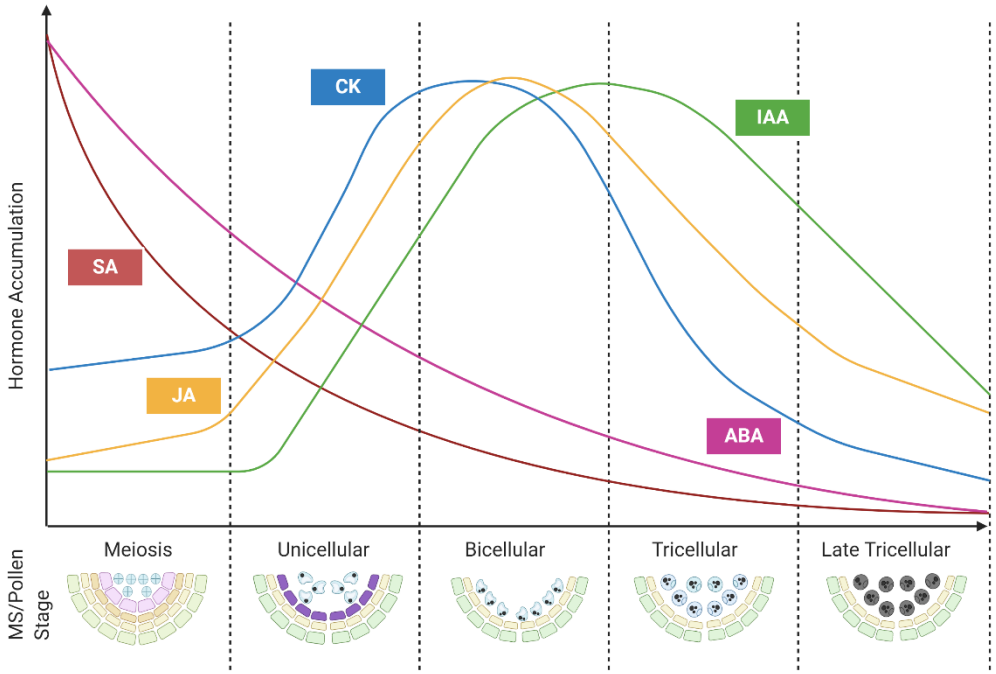

Figure 4.22: *Phytohormone accumulation in wheat anthers according to pollen stage.*

JA (Jasmonic acid), IAA (Indole-3-acetic acid), CK (Cytokinins), ABA (Abscisic acid) and SA (Salicylic acid). This is based on the accumulation pattern of the bioactive forms. Created with BioRender.com.

As heat stress accelerates male reproductive development(Ruiz-Vera *et al.*, 2018), we used a pollen staging approach whereby we ensured both the control and heat stress plants were at the same stage when making a comparison of the heat stress affects. In a conventional time course experiment this would mean we would be comparing different developmental stage on their hormone and transcript profile. We found a significant increase in JA/JA-Ile and decrease in various bioactive CKs (Figure 4.23). We also found a significant decrease in $GA_{1/4}$ in response to heat stress, however this was not shown in Figure 4.23 due to concerns over the measurements. Expression of orthologous genes known to be involved in hormone synthesis/degradation have linked the genetic data to changes in hormone accumulation. Overall, this study has provided new insights into the hormonal and genetic control of anther development, and how heat stress interrupts this, resulting in male sterility. It is worth mentioning that although we are comparing anthers at the same stages of pollen development, this does not account for the

reduction in pollen viability (Table 3.2) which occurs as a result of the heat treatment and could impact the hormone levels and transcriptome of the anthers.

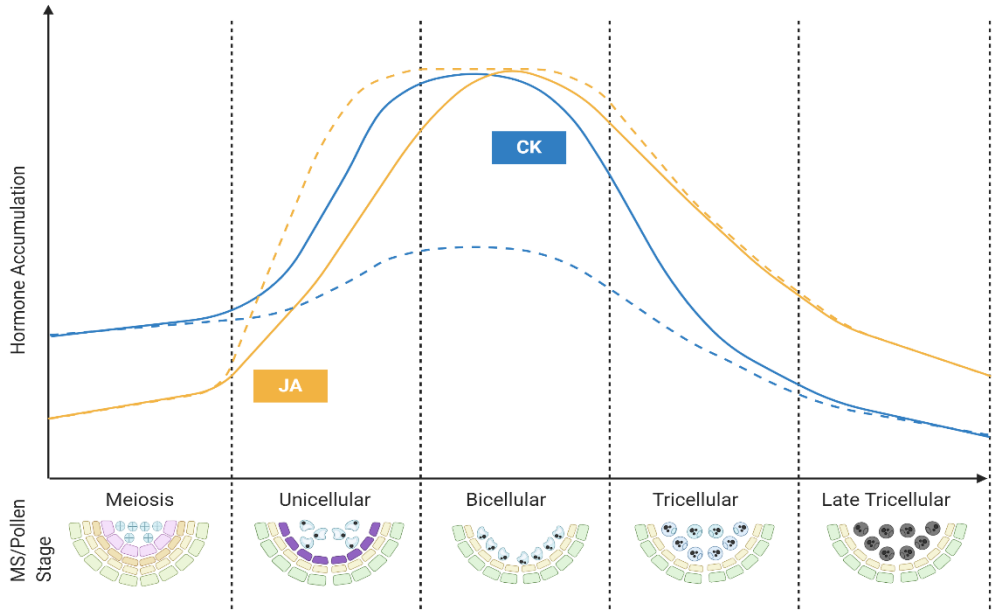

Figure 4.23: *Phytohormone accumulation in wheat anthers in response to heat.*

JA (Jasmonic acid), IAA (Indole-3-acetic acid), CK (Cytokinins), ABA (Abscisic acid) and SA (Salicylic acid). This is based on the accumulation pattern of the bioactive forms. Solid line shows accumulation in control conditions (20/15°C d/n) and dashed line shows response to heat treatment (33/26°C d/n for 4 days from meiosis). Created with BioRender.com.

4.4.1 Hormone accumulation and genetic causes

<u>Auxin</u>

The global hormone data shows an accumulation of auxin in anthers towards the later stages of development (Figure 4.2). IAA content has been measured in rice anthers at mature tricellular stage and it was found to accumulate to much greater levels than the leaf blade and pistil(Hirano *et al.*, 2008). IAA was predicted from gene expression data to accumulate towards the later stages of pollen development in the developing pollen (Hirano *et al.*, 2008). In Arabidopsis, auxin accumulation occurs primarily in the tapetum and the pollen grains and is at its highest during mitosis(Feng *et al.*, 2006). It is hypothesised that auxin is important in controlling

mitosis, since continuous treatment of IAA lead to an increased transition period between G1 to S phase and G2 to M phase in root meristem of *Vicia faba*(Polit *et al.*, 2003).These findings support our results that in wheat IAA accumulates with the maturation of the pollen, reaching its highest during bicellular and tricellular stages (Figure 4.2).

There was found to be no significant effect of heat on auxin accumulation within the wheat anther (Figure 4.8). This is contrasts with other studies. In barley and rice, endogenous levels of auxin were reduced in the anther in response to heat(Tang *et al.*, 2008; Sakata *et al.*, 2010). It could be the case that this is a wheat specific response. However, we hypothesise that the contrasting results could be due to the nature of the experiment. Samples in other studies were taken during heat treatment, whereas in this study samples were taken at unicellular, bicellular and tricellular stages after heat stress had already occurred and the plants were in normal conditions. Therefore, the change in IAA content could be a temporal one during heat treatment. Future experiments could establish this by accurately staging the tillers and then exposing them to shorter heat treatments, for example 1 hour. This way the plants have been exposed to the heat, but the anthers have not had enough time to rapidly progress onto the next stage of pollen development.

RNAseq data suggests that some auxin biosynthesis genes such as the wheat *NIT1/2* were upregulated at bicellular and tricellular stages after heat stress (Figure 4.14). The auxin biosynthesis gene *YUCCA6* was found to be upregulated in response to heat at the unicellular stage. Although not significant, there was a 2.7-fold increase in IAA content in response to the heat treatment at unicellular stage. This result warrants further investigation, into the short- and long-term role of IAA in the heat stress response.

Jasmonic Acid

There was found to be an accumulation of JA in the anthers towards the later stages of pollen development. In the initial experiment this was found to peak at the bicellular and tricellular stages, whereas in the control conditions of the second experiment it was found to peak at the bicellular stage (Figure 4.1; 4.7). Both JA and

its bioactive form JA-Ile follow the same pattern of accumulation. This pattern of accumulation is similar to what was predicted to occur in rice microspores/pollen(Hirano *et al.*, 2008). The accumulation of JA towards the later stages of pollen development has been linked to its role in pollen dehiscence. Delayed or even absent dehiscence has been found in mutants defective in JA biosynthesis(McConn and Browse, 1996; Sanders *et al.*, 2000; Ishiguro *et al.*, 2001; Park *et al.*, 2002; Von Malek *et al.*, 2002). These mutants were rescued by the application of JA, which recovers dehiscence. JA signal transduction mutants, however cannot be rescued by the application of JA (Devoto *et al.*, 2002), therefore supporting the fact that JA signalling is crucial in the later stages of anther development. JA is thought to regulate the water transport from the endothecium, connective locules into the anther filament(Ishiguro *et al.*, 2001). Dehydration and shrinkage of the endothecium and connective tissue is thought to be critical to break the stomium and release the mature pollen(Ishiguro *et al.*, 2001). The highest levels of JA accumulation were during the bicellular and tricellular phases of pollen development, being over 10x higher than at meiosis and the unicellular stage (Figure 4.1). This indicates that during these stages dehydration of the anthers is beginning to be initiated.

In response to heat stress there was found to be a significant accumulation of JA at the unicellular stage relative to the control conditions (Figure 4.7). The accumulation of JA could be attributed to the apparent upregulation of JA biosynthesis gene expression in the heat-treated plants at unicellular stage. *AOC* is one of these genes, which showed upregulation at unicellular stage across all three of its homoeologues (Figure 4.15). *TraesCS6B02G365200* is the wheat AOC homoeologue on the B sub-genome. *TraesCS6B02G365200* has previously been identified in wheat and was named *TaAOC1*. Its expression was found to be induced in wheat seedlings exposed to salt stress and drought stress and was actually found to be upregulated by JA, with constitutive expression of *TaAOC1* leading to increased JA accumulation and salinity tolerance(Zhao *et al.*, 2014). Therefore, wheat AOC appears to play a role in the abiotic stress response.

Abnormal inflorescence meristem1 (AIM1) is another JA biosynthesis gene whose expression of its wheat orthologues was significantly upregulated by the heat treatment. The Arabidopsis mutant *aim1* was found to show defects in male fertility, with few matured pollen grains and missing stamens(Richmond and Bleecker, 1999). This suggests its key role in JA biosynthesis in anthers.

There was also found to be a significant accumulation of the conjugated JA, JA-Ile, at the unicellular stage (Figure 4.7). This could be attributed to the increased expression of the wheat orthologues of *JAR1,* an enzyme is involved in synthesis of JA-Ile (Figure 4.15)(Staswick *et al.*, 2002). The expression of *JAR1* has been found to correlate with JA-Ile accumulation, with JA-Ile beginning to accumulate and *JAR1* transcript levels increasing dramatically(Suza and Staswick, 2008).

Gibberellins

GA is also important for ensuring normal pollen development in plants. Transcriptome studies on rice pollen have shown an increased expression of GA biosynthetic genes towards the later stages of pollen development(Hirano *et al.*, 2008), therefore indicating the increased importance of GA especially towards the later stages of pollen development.

Arabidopsis mutants defective in GA biosynthesis were found to have shorter anther filaments and failed dehiscence(Cheng *et al.*, 2004; Hu *et al.*, 2008; Rieu *et al.*, 2008). GA signalling pathway has also been shown to be involved in initiating tapetum PCD. GA controlled tapetum degradation by upregulation of the transcription factor GAMYB, is critical for initiating tapetal PCD in rice(Murray *et al.*, 2003; Kaneko *et al.*, 2004; Aya *et al.*, 2009; Liu *et al.*, 2010). In wheat, *Tagamyb* mutants, defective in GA signalling, were found to be male sterile, with the tapetum failing to go through PCD(Audley, 2016). GAs are also known to be involved in pollen tube germination and elongation(Chhun *et al.*, 2007), thus ensuring successful pollination. Together this suggests that GA is important in the later stages of pollen development and we would predict it to accumulate most highly there in wheat. Indeed transcriptional data from rice pollen predicted an increase in GA content towards the later stages of pollen development(Hirano *et al.*, 2008). In the

wheat anthers, GA_3 was found to accumulate most highly during meiosis, GA_1 at unicellular/bicellular stage and GA_4 was relatively consistent; a stark contrast from the findings from transcriptome data in rice(Hirano *et al.*, 2008) (Figure 4.11). This is likely to be due to issues with the hormone extraction protocol and therefore we would not recommend inferring any solid conclusions from our data.

At the bicellular stage, the GA_1 content was found to be nearly 12x higher in the control treatment compared to the heat treatment and at the unicellular stage the GA_4 content was 6.6x higher in the control. The results confirm previously findings which also show reduced endogenous content of GAs in the anthers in response to heat stress in rice(Tang *et al.*, 2008).

The RNAseq data found an increased accumulation of *EUI* orthologues in response to heat stress at the bicellular stage (Figure 4.17). EUI is a cytochrome P450 monooxygenase (CYP714D1) which reduces the bioactivity of GA_4 in rice(Zhu *et al.*, 2006). Despite this there was not found to be a significant reduction in GA_4 at bicellular stage after heat treatment. Overall, the RNAseq results appear to show a high expression of bioactive GA biosynthesis enzymes *GA20ox2/4* and *GA3ox2* at tricellular stages of pollen development after heat treatment.

Cytokinin

In control conditions there was found to be an overall accumulation of bioactive CKs from meiosis to unicellular/bicellular stage, following by a reduction till late tricellular stage (Figure 4.3). In contrast, Hirano et al., 2008 predicted a deaccumulation of CKs in the pollen from meiosis to tricellular stage in rice pollen, although this did not take into consideration the whole anther tissue.

In response to heat there was found to be a significant deaccumulation of bioactive cytokinins, iP and cZ, at bicellular stage after heat stress and tZ and cZ at unicellular stage after heat stress (Figure 4.9). This has not been found to occur in reproductive growth in response to heat stress in previous studies(Ozga *et al.*, 2017), and offers a potential new insight into the possible role of CK in the heat stress response in wheat. The lower CK content could be attributed to cytokinin inactivation enzyme,

CKX1, being more highly expressed in anthers at unicellular stage which had previously been heat stressed (Figure 4.19).

Ethylene

In rice, transcriptional data suggested that ethylene increased in accumulation in rice pollen towards the later stages of pollen development(Hirano *et al.*, 2008). However, in this study ethylene accumulation was not measured. Ethylene is difficult to measure as it is gaseous and therefore it would require fresh tissue rather than freeze dried, as in this instance. Alternatively, measurements could be taken of the ethylene precursor 1-Aminocyclopropane-1-carboxylic acid (ACC), which is easier to measure.

Our transcriptional data infers that ethylene levels rise in the anthers in response to heat stress (Figure 4.16). There was an accumulation of *ACO1/3*, involved in converting the precursor ACC to ethylene(Hamilton *et al.*, 1990), under heat treatment at the unicellular, bicellular and tricellular stages. Ethylene is implicated to be involved in the heat stress response. Tomato *Never ripe* (*Nr*) mutants which are ethylene-insensitive were more sensitive to heat stress compared to the WT, showing reduced pollen production and viability(Firon *et al.*, 2012). Pollen viability and germination was increased when heat stressed tomato plants were pre-treated with ethephon, an ethylene-releasing agent, and decreased when treated with AVG, an ethylene biosynthesis inhibitor (Firon *et al.*, 2012). Ethylene was also found to accelerate anther dehiscence in tobacco and treatment with an inhibitor of ethylene perception (MCP) was found to delay dehiscence (Rieu *et al.*, 2003). The predicted increased accumulation of ethylene in wheat could be a contributing factor to the increase in the rate of anther development as a result of the heat treatment (Section 5.3.8; Table 5.8).

ABA

Transcriptional studies of rice have predicted a relatively uniform accumulation of ABA in the microspores/pollen throughout the different stages of pollen development(Hirano *et al.*, 2008). However, in this experiment we measured ABA content from the whole anther. There was found to be a reduction of ABA

concentration from meiosis to late tricellular stages in the first experiment, without heat stress (Figure 4.4). A similar pattern was observed in the control treatment for the heat stress experiment, although there was considerable variability between the replicates, and the highest levels were found at the unicellular stage.

There appears to be no significant effect of heat on ABA accumulation in the anther (Figure 4.10). In contrast it has been found that in rice anthers there was an accumulation of ABA in response to heat treatment (Tang *et al.*, 2008), although in this experiment anthers were taken directly after heat treatment and not staged. Exogenous application of ABA has been linked to pollen sterility in rice (Oliver *et al.*, 2007), therefore the heat stress induced accumulation of ABA has been linked to male sterility.

Summary

The phytohormone analysis of wheat anthers at meiosis, unicellular, bicellular, tricellular and late tricellular stage, shows IAA, JA and CK accumulate in the anthers at bicellular and tricellular stages of pollen development (Figure 4.22). In contrast there was found to be a reduced concentration of SA and ABA from meiosis to late tricellular stage. All hormones showed reduced hormone content from tricellular to tricellular late stages of pollen development as the anthers neared dehiscence. Surprisingly, there was found to be very low levels of bioactive GA_4, with it only being found at the unicellular stage. This is thought to be an issue with the protocol. Even when repeating the GA analysis using a different protocol, the results were dubious and therefore GA was excluded from the schematic. The complex pattern of hormone accumulation is consistent with the roles of these hormones at controlling specific stages of anther and pollen development. The data implies that the hormone function in anther development of wheat is shared with that of other angiosperms.

4.4.2 Cluster analysis of stage specific gene expression

Meiosis has been previously found to be the stage at which there was a marked upregulation of genes known to be involved in sporopollenin biosynthesis in Arabidopsis(Pearce *et al.*, 2015). In contrast, the GO cluster analysis indicated that

sporopollenin biosynthesis occurs mainly in the unicellular stage of wheat (Figure 4.13). At meiosis, genes which are involved in chromosome remodelling, DNA replication and chromosome segregation were most highly expressed. At the unicellular stage genes which are specific to pollen exine formation were highly expressed, as was also found in cluster analysis of Arabidopsis transcripts at mitosis I(Pearce *et al.*, 2015). In Arabidopsis genes mostly involved in pollen exine formation were expressed at bicellular stage(Pearce *et al.*, 2015). We found that at bicellular stage many of the upregulated genes are involved in transmembrane transport. Finally, at the tricellular stage, genes involved in polysaccharide catabolism, cell wall modification and actin filament organisation were highly expressed (Figure 4.13). Likewise, in Arabidopsis, expression of genes involved in actin filament movement, cell wall modification as well as sugar transport occurred most strongly at mitosis II (Pearce *et al.*, 2015).

When comparing wheat with Arabidopsis we can see a similarity in the anther expression profiles of key pollen developmental genes. This is to be expected due to anther and pollen development being highly conserved physiologically. There are however key differences, such as the sporopollenin biosynthesis genes being expressed earlier in Arabidopsis, starting at meiosis rather than the unicellular stage, as was found in wheat. This could be linked to differences in the timing of tapetum formation and breakdown between Arabidopsis and wheat.

4.4.3 Changes in expression of key genes involved in male fertility

Orthologue searches were performed on key genes known to be involved in ensuring normal anther and pollen development. The results indicate that there is a high level of homology of these genes between wheat and other species, indicating that the signalling pathways described in Arabidopsis and rice can be applied to wheat.

Genes which are known to be involved in regulating tapetal breakdown are all highly expressed at the meiosis stage, indicating that the signalling which initiates tapetal breakdown is starting to occur (Figure 4.21). This seems to be carried forward to the unicellular stage after control conditions for *TDR*, *EAT* and *AP25*, indicating that tapetal breakdown is still occurring at this stage. Whereas after heat

treatment there is a lower expression of these genes at the unicellular stage compared to the unicellular anthers after control treatment, suggesting that tapetal breakdown has already been initiated.

Genes which are known to be involved in pollen exine formation, *DEX1* and *NEF1*(Ariizumi *et al.*, 2004; L. J. Ma *et al.*, 2013), seemed to be most highly expressed during meiosis, but interestingly were also highly expressed at unicellular heat and bicellular control stages. This suggests that these genes are being switched on earlier in the heat stressed plants. *RAFTIN* is a gene required for formation of Ubisch bodies and is expressed in both the tapetum and microspores(Wang *et al.*, 2003). The expression of the three homoeologues of *RAFTIN* was found to be extremely high in wheat anthers, indicating it maybe of crucial importance in wheat pollen development. The expression peaks at the unicellular stage after heat treatment and bicellular stage after control conditions (Figure 4.21). Once again, this suggests that also this gene is being expressed earlier in the heat stressed plants.

The differences in the timing of expression of these key regulatory genes in pollen development could be a major contributing factor to the lower pollen viability (section 3.3.5) as a result of heat stress. Possibly due to the disruption of the careful coordination of developmental processes required to ensure correct pollen viability.

4.5 Conclusion

The results show the complexity of hormone signalling in the anther under normal conditions and in response to heat stress. Each pollen stage is defined by a very different hormone and gene expression profile. Heat perturbs the accumulation of certain hormones. The findings revealed that heat stress led to a greater accumulation of JA and its bioactive form JA-Ile at the unicellular stage, whereas a deaccumulation of bioactive CKs at unicellular and bicellular stages and a deaccumulation of GA_1 at the bicellular stage. This was associated with changes in expression of genes encoding key proteins involved in the synthesis and degradation of these hormones. These are part of the very complex transcriptional changes which are occurring in the anther throughout pollen development and in

response to heat stress. GO analysis and analysis of orthologues of key genes involved in pollen development revealed a high level of homology in male reproductive development between Arabidopsis, rice and wheat. It indicates that research in anther development of model plant species can be applied to wheat. The results from this study have discovered genes which from their expression profile could play an important role in anther/pollen development and heat stress tolerance of wheat.

Chapter 5: Identification and characterisation of auxin signalling mutants in wheat

5.1 Introduction

Auxin has been studied since the 19th century, making it one of the oldest areas of plant biology research. Charles Darwin in fact began experimentation on this mysterious substance by investigating shoot elongation towards a light source, although at the time, the cause of this was unknown (Darwin, 1880). Since then, the substance responsible has been determined to be indole-3-acetic acid (IAA), better known as auxin. Auxin is an important plant phytohormone known to be involved in a diversity of different developmental processes. It is a key component of regulating vascular tissue formation, apical dominance, flowering, lateral root formation, as well as controlling various cellular processes such as division, enlargement and differentiation(Mockaitis and Estelle, 2008). Auxin regulates these developments through a complex interplay of regulatory proteins, their targeted degradation, and the consequential activation of auxin-responsive genes. The complexity of these controlling components of the auxin signalling pathway means that different cells/tissues can respond in a tissue specific way, ensuring as precise level of control and adaptability.

Auxin regulates transcription of auxin-responsive genes by targeted protein degradation of transcriptional repressors of these genes, known as *Auxin/Indole-3-Acetic Acids* (*Aux/IAAs*) (Figure 5.1). Auxin forms a complex with F-box proteins of the TRANSPORT INHIBITOR RESPONSE1/AUXIN SIGNALING F-BOX (TIR1/AFB) family and members of the Aux/IAA transcriptional repressor family(Tan *et al.*, 2007). TIR1 is the F-box subunit of an SCF-type ubiquitin protein ligase complex, consisting of two other subunits: Skp1 and Cullin(Smalle and Vierstra, 2004). TIR1 contains Leucine-rich repeat domain which recognises auxin and Aux/IAAs through a single surface pocket(Tan *et al.*, 2007). Aux/IAAs are recognised by TIR1 by a short and highly conserved motif in domain II(Ramos *et al.*, 2001; Tan *et al.*, 2007). Subsequent to binding, the Aux/IAA is ubiquitinated and degraded by the 26S proteasome(Gray *et al.*, 2001; Dos Santos Maraschin *et al.*, 2009). Relieved from the repression of the Aux/IAAs, ARFs bind to Auxin Response Elements (AREs)

containing the consensus sequence “TGTCTC” in the promoter of auxin responsive genes and recruit chromatin remodelling enzymes to activate transcription of these auxin responsive genes(Abel and Theologis, 1996; Ulmasov *et al.*, 1997; Mironova *et al.*, 2014; Wu *et al.*, 2015).

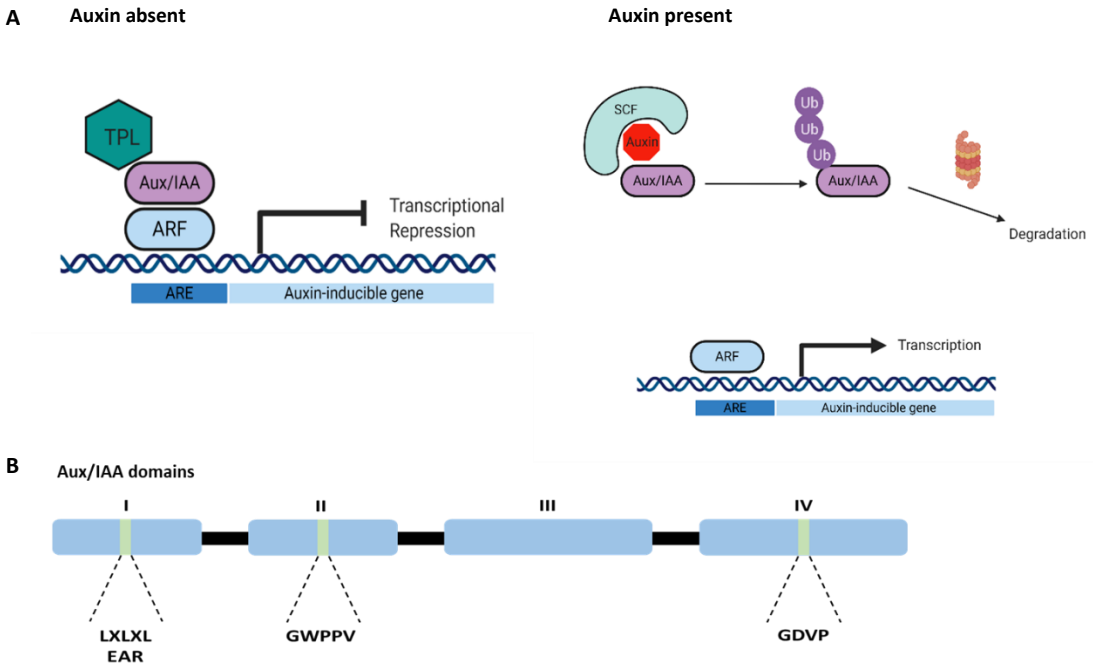

Figure 5.1: *Schematic diagram of the auxin signalling pathway in the presence/absence of auxin and conserved domains of Aux/IAA proteins.*

A: *In the absence of auxin, Aux/IAAs actively repress the transcription of auxin responsive genes, by recruiting transcriptional corepressor TOPLESS (TPL) and oligomerisation with ARFs to prevent their activation of auxin responsive genes. When auxin is present it facilitates an interaction between the GWPPV motif of domain II of the Aux/IAA with SCF-type ubiquitin protein ligase complex, which subsequently tags the Aux/IAA with ubiquitin for degradation by the proteasome. This frees ARFs to activate auxin responsive gene expression.* **B**: *The domains of a typical Aux/IAA protein. Domain I contain a repression domain involved in recruiting a TOPLESS (TPL) co-repressor. Domain II contains a conserved “GWPPV” motif. Domain III contains a βαα-fold which is involved in homo and heterodimerisation with Aux/IAAs and/or ARF proteins. Domain IV is thought to contribute to electrostatic protein interactions. Created with BioRender.com.*

In the absence of Auxin, Aux/IAA oligomerisation with Auxin Response Factors (ARFs) prevents their activation of auxin responsive genes (Figure 5.1). Aux/IAAs also directly repress transcription of auxin responsive genes(Ulmasov *et al.*, 1997). Their EAR motif, in domain I, recruits corepressor TOPLESS (TPL) to the promoter and TPL in tern recruits chromatin remodelling proteins to induce transcriptional repression of the bound gene(Tiwari *et al.*, 2004; Szemenyei *et al.*, 2008). A combination of passive prevention of activation and direct repression ensures reduced auxin-responsive gene expression.

The Aux/IAA family was first discovered as a family of genes whose expression is rapidly induced in response to auxin(Abel *et al.*, 1995; Abel and Theologis, 1996) indicating their key roles in the auxin-signalling pathway. They are a dynamic protein family which along with ARFs, small auxin upregulated RNAs (SAUR), aminocyclopropane-1-carboxylic acid synthases (ACS), glutathione-S-transferases (GH2/4-like), and the auxin-responsive Gretchen Hagen3 (GH3) family all respond to changes in auxin accumulation(Luo *et al.*, 2018).

Aux/IAAs are found in both gymnosperms and angiosperms and are thought to be unique to plants(Reed, 2001). This gene family has undergone extensive duplication(Jain *et al.*, 2006) and has diversified into 29 members in Arabidopsis(Overvoorde *et al.*, 2005), 31 members in rice and maize(Jain *et al.*, 2006; Y. Wang *et al.*, 2010) 26 in tomato and sorghum(S. Wang *et al.*, 2010; Wu *et al.*, 2012), 36 in barley(Shi *et al.*, 2020) and at least 84 Aux/IAA homoeologues in wheat(Qiao *et al.*, 2015).

Aux/IAAs consist of 4 conserved domains which are shared by most members of the protein family (Figure 5.1B)(Hagen and Guilfoyle, 2002). Domain I contains a repression domain containing ethylene response factor (ERF)–associated amphiphilic repression (EAR) motif, “LxLxL”, involved in recruiting a TOPLESS (TPL) co-repressor(Szemenyei *et al.*, 2008). Domain II contains a conserved “GWPPV” motif, which forms a complex with auxin and with the TIR1 subunit of the SCF complex (Ramos *et al.*, 2001). Domain III contains a βαα-fold which is involved in homo and heterodimerisation with Aux/IAAs and/or ARF proteins(Hagen and Guilfoyle, 2002; Guilfoyle and Hagen, 2012). Domain IV is comprised of a number of

conserved regions: an acid region, SV40 type Nuclear Localisation Signal (PKKKRKV) and a conserved "GDVP" motif which is thought to contribute to electrostatic protein interactions(Guilfoyle and Hagen, 2012). Collectively domain III and IV are shared with the carboxy-terminal dimerization domain (CTD) in ARF proteins, therefore allowing interaction with Aux/IAAs via these domains(Kim *et al.*, 1997).

Forward genetic studies screening for auxin-insensitive phenotypes discovered that missense mutations within the GWPPV motif of various members of the Aux/IAA gene family result in an auxin-insensitive phenotype (Table 5.1). These mutations within the GWPPV conserved domain led to increased protein stability(Ramos *et al.*, 2001). These mutated Aux/IAA proteins fail to be recognised by the SCF^{TIR1} ubiquitin E3 ligase and remained stable even in the presence of auxin(Ramos *et al.*, 2001; Dreher, 2006). Consequently they continue to repress the expression of auxin responsive genes (Worley *et al.*, 2000; Ramos *et al.*, 2001; Zenser *et al.*, 2001; J. Y. Park *et al.*, 2002; Yang *et al.*, 2004). This results in gain-of-function auxin-insensitive phenotypes in both rice and Arabidopsis(Tian and Reed, 1999; Gray *et al.*, 2001; Ouellet *et al.*, 2001; Ramos *et al.*, 2001; Fukaki *et al.*, 2002; J. Y. Park *et al.*, 2002; Yang *et al.*, 2004; Tatematsu *et al.*, 2004; Uehara *et al.*, 2008; Zhu *et al.*, 2012; Kitomi *et al.*, 2012; Rinaldi *et al.*, 2012). Only certain missense mutations have been demonstrated to confer insensitivity: G>E/R/S, P>S/L/A and V>G (Table 5.1). These mutations are likely to interfere with the binding between the Aux/IAA, auxin and the SCF^{TIR1} ubiquitin E3 ligase.

Table 5.1: *Aux/IAA mutants in the GWPPV motif of domain II known to confer auxin-insensitivity in Arabidopsis and rice. Adapted and updated from Uehara et al., 2008.*

Species	Mutant	Gene	GWPPV motif
Arabidopsis	*axr5-1*	AtIAA1	GWP**S**V
Arabidopsis	*shy2-1/2*	AtIAA3	GW**S**PV
Arabidopsis	*shy2-3*	AtIAA3	**E**WPPV
Arabidopsis	*shy2-6*	AtIAA3	GWP**L**V
Arabidopsis	*axr2-1*	AtIAA7	GW**S**PV
Arabidopsis	*bodenlos*	AtIAA12	GW**S**PV
Arabidopsis	*slr-1/4*	AtIAA14	GWP**S**V
Arabidopsis	*slr-2*	AtIAA14	GW**S**PV
Arabidopsis	*slr-3*	AtIAA14	GW**A**PV
Arabidopsis	*iaa16-1*	AtIAA16	GW**L**PV
Arabidopsis	*axr3-1*	AtIAA17	GWP**L**V
Arabidopsis	*axr3-3*	AtIAA17	GWPP**G**
Arabidopsis	*axr3-101*	AtIAA17	**E**WPPV
Arabidopsis	*crane-1*	AtIAA18	**R**WPPV
Arabidopsis	*crane-2*	AtIAA18	**E**WPPV
Arabidopsis	*iaa18-1*	AtIAA18	**E**WPPV
Arabidopsis	*msg2-1*	AtIAA19	GWP**S**V
Arabidopsis	*msg2-2*	AtIAA19	**R**WPPV
Arabidopsis	*msg2-3*	AtIAA19	GWP**L**V
Arabidopsis	*msg2-4*	AtIAA19	GW**L**PV
Arabidopsis	*iaa28-1*	AtIAA28	GW**L**PV
Rice	*Osiaa11*	OsIAA11	GWP**L**V
Rice	*Osiaa13*	OsIAA13	**S**WPLV

Aux/IAA mutants often show characteristic defects in lateral root/hypocotyl development, gravitropism, and flower fertility(Tian and Reed, 1999; Gray *et al.*, 2001; Ouellet *et al.*, 2001; Ramos *et al.*, 2001; Fukaki *et al.*, 2002; J. Y. Park *et al.*, 2002; Yang *et al.*, 2004; Tatematsu *et al.*, 2004; Uehara *et al.*, 2008; Zhu *et al.*, 2012;

Kitomi *et al.*, 2012; Rinaldi *et al.*, 2012). The severity of the phenotype depends on which Aux/IAA is mutated and the type of amino acid change. Different Aux/IAAs show different tissue specific expression and levels of expression. More conservative mutations are more likely to still be recognised by the SCF^{TIR1} complex and targeted for degradation and subsequently show less extreme phenotype. Tissue specific expression of Aux/IAAs means auxin-insensitivity will only occur in the plant organs/tissue where they are locally expressed. Mutations in Aux/IAAs which are highly expressed are likely to result in a greater repression of auxin responsive genes and therefore a more extreme auxin-insensitive phenotype. As an added layer of complexity, the ability for Aux/IAAs to repress the expression of an auxin-responsive gene depends on the presence of an ARF bound to the ARE region. The presence or absence of ARFs in different cells and tissue types ensure auxin signalling specificity(Rademacher *et al.*, 2012; Bargmann *et al.*, 2013).

Auxin is central to the development of lateral roots. Lateral roots arise from cell divisions in the pericycle forming a projection of tissue from the central root forming lateral root primordia (LRP)(Laskowski *et al.*, 1995). Eventually the root primordia develop a root cap and apex and penetrate outward through the cortex, emerging laterally. Auxin accumulation in the root pericycle cells at the basal meristem is required to initiate the formation of LRP(De Smet *et al.*, 2007). One of the most defining phenotypic characteristics of Aux/IAA mutants is the distinctive root architectural phenotype. AUX/IAA mutants commonly have reduced or absent lateral roots in Arabidopsis (Tian and Reed, 1999; Fukaki *et al.*, 2002; Tatematsu *et al.*, 2004; Yang *et al.*, 2004; Uehara *et al.*, 2008; Rinaldi *et al.*, 2012). In rice, *OsIaa11* and *OsIaa13*, was found to have a complete absence of lateral roots, this severe root phenotype was linked to the expression of the IAA in the lateral root primordia, therefore the primordia fail to initiate lateral root formation normally triggered by auxin(Kitomi *et al.*, 2012; Zhu *et al.*, 2012). These mutant phenotypes in both rice and Arabidopsis failed to be rescued by the application of auxin(Fukaki *et al.*, 2002; Yang *et al.*, 2004; Rinaldi *et al.*, 2012; Zhu *et al.*, 2012), or were only partially rescued(Tatematsu *et al.*, 2004), indicating that they are either partially or completely insensitive to auxin.

Some Aux/IAA mutants also failed to maintain an apical hook(Tatematsu *et al.*, 2004; Yang *et al.*, 2004) and possessed a shortened hypocotyl and plant height(Tian and Reed, 1999; Yang *et al.*, 2004; Rinaldi *et al.*, 2012; Zhu *et al.*, 2012). Many auxin insensitive mutants in both Arabidopsis and rice also display agravitropic responses, this is most evident from the roots(Tian and Reed, 1999; Fukaki *et al.*, 2002; Yang *et al.*, 2004; Kitomi *et al.*, 2012; Rinaldi *et al.*, 2012; Zhu *et al.*, 2012). Asymmetric distribution of auxin within the root tip enables the plant to respond to a gravistimulation. Auxin is directed disproportionately to the lower root surface, resulting in asymmetric growth(Leyser, 2018). The formation of the root cap is controlled by ARFs, unfunctional ARFs result in developmental defects of the root cap in abnormal root gravitropism(Wang *et al.*, 2005). It is hypothesised that mutant Aux/IAAs may continue to repress the action of ARFs in promoting auxin responsive gene expression and therefore have developmental defects in the root cap and fail to show gravitropism.

Auxin also has an important role in the development of pollen. In rice, IAA was found to accumulate 64-90 times higher in the anthers than in the leaf(Hirano *et al.*, 2008). Auxin signalling is known to play an important role in pollen development, with Aux/IAAs being implicated to be an important component of this(Hirano *et al.*, 2008; Sakata *et al.*, 2010; Rinaldi *et al.*, 2012). Studies in Arabidopsis have shown that when Aux/IAA mutations are homozygous there is either a reduction of seed set(Yang *et al.*, 2004; Uehara *et al.*, 2008) or completely abolished seed set as observed in *iaa16-1*(Rinaldi *et al.*, 2012). However, when *iaa16-1* was hand pollinated with WT pollen they successful set seed, indicating that the female part of the flower develops as normal and the only reduction in fertility is loss of pollen viability(Rinaldi *et al.*, 2012). However, the *Osiaa11* mutant in rice showed no difference in fertility compared to the WT, despite having a strong auxin-insensitive root phenotype(Zhu *et al.*, 2012). This can be attributed to relatively low expression in the flower compared to the root(Sakai *et al.*, 2011). Therefore, indicating that OsIAA11 is more involved in regulating auxin signalling in the root rather than the flower.

Auxin has also been implicated to be involved in abiotic stress tolerance. During heat stress, most Aux/IAA proteins were found to be downregulated in rice and wheat leaf tissue(Qin *et al.*, 2008; Du *et al.*, 2013), thus allowing more auxin responsive gene expression. It was found that in barley and rice anthers, increased temperatures during early stages of anther development, reduced the accumulation of auxin and male sterility occurred; this was reversed by the application of IAA/NAA (Sakata *et al.*, 2010; Sharma *et al.*, 2018). When comparing heat sensitive and heat tolerant varieties of rice, there was found to be a greater reduction in IAA accumulation in heat sensitive lines(Tang *et al.*, 2008). The findings indicate the vital role of auxin signalling in ensuring normal pollen development and viability. It implies that heat stress disrupts auxin regulated pollen development by reducing auxin accumulation in the anther.

So far, no studies have investigated the role of Aux/IAAs in wheat development and abiotic stress tolerance. The recent annotation of the wheat genome, combined with the creation of a TILLING population in wheat var. Cadenza as a resource for mutants in genes of interest(Krasileva *et al.*, 2017), meant a reverse genetics approach was implemented to determine the role of auxin in development and abiotic stress tolerance in wheat. A number of wheat Aux/IAA mutants were discovered, and their phenotypes characterised. The heat stress tolerance of select Aux/IAA mutants was also investigated, along with exogenous application of synthetic auxin 1-Naphthaleneacetic acid (NAA). These studies have given vital insights into the role of auxin in wheat development and heat stress tolerance.

5.2 Materials and Methods

All experimental details are described in section 2.

5.3 Results

5.3.1 The Aux/IAA gene family in wheat

A list of the Aux/IAA gene family in hexaploid wheat has already been characterised(Qiao *et al.*, 2015). However, since this paper was published there have been a number of updates on the annotation of the wheat genome. Consequently, it is necessary to establish an updated list of Aux/IAA genes in

hexaploid wheat from the recent iwgsc_refseqv1.0 annotation available on Ensemble (https://plants.ensembl.org/Triticum_aestivum/Info/Index).

A complete list of Aux/IAA genes in wheat were found by obtaining a sequence list of *Oryza sativa Japonica* Aux/IAA genes from Ensembl. Using the rice protein sequences, BLAST searches were performed against the protein database and the hits downloaded. More wheat Aux/IAAs were found by searching for proteins which contain the Aux/IAA domain with the InterPro domain number IPR033389. Paralogue searches were also performed using this list.

The amino acid sequences were obtained and aligned, with the complete list of Arabidopsis and rice sequences(Jain *et al.*, 2006), using genomics software Geneious (v10.0.02, Biomatters Ltd, Auckland, New Zealand). The alignment was performed using the clustalW alignment tool using the cost matrix PAM. A phylogenetic tree was constructed in Geneious using the Jukes-Cantor genetic distance model and built with the Neighbour-Joining tree building method.

Phylogenetic analysis of the Aux/IAA proteins suggests extensive duplication has occurred within the wheat genome (Figure 5.2). In total 84 different Aux/IAA homoeologues were found, as was previously found using the older CSS wheat annotation(Qiao *et al.*, 2015). However, when converting the list of Aux/IAAs from the CSS annotation to the latest iwgsc_refseqv1.0 annotation there was only found to be 66 genes, 58 of which matched those found from our searches. The remaining 8 additional homoeologues were *TraesCS3A02G442000*, *TraesCS3D02G434700*, TraesCS2B02G578500, TraesCS7A02G252000, *TraesCS6A02G111900*, *TraesCS6A02G112000*, *TraesCS6D02G100800* and *TraesCS6D02G100900.* These were not included in phylogenetic analysis, as their rice orthologues were all ARFs, not Aux/IAAs. They all also lack domains I and II and some contained an extensive amino acid sequence on the N terminus of the protein which is not seen in any other Aux/IAAs.

The majority of the Aux/IAA genes contain 3 copies due to the hexaploidy of *Triticum aestivum*, having a homoeologue on each of the 3 genomes: A, B and D. In total, *Triticum urartu* (A) contributed 27 genes, *Aegilops speltoides* (B) 27 and

Triticum tauschii (D) 30 genes. The wheat orthologue of *OsIAA14* is missing a copy on the A genome and *OsIAA7* on the B genome. Three rice Aux/IAAs: OsIAA8, OsIAA16 and OsIAA22 were removed due to poor alignment with the rest of the Aux/IAA protein family. Despite these exceptions there is a high degree of homology between wheat and rice, whereby the majority of rice genes have a wheat orthologue. There is less homology between Arabidopsis and wheat, however this is to be expected due to being more distantly related.

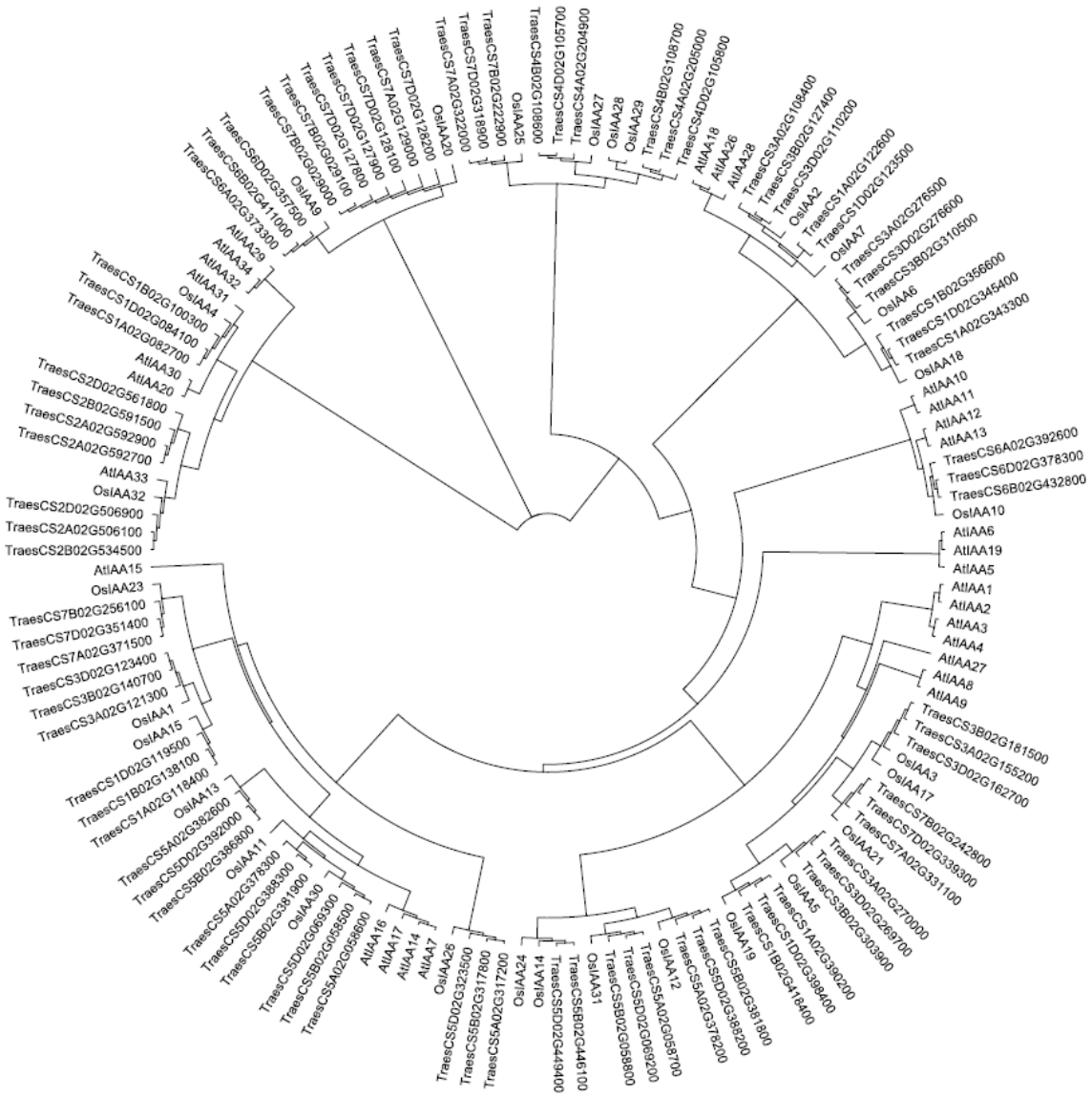

Figure 5.2*: Phylogenetic relationship of the Aux/IAA gene family in Arabidopsis,* Oryza sativa Japonica and Triticum aestivum.

Amino acid sequences were aligned in ClustalW alignment tool using the cost matrix PAM and constructed using the Jukes-Cantor genetic distance model and built with the Neighbour-Joining tree building method in bioinformatics software Geneious.

The majority of the wheat Aux/IAAs contain the classic 4 domain structure. Sharing the domain homology shown in Figure 5.3B. However, some wheat homoeologues show a complete absence of these domains; for example, *TraesCS7D02G128200*, *TraesCS7A02G129000*, *TraesCS4D02G105800*, *TraesCS4B02G108700*, *TraesCS4A02G205000*, *TraesCS2B02G591500* and *TraesCS2A02G592700* show a complete absence of domain I. Domain II is also completely absent in *TraesCS7A02G129000* and *TraesCS4D02G5800*.

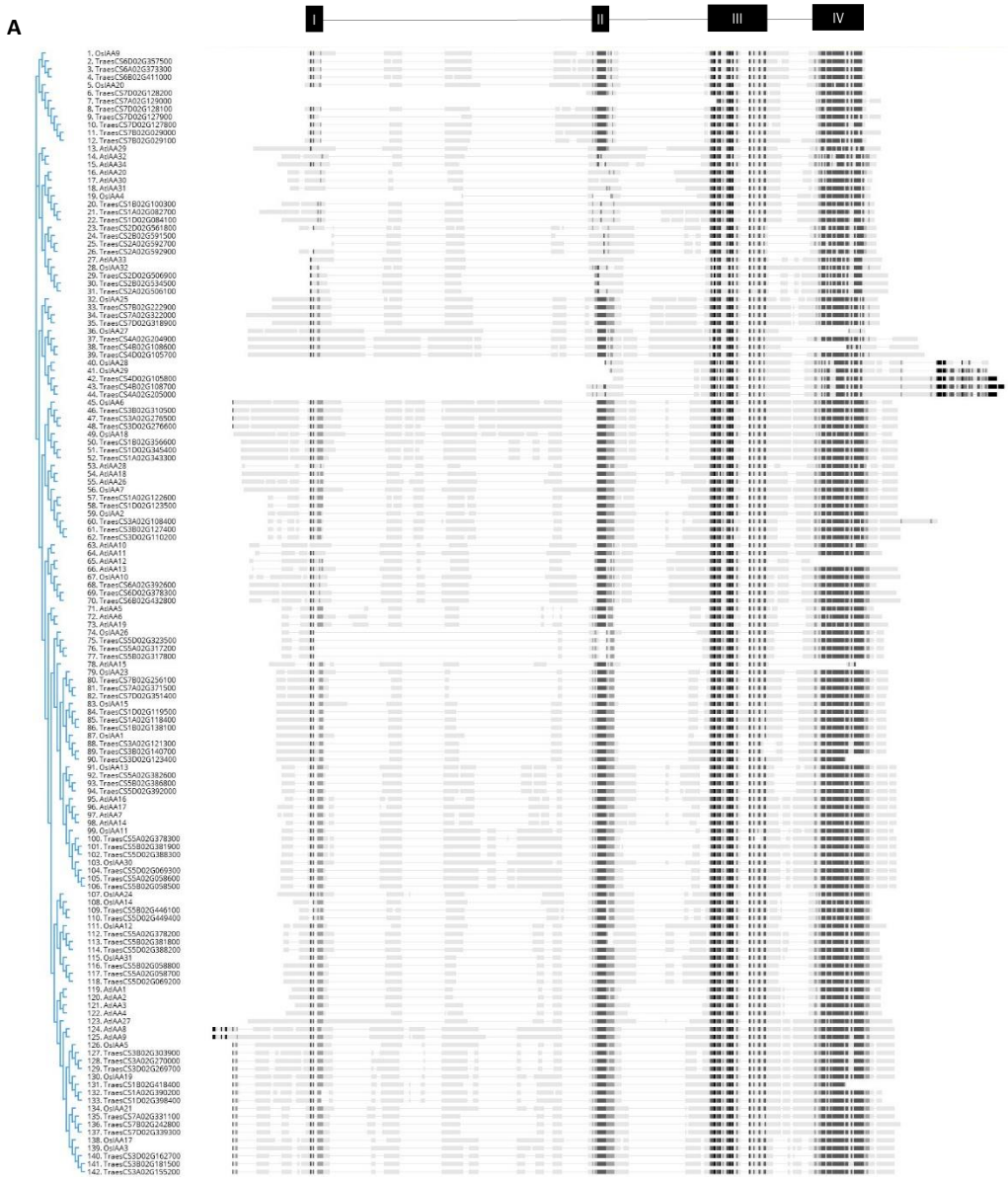
A
I
II
III
IV
B
Motif 1
Motif 2
Motif 3
Motif 4
bits

Figure 5.3: *The domain structure of the Aux/IAA gene family in Arabidopsis, rice and wheat.*

A*: A ClustalW alignment using the cost matrix PAM of Arabidopsis, rice and wheat protein sequences. The positions of the 4 conserved motifs I, II, III and IV are labelled and shared by most members of the Aux/IAA gene family.* **B***: Motif structure of wheat Aux/IAA proteins. Positions of conserved domains are boxed. Taken from Qiao et al., 2015.*

5.3.2 Finding Aux/IAA mutants

Using the established list of Aux/IAAs from the latest iwgsc_refseqv1.0 wheat genome annotation, TILLING lines containing missense mutations in the GWPPV motif of domain II conferring amino acid changes were brought forward (Section 2.7). Mutations within the GWPPV motif are known to confer auxin-insensitive phenotypes in both Arabidopsis and rice(Tian and Reed, 1999; Gray *et al.*, 2001; Ouellet *et al.*, 2001; Ramos *et al.*, 2001; Fukaki *et al.*, 2002; J. Y. Park *et al.*, 2002; Yang *et al.*, 2004; Tatematsu *et al.*, 2004; Uehara *et al.*, 2008; Zhu *et al.*, 2012; Kitomi *et al.*, 2012; Rinaldi *et al.*, 2012). These mutations interfere with the normal interaction of the Aux/IAA with auxin and the TIR1 subunit of the SCF complex, causing it to no longer be poly-ubiquitinated and subsequently degraded(Dos Santos Maraschin *et al.*, 2009). Therefore, this is a reverse genetics approach to identify auxin-insensitive wheat mutants by targeting Aux/IAAs (repressors of auxin signalling) which are resistant to auxin mediated degradation.

All the identified wheat Aux/IAA TILLING mutations conferring missense mutations in the GWPPV motif are shown in Table 5.2. The mutants chosen to investigate were selected based on three criteria. Firstly, whether the identified missense mutation is known to confer an auxin-insensitive phenotype in Arabidopsis or rice, whether the gene is an orthologue of a gene known to induce an auxin-insensitive phenotype and also whether the gene is expressed in the anther from RNAseq data (Figure 5.4). This is because one of our aims was to investigate the role of auxin in pollen development and therefore, we hoped to induce a partial sterility phenotype.

Table 5.2*: A list of the wheat Aux/IAA TILLING lines, their corresponding IWGSC_ refseqv1.0 scaffold name and abbreviated gene name*(Qiao *et al.*, 2015) *and the predicted amino acid substitutions that occur within domain II.*

Tilling Line	Mutant name	IWGSC_ refseqv1.0	Domain II substitution
Cad0188	*Talaa22-Bb*	*TraesCS5B02G381900*	**G** to **R** **R**WPPV
Cad1305	*Talaa34-Ab*	*TraesCS7A02G322000*	**P** to **L** GWP**L**V
Cad1420	*Talaa22-Bc*	*TraesCS5B02G381900*	**P** to **L** GW**L**PV
Cad1806	*Talaa24-Bb*	*TraesCS5B02G446100*	**P** to **R** GWPPV**R**
Cad0139	*Talaa3-Bb*	*TraesCS1B02G138100*	**G** to **D** **D**WPPV
Cad1812	*Talaa22-Ab*	*TraesCS5A02G378300*	**V** to **M** GWPP**M**
Cad1374	*Talaa23-Ab*	*TraesCS5A02G382600*	**V** to **I** GWPP**I**
Cad1366	*Talaa22-Db*	*TraesCS5D02G388300*	**P** to **L** GWP**L**V
Cad0161	*Talaa18-Bb*	*TraesCS5B02G058500*	**P** to **L** GW**L**PV
Cad1673	*Talaa21-Bb*	*TraesCS5B02G381800*	**V** to **M** GWPP**M**
Cad0275	*Talaa33-Db*	*TraesCS7D02G351400*	**G** to **R** **R**WPPV
Cad0388	*Talaa33-Dc*	*TraesCS7D02G351400*	**P** to **S** GWP**S**V

Talaa18-Bb, Talaa22-Bb, Talaa22-Bc, Talaa34-Ab, Talaa22-Db, Talaa33-Db and *Talaa33-Dc,* all contain missense mutations in domain II which have previously been defined to confer auxin insensitivity in Arabidopsis and rice (Table 5.1/2). Therefore, are likely to result in an Aux/IAA protein which is resistant to degradation. *Talaa3-Bb* contains a mutation which has not previously been characterised. The missense

mutation is glycine>aspartic acid (G>D), but was still of interest as conversations of G>glutamic acid (E) conferred an auxin-insensitive phenotype in Arabidopsis *shy2-3*, *axr3-101, crane-2* and *iaa18-1* mutants(Tian and Reed, 1999; Uehara *et al.*, 2008). Both E and D are amino acids which have similar biochemical properties of negatively charged side chains and therefore could still interfere with auxin and SCF^{TIR1} binding. *TaIaa21-Bb, TaIaa22-Ab, TaIaa23-Ab* and *TaIaa24-Bb* all contain more conservative mutations in their GWPPV motif, which have not been documented to cause auxin insensitivity and confer amino acid changes with similar properties.

The majority of the wheat tilling mutants are in genes which are putative orthologues of Arabidopsis and rice genes which have been found to cause auxin-insensitivity. *TaIaa18* the orthologue of rice *OsIAA30* and clusters with *AIAA7/14/16/17* which all have shown to induce auxin-insensitivity in Arabidopsis from mutants *axr2-1*, *slr-1-4*, *iaa16-1* and *axr3-1/3/101* (Table 5.1)(Timpte *et al.*, 1994; Rouse *et al.*, 1998; Fukaki *et al.*, 2002; Uehara *et al.*, 2008; Rinaldi *et al.*, 2012). *TaIaa22* is a putative orthologue of rice *OsIAA10* and Arabidopsis *AtIAA10/11/12/13*, *AtIAA12* has produced the auxin-insensitive mutant *bodenlos*(Hamann *et al.*, 2002). *TaIaa23* is the orthologue of *OsIAA13* has been shown to produce in auxin-insensitive phenotype in rice(Kitomi *et al.*, 2012). The closest Arabidopsis Aux/IAAs it clusters with are also *AtIAA10/11/12/13* as described above. *TaIaa24* is the orthologue of *OsIAA24* and *OsIAA14*, the closest Arabidopsis genes are *AtIAA1/2/3/4/8/9/27*. Mutations in *AtIAA1*, *axr5-1*, and in *AtIAA3 shy2-1/2/3/6* were also found to confer auxin-insensitivity(Kim, 1996; Reed *et al.*, 1998; Tian and Reed, 1999; Yang *et al.*, 2004; Uehara *et al.*, 2008).

When determining which TILLING lines are likely to yield an auxin-insensitive phenotype the level and location of expression is important. Higher expression of the degradation resistant Aux/IAA is likely to result in greater repression of the auxin-signalling pathway. We are most interested in the involvement of auxin in pollen development and heat stress tolerance and therefore examination of the expression of the RNA-seq data generated in chapter 4 is shown (Figure 5.4). All the genes are expressed in the anthers at all stages of pollen development and in

response to heat stress. *TaIaa24-B* consistently shows the highest expression across all stages and treatments, followed by *TaIaa3-B* and *TaIaa18-B*. *TaIaa33-D* and *TaIaa34-A* were found to show the lowest expression, especially *TaIaa33-D* during the early stages and *TaIaa34-A* during the later stages of pollen development.

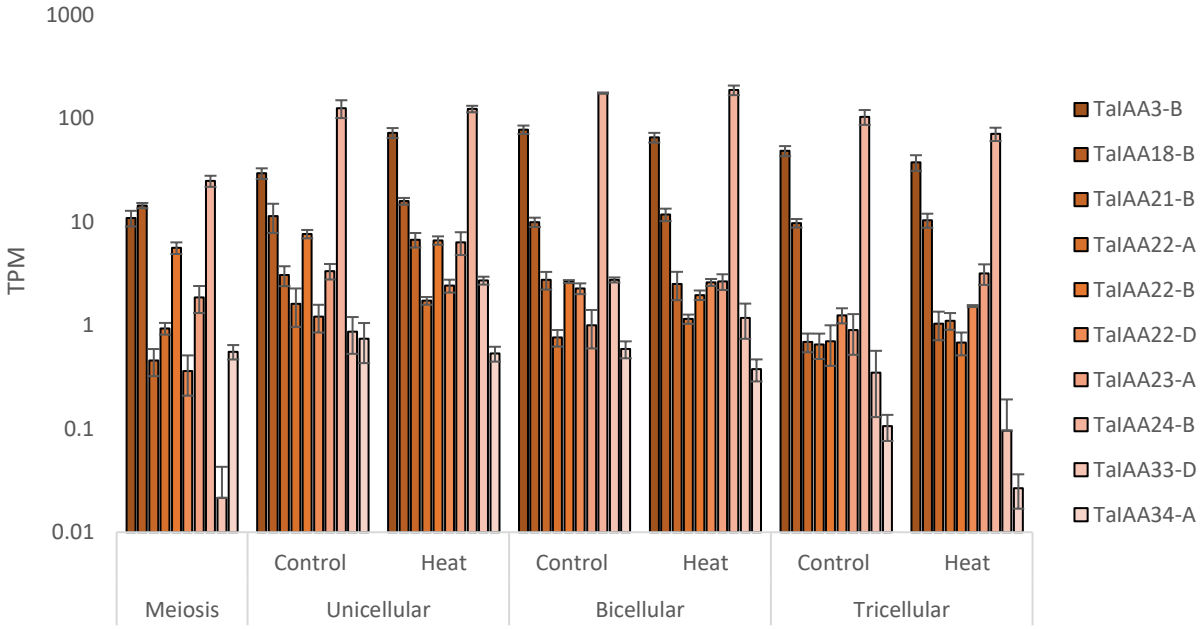

Figure 5.4: *Expression of auxin-insensitive Aux/IAAs across 4 main stages of pollen development and in response to control and heat treatment.*

Anther samples were initially taken at meiosis stage, followed by unicellular, bicellular and tricellular stages in control conditions and after heat stressing for 4 days 33/26°C day/night from meiosis stage. Samples were staged using the Ampha Z32 Pollen Analyzer. Bars represent the mean TPM of 4 biological replicates, error bars represent one S.E.

Carefully taking into the consideration the nature of the mutation, the known knowledge about the orthologues and the expression in the anthers in control conditions and in response to heat stress *TaIaa21-Bb*/*TaIaa33-Db*/*TaIaa33-Dc* were chosen to be omitted from experiments due to low expectations that they would yield an auxin-insensitive phenotype, in particular when it came to investigating pollen development and heat stress. *TaIaa21-B* was found to have low expression in the anthers, conferred a conservative amino acid change and no orthologous

mutants have yet been discovered. *TaIaa33-Db* and *TaIaa33-Dc* were omitted as although they contained amino acid changes in the GWPPV motif which are known to cause auxin-insensitivity; the genes were found to show low expression in the anther, especially at meiosis stage which is the stage most vulnerable to heat stress (Table 5.1) and the rice orthologue (OsIAA23) has not been found to induce an auxin-insensitive phenotype and it does not cluster closely with any Arabidopsis genes.

The selected TILLING lines were subsequently backcrossed twice to Cadenza to remove approximately 75% of EMS-induced SNPs that are present in the background and which could impact on the phenotype.

5.3.3 Root development and auxin sensitivity in wheat Aux/IAA mutants

Aux/IAAs are known to be involved in lateral root development in Arabidopsis and rice (Tian and Reed, 1999; Fukaki *et al.*, 2002; Tatematsu *et al.*, 2004; Yang *et al.*, 2004; Uehara *et al.*, 2008; Kitomi *et al.*, 2012; Rinaldi *et al.*, 2012; Zhu *et al.*, 2012). An initial investigation into the seminal root phenotype of *TaIaa18-Bb, TaIaa22-Bb, TaIaa22-Bc* and *TaIaa22-Db* was executed after initial observations of a divergent root phenotype from WT Cadenza. To investigate the seminal root phenotype a 2D phenotyping approach was implemented. *TaIaa18-Bb, TaIaa22-Bb, TaIaa22-Bc* and *TaIaa22-Db* mutants were grown alongside Cadenza in a randomised 3 block design (section 2.10.1). Measurements of the length of the primary seminal root and the number of laterals on the primary seminal root were taken. The statistical test ANOVA was used for analysis of the untransformed data. All statistical analysis was performed using statistical handling software Genstat (v20, VSNI, Hemel Hempstead, U.K.).

TaIaa18-Bb and *TaIaa22-Db* show a significantly shorter length of primary seminal root compared to the other genotypes, showing a reduction of 53% and 29% compared to Cadenza respectively (Table 5.3). All 4 mutants showed a complete absence of lateral roots in the primary seminal root compared to on average 7.87 in WT Cadenza, therefore suggesting a key role of Aux/IAAs and auxin signalling in lateral root formation of wheat.

Table 5.3: *Seminal root phenotype of 10-day old WT Cadenza and Aux/IAA mutants.*

ANOVA output of measurements of primary seminal root length and the number of lateral roots from the primary seminal root. Pairwise comparisons were made between each genotype using 5% LSDs to determine the significance. * *= significantly different from Cadenza. The values are shown in brackets are the arithmetic mean.*

Genotype	Length of primary root (mm)	Number of lateral roots
Cadenza	170.5	8.67(7.87)
Talaa18-Bb	79.7*	-0.46*(0)
Talaa22-Bb	164.2	-0.03*(0)
Talaa22-Bc	184.9	-0.15*(0)
Talaa22-Db	121.7*	-0.36*(0)
P-value	<.001	<.001
SED	22.37	0.981
LSD (5%) (83 d.f)	44.49	1.951

Following on from this we wanted to investigate the impact of endogenous application of NAA on lateral root formation in Cadenza and the Aux/IAA mutants. Auxin is known to be involved in the formation of lateral root primordia (LRP) which eventually develop into lateral roots(De Smet *et al.*, 2007). We sought to investigate if NAA could induce formation of lateral roots in both WT Cadenza and the Aux/IAA mutants.

Cadenza, *Talaa18-Bb, Talaa22-Bb, Talaa22-Bc* and *Talaa22-Db* were used in this experiment. The plants were treated with either 0µM or 5µM NAA. The set up was described in section 2.10.2. The experiment conducted was a randomised block design where each role is considered a randomised block, and this was replicated 4 times for each treatment (a total of 4 roles and 4 biological replicates per treatment). Measurements of root length, diameter and number of laterals were taken for all the seminal roots. Lateral root number was transformed by $\log_{10}+1$ to ensure normal distribution. REML analysis was performed.

There was found to be a significant impact of genotype (P<0.001) and NAA treatment (P=0.012) on lateral root number, however there was no significant interaction between genotype and NAA treatment (P=0.632). Results demonstrate that WT Cadenza exposed to 5µM NAA shows a significantly greater number of lateral roots than the control (5% LSD = 0.2321) (Table 5.4), however there was no significant increase in lateral root number in *TaIaa18-Bb, TaIaa22-Bb, TaIaa22-Bc and TaIaa22-Db* (5% LSD = 0.2839, 0.2277, 0.2298 and 0.2424 respectively). No lateral root formation was observed in *TaIaa18-Bb* and *TaIaa22-Db* in the absence of NAA, as was also initially found using 2D phenotyping (Table 5.3). However, when exposed to 5µM NAA for 3 days there was the occasional formation of a lateral root, being on average 0.125 per root at *TaIaa18-Bb* and 0.1 per root at *TaIaa22-Db* (Table 5.4). Out of all the mutants *TaIaa22-Bc* produced the greatest number of lateral roots with on average 4.16 per root at 0µM NAA and 4.96 per root at 5µM NAA. However, this is still significantly less than Cadenza in both treatments. The occasional appearance of lateral roots in *TaIaa22-Bc* and *TaIaa22-Db* using the cigar role experiment compared to the complete absence using 2D phenotyping could be due to the observed difference in rate of development. The cigar rolled plants were noted to grow faster compared to the 2D phenotyped plants and therefore the 2D phenotyped plants were a little behind in lateral root formation.

There was found to be no effect of NAA treatment on diameter of the roots (P=0.43), however there was a significant effect of genotype (P<0.001). The average diameter was 0.4874mm, 0.3518mm, 0.4086mm, 0.4274mm and 0.4772mm for Cadenza, *TaIaa18-Bb, TaIaa22-Bb, TaIaa22-Bc* and *TaIaa22-Db* respectively (5% LSD compared to Cadenza = 0.03357, 0.03088, 0.03098 and 0.03156 respectively). Therefore, all mutants showed a significantly smaller seminal root diameter than Cadenza, with the exception of *TaIaa22-Db.*

There was not found to be a significant reduction in root growth of Cadenza in response to 3 days of 5µM NAA (P=0.034; 5% LSD = 5.693) despite showing on average a 14% reduction in elongation. Indeed *TaIAA18-Bb* showed a significantly increased length of seminal root (5% LSD=6.019), suggesting no auxin induced inhibition of root growth.

Table 5.4: *Effect of NAA treatment on the average diameter, length and number of lateral roots of seminal roots. 10-day old Cadenza, Talaa18-Bb, Talaa22-Bb, Talaa22-Bc and Talaa22-Db were investigated.*

*Output of REML analysis. Pairwise comparisons were made between each genotype and treatment using 5% LSDs to determine the significance. *= significantly different from control of same genotype. Lateral root number was transformed by log_{10}+1 to ensure normal distribution.*

Genotype	Treatment	Diameter (mm)	Length (cm)	Nom laterals
Cadenza	Control	0.4791	25.54	25.725(1.3034)
	5 µM NAA	0.4957	22.02	37.45(1.5618)*
Talaa18-Bb	Control	0.3568	17.57	0(0)
	5 µM NAA	0.3469	26.12*	0.125(0.0343)
Talaa22-Bb	Control	0.4002	22.19	0.4(0.0991)
	5 µM NAA	0.4170	23.88	1.65(0.2597)
Talaa22-Bc	Control	0.4271	28.17	4.1625(0.3957)
	5 µM NAA	0.4277	24.40	4.9625(0.5716)
Talaa22-Db	Control	0.4793	27.10	0(0)
	5 µM NAA	0.4751	24.39	0.1(0.0340)
Genotype		<0.001	0.055	<0.001
Treatment		0.43	0.669	0.012
Genotype*Treatment		0.875	0.034	0.632
Max SED		0.02480	3.192	0.1391
Max LSD 5% (d.f.)		0.05980	7.651	0.2839

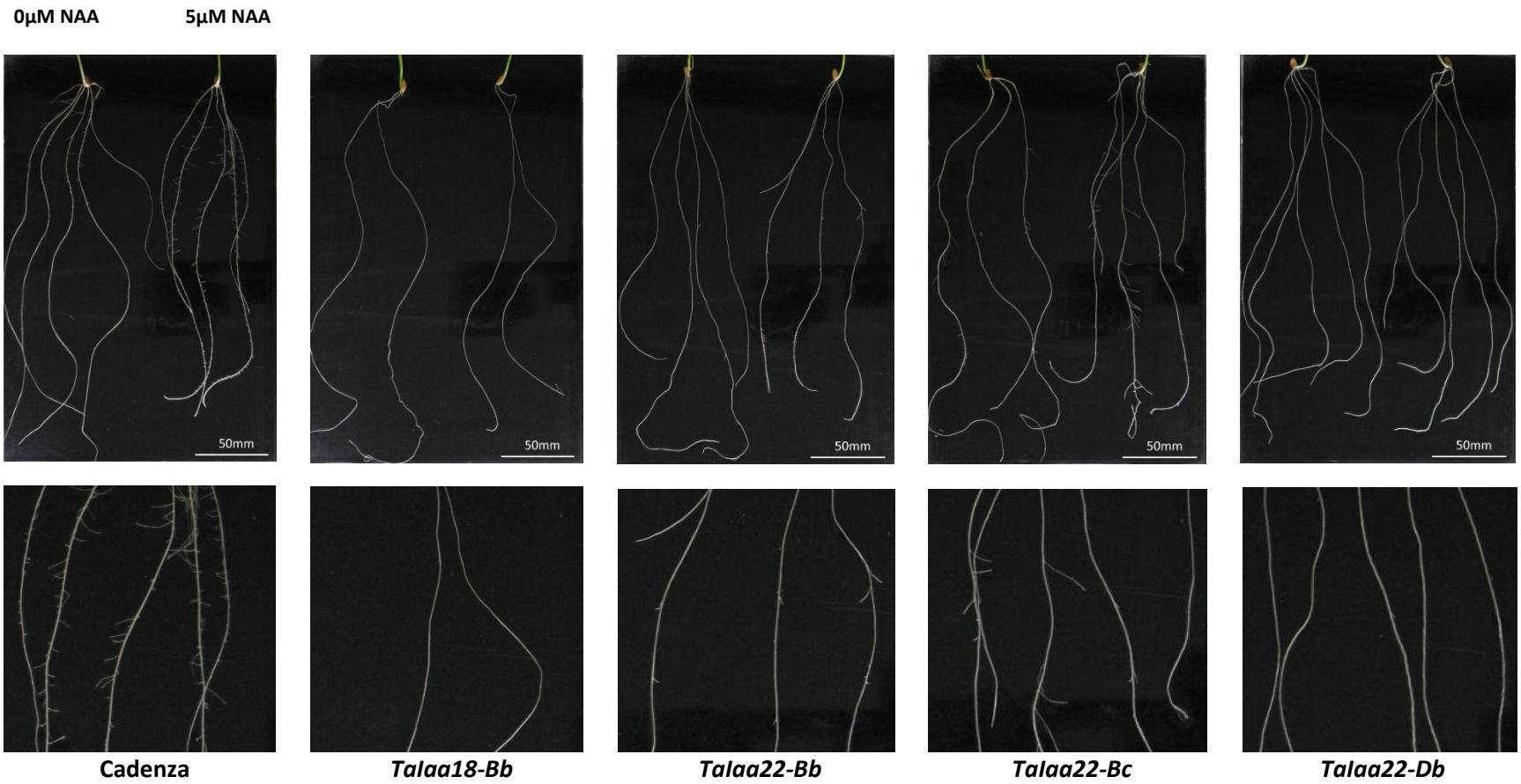

Figure 5.5: *Effect of NAA on the seminal root length and lateral root number of Cadenza and auxin-insensitive mutants.*

Phenotype of Cadenza, Talaa18-Bb, Talaa22-Bb, Talaa22-Bc and Talaa22-Db grown for 7 days on rolled germination paper and ¼ Hoagland's solution, before being treated with either 0µM or 5µM NAA for 3 more days. The photographs below are closeups of plants treated with 5µM NAA.

Longitudinal cross sections were taken across the length of the root of *Taiaa18-Bb,* the mutant with the most severe phenotype. The cross sections demonstrate the absence of LRP (Figure 5.6), even when treated with 5µM NAA.

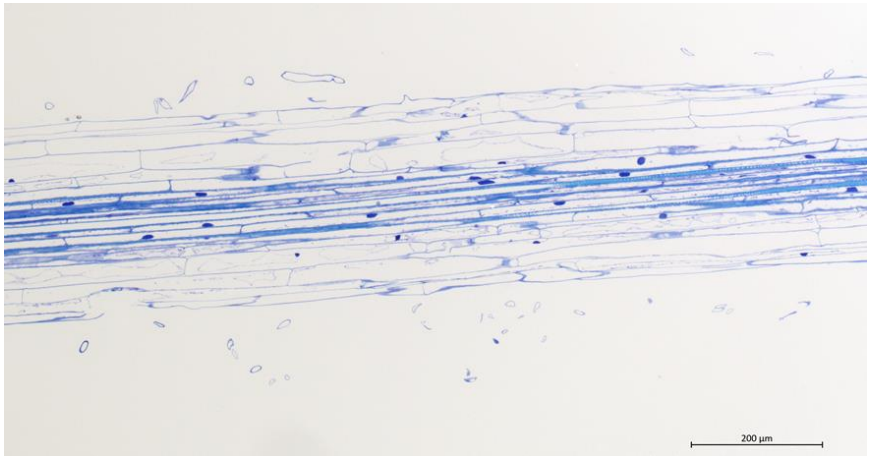

Figure 5.6: *Longitudinal sections of 10-day old TaIaa18-Bb treated with 5µM NAA. TaIaa18-Bb shows no initiation of lateral root primordia. Toluidine blue staining.*

Following on from this we wanted to investigate the nodal root phenotype of these mutants. Due to the size of wheat, we could not use the 2D phenotyping or cigar role method to examine structure of the nodal roots. Instead, plants were grown for 23 days in sand columns, before they were harvested, and measurements of their physiology were taken (Section 2.10.4). Selected genotypes *TaIaa22-Bb, TaIaa22-Bc, TaIaa22-Db* and Cadenza, were incorporated into the experiment. A total of 6 trays were used for the experiment; these were treated as blocks. Different genotypes were arranged in a randomised balanced block design leading to a total of 9 biological replicates for each genotype across the 6 blocks. *TaIaa18-Bb* was not included in the experiment, despite being shown to be auxin insensitive, due to very poor root architecture likely disrupting the measurements. From each plant, 5 seminal roots were taken, and their phenotype analysed. The data was all found to be normally distributed and ANOVA analysis was applied to all measurements.

Figure 5.7: *Seminal root phenotype of Cadenza, Talaa22-Bb, Talaa22-Bc and Talaa22-Db.*

Photograph of 24-day old plants grown on sand columns.

From initial observation *Talaa22-Bb, Talaa22-Bc* and *Talaa22-Db* possess a sparser network of nodal roots compared to WT Cadenza (Figure 5.7). All three mutants show significantly fewer nodal roots compared to Cadenza ($P<0.001$; 5% LSD=2.409), all having around 30% fewer nodal roots (Table 5.5) and fewer lateral roots (although not absent as was found with *Talaa22-Db* in the seminal roots (Table 5.4)) ($P<0.001$; 5% LSD=1.853). The roots on average were longer in the mutants compared to Cadenza ($P=0.048$; 5% LSD=1.898), with *Talaa22-Db* being significantly longer. There was also found to be no difference in the diameter of the seminal roots of the mutants and Cadenza ($P=0.282$; 5% LSD=0.0765). Overall, however, the total root dry weight was significantly lower in each of the mutants compared to Cadenza ($P<0.001$; 5% LSD=0.1352), being around 50% lower in *Talaa22-Bb* and *Talaa22-Db*. At this early stage there appears to be a more severe difference in stem physiology than later. Mutants appear shorter (Figure 5.7) and have a significantly lower shoot DW compared to Cadenza (($P<0.001$; 5%

LSD=0.1352). There was, however, no difference in tiller number compared to Cadenza (P=0.345; 5% LSD=0.711).

Table 5.5: *Phenotypic analysis of 24-day old WT Cadenza and Aux/IAA mutants grown in sand columns.*

*ANOVA output of phenotypic measurements of the roots and shoots. Pairwise comparisons were made between each genotype using 5% LSDs to determine the significance. *Significantly different from Cadenza.*

Genotype	Tiller Nom	Shoot DW (g)	Nodal root nom	Root DW (g)	Nodal root length (cm)	Lateral root nom/root	Diameter (mm)
Cadenza	4.36	1.003	21.51	0.402	5.49	6.81	1.207
Talaa22-Bb	3.76	0.501*	14.45*	0.179*	6.73	0.78*	1.175
Talaa22-Bc	3.90	0.657*	14.68*	0.222*	6.00	0.55*	1.249
Talaa22-Db	3.88	0.408*	14.24*	0.212*	8.09*	0.17*	1.212
P-value	0.345	<.001	<.001	<.001	0.048	<.001	0.282
SED	0.346	0.0659	1.174	0.0440	0.925	0.903	0.0373
LSD (5%) (27 d.f)	0.711	0.1352	2.409	0.0903	1.898	1.853	0.0765

Talaa18-Bb, Talaa22-Bb, Talaa22-Bc and *Talaa22-Db* all show a root phenotype indicative of auxin-insensitivity. In order to quantify this, it is necessary to investigate how the mutants respond to treatment of synthetic auxin NAA (1-Naphthaleneacetic acid). Auxins inhibit the elongation of the root, by inhibiting the elongation of root epidermal cells(Fendrych *et al.*, 2018). Measurements of root elongation allow a rapid way to quantify the severity of auxin-insensitivity of the mutants. To quantify the degree of auxin-insensitivity 4 Aux/IAA mutants, *Talaa18-Bb, Talaa22-Bb, Talaa22-Bc* and *Talaa22-Db* were grown along with WT Cadenza on plates containing 0µM, 1µM or 5µM NAA following the methods detailed in section 2.10.3. Each plate contained the 4 Aux/IAA mutants and WT Cadenza randomised. Each NAA treatment was repeated 4x over 4 plates. An ANOVA analysis was performed on non-transformed data.

In the absence of NAA there was no significant difference in root elongation between any of the mutants and the Cadenza (Figure 5.8C). *TaIaa18-Bb, TaIaa22-Bc* and *TaIaa22-Db* all show a significantly lower reduction in root elongation compared to Cadenza when treated with NAA (Figure 5.8C). 1 µM NAA led to a reduction in root elongation in Cadenza by 49% and 5 µM led to a reduction by 77%. The most extreme mutant was *TaIaa18-Bb,* which showed no significant reduction in root length across both concentrations of NAA. *TaIaa22-Bc and TaIaa22-Db* showed no significant reduction in root elongation in response to 1 µM NAA treatment, however at 5 µM NAA there was a significant reduction in root elongation by 50% and 41% respectively. However, *TaIaa22-Bb* showed a significant reduction in root length at both 1 µM and 5 µM NAA, showing a reduction of 40% at 1 µM and 53% at 5 µM. However, *TaIaa22-Bb* does have a significantly longer average root length at 5 µM compared to Cadenza (average root length of 37.5mm and 15.7mm respectively), therefore suggesting a greater degree of auxin-insensitivity than Cadenza. There was found to be no significant effect of NAA treatment on shoot elongation across all genotypes. In the presence and absence of NAA *TaIaa18-Bb* and *TaIaa22-Db* both showed significantly shorter shoots compared to Cadenza and the other two mutants (Figure 5.8D).

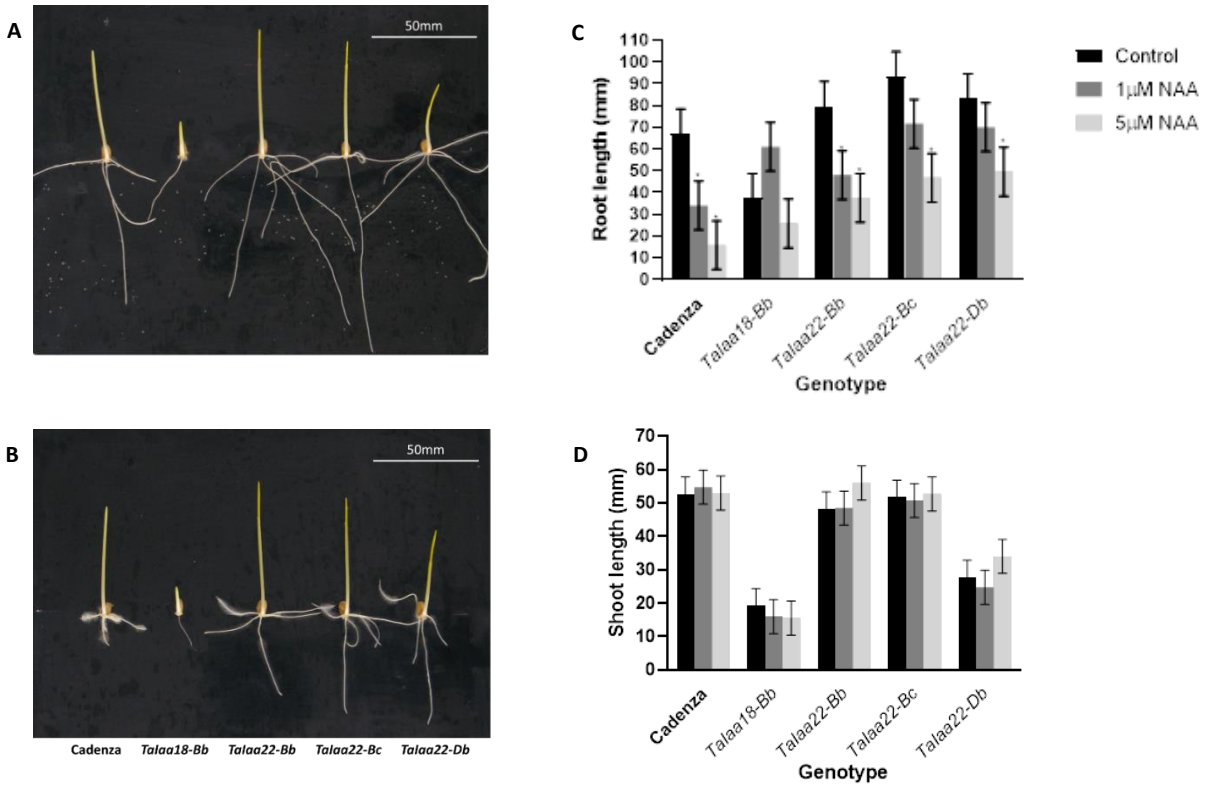

Figure 5.8: *Sensitivity of Cadenza and 4 Aux/IAA mutants to NAA treatment.*

***A-B**: Left to right WT Cadenza, Talaa18-Bb, Talaa22-Bb, Talaa22-Bc and Talaa22-Db grown on control (A) and 5μM NAA media (B) for 3 days. **C**: Length of primary seminal root in response to three treatments: control, 1μM NAA and 5μM NAA after 3 days. Bars are the ANOVA output of the predicted means for 4 biological replicates. Error bars = +/- 1. SED (5%) = 11.2 comparing means of the same treatment. LSD (5%) = 21.81 (44.12 d.f) and 22.71 (36 d.f) when comparing means between treatments and within treatments respectively. *Significantly different from control treatment of the same genotype. P=0.042. **D**: Length of shoot in response to three treatments: control, 1μM NAA and 5μM NAA after 3 days. Bars are the ANOVA output of the predicted means for 4 biological replicates. Error bars =+/- 1 SED (5%) = 5.103 comparing means of the same treatment. LSD (5%) = 10.311 (44.99 d.f) and 10.35 (36 d.f) when comparing means between treatments and within treatments respectively. P=0.733. Bar graphs created using GraphPad Prism Software.*

When grown on control phytagel, Cadenza seedlings show root hair formation, whilst the mutants show sparser and shorter root hairs (Figure 5.9). In response to

5µM NAA there is a clear proliferation of root hairs in Cadenza, both in density and length. The mutants also showed a proliferation in length and density; however, this was not as dramatic as Cadenza. *TaIaa22-Db*'s root hairs were the least responsive to NAA.

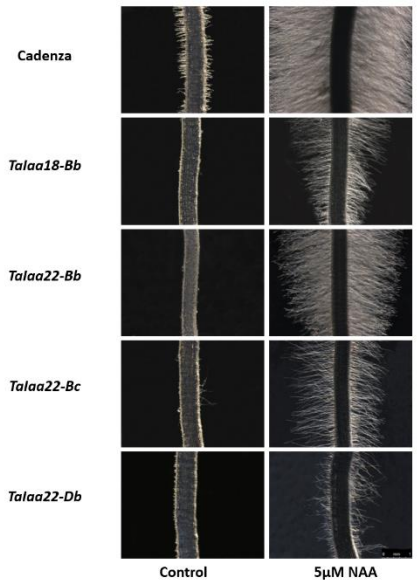

Figure 5.9: *Root hair phenotype of Cadenza and 4 Aux/IAA mutants.*

Cadenza, TaIaa18-Bb, TaIaa22-Bb, TaIaa22-Bc and TaIaa22-Db grown on control or 5µM NAA media for 3 days. Photograph taken from the middle of the root.

5.3.4 Responsiveness to changes in the direction of gravity

Auxin in known to play a key role in the perception of gravity and the growth in the direction of gravity(Morita and Tasaka, 2004). Many Arabidopsis Aux/IAA auxin-insensitive mutants have been found to be agravitropic(Tian and Reed, 1999; Fukaki *et al.*, 2002; Tatematsu *et al.*, 2004; Yang *et al.*, 2004; Rinaldi *et al.*, 2012). An investigation into the gravitropic phenotype of these auxin-insensitive wheat mutants was implemented to investigate the role of auxin in gravity perception in wheat. Rotation studies on seedlings were used to quantify the responsiveness of growth to changes in the direction of gravity.

Cadenza, TaIaa18-Bb, TaIaa22-Bb, TaIaa22-Bc and TaIaa22-Db were all incorporated into a gravitropism experiment (Section 2.10.5). Each plate consisted of one biological replicate of each genotype, which were all randomised. This was repeated 4 times across 4 plates. Cadenza, being a monocot, has a fibrous root structure, with 5 seminal roots emerging from the seed at different angles. Measurements of the primary seminal root were taken as it is the only root which directly grows directly downwards following the direction of gravity. ANOVA analysis was applied to all measurements, with no transformation required.

After 1 day after being rotated 90° *Cadenza, TaIaa18-Bb* and *TaIaa22-Bb* all showed a root angle below 90°, showing that the primary seminal root is already responding to the direction of gravity. However, the roots of *TaIaa22-Db* show a significantly reduced gravitropic response compared to Cadenza (P=0.012; 5% LSD = 36.17), having an average root angle of above 90°, suggesting that on average it grew in the opposite direction to gravity (Figure 5.10A).

The shoots of *Cadenza, TaIaa18-Bb, TaIaa22-Bb, TaIaa22-Bc and TaIaa22-Db* all showed a change in growth direction in the opposite direction to gravity. Therefore, indicating that the shoots are perceiving and responding to the change in the direction of gravity. However, the angle of response differed depending on the genotype. *TaIaa22-Db* showed a significantly greater angle compared to Cadenza (P=0.026; 5% LSD = 11.03), indicating that it is not perceiving or responding to the change in direction of gravity as rapidly as the other genotypes. *TaIaa18-Bb, TaIaa22-Bb, TaIaa22-Bc* do not show a significantly different gravitropic response compared to Cadenza (Figure 5.10B).

As well as Aux/IAAs being involved in growth response to gravity they are also thought to be involved in regulating starch granule accumulation and distribution in the root tip(Luo *et al.*, 2015; Zhang *et al.*, 2019). Perception of the direction of gravity relies on starch granules (statoliths) which sediment in the direction of the pull of gravity (Leitz *et al.*, 2009; Band *et al.*, 2012; Baldwin *et al.*, 2013; Sato *et al.*, 2015). To determine whether the agravitropism is due to failure to perceive the

direction of gravity the root tips were stained with Lugol's solution to determine the presence of starch (Section 2.5.4). It revealed that Cadenza has less accumulation of starch compared to the Aux/IAA mutants, with the greatest accumulation occurring in *TaIaa22-Bb, TaIaa22-Bc* and *TaIaa22-Db* (Figure 5.10C). This surprising result indicates no change in the ability to perceive the direction of gravity in the Aux/IAA mutants.

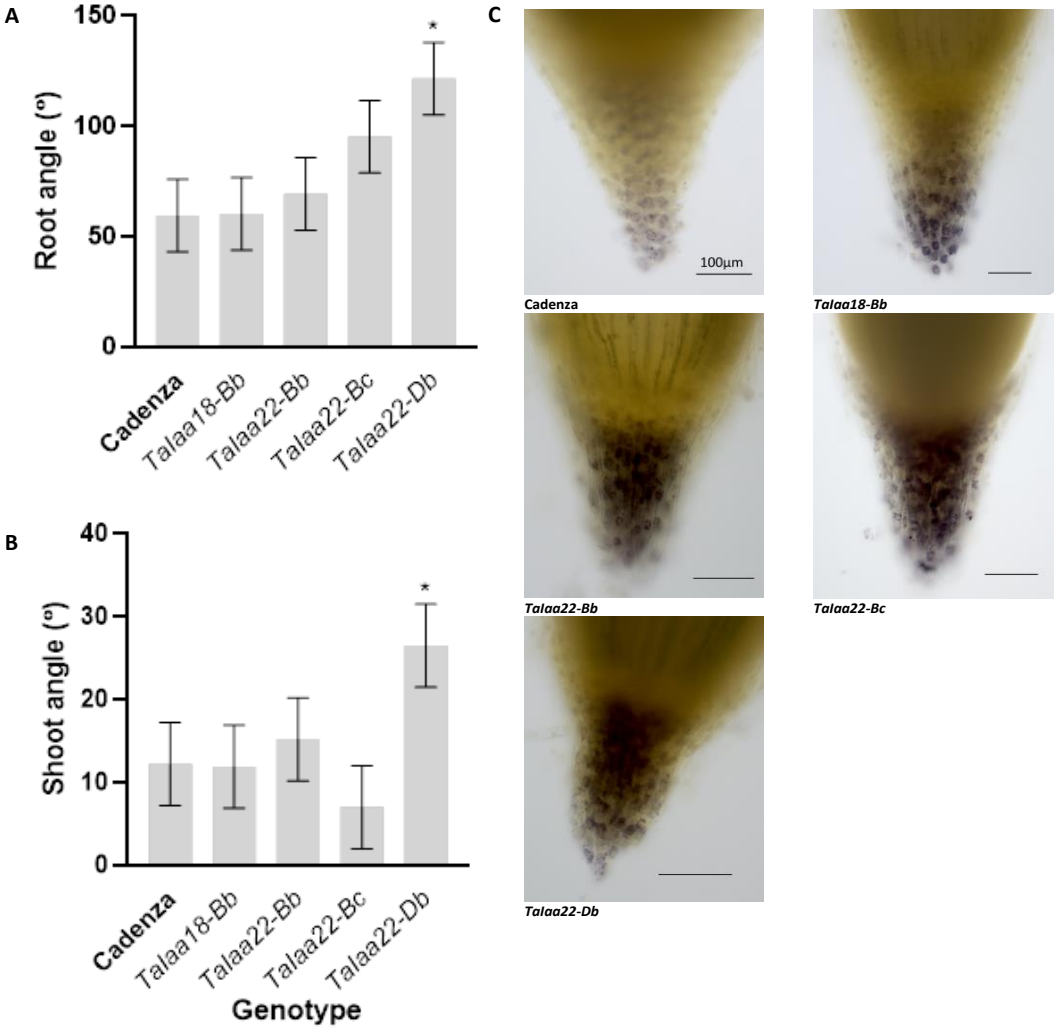

Figure 5.10: *Gravitropic response of the roots and shoots of Cadenza, Talaa18-Bb, Talaa22-Bb, Talaa22-Bc and Talaa22-Db*

***A**: ANOVA output of the angle of the root to the direction of gravity after 2-day old seedlings grown vertically on media were turned 90° and allowed to grow for 1 more day. Error bars =+/- 1 SED (5%) = 16.43. LSD (5%) = 36.17 (11 d.f). *Significantly different from Cadenza. (P=0.012). **B**: ANOVA output of the angle of the shoot to the direction of gravity after 2-day old seedlings grown vertically on media were turned 90° and allowed to grow for 1 more day. Error bars =+/- 1 SED (5%) = 5.01. LSD (5%) =11.03 (11 d.f). *Significantly different from Cadenza. (P=0.026).* **C**: *Accumulation of starch granules in the root tips. Root tips were fixed in resin, before being stained with Lugol's solution. Scale bar = 100µM. Bar graphs created using GraphPad Prism Software.*

5.3.5 General above ground phenotype

A detailed investigation into the general phenotype of the Aux/IAAs mutants was conducted. This characterisation was used to determine the effect of the Aux/IAA mutations on the above ground phenotype of the plants and to investigate whether there are any indicative signs of auxin-insensitivity. Aux/IAA mutants in Arabidopsis and rice have been shown to have a reduced plant height and tiller number(Tian and Reed, 1999; Zhu *et al.*, 2012).

A 4-bock randomised glasshouse experiment was implemented, each block consisted of one biological replicate of each of 9 Aux/IAA lines with the mutant and null segregant (NS) in each of these along with WT Cadenza. This led to a total of 19 plants per block. Plants were grown in glasshouse conditions (Section 2.1) until maturity. Whole plant data was collected on tiller number, heading date; and from three of the tallest tillers measurements of internode length, spike length and average grain number were taken. Only tillers which produced a spike were counted and heading date was recorded when the spike had completely emerged from the flag leaf sheath. Internodes 1-4 (1 being the highest internode of the tiller) were measured individually. Measurements were completed when all plants had reached GS93 (harvest) of the Zadoks scaling system of wheat (Figure 3.1). All measurements were determined to be normally distributed and therefore no transformation was required. ANOVA analysis was used. For all these measurements there was found to be a significant effect of genotype ($P<0.001$) (Table 5.6).

Figure 5.11: *Phenotypes of hexaploid wheat (var. Cadenza) Aux/IAA mutants.*

Phenotype of Aux/IAA mutants grown in glasshouse conditions. Cad: Cadenza, NS: Null Segregant and Mut: Mutant. Scale bar = 100mm. Photographs were taken at GS93 of the Zadoks scale.

TaIaa18-Bb was found to show the most divergent phenotype from both its NS (*TaIaa18-Ba*) and WT Cadenza (Table 5.6; Figure 5.11). Spike emergence was found to occur on average 9 days later, on average it produced only 1.5 tillers, possessed shorter spikes, and reduced length of each of the internodes. There was also found to be a 76% reduction in grain set/spike compared to *TaIaa18-Ba* and a 77.5% reduction compared to Cadenza.

TaIaa22-Bb and *TaIaa22-Bc* are both different missense mutations within the GWPPV domain in the same gene (Table 5.2). Although both show a phenotype significantly different to that of the WT and their NS (*TaIaa22-Ba*). *TaIaa22-Bb* shows a more severe phenotype, indicating that this missense mutation is producing an Aux/IAA which is more resistant to degradation (Table 5.6). *TaIaa22-Bb* was found to have around a 50% reduction in grain set compared to its NS and Cadenza, whereas *TaIaa22-Bc* had significantly fewer grain compared to Cadenza but not its NS despite having an 18% reduction in grain set. Both *TaIaa22-Bb* and *TaIaa22-Bc* also show a significantly shorter spike length compared to their NS and Cadenza. Both *TaIaa22-Bb* and *TaIaa22-Bc* have a similar height phenotype. The second internode of both mutants is significantly longer than WT Cadenza, but not the NS, suggesting that a background mutation is present in both lines which is affecting elongation of this node and has not been removed by backcrossing. The third internode of *TaIaa22-Bb* is also significantly longer than the NS and Cadenza, and for *TaIaa22-Bb* significantly longer than the NS.

TaIaa22-Db showed a less severe phenotype, but there is evidence of some degree of auxin-insensitivity (Table 5.6). *TaIaa22-Db* showed significantly later ear emergence compared to WT Cadenza, but not the NS (*TaIaa22-Da*) and a shorter spike length compared to the NS. Both *TaIaa22-Db* and its NS showed significantly fewer tillers compared to Cadenza, suggesting that this is a result of a background mutation still present in both lines.

TaIaa23-Ab showed a significantly reduced grain set compared to WT Cadenza and its NS (*TaIaa23-Aa*). Both *TaIaa24-Bb* and *TaIaa34-Ab* showed significantly reduced

grain set compared to WT Cadenza, but not their NS. *TaIaa24-Bb* also showed a shorter spike length and for *TaIaa34-Ab* a shorter 3rd internode than WT Cadenza, but once again not the NS. This indicates that the phenotypes evident in both lines could be due to the effect of a background mutation.

Table 5.6: *Effect of missense mutations in the GWPPV motif of Aux/IAAs on phenotype.*

A phenotypic comparison of WT Cadenza with the 9 Aux/IAA mutants (Mut) and their null segregant (NS). ANOVA output of grain count/spike, spike length, tiller number, spike emergence and internode length). P<0.001. Pairwise comparisons were made between each phenotype using 5% LSDs to determine the significance. [a]= significantly different from NS segregant, [b]=significantly different from WT Cadenza.

Genotype		Spike emergence (days)	Grain count/spike	Spike length (cm)	Tiller number	Internode lengths			
						1	2	3	4
Cadenza		79.75	78.00	11.05	10.75	36.6	17.525	12.417	8.37
Talaa3-Ba	NS	80.50	75.67	10.292	6.25 [ab]	37.26	16.292	11.017	6.65
Talaa3-Bb	Mut	79.75	67.58	9.883 [b]	10.00	36.39	17.442	12.475	8.92 [a]
Talaa18-Ba	NS	81.50	73.17	11.925	7.25 [a]	34.42	17.100	11.508	6.68
Talaa18-Bb	Mut	90.33[ab]	17.56 [ab]	8.454 [ab]	1.50 [ab]	27.65 [ab]	14.015 [ab]	8.738 [ab]	4.87 [ab]
Talaa22-Aa	NS	82.25	82.50	11.258	8.00 [a]	38.34	17.633	11.9	8
Talaa22-Ab	Mut	84.75	70.42	11.017	7.25 [a]	36.4	16.550	12.142	8.14
TalAA22-Ba	NS	89.50 [a]	75.25	11.775	9.25	39.46	17.917	13.55	10.68 [b]
TalAA22-Bb	Mut	92.50 [b]	38.25 [ab]	9.567 [ab]	8.75	37.12	19.692 [b]	15.242 [ab]	11.96 [b]
TalAA22-Ba	NS	80.75	72.42	10.358	11.25	35.73	18.383	12	7.53
TalAA22-Bc	Mut	84.25	59.25 [b]	9.042 [ab]	10.50	33.88	20.033[b]	13.658 [a]	7.65
Talaa22-Da	NS	78.00	65.50	9.992	7.25 [a]	33.11	15.933	10.95	6.13 [b]
Talaa22-Db	Mut	85.25[a]	57.25	8.883 [b]	6.00 [a]	33.54	15.558	10.617	6.74
Talaa23-Aa	NS	81.00	81.83	10.908	7.50 [a]	33.02	17.617	12.658	8.26
Talaa23-Ab	Mut	80.50	64.72 [ab]	10.008	8.25	30.33[b]	16.450	11.992	7.6
Talaa24-Ba	NS	79.25	60.83 [b]	9.342 [b]	9.25	32.43[b]	16.333	11.45	7.62
Talaa24-Bb	Mut	82.50	63.83 [b]	9.55 [b]	9.00	33.13	16.983	11.508	7.17
Talaa34-Aa	NS	80.25	70.33	10.442	9.25	33.11	16.533	11.608	8.19
Talaa34-Ab	Mut	78.00	58.42[b]	10.008	11.50	33.54	15.658	10.683 [b]	6.96
P-value		<0.001	<0.001	<0.001	<0.001	<0.001	<0.001	<0.001	<0.001
SED		3.027	6.811	0.557	1.273	1.932	1.0087	0.7543	0.888
LSD (5%) (d.f)		6.072(53)	13.668(52)	1.1172(52)	2.552(54)	3.875(53)	2.0233(53)	1.5130(53)	1.7891(53)

.

5.3.6 Spike morphology and pollen development

The findings of reduced grain set coupled with evidence of sterility occurring towards the tip of the spike warranted further investigation into the grain set and spike morphology of select mutants (Table 5.6). Grain set data from the tip of the spike was counted from the top 8 spikelets (Figure 5.12) of *TaIaa18-Bb, TaIaa22-Bb, TaIaa22-Bc*, *TaIaa22-Db,* their NS and WT Cadenza. ANOVA analysis was performed on grain set data which had been transformed using the function logit+1.

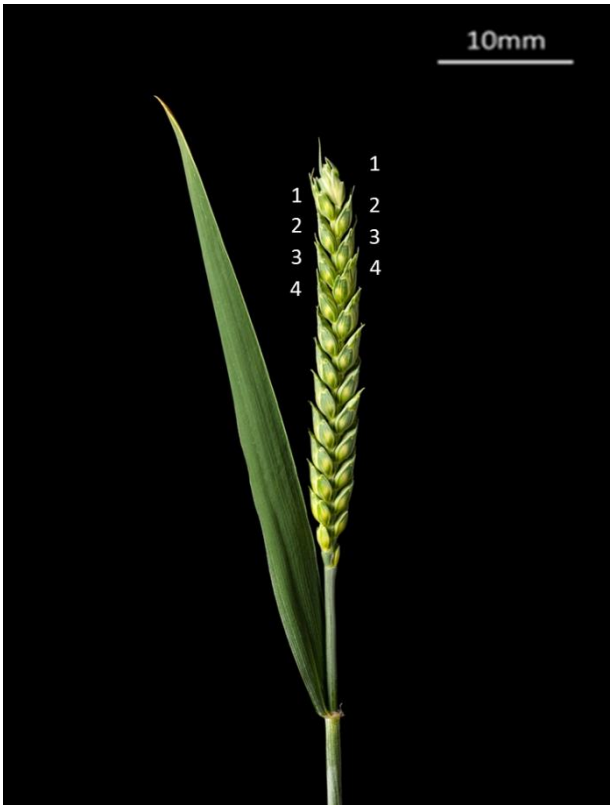

Figure 5.12: *The top 8 spikelets which were used to examine grain count in selected Aux/IAA mutants, labelled 1-4 running along either side of the spike.*

Studies in Arabidopsis have shown that some Aux/IAA gain-of-function mutants result in a reduction of seed set(Yang *et al.*, 2004; Uehara *et al.*, 2008) or completely abolished seed set (Rinaldi *et al.*, 2012). However, the impact on fertility depends

on which Aux/IAA is mutated, with the *Osiaa11* mutant in rice showing no reduction in grain set despite showing an auxin-insensitive root phenotype(Zhu *et al.*, 2012). Our wheat Aux/IAA mutants *TaIaa18-Bb, TaIaa22-Bb, TaIaa22-Bc* and *TaIaa22-Db* all showed a significant reduction in grain set towards the tip of the spike (ANOVA: P<0.001, Figure 5.13A/B). This is most pronounced in *TaIaa18-Bb* and *TaIaa22-Bc,* which both show less than 10% grain set in the top 8 spikelets compared to WT Cadenza which on average had 75% grain set.

The reduction in grain set of the Aux/IAA mutants has been linked to reductions in pollen viability(Rinaldi *et al.*, 2012). Auxin is known to be involved in facilitating anther developmental processes of filament elongation, tapetal degradation and dehiscence as evident from the phenotypes of auxin deficient or insensitive phenotypes which are defective is one or more of these developmental processes(Ellis *et al.*, 2005; Nagpal *et al.*, 2005; Cheng *et al.*, 2006; Cecchetti *et al.*, 2008; Xu *et al.*, 2019). Measurements of pollen viability were taken to determine the reason for this reduction in grain set. 3 biological replicates of the 4 mutant genotypes and the Cadenza control were grown in 4 15-well trays (each tray representing a block). Due to certain mutants showing a lower success rate of germination, not all contained 3 biological replicates in each of the blocks. Anther samples were taken from the top and middle of the spikes and stained using iodine staining (2.5.3). REML analysis was performed on the transformed data using the function logit+1.

The reduction of pollen viability between the mutants was most evident at the top of the spike with *TaIaa18-Bb* showing the most severe phenotype with less than 1% pollen viability, compared with 40% for *TaIaa22-Bb* and 60%-70% in Cadenza, *TaIaa22-Bc* and *TaIaa22-Db* (Figure 5.13C). This severity of phenotype corresponds closely with the severity of the reduction in grain set (Table 5.6). There was found to be significantly lower pollen viability at the top part of the spike of *TaIaa18-Bb* and *TaIaa22-Bb* compared to both the middle of the spike (5% LSD= 0.7798/0.3899 respectively) and the top of WT Cadenza (5% LSD= 0.8754/0.5727 respectively)

(REML, P<0.001, Figure 5.13C). In comparison there was no significant difference between the top of *TaIaa22-Bc* and *TaIaa22-Db* compared to the middle of the spike (5% LSD= 0.4072/0.3899 respectively) and the top of WT Cadenza (5% LSD= 0.5840/0.5727 respectively).

All 4 of these Aux/IAA mutants were backcrossed with WT Cadenza pollen to determine whether the loss of grain set was also due to infertility of the female part of the flower. In all instances there was successful grain set towards the tip of the spike, therefore suggesting the loss of grain set is predominantly due to loss of male fertility (Figure 5.13D).

A

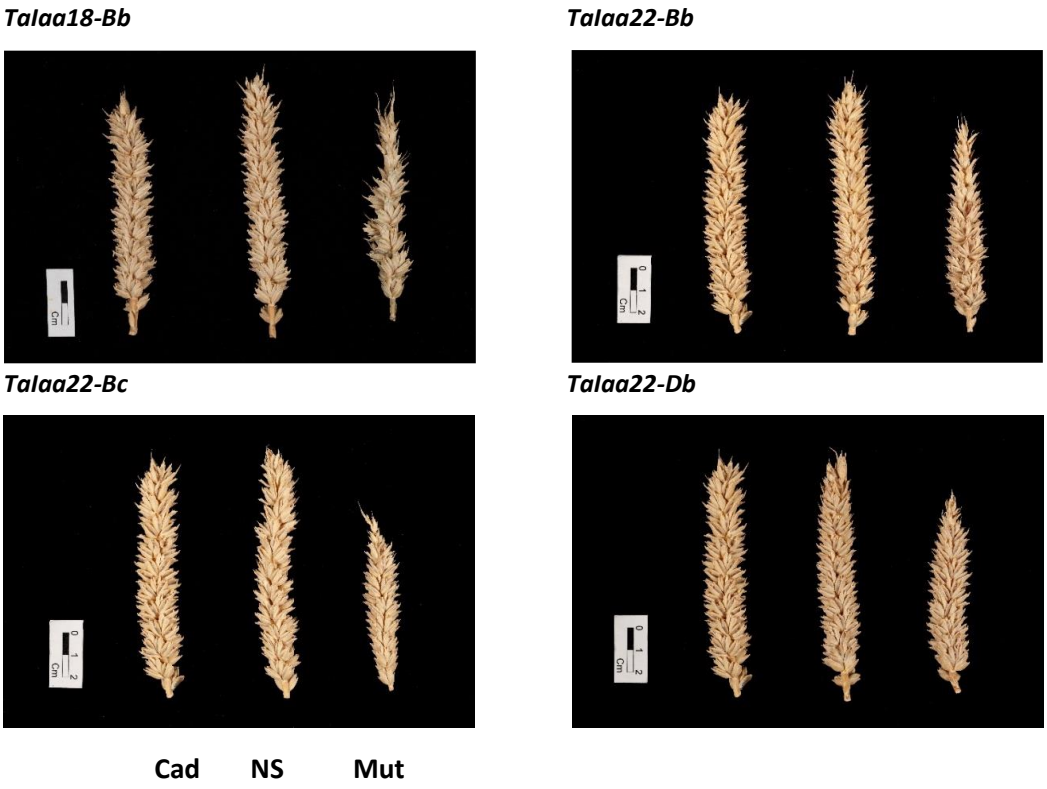
Talaa18-Bb
Talaa22-Bb
Talaa22-Bc
Talaa22-Db
Cad
NS
Mut

B

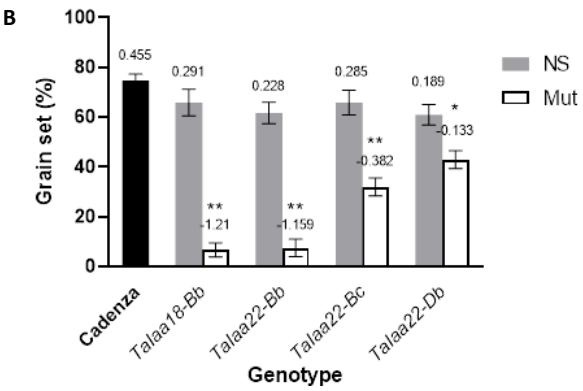
Grain set (%)
NS
Mut
0.455
0.291
0.228
0.285
0.189
**
-1.21
**
-1.159
**
-0.382
*
-0.133
Cadenza
Talaa18-Bb
Talaa22-Bb
Talaa22-Bc
Talaa22-Db
Genotype

C

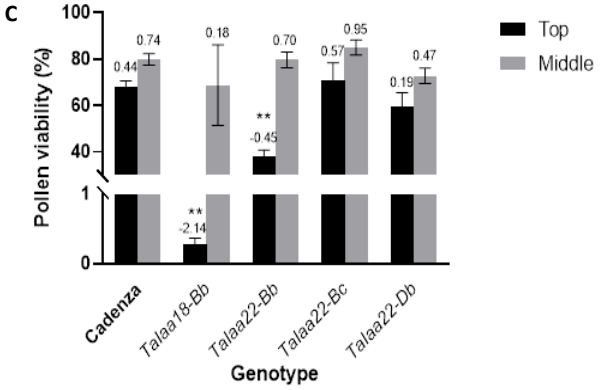
Pollen viability (%)
Top
Middle
0.44
0.74
0.18
**
-2.14
0.70
**
-0.45
0.57
0.95
0.19
0.47
Cadenza
Talaa18-Bb
Talaa22-Bb
Talaa22-Bc
Talaa22-Db
Genotype

D


Talaa18-Bb
Talaa22-Bb
Talaa22-Bc
Talaa22-Db

Figure 5.13: *Differences in fertility across the length of the spike of wheat Aux/IAA mutants.*

A*: Spike morphology of auxin-insensitive mutants: TaIaa18-Bb, TaIaa22-Bb, TaIaa22-Bc and TaIaa22-Db and direct comparisons with their respective null segregants (NS) and WT Cadenza. Photograph was taken at GS93 of the Zadoks scale.* **B***: Grain set across the top 8 spikelets (4 either side of the spike, including the terminal spikelet) of TaIaa18-Bb, TaIaa22-Bb, TaIaa22-Bc and TaIaa22-Db and WT Cadenza. Each bar is the mean of 4 biological replicates (each consisting of the three main tillers taken from each plant). Error bars = +/- 1 S.E. P<0.001. ANOVA analysis was performed on the transformed scale* (*logit+1 transformation*) and values are indicated in parentheses above the bars*. Pairwise comparisons were made using a 5% LSD = 0.3245 (23 d.f.) between genotypes to determine significance. *Significantly different from WT Cadenza, ** Significantly different from WT Cadenza and NS.* **C***: Pollen viability at tricellular stage, determined by iodine staining, at the top and middle part of the spike of TaIaa18-Bb, TaIaa22-Bb, TaIaa22-Bc and TaIaa22-Db and WT Cadenza. P<0.001. Mean +/- SE. REML analysis was performed on the transformed scale* (*logit+1 transformation*)*. Pairwise comparisons were made using a 5% LSD to determine significance. The LSD value varied depending on the comparison. ** Significantly different from WT Cadenza and the middle of the mutant spike.* **D**: *TaIaa18-Bb, TaIaa22-Bb, TaIaa22-Bc and TaIaa22-Db spikes* backcrossed with WT Cadenza pollen. *Bar graphs created using GraphPad Prism Software.*

On closer examination of the reproductive physiology of these mutants there was a clear difference in phenotype of *TaIaa22-Bb* and Cadenza (Figure 5.14), with the anthers of the auxin-insensitive mutant appearing to be shorter and more yellow as opposed to green. Auxin is thought to be an inhibitor of dehiscence, with auxin-receptor mutants showing earlier dehiscence(Cecchetti *et al.*, 2008). The yellower anther phenotype of *TaIaa22-Bb* could be a result of premature dehiscence due to being auxin-insensitive. The reproductive physiology of *TaIaa22-Bc* and *TaIaa22-Db* showed similar phenotypes to that of Cadenza, corresponding with the apparent lack of obvious reduction in pollen viability (Figure 5.14C). Although we have not investigated thoroughly, there does appear to be a difference in phenotype of the stigma of *TaIaa22-Bb* compared to the other genotypes being smaller and less fluffy

in appearance. Therefore, although there was successful grain set after backcrossing (Figure 5.13D) there could be a reduction of female fertility at the tip of the spike which is also contributing to the loss of grain set.

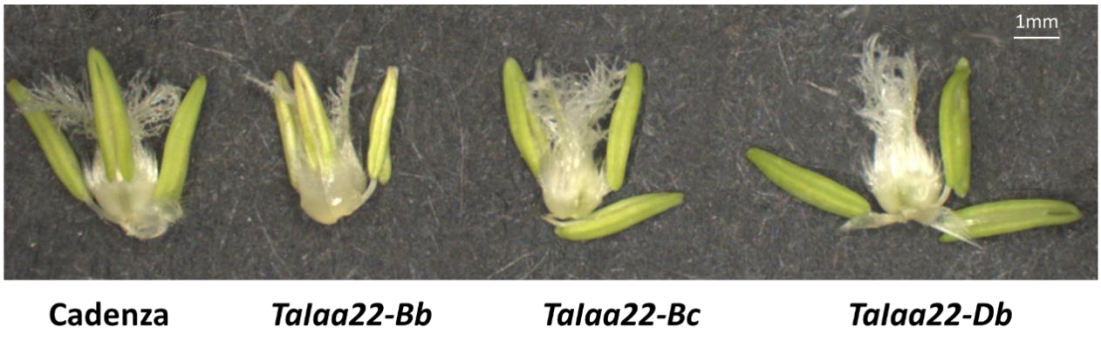

Figure 5.14: *Reproductive morphology of auxin-insensitive wheat mutants.*

Reproductive morphology of WT Cadenza, Taiaa22-Bb, Taiaa22-Bc and Taiaa22-Db. Samples were taken from the tip of the spike and either of the two outer florets. Anthers were all at late tricellular stage, approaching dehiscence. Scale bar = 1mm

5.3.7 Heat stress tolerance

There is evidence that a heat stress induced depletion of auxin in the anther is one possibly cause of loss of pollen viability and therefore yield in barley and rice (Sakata *et al.*, 2010; Sharma *et al.*, 2018). Endogenous application of IAA was found to relieve heat stress induced pollen sterility and recover the yield (Sakata *et al.*, 2010; Sharma *et al.*, 2018).

Considering the literature, we hypothesise that our auxin-insensitive mutants will be more sensitive to heat stress, owing to the apparent role of auxin in heat stress tolerance of cereals. To determine whether this is the case, *Taiaa22-Bc, Taiaa22-Db* and *Taiaa34-Ab* were chosen based on them not showing a severe spike phenotype and often still showing grain set in the middle 6 spikelets. All three contained missense mutations which are known to cause an auxin-insensitive phenotype in Arabidopsis and rice. To investigate the impact of heat treatment on the fertility of these mutants, a 4-cohort experiment was constructed where all 3 mutant plants

and WT Cadenza were subjected to heat treatment. The heat stress assay applied was the same assay that had been already optimised for hexaploid wheat var. Cadenza (see chapter 3/Section 2.8). REML analysis was performed on the transformed scale (logit+1 transformation).

There was found to be a significant impact of heat treatment ($P<0.001$) and genotype ($P<0.001$) on grain set, however there was found to be no interaction between treatment and genotype ($P=0.308$). However, there was found to be a significant reduction in grain set in response to heat treatment in *TaIaa22-Bc, TaIaa22-Db* and *TaIaa34-Ab* compared to the control (5% LSD= 0.3625, 0.4996 and 0.4072 respectively), showing on average a reduction of 37%, 26% and 20% grain set respectively. However, there was found to be no significant reduction in grain set in the heat treatment of Cadenza (5% LSD = 0.4847), showing on average a reduction of 7% grain set. In the control treatment there was found to be no significant difference in grain set between the controls of Cadenza and *TaIaa22-Bc, TaIaa22-Db* and *TaIaa34-Ab* (5% LSD = 0.4463, 0.4554 and 0.4996 compared to Cadenza respectively). All three Aux/IAA mutants show a significantly lower grain set in response to heat treatment compared to heat treated Cadenza (5% LSD = 0.4115, 0.4847 and 0.3962 compared to Cadenza correspondingly), with 38%, 24% and 16% less grain set respectively. Therefore, fertility in the three Aux/IAA mutants is more sensitive to the heat treatment compared to the WT.

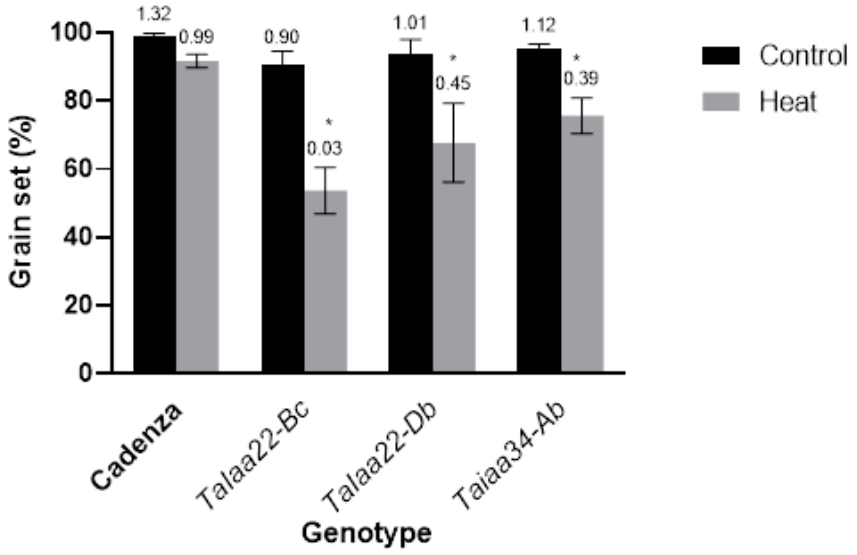

Figure 5.15: *The effect of heat stress on spike fertility.*

Grain set of Cadenza, Talaa22-Bc, Talaa22-Db and Talaa34-Ab grown in normal conditions and after being exposed to 33/26°C day/night for 4 days after meiosis. P = 0.308. Each bar is the mean of at least 4 biological replicates. Error bars =+/- S.E. REML analysis was performed on the transformed scale (*logit+1 transformation*) and values are indicated in parentheses above the bars*. Pairwise comparisons were made using a 5% LSD to determine significance, each comparison has a different LSD value. P = 0.308. * Significantly different from Cadenza of the same treatment and from the control treatment within the same genotype. Created using GraphPad Prism Software.*

Following on from the increased sensitivity to heat stress, we sought to investigate whether this was linked to reductions in pollen viability. A 3-cohort experiment was constructed where all 3 mutant plants and WT Cadenza were subjected to heat treatment (Section 2.8). Once the spikes had reached the beginning of tricellular stage of pollen development, 3 anthers were taken from a single floret and considered to be a single replicate. Samples were taken only from the central 6 spikelets, as was used to record the grain set. Samples were taken from the either of the outer florets of the top, middle and bottom spikelet of these central 6 spikelets (Figure 3.7; Section 3.3.5). These measurements were used to investigate whether the greater reduction in grain set findings is a result of greater reductions in male fertility in the mutants.

Heat treated *TaIaa22-Db* and *TaIaa34-Ab* showed a significantly lower pollen number at the top of the spike compared to heat treated Cadenza (5% LSD=1114 and 1004) and in heat treated *TaIaa22-Db* compared to the control treatment (5% LSD=1171) (Table 5.7). However, there was found to be no significant interaction of genotype and heat treatment on pollen number in the top, middle and lower parts of the spike (P=0.082, 0.176 and 0.127 respectively). The heat treatment alone was not found to have a significant impact on pollen number at the top, middle and bottom parts of the spike (P=0.336, 0.966 and 0.844). However, *TaIaa22-Bc, TaIaa22-Db* and *TaIaa34-Ab* were all found to have a significantly lower pollen number at the top of the spike with an average of 4142, 3387 and 3477 pollen/ml compared to 4269 pollen/ml in Cadenza (P=0.05; 5% LSD compared to Cadenza being 772.5, 807.6 and 743.7 respectively). The middle part of the spike of *TaIaa34-Ab* showed a significantly lower pollen number with an average of 4013 pollen/ml compared to 4625 pollen/ml in Cadenza (P<0.001; 5% LSD 354.5).

There was no interaction between genotype and heat treatment on pollen viability (P=0.399, 0.386 and 0.644 for top, middle and lower parts of the spike). However, *TaIaa22-Bc* showed significantly lower pollen viability in the lower part of the spike compared to both the control treatment of *TaIaa22-Bc* (43% reduction) and heat-treated WT Cadenza (28% reduction) (5% LSD=19.3 and 19.64 respectively). There was found to be no significant difference in pollen viability between the different genotypes and in response to the treatment in the top, middle and bottom parts of the spike.

Table 5.7: *Effects of heat stress on pollen number and viability of Cadenza and 3 Aux/IAA mutants.*

REML output of Ampha Z32 Impedance Flow Cytometer measurements of pollen number and viability from anthers taken from the top, middle and lower parts of the spike. Pairwise comparisons were made between each genotype and treatment using 5% LSDs to determine the significance. [a]*= significantly different from control of same genotype,* [b]*=significantly different from WT Cadenza in the same treatment. Minimum of 4 biological replicates for the treatment and genotype combination, across 3 cohorts.*

Genotype	Treatment	Pollen number/ml			Pollen viability (%)		
		Top	Middle	Lower	Top	Middle	Lower
Cadenza	Control	4136	4501	4335	34.18	46.83	48.55
	Heat	4401	4748	4259	26.24	38.15	40.57
TaIaa22-Bc	Control	3975	4373	3917	18.47	34.47	51.32
	Heat	4310	4794	4091	28.74	39.98	29.44 [ab]
TaIaa22-Db	Control	4165	4942	3950	23.44	43.57	43.83
	Heat	2609 [ab]	4523	4757	16.43	24.50	34.36
TaIaa34-Ab	Control	3614	4016	4204	29.8	35.87	42.92
	Heat	3340 [b]	4009	3749	36.94	36.69	36.40
Genotype		0.05	<0.001	0.326	0.143	0.827	0.886
Treatment		0.336	0.966	0.844	0.616	0.475	0.024
Genotype*Treatment		0.082	0.176	0.127	0.399	0.386	0.644
Max SED		571.5	350.7	409.7	10.99	12.29	10.65
Max LSD (5%)		1171	3833	839.9	22.65	25.30	21.82

5.3.8 Application of NAA to mitigate heat stress

The findings from section 5.3.7 indicate that auxin plays an important role in heat stress tolerance during male reproductive development in wheat. We sought to replicate experiments in barley and rice(Sakata *et al.*, 2010; Sharma *et al.*, 2018), to investigate whether the exogenous application of synthetic auxin NAA mitigated the grain set losses in wheat.

A 5-cohort experiment was conducted following methods detailed in section 2.9. Treatments included spraying tillers with control, 10µM and 100µM NAA, and taking measurements of grain set, days until anthesis and elongation of the FLS. REML analysis was performed for grain set, days until anthesis and elongation rate of the FLS. For the grain set the data was transformed (logit+1) prior to analysis to ensure a normal distribution of data.

There was found to be no interaction between spray treatment and temperature treatment on grain set (P=0.159; Table 5.8). Therefore, showing that spraying with NAA is not mitigating the reduction in grain set caused by heat treatment. Throughout all spray treatments there was on average a 30% reduction in grain set in response to heat treatment (P<0.001). There was also no significant impact of spray or heat treatment and interaction of the two factors on FLS elongation (P=0.15, 0.094 and 0.448 respectively).

There was found to be an increased rate of anther development in response to heat treatment (P<0.001), with anthesis being reached on average 2.87 days faster in the heat-treated plants. Spraying also has a significant impact on rate of development (P=0.006), with application of 0µM, 10µM or 100µM NAA taking on average 13.75, 15 and 14.88 days respectively to reach anthesis. Thus, auxin treatment appears to slow down the rate of anther and therefore pollen development. However, there was found to be no significant interaction of spray and temperature treatment on days until anthesis (P=0.33).

Table 5.8: *Effect of NAA application on heat stress tolerance of Cadenza. REML output of grain set, rate of FLS elongation and time to reach anthesis after application of either 0µM, 10µM or 100µM NAA and its interaction with heat treatment. Pairwise comparisons were made between each genotype and treatment using 5% LSDs to determine the significance. *= significantly different from control of same spray treatment. Grain set data underwent a logit+1 transformation prior to analysis.*

Spray	Temperature	Grain set	Days until	FLS
Wet	Control	1.0006	14.99	7.924
	Heat	0.7292*	12.50*	7.940
10 μM	Control	0.9929	16.23	9.660
	Heat	0.6796*	13.77*	8.255
100 μM	Control	0.9074	16.72	8.540
	Heat	0.7391*	13.05*	7.302
Spray Treatment		0.660	0.006	0.15
Temperature Treatment		<0.001	<0.001	0.094
Spray*Treatment		0.159	0.33	0.448
Max SED		0.05548	0.67	0.9011
Max LSD		0.1119	1.354	1.818

5.4 Discussion

Auxin is a plant hormone known to be involved in a wide variety of plant developmental processes and is essential to regulating plant growth and development(Luo *et al.*, 2018). One of the fundamental ways in which the role of auxin has been investigated has been through the identification and phenotypic characterisation of auxin-insensitive mutants. Although, auxin-insensitivity has been extensively studied in Arabidopsis, little research has been conducted on cereal crops, with only a few studies on rice confirming that a similar mutation in the GWPPV motif of an Aux/IAAs lead to an auxin-insensitive phenotype exhibited in Arabidopsis(Kitomi *et al.*, 2012; Zhu *et al.*, 2012). We therefore aimed to apply a reverse genetics approach to acquire missense mutants within the GWPPV motif and discover the first auxin-insensitive mutants in hexaploid wheat. Using the hexaploid wheat TILLING resources available, a total of 12 independent missense mutations in 10 Aux/IAA genes were identified. These mutations confer amino acid substitutions in the GWPPV motif of wheat AUX/IAA proteins (Table 5.2).

Certain mutations in this conserved motif confer clear auxin-insensitive phenotypes like that seen in model plants. The roots were found to have reduced lateral roots, root hairs and agravitropism. The auxin-insensitive phenotype was also carried above ground with evidence of reduced grain set and pollen viability in some lines, especially towards the tip of the spike. The severity of the mutant phenotype depended on several factors: the type of missense mutation, the expression level of the Aux/IAA and the tissue specific expression. These mutants also showed increased sensitivity to heat stress, indicating the crucial role of auxin in pollen development and heat stress tolerance.

5.4.1 The Aux/IAA gene family in wheat

In total there were found to be 84 homoeologues of Aux/IAAs from the latest iwgsc_refseqv1.0 annotation. This is the same as how many were previously found using an older CSS annotation of the wheat genome(Qiao *et al.*, 2015). However, when converting the CSS list to the iwgsc_refseqv1.0 we found only 66 genes, 8 of which were unique homoeologues, but are possibly ARFs rather than Aux/IAAs. This shows the importance of using the more recent annotation, as it is both more complete and more accurate.

This high number is due to the hexaploidy of wheat meaning that in most circumstances each gene possesses a copy on each of the 3 sub-genomes: A, B and D. Modern hexaploid wheat, *Triticum aestivum*, is the product of hybridisation of three closely related grass species: *T.urartu*, *Aegilops speltoides* and *T.tauschii* (Mcfadden and Sears, 1946; Heun *et al.*, 1997; Dubcovsky and Dvorak, 2007), each contributing to the A, B and D genomes respectively. In total, *Triticum urartu* (A) contributed 27 Aux/IAA genes, *Aegilops speltoides* (B) contributed 27 and *Triticum tauschii* (D) contributed 30.

The total number of Aux/IAA genes in wheat, when taking into consideration hexaploidy, were found to be comparable to other monocots and dicots. There were found to be a total of 29 Aux/IAA members in Arabidopsis(Overvoorde *et al.*, 2005), 31 members in rice and maize(Jain *et al.*, 2006; Y. Wang *et al.*, 2010), 26 in

tomato and sorghum(S. Wang *et al.*, 2010; Wu *et al.*, 2012) and 36 in barley(Shi *et al.*, 2020). On examination of the phylogeny of the Aux/IAAs there many examples of homology between rice and wheat (Figure 5.2). Most of the rice Aux/IAAs have a direct homoeologue in wheat, corresponding to the closer genetic relationship between wheat and rice, both being monocots, compared to the dicot Arabidopsis.

From the list of 84 Aux/IAAs a total of 12 lines from the TILLING population contain missense mutations within the conserved GWPPV motif of domain II. Only 9 of the 12 had their phenotype characterised, considering three factors which determine the likelihood of showing an auxin-insensitive phenotype: the nature of the missense mutation, the expression level of the mutated gene and whether orthologues in other species have resulted in an auxin-insensitive phenotype.

5.4.2 Role of auxin in root development

Auxin is known to play a crucial role in root development, with many auxin-insensitive/deficient mutants showing an absence/reduced number of lateral roots formation, fewer root hairs and agravitropism(Tian and Reed, 1999; Fukaki *et al.*, 2002; J. Y. Park *et al.*, 2002; Tatematsu *et al.*, 2004; Yang *et al.*, 2004; Kitomi *et al.*, 2012; Rinaldi *et al.*, 2012; Zhu *et al.*, 2012). *TaIaa18-Bb, TaIaa22-Bb, TaIaa22-Bc* and *TaIaa22-Db* were all found to be insensitive to auxin on examination of the elongation of the developing seminal roots in response to NAA (Figure 5.8A-C), although to different levels of insensitivity. Mutations in domain II have shown to result in Aux/IAA proteins which fail to be recognised by the SCF^{TIR1} ubiquitin E3 ligase and remained stable even in the presence of auxin(Ramos *et al.*, 2001; Dreher, 2006). The severity of the phenotype appeared to correspond closely with the expression level of these mutant Aux/IAAs within the roots (Figure 5.16). *TaIaa18-B* shows the highest level of expression within the root, corresponds with having the most severe auxin-insensitive root phenotype (Figure 5.16; Figure 5.8A-C).

TaIaa18-Bb, TaIaa22-Bb, TaIaa22-Bc and *TaIaa22-Db* showed defects in root hair development, with fewer and shorter root hairs (Figure 5.9). The auxin-insensitive

mutants failed to show the level of proliferation of root hairs induced by NAA, however all did show some increase in density and length of hair. This phenotype has shown to be typical in Aux/IAA mutants, Arabidopsis Aux/IAA gain-of-function mutants, *slr1-1* and *iaa16-1,* showing fewer and shorter root hairs(Fukaki *et al.*, 2002; Rinaldi *et al.*, 2012). With endogenous application of NAA inducing a proliferation of root hairs in WT rice, but not the *Osiaa11* mutant(Zhu *et al.*, 2012).

TaIaa18-Bb, TaIaa22-Bb, TaIaa22-Bc and *TaIaa22-Db* showed defects in lateral root development in both the seminal (Table 5.3/5.4; Figure 5.5A) and nodal roots (Table 5.5). This is likely due to defects in formation of lateral root primordia (Figure 5.6)(Zhu *et al.*, 2012). Defects in lateral root formation (Tian and Reed, 1999; Fukaki *et al.*, 2002; Tatematsu *et al.*, 2004; Yang *et al.*, 2004; Uehara *et al.*, 2008; Kitomi *et al.*, 2012; Rinaldi *et al.*, 2012; Zhu *et al.*, 2012) and root hair formation (Fukaki *et al.*, 2002; Kitomi *et al.*, 2012; Rinaldi *et al.*, 2012; Zhu *et al.*, 2012) are known in both dicots and monocots from auxin-insensitive mutants. *TaIaa22* and *TaIaa18* cluster closely with genes Arabidopsis *AtIAA14* (Figure 5.2), this mutant was found to be completely lacking in lateral roots(Fukaki *et al.*, 2002). This indicates that there is a considerable degree of homology in the function of specific Aux/IAAs in root development in both monocots and dicots, and role of auxin is conserved in promoting lateral root development.

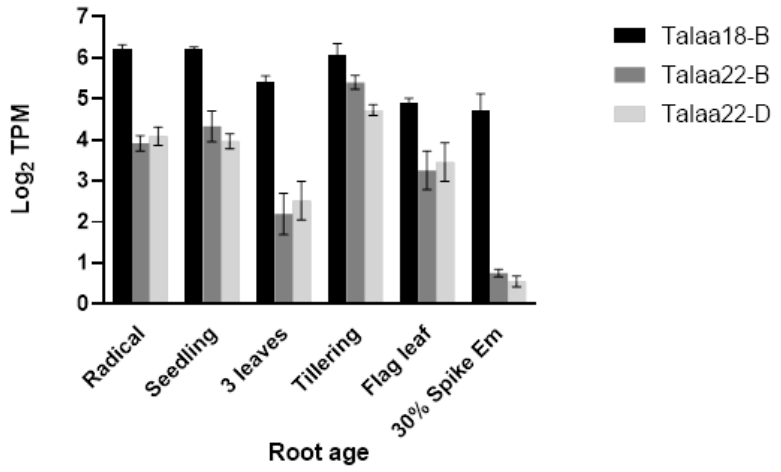

Figure 5.16: *Expression of TaIaa18-B, TaIaa22-B and TaIaa22-D in root tissue.*

Root samples were taken at 6 different stages of development: radical emergence, seedling, 3 leaf, tillering, emergence of flag leaf and 30% spike emergence. Bars represent the mean expression of 3 biological replicates (Log_2). Error bars represent one S.E. (Ramírez-González *et al.*, 2018). *Created using GraphPad Prism Software.*

TaIaa18-Bb, TaIaa22-Bb, TaIaa22-Bc were all found to have a reduced diameter of seminal roots (Table 5.4), in contrast to the findings that *Osiaa11* had a greater diameter than the WT roots(Zhu *et al.*, 2012). *TaIaa22-Db* did however have significantly longer nodal roots than Cadenza, as was found with the *Osiaa11* mutant (Zhu *et al.*, 2012), however the length of the seminal roots of *TaIaa18-Bb* and *TaIaa22-Db* was significantly shorter (Table 5.4). These defects in root formation are likely to result in reduction in supply of water and nutrients to the developing stem and are likely to be at least partially responsible for the smaller above ground phenotype of these mutants, which is most evident in the nutrient starved phenotype of *TaIaa18-Bb* (Figure 5.11).

Further investigation into the mechanisms behind lack of lateral root formation should be implemented. Tissue specific expression patterns of the mutant Aux/IAAs

could be determined by producing *Aux/IAA::GUS* transgenic reporter lines and subsequent cross sectioning to see the localisation of these proteins.

5.4.3 Role of auxin in gravitropism

Perception of the direction of gravity is determined by the root tip. Surgical removal of the root cap results in agravitropic roots(Morita and Tasaka, 2004). Perception of the direction of gravity begins in the columella cells in the tip of the roots, whereby starch-filled amyloplasts (statoliths) sediment in the direction of the pull of gravity (Leitz *et al.*, 2009; Band *et al.*, 2012; Baldwin *et al.*, 2013; Sato *et al.*, 2015). After this, auxin efflux facilitators PIN3 and PIN7 in Arabidopsis transfer to the lower side of the columella cells creating an asymmetry of auxin accumulation towards the lower side of the columella cells(Friml *et al.*, 2002; Kleine-Vehn *et al.*, 2010). Auxin in the columella cells is then transported by AUX1/PIN2 into the epidermal cells of the elongation zone of the root(Blilou *et al.*, 2005).

Many Aux/IAA gain-of-functions mutants have been found to be defective in gravity perception(Tian and Reed, 1999; Fukaki *et al.*, 2002; Tatematsu *et al.*, 2004; Yang *et al.*, 2004; Kitomi *et al.*, 2012; Rinaldi *et al.*, 2012). *TaIaa22-Db* shows the most severe agravitropic phenotype in both the root and shoot (Figure 5.10A/B), despite showing the lowest level of Aux/IAA expression in the roots compared to the other genes (Figure 5.16). This could be due to perception of gravity mostly occurring in the root tip, where possibly the expression of *TaIaa22-D* is very high.

Auxin has long been known to be involved in the transmission of the gravitropic signal and the growth response, but results elude to its function as a perceiver of the gravity signal as well, with auxin being essential for the accumulation of starch in the root apex(Zhang *et al.*, 2019). Gain-of-function mutant *axr3-1 (AtIAA17)* was found to have completely absent starch accumulation within the root cap(Zhang *et al.*, 2019). When *OsIAA9* was overexpressed in rice there was found to be a significant decrease in accumulation of starch(Luo *et al.*, 2015). In contrast, however, none of the wheat Aux/IAA mutants show a decrease in starch staining in the root cap, despite there being evidence of agravitropism (Figure 5.10). This

suggests that these Aux/IAAs are not expressed within the columnar cells of the root cap but are expressed in the epidermal cells of the elongation zone. This leads to the conclusion that these mutants are successfully perceiving the direction of gravity, but they are not able to produce the growth induced bending in response. This once again indicates the cell specificity of the Aux/IAAs, with none of the mutants from the TILLING population being direct orthologues of either *OsIAA9* or *AtIAA17* (Figure 5.2). Future research could target the wheat orthologues of these genes, either by directly producing gain-of-function mutants in the GWPPV motif or overexpression, and examine the starch accumulation within the cap.

Further investigation into gravity sensing in wheat could be further implemented with the *TaIaa22-Db* agravitropic mutant. Specifically, investigation into the expression of PIN genes could be used to uncover the cause of this agravitropic phenotype. Single cell RNAseq can be used to ascertain the localised expression of certain PIN genes in the root and ascertain the point the gravity response is disrupted.

5.4.4 Role of auxin in pollen development

Auxin is known to be an essential component of ensuring normal anther development and pollen viability. Auxin deficient or insensitive phenotypes commonly have defects in anther filament elongation, tapetal degradation and dehiscence (Ellis *et al.*, 2005; Nagpal *et al.*, 2005; Cheng *et al.*, 2006; Cecchetti *et al.*, 2008; Xu *et al.*, 2019).

TaIaa18-Bb, TaIaa22-Bb, TaIaa22-Bc and *TaIaa22-Db* all showed evidence of an auxin-insensitive phenotype (Table 5.6). Closer analysis of the spike morphology showed that all 4 of these mutants showed a tapered spike phenotype, with a significant reduction in grain set in the last 8 spikelets (Figure 5.13A/B). This grain set reduction has been linked to a reduction in pollen viability towards the tip of the spike in *TaIaa18-Bb* and *TaIaa22-Bb* (Figure 5.13C), and backcrossing with WT Cadenza pollen led to the successful restoration of grain set, indicating that there is no reduction of fertility of the female part of the flower (Figure 5.13D). This

concludes that, like Arabidopsis and rice, certain missense mutations in the GWPPV motif of Aux/IAAs also causes defects in male fertility(Yang *et al.*, 2004; Uehara *et al.*, 2008; Rinaldi *et al.*, 2012). The findings implicate that Aux/IAA degradation is crucial for ensuring successful anther development and consequently grain set in wheat. This shows the importance of the auxin-signalling pathway in anther development(Hirano *et al.*, 2008; Sakata *et al.*, 2010; Rinaldi *et al.*, 2012).

TaIaa18, TaIaa22 and TaIaa23 are all orthologues of Arabidopsis *AtIAA16* (Figure 5.2). The auxin-insensitive mutant *iaa16-1* was found to be completely male sterile, owing to its stamen not being able to reach the stigma, due to reduced filament elongation(Rinaldi *et al.*, 2012). However, in rice *OsIAA11* there was found to be no difference in fertility compared to the WT but a strong root phenotype(Zhu *et al.*, 2012). This disparity strongly corresponds with the tissue specific expression of *OsIAA11* in rice, with much higher expression in the root(Sakai *et al.*, 2011). Therefore, indicating the tissue specific nature of Aux/IAAs causing localised repression of the auxin-signalling pathway. The degree of grain reduction appears to correlate to a combination of tissue specific expression and the type of missense mutation. *TaIaa18-Bb, TaIaa22-Bb, TaIaa22-Bc, TaIaa22-Db* and *TaIaa34-Ab* all contain missense mutations shared with those found in Arabidopsis or rice which were found to be auxin-insensitive (GWPPV > **R**WPPV/ GWP**L**V/ GW**L**PV). Of these, *TaIaa18-Bb, TaIaa22-Bb, TaIaa22-Bc, TaIaa22-Db* all show auxin-insensitivity in the root (Figure 5.8). Despite encoding a degradation resistant Aux/IAA produce, *TaIaa34-Ab* is likely to not show a strong sterility phenotype due to the low expression of this gene in wheat anthers, especially towards the later stages of pollen development where auxin accumulates (Figure 5.4).

TaIaa18-Bb has the most severe spike morphology, with the most reduced grain set and pollen viability (Table 5.6; Figure 5.13). This corresponds with it having a high level of gene expression in the anthers (Figure 5.16). Consequently, the degradation resistant *TaIaa18-Bb* is not degraded by auxin accumulation and the higher expression means it will have a greater repression on the auxin signalling pathway

and auxin-responsive gene expression, leading to the severity of the phenotype observed.

Complete sterility was not found in any of the Aux/IAA mutants from the TILLING population. This is likely due to the TILLING population being at the M4 generation, whereby any complete male sterile phenotypes would not be carried through the generations, except possibly through outcrossing, which rarely occurs in wheat.

The partial male sterility of auxin-insensitive mutants verifies the evidence from the previous chapter that auxin accumulates towards the later stages of pollen development (Figure 4.1), therefore indicating the importance of auxin signalling. Auxin is found to accumulate mostly in the tapetum and pollen grains and peaks in accumulation during mitosis, suggesting its involvement in controlling mitosis(Polit *et al.*, 2003; Feng *et al.*, 2006). Potentially these Aux/IAA mutants are failing to complete mitosis due to continued repression of auxin responsive gene expression even in the presence of auxin.

What is noticeable is that pollen viability reduces towards the top of the spike in these mutants (Figure 5.13C). This could be due to an auxin gradient across the length of the spike, whereby there is lower auxin synthesis occurring towards the tip of the spike, meaning that is more vulnerable to sterility. Another possible explanation is greater expression of these Aux/IAAs towards the tip of the spike leading to greater repression of auxin signalling.

The results indicate the importance of the type of missense mutation within the GWPPV motif. Missense mutations in genes which are more conservative amino acid changes (GWPPV > GWPP**M** and GWPP**I**) do not show an auxin-insensitive phenotype (*TaIaa3-Bb* and *TaIaa24-Bb*) despite being very highly expressed within the anther (Figure 5.4). Therefore, it is likely that the mutated Aux/IAA is still able to form a complex with auxin and SCF^{TIR1} and can therefore still be targeted for degradation. Whereas less conservative amino acid changes, such as G to R (glycine to arginine, containing a positively charged side chain) and P to L (proline to leucine,

containing a hydrophobic side chain) form an active site which is unable form a complex with auxin and SCF^{TIR1} (Ramos *et al.*, 2001). This is because the missense mutations have affected the stereochemistry of the GWPPV active site. This results in continued repression of the auxin-responsive gene expression by the Aux/IAA despite the presence of auxin. The results indicate the high degree of homology in auxin signalling between monocots and dicots, with the GWPPV active site being essential for recognition by auxin in wheat.

Future work will aim to understand mechanisms behind reduced floret fertility. This will primarily be focused on sectioning the anthers throughout their development to identify key stages of development which are being disrupted in these auxin-insensitive mutants. RNAseq analysis could be used to identify changes in transcriptional networks of various auxin responsive genes which are continuously being repressed by the degradation resistant Aux/IAAs.

5.4.5 Role of auxin in the heat stress response

Auxin has also been implicated to be involved in the heat stress response. Endogenous levels of IAA in the anthers of rice and barley were found to decrease in response to heat stress, with this decrease being linked to reduced expression of YUCCA genes involved in auxin synthesis and signalling(Tang *et al.*, 2008; Sakata *et al.*, 2010). Endogenous application of IAA/NAA was found to recover grain set and pollen viability of heat stressed barley and rice(Sakata *et al.*, 2010; Sharma *et al.*, 2018). To investigate the role of auxin in heat stress tolerance of wheat we hypothesised that the Aux/IAA mutants should be more sensitive to heat stress, as this deficiency of auxin is exacerbated in the auxin-insensitive mutants.

TaIaa22-Bc, *TaIaa22-Db* and *TaIaa34-Ab*, were found to show a greater reduction in grain set in response to heat stress than Cadenza (Figure 5.15). This has been attributed at least partially to reduced pollen number in the top florets of the central 6 spikelets in *TaIaa22-Db* and *TaIaa34-Ab* and significantly reduced pollen viability in the lower region of *TaIaa22-Bc* (Table 5.7). This result suggests that possibly there are other factors at play, other than just pollen viability and pollen

number in reduced grain set. It is worth noting that pollen viability was determined when pollen had just completed mitosis II, therefore had just entered tricellular stage and would possibly be better to investigate this again when pollen has reached anthesis.

Following on from these findings we sought to investigate whether exogenous application of NAA was able to mitigate the effect of heat stress. However, it was found to result in no significant recovery of grain count in response to heat stress. Interestingly, there was found to be a significantly decreased time to reach anthesis in response to heat treatment (2.87 days faster in the heat treatment).

When spraying with NAA it was found to take 1 day slower to reach anthesis (Table 5.8). Auxin is thought to be involved in controlling the rate of pollen/anther development and dehiscence, primarily acting to slow down the rate of development. Arabidopsis mutants with increased sensitivity to auxin have shown delayed anther dehiscence, whereas auxin-insensitive mutants show earlier pollen maturation and anther dehiscence (Cecchetti *et al.*, 2008). This indicates that the reduction in grain set could be due to both a reduction in pollen viability, but also the increased rate of development of anthers and pollen which results in a lack of synchrony between male and female reproductive development within the flower. Consequently, pollen could be ready for fertilisation before the stigma is receptive. Therefore, fertilisation does not occur as the rest of the pollen is released.

This is possibly another reason why the auxin-insensitive mutants are more sensitive to heat stress. As heat stress quickens the rate of pollen development auxin would normally act to reduce the rate of pollen development to keep the synchrony between male and female reproduction, however the auxin-insensitive mutants do not respond to this.

Future study should aim to characterise differences in the rate of female reproductive development, to investigate whether anthesis and a receptive stigma are happening simultaneously in heat stressed plants like in control plants. Further

investigation into the rate of reproductive development of auxin-insensitive mutants should also be implemented.

5.5 Conclusion

The results confirm that auxin plays an important role in wheat reproductive development, abiotic stress tolerance and root development. There is also clear evidence of a high degree of homology in the role and structure of Aux/IAAs in both monocots and dicots, with only certain missense mutations in the GWPPV motif, which are known to induce auxin-insensitivity in either Arabidopsis or rice, also causing an auxin-insensitive phenotype in wheat. Mutations in the GWPPV motif led to similar phenotypes of reduced gravitropism, reduced root hair density, fewer/absent lateral roots and male sterility which have also been found in mutants in Arabidopsis and rice. The severity of the phenotype also being dependent on the tissue specific expression and level of gene expression. Overall, the evidence suggests a high level of homology in the auxin signalling pathway of wheat and other plants.

Exogenous application of synthetic auxin, NAA, showed no evidence of mitigating the grain set losses as a result of heat stress (Table 3.3), in contrast to findings in barley(Sakata *et al.*, 2010). However, there was evidence of NAA slowing down the rate of anther development by 1 day. The heat treatment was found to increase the rate of pollen development by 2.87 days. Consequently, we conclude that synchrony between male and female development is also an important part of the heat stress induced losses in grain set. Heat stress could be causing the anthers to have already released their mature pollen before the pistil is ready to receive the pollen. Consequently, successful fertilisation of the ovule does not occur, thus resulting in the loss of grain set.

Chapter 6: Identification and characterisation of ethylene-receptor mutants in wheat

6.1 Introduction

Ethylene is an olefin gas which also acts as a plant hormone. Since its discovery it has been found to be involved in a plethora of different functions, most notably stem elongation, seed germination, fruit ripening, senescence and abscission, but also abiotic/biotic stress tolerance(Binder, 2020). Ethylene has also been implicated to be involved in acclimation to a low oxygen environment caused by flooding. As a result of flooding ethylene gas diffusion is decreased and consequently it begins to accumulate in the submerged plant tissues, initiating a number of physiological and metabolic adaptive responses to hypoxia (Reviewed by Hartman, Sasidharan and Voesenek, 2021).

In Arabidopsis, ethylene is known to induce three characteristics to etiolated seedlings: shorter and thicker roots and hypocotyls and increased curvature of the apical hook, collectively known as the 'triple response'(Knight and Crocker, 1913). The triple response has been exploited to identify ethylene related mutants in Arabidopsis and has been a crucial part in identifying key components of the ethylene signalling pathway(Guzman and Ecker, 1990). Variations of this triple response have been found in monocot species. Maize, wheat, sorghum and *Brachypodium distachyon* showed a response of shorter roots and coleoptiles(Yang *et al.*, 2015). Rice etiolated seedlings show a so called double response where, like other monocots there is an inhibition of root growth, but unlike other monocots there is a promotion of coleoptile growth(Han San Ku , Hiroshi Suge, 1970; Satler and Kende, 1985; B. Ma *et al.*, 2013; Yin *et al.*, 2015). This difference in response has been linked to rice evolving in water-saturated soil and as a seedling must rapidly grow above the water to reach air and light(Magneschi and Perata, 2009).

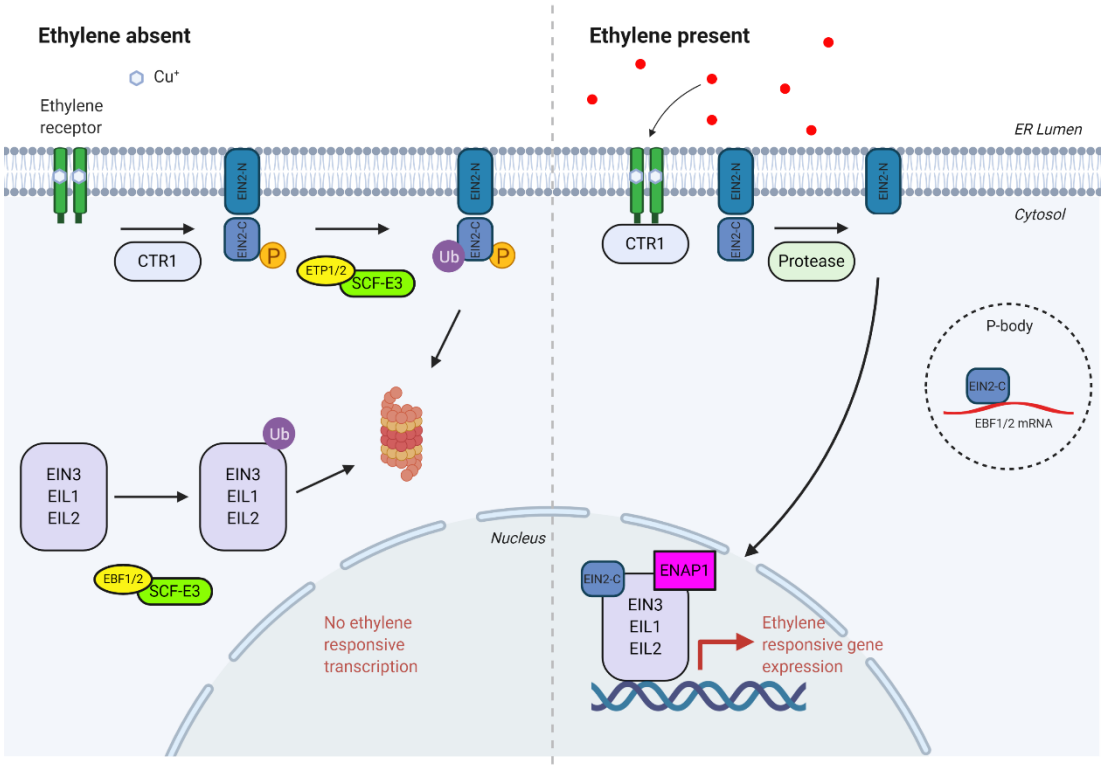

Figure 6.1: *Schematic diagram of the ethylene signalling pathway in Arabidopsis.*

In the absence of ethylene, the 5 rice ethylene receptors, located in the endoplasmic reticulum membrane, are in a transmitter on state. Here they recruit the CTR1 like proteins which phosphorylate EIN2, which subsequently leads to ubiquitination by an SCF E3 complex containing EBF1/2 F-box proteins and degradation by the proteasome. Simultaneously there is the ubiquitination of transcription factors EIN3, EIL1 and EIL2 by SCF-E3 complex containing the EBF1/2 F-box proteins and subsequent degradation by the proteasome. The result is no ethylene responsive gene expression. In the presence of ethylene, the ethylene binds to ethylene receptors, in doing so induces a conformational change which either reduces CTR1 kinase activity or CTR1 is sequestered to the cytosolic domains of the ethylene receptor, thus preventing it from phosphorylating EIN2. The result is an increase in EIN2 abundance. A so far undescribed protease cleaves the EIN2 protein in two, releasing the C-terminal end (EIN2-C) from the N-terminal end (EIN2-N), which remains within the membrane. EIN2-C then moves to the nucleus whereby it increases the transcriptional activity of EIN3/EIL1/2. This results in the activation of ethylene responsive gene expression. EIN2-C also binds to the mRNAs of EBF1 and EBF2 F-box proteins. This complex then associates with processing bodies resulting in degradation of the mRNAs by XRN4 (EIN5). Figure simplified and adapted from Binder, 2020. Adapted from "Wnt Signaling Pathway Activation and Inhibition", by BioRender.com (2021). Retrieved from https://app.biorender.com/biorender-templates.

The signalling pathway consists of a family of membrane receptors, a CTR1 protein kinase, EIN2 and transcription factors EIN3, EILs and further downstream the ERFs(Binder, 2020) (Figure 6.1). In the absence of ethylene, the ethylene receptors keep a serine/threonine protein kinase called CTR1 active(Kieber *et al.*, 1993). CTR1 regulates the activity of EIN2. EIN2 is a transmembrane protein which is part of the NRAMP (natural resistance associated microphage protein) family of metal transporters(Alonso *et al.*, 1999). It is a positive regulator of the ethylene response. CTR1 targets EIN2 for degradation by phosphorylation via a Skp1 Cullen F-box (SCF) E3 ubiquitin ligase complex containing the EIN2-targeting protein 1 (ETP1) and ETP2 F-box proteins. EIN2 then undergoes proteolysis by the 26s proteasome(Qiao *et al.*, 2009). This subsequently leads to ubiquitination of downstream EIN3, EIL1 and EIL2 transcription factors by the SCF E3 complex consisting of EBF1 and EBF2 F-box proteins(Guo and Ecker, 2003; Potuschak *et al.*, 2003; Gagne *et al.*, 2004; Binder *et al.*, 2007; An *et al.*, 2010). Consequently, there is reduced expression of ethylene responsive genes. Figure 6.1.

In the presence of ethylene, ethylene binds to the N-terminal transmembrane portion of the receptor resulting in a conformational change which either reduces CTR1 kinase activity or CTR1 is sequestered to the cytosolic domains of the ethylene receptor(Binder, 2020). Consequently, EIN2 is not degraded by the action of CTR1 and the ethylene signalling pathway can occur. Without being degraded, there is a subsequent increase in EIN2 levels. The EIN2 protein is then cleaved in two by a thus far undescribed protease, releasing the C-terminal protein (EIN2-C) from the transmembrane N-terminal protein (EIN2-N)(Wen *et al.*, 2012).

EIN2-C promotes ethylene responsive signalling in two ways. It binds to mRNAs that encode for EBF1 and EBF2 F-box proteins (two components of the SCF E3 complex). This complex then associates with processing bodies (P-bodies) resulting in degradation of the mRNAs by XRN4 (EIN5)(Olmedo *et al.*, 2006; Potuschak *et al.*, 2006; Li *et al.*, 2015; Merchante *et al.*, 2015). This subsequently results in reduced degradation of EIN3 and EIL1/2 by EBF1/2 and greater ethylene signalling(An *et al.*, 2010). EIN2-C also diffuses into the nucleus and binds to EIN2 nuclear associated

protein 1 (ENAP1) and increases the transcriptional activity of EIN3 and EIL1(Zhang *et al.*, 2017). An increase in EIN3, as well as other transcription factors EIL1/2 leads to changes in transcription of ethylene responsive genes(Chao *et al.*, 1997; Solano *et al.*, 1998; Alonso *et al.*, 2003). Figure 6.1.

The first part of ethylene perception is mediated by the receptor. Ethylene receptors consist of a basic structure of a transmembrane domain at the N-terminus of the protein, followed by a GAF domain (cGMP-specific phosphodiesterases, adenylyl cyclases, and FhlA), a kinase domain and finally in some receptors a receiver domain(Müller-Dieckmann *et al.*, 1999; Mayerhofer *et al.*, 2015). The transmembrane domain is embedded in the ER membrane and the C-terminal region extends into the cytosol. Receptors form homodimers which are stabilised by two disulphide bonds on the N termini. These bonds are formed between the two conserved cysteine residues cys-4 and cys-6 (Schaller *et al.*, 1995; Hall *et al.*, 2000; Chen *et al.*, 2010). However, these interactions are not required for ethylene binding or the receptor function(Xie *et al.*, 2006; Chen *et al.*, 2010). It is also thought that dimerization can also occur from the kinase domain (Mayerhofer *et al.*, 2015).

The ethylene receptor gene families in Arabidopsis consists of 5 members: *ETR1, ERS1, ETR2, ERS2* and *EIN4*(Chang *et al.*, 1993; Hua *et al.*, 1995; Hua and Meyerowitz, 1998; Sakai *et al.*, 1998). The receptors can be divided into two subfamilies, in subfamily I (*ETR1* and *ERS1*) and subfamily II (ETR2, ERS2 and EIN4). Subfamily 2 receptors have additional amino acids on the N-terminus of the protein extending into the ER lumen which are of unknown function. These receptors can be classified further by their type of kinase activity. ETR1 has histidine kinase activity, whereas ETR2, ERS2 and EIN4 have serine/threonine kinase activity and ERS1 appears to have both(Gamble *et al.*, 1998; Moussatche and Klee, 2004). ERS1 and ERS2 also both lack a receiver domain, which is present in the other receptors. Figure 6.2.

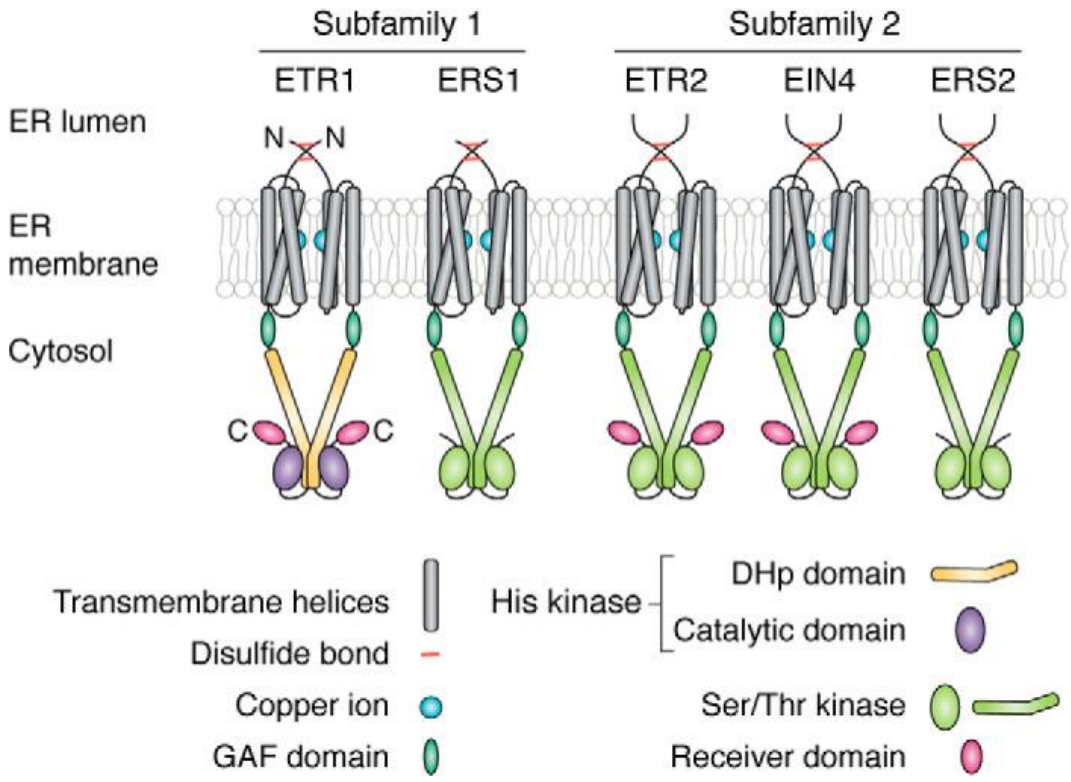

Figure 6.2*: Diagram of domains of Arabidopsis ethylene receptors.*

Arabidopsis possesses 5 known ethylene receptors. The receptors all have a basic structure of three transmembrane domains with a single copper ion cofactor required for ethylene binding. In the cytosol there is first a GAF domain, followed by a kinase domain which either has histidine kinase or serine/threonine kinase activity or both in the case of ERS1. Three of the five also contain a receiver domain. Receptors form dimers on the ER membrane. The dimers are thought to be partially stabilised by disulphide bonds at the N-terminus. Figure taken from Binder., 2020.

Ethylene receptors in other species have also been studied, however not to the same extent as Arabidopsis. Like Arabidopsis, rice has 5 receptors *OsERS1, OsERS2, OsETR2, OsETR3* and *OsETR4*. *OsERS1* and *OsERS2* are members of subfamily I and *OsETR2, OsETR3* and *OsETR4* are members of subfamily II(Watanabe *et al.*, 2004; Yau *et al.*, 2004). Orthologues of ethylene receptors have also been found in other monocots such as maize, wheat and sorghum(Yang *et al.*, 2015).

ETR1 of Arabidopsis has been most extensively studied and key amino acid residues which are essential to its function have been elucidated. Like other ethylene

receptors ETR1 has 3 α-helices which span across the membrane, these make the transmembrane domain (Figure 6.3). It was found that a copper ion binding to residues C65 and H69 on helix 2 of the transmembrane domain is an essential cofactor to allow ethylene to bind(Rodríguez *et al.*, 1999; Schott-Verdugo *et al.*, 2019). Mutational studies have identified a number of amino acids in helices 1 and 2 to be essential for ethylene binding(Rodríguez *et al.*, 1999; Wang *et al.*, 2006). On binding of ethylene a possible conformational change occurs which is transmitted through the third helix(Schott-Verdugo *et al.*, 2019), this causes a dissociation between CTR1 and EIN2. Consequently, phosphorylation and ubiquitination of EIN2 occurs and subsequently an increase in EIN2 levels and increased expression of ethylene responsive genes. The transmembrane residues are highly conserved between the 5 different ethylene receptors, suggesting that they all bind ethylene in a similar way.

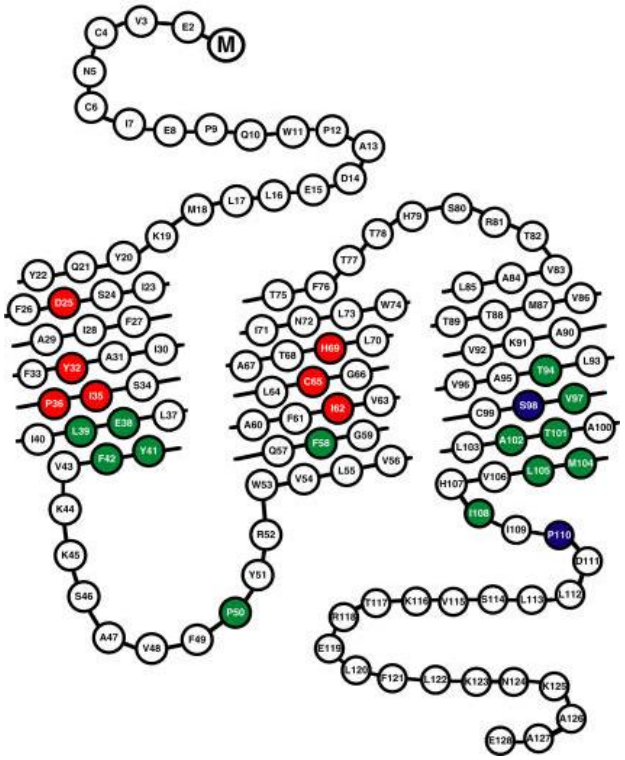

Figure 6.3: *Transmembrane domain of Arabidopsis ETR1.*

The transmembrane domain consists of three α-helices, spanning the length of the ER membrane. Mutations in the coloured aa residues were found to confer ethylene-insensitivity. Green: Mutants showed substantial ethylene binding activity. Red: Mutants showed negligible ethylene binding activity. Blue: Mutants with partial loss of function showing substantial binding activity. Taken from(Wang *et al.*, 2006).

The GAF, kinase and receiver domains are thought to be involved in the signal output. The function of the GAF domain in ethylene signalling is unknown. The histidine kinase domain of ETR1 consists of a dimerization and catalytic domain(Mayerhofer *et al.*, 2015). It is thought to act in a similar fashion to bacterial two-component receptors where there is autophosphorylation of histidine residues in the histidine kinase followed by the relay of the phosphoryl to an aspartate residue on the receiver domain(Gao and Stock, 2006). The histidine kinase activity of receptor ETR1 has been determined to be modulated by ethylene(Gamble *et al.*, 1998; Voet-Van-Vormizeele and Groth, 2008). However, the activity is not required for an ethylene response and instead is thought to be a form of moderation of receptor signalling(Qu and Schaller, 2004; Hall *et al.*, 2012). The histidine kinase

domain of ETR1 is essential for the interaction with EIN2, whereby abolishing autophosphorylation increases affinity for EIN2 and permanent autophosphorylation releases the interaction(Bisson and Groth, 2010). The conserved histidine residues in the histidine kinase domain of ETR1 is His-353 and in the catalytic domain two groups of conserved glycine residues (G1 and G2 boxes), these are autophosphorylation sites(Gamble *et al.*, 1998, 2002; Moussatche and Klee, 2004). Mutations in these sites eliminate the autophosphorylation of ETR1. As previously discussed, the kinase domains of ETR2, ERS2 and EIN4 were found to have serine/threonine kinase activity, and ERS1 has both types of kinase activity(Moussatche and Klee, 2004). This is evident from the peptide sequence of their kinase domains not possessing the motifs required for histidine kinase activity(Moussatche and Klee, 2004). Like the histidine kinase activity this activity is not required for ethylene responses, but possibly playing a modulatory role(Chen *et al.*, 2009).

Specific missense mutations within conserved residues of the transmembrane domain of ethylene receptors can lead to a dominant gain-of-function ethylene-insensitive phenotype caused by constitutive repression of the ethylene signalling pathway(Sakai *et al.*, 1998; Alonso *et al.*, 1999; Hall *et al.*, 1999; Gamble *et al.*, 2002; Takada *et al.*, 2005, 2006; Binder *et al.*, 2006; Wang *et al.*, 2006; Ishimaru *et al.*, 2006; Kim *et al.*, 2011; Okabe *et al.*, 2011; Shinoyama *et al.*, 2012; Mubarok *et al.*, 2019; Schott-Verdugo *et al.*, 2019). Some mutations prevent ethylene binding to the receptor, whereas others still allow ethylene binding but still result in constitutive signalling (Figure 6.3)(Wang *et al.*, 2006).

Monocots are believed to share a similar ethylene signalling pathway to dicots. Ethylene receptors are thought to have a shared function. Relatively few studies have looked at ethylene-receptor transmembrane domain mutants in monocots. One study on maize receptors found that when mutant *Zmers1b* and *Zmetr2b* receptors containing a C65Y mutation, were expressed in Arabidopsis, this induced ethylene insensitivity(Chen and Gallie, 2010). When grown in air the mutants displayed larger leaves and took longer to senesce. Therefore suggesting that the Cys-65 plays the same role in maize, with an essential role in binding the copper

cofactor required for ethylene binding, as it does in Arabidopsis receptors (Rodríguez *et al.*, 1999; Schott-Verdugo *et al.*, 2019). The function of these receptors is also thought to be shared between monocots and dicots. In rice, overexpression of *OsETR2* led to reduced ethylene-sensitivity, whereas knockdown mutants showed the opposite(Biao Ma, 2015). The roots of air grown *Osers1* rice mutant were found to be significantly shorter than the WT and were found to show increased sensitivity to ethylene(Ma *et al.*, 2014).

Orthologue analysis between Arabidopsis and rice shows that there are many other shared components of the ethylene signalling pathway. In rice, *B. distachyon*, maize, wheat, and sorghum there were found to be a number of CTR like genes(Yang *et al.*, 2015), with *osctr2* rice mutants showing a classic constitutive ethylene response phenotype of delayed flowering, increased tillering and reduced height(Wang *et al.*, 2013). An EIN2 orthologue has been found in rice, MHZ7/ OsEIN2. Various *mhz7* mutants were found to be completely insensitive to ethylene(B. Ma *et al.*, 2013). EIN3 also has orthologues in the rice genome, *OsEIL1-6*(Mao *et al.*, 2006) and wheat genome, *TaEIL1*(Duan *et al.*, 2013).

Amongst a plethora of different roles, ethylene is thought to be involved in anther/pollen development with a role in promoting the degradation of the tapetum, anther filament elongation and dehiscence. Ethylene signalling genes were found to be highly expressed in the tapetum during the stages, of pollen development just prior to its programmed cell death (Hirano *et al.*, 2008). When an ethylene insensitive form of ethylene receptor, *CmETR1* (H69A/H70A), was constitutively expressed in both *Nicotiana tabacum* and *Chrysanthemum morifolium* there was found to be male sterility due to delayed tapetum degradation and reduced anther filament elongation(Takada *et al.*, 2005, 2006; Ishimaru *et al.*, 2006; Shinoyama *et al.*, 2012).

Ethylene was also found to accumulate sevenfold during maturation of pollen grain(Jegadeesan *et al.*, 2018).This has been related to increased expression of ethylene biosynthesis genes towards the later stages of pollen development(Hirano *et al.*, 2008; Jegadeesan *et al.*, 2018). This accumulation could be due to ethylene's role in controlling dehiscence. Ethylene-insensitive tobacco and plants treated with

MCP, an ethylene perception inhibitor, showed delayed dehiscence, whereas when treated with ethylene there was an acceleration in dehiscence(Rieu *et al.*, 2003). Antisense suppression of PhETR2 in petunia led to premature dehiscence before anthesis(Wang and Kumar, 2007). Therefore, ethylene appears to have roles in regulating both the PCD of the tapetum and also anther dehiscence, both critical steps in ensuring successful pollen development and release.

Ethylene is also thought to play a role in abiotic stress tolerance. The impact of ethylene on abiotic stress tolerance seems to act in both an age dependent and tissue specific way. Ethylene signalling has been linked to reducing oxidative damage as a result of heat stress in rice seedlings (Wu and Yang, 2019). Ethylene was found to increase activity of scavenger enzymes involved in relieving oxidative damage, such as CAT, APX and POX(Wu and Yang, 2019). Ethylene-insensitive Arabidopsis seedlings were found to be more susceptible to heat, showing greater oxidative damage and reduced survival rate(Larkindale and Knight, 2002; Larkindale *et al.*, 2005). Treating seedlings with the ethylene precursor, 1-aminocyclopropane-1-carboxylic acid (ACC), led to increased thermotolerance with higher chlorophyll content, greater cell membrane stability and reduced oxidative damage of vegetative tissue (Larkindale and Knight, 2002; Wu and Yang, 2019).

Ethylene also has implications on the viability of pollen under heat stress. In tomato pollen there was found to be a significant deaccumulation of ethylene after heat treatment(Jegadeesan *et al.*, 2018). Pollen viability under heat stress was increased by pre-treatment of tomato plants with an ethylene-releasing agent and decreased with application of an ethylene biosynthesis inhibitor (Firon *et al.*, 2012). Therefore, ethylene appears to be responsive to heat stress and its presence is crucial for maintaining pollen viability.

In this study we aimed to begin to investigate the ethylene signalling pathway in hexaploid wheat. A reverse genetics approach was implemented, by which the TILLING population in wheat var. Cadenza was used to identify missense mutations in conserved residues of the transmembrane domain of wheat orthologues of ethylene receptors, in order to produce gain-of-function mutants which are ethylene-insensitive. 5 missense mutations were found, their phenotype

characterised, the degree of ethylene-insensitivity and heat stress tolerance determined.

6.2 Materials and Methods

All experimental details are described in section 2.

6.3 Results

6.3.1 The ethylene receptor gene family in wheat

The ethylene receptor family in Arabidopsis and rice consists of 5 members: AtETR1, AtERS1, AtETR2, AtERS2 and AtEIN4; OsERS1, OsERS2, OsETR2, OsETR3 and OsETR4(Gamble *et al.*, 2002; Yau *et al.*, 2004). Using the peptide sequences of these genes, BLAST searches were performed against the wheat iwgsc_refseqv1.0 annotation of the hexaploid wheat genome available on Ensembl and the hits downloaded. Repeats were removed and the protein domains were annotated in Geneious (v10.0.02, Biomatters Ltd, Auckland, New Zealand) using the InterProScan plugin. This located the transmembrane, GAF, kinase and receiver domains. Alignments of the peptide sequences were performed in Geneious software (v10.0.02, Biomatters Ltd, Auckland, New Zealand) using the MUSCLE alignment tool. A phylogenetic tree was constructed using all the Arabidopsis, rice and wheat peptide sequences. This was performed using the Geneious tree building tool PHYML, substitution model Blosum62. The close homology between rice and wheat led to an adoption of the rice gene names, combined with standard wheat nomenclature.

23 ethylene receptor genes were detected in the hexaploid wheat genome through orthologue and paralogue searches in Ensembl Plant BLAST function, using the complete protein sequence of the Arabidopsis and rice ethylene receptor genes (Table 6.1; Figure 6.4). The 23 ethylene receptors consisted of 7 genes with 3 homoeologues on each of the three hexaploid wheat genomes (A, B, D) and 2 genes without homoeologues (*TaErsl1-A1* and *TaErsl2-B1*). *TaErsl1-A1* and *TaErsl2-B1* were removed from the alignment used to construct the phylogenetic tree, due to them missing large parts of the peptide sequence.

So far, a complete establishment of wheat ethylene receptors has not been established in hexaploid wheat. Past studies have determined only 1 ethylene receptor, *W-er1*, in *Triticum aestivum*(Ma and Wang, 2003). BLAST studies of the provided peptide sequence determined that *W-er1* is closest to both *TaErs1-D1*, *TaErs1-A1* and *TaErs1-B1*, sharing 95.5%, 95.5% and 93.2% homology respectively. A total of 5 ethylene receptors have been found in the wheat progenitor *T. urartu*, as well as 5 in maize, sorghum and *B. distachyon*(Yang *et al.*, 2015). *T. urartu* contributes to the A genome of wheat. We found that in total there were 8 ethylene receptor and ethylene receptor like genes on the A sub-genome from the latest iwgsc_refseqv1.0 annotation.

Table 6.1: *A complete list of Arabidopsis, rice and wheat ethylene receptors. The names refer to their abbreviated name and accession number.*

Gene	Sequence ID
AtETR1	*AT1G66340*
AtERS1	*AT2G40940*
AtETR2	*AT3G23150*
AtERS2	*AT1G04310*
AtEIN4	*AT3G04580*
OsETR3	*Os02g0820900*
OsETR2	*Os04g0169100*
OsETR4	*Os07g0259100*
OsERS2	*Os05g0155200*
OsERS1	*Os03g0701700*
TaEtr3-A1	*TraesCS6A02G399400*
TaEtr3-B1	*TraesCS6B02G439600*
TaEtr3-D1	*TraesCS6D02G383600*
TaEtr2-A1	*TraesCS2A02G000200*
TaEtr2-B1	*TraesCS2B02G023800*
TaEtr2-D1	*TraesCS2D02G000500*
TaEtr4-A1	*TraesCS6A02G329400*
TaEtr4-B1	*TraesCS6B02G360200*
TaEtr4-D1	*TraesCS6D02G308300*
TaEtr4-A2	*TraesCS6A02G285800*
TaEtr4-B2	*TraesCS6B02G314600*
TaEtr4-D2	*TraesCS6D02G266200*
TaErsl1-A1	*TraesCS4A02G344200*
TaErsl2-B1	*TraesCS5B02G527300*
TaErs2-A1	*TraesCS1A02G096600*
TaErs2-B1	*TraesCS1B02G127000*
TaErs2-D1	*TraesCS1D02G105600*
TaErs1-A1	*TraesCS4A02G274300*
TaErs1-B1	*TraesCS4B02G039300*
TaErs1-D1	*TraesCS4D02G036400*
TaErs3-A1	*TraesCS5A02G002600*
TaErs3-B1	*TraesCS5B02G001600*
TaErs3-D1	*TraesCS5D02G002600*

As is expected, there is a considerably greater homology between rice and wheat, than Arabidopsis, attributed to both being more closely related. *OsETR2, OsETR3, OsERS1* and *OsERS2* have direct orthologues in the wheat genome with three homoeologues each. *OsETR4* has 6 orthologues suggesting duplication of this gene has occurred. *OsERS1* also clusters closely with 6 wheat homoeologues. Comparing with the Arabidopsis ethylene receptors *AtEIN4*, *AtETR2* and *AtERS2* form a clear outgroup from all the wheat and rice receptors, whereas *AtETR1* and *AtERS1* cluster most closely with *OsERS2*.

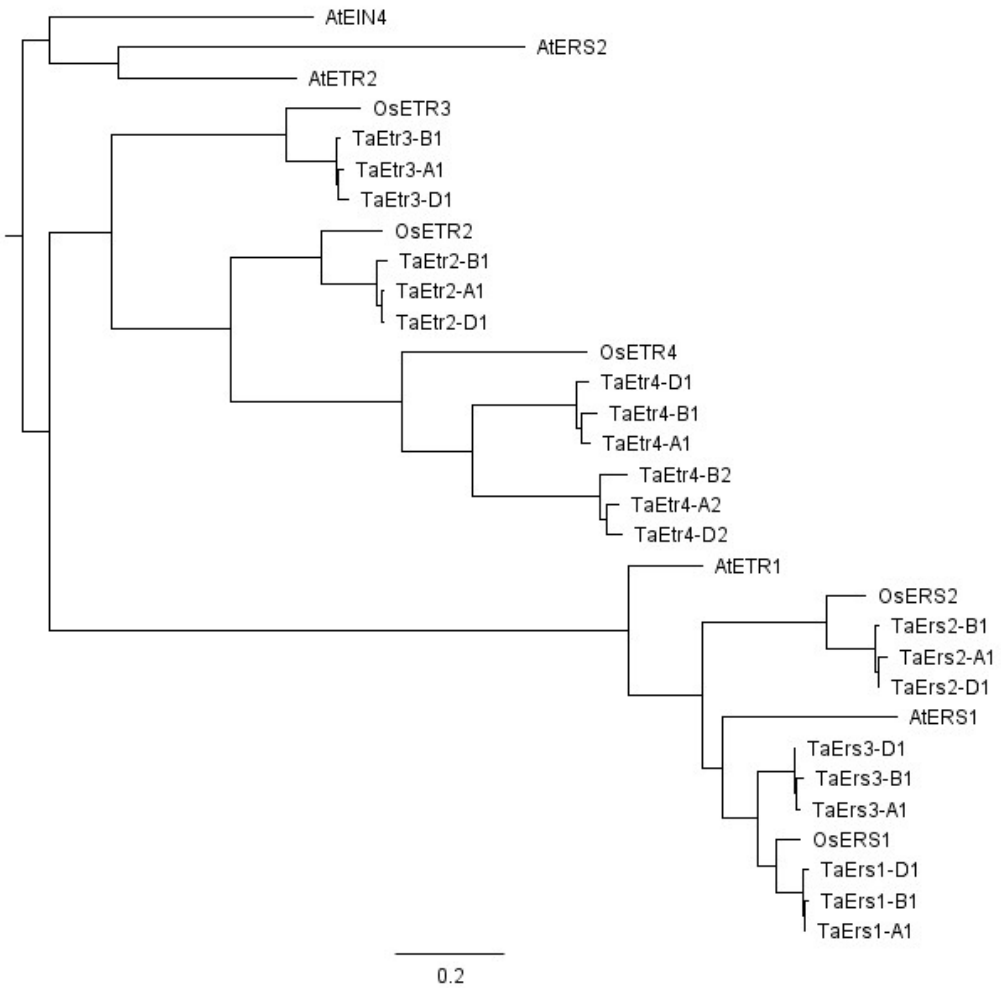

Figure 6.4: *A phylogenetic tree of Arabidopsis, rice and wheat ethylene receptors.*

The phylogenetic tree of ethylene receptors constructed from a complete alignment of 21 wheat, 5 Arabidopsis and rice ethylene receptor peptide sequences. This was completed using the Geneious tree building tool PHYML, substitution model Blosum62.

Domain analysis revealed that most of the receptor genes contain the 4 key domains which are indicative of ethylene receptors: three transmembrane domains, a single GAF domain, a kinase of either histidine and/or serine/threonine activity and in certain proteins a receiver domain(Gallie, 2015) (Figure 6.5). TaErsl1-A1 and TaErsl2-B1 both lack the kinase and receiver domain. AtERS1/2 also lack a receiver domain, as well as OsERS1/2 and their wheat orthologues TaErs2-A1, TaErs2-D1, TaErs2-B1, TaErs3-B1, TaErs3-D1, TaErs3-A1, TaErs1-D1, TaErs1-A1 and TaErs1-B1. Interestingly, like rice and maize, wheat does not contain an ETR1-like (subfamily I receptor with a receiver domain)(Gallie and Young, 2004; Pareek *et al.*, 2006).

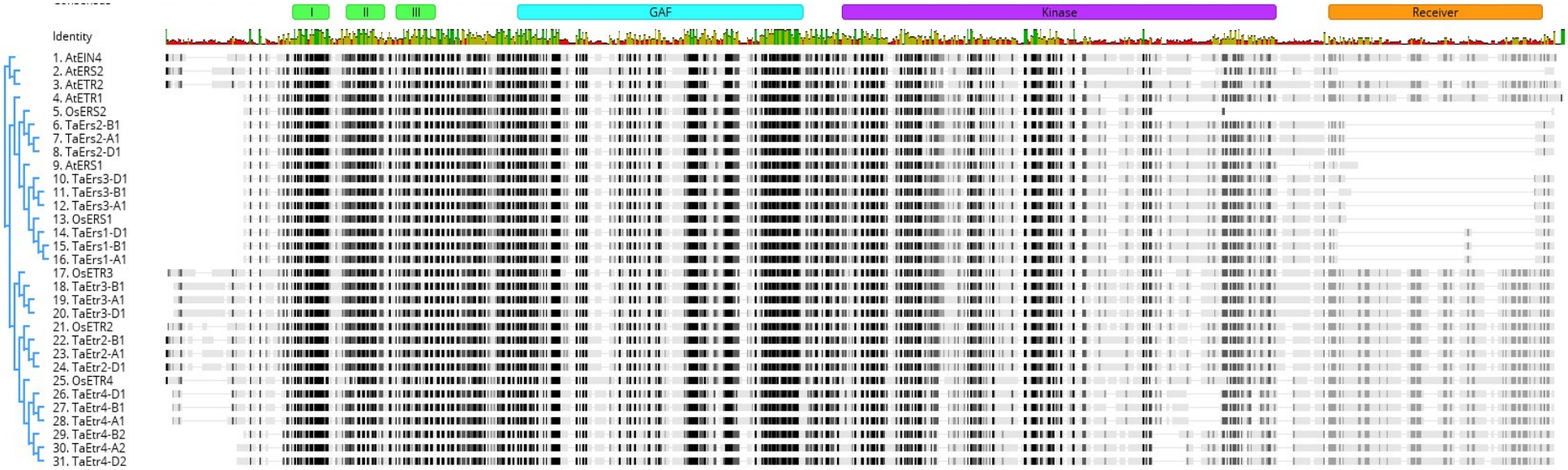

Figure 6.5: *Alignments of conserved domains of ethylene receptors.*

Domain structure of *Arabidopsis, rice and Triticum aestivum ethylene receptors. Alignments show conserved transmembrane (green), GAF (violet), kinase (purple) and receiver domains (yellow).*

The transmembrane domain is the site where ethylene binds. An alignment of the transmembrane domain of Arabidopsis, rice and wheat ethylene receptors shows the high degree of homology of peptide sequence (Figure 6.6). The residues are highly conserved across the three transmembrane α-helices. H69, which is essential for copper binding and therefore essential for ethylene binding(Schott-Verdugo *et al.*, 2019), is present in all of the Arabidopsis, rice and wheat receptors. However, it must be noted that cys-65 in helix II, which is also required for coordination of copper and therefore ethylene binding(Schott-Verdugo *et al.*, 2019), is absent in TaEtr4-B1, TaEtr4-D1, TaEtr4-A2, TaEtr4-B2, TaEtr4-D2 and TaEtr4-A1, being replaced instead with glycine. These are all orthologues of OsETR4, which still possesses the cys-65 residue. All the Arabidopsis, rice and the rest of the wheat ethylene receptors have retained this essential amino acid residue.

Extending into the ER lumen, the N-terminal end of the ETR1 protein contains cysteine residues at positions 4 and 6 which have both been determined to be essential for ensuring homodimer formation by means of two disulphide bonds(Schaller *et al.*, 1995; Hall *et al.*, 2000; Chen *et al.*, 2010). Most receptors possess at least one of these cystine residues, however rice OsETR2 along with its orthologues TaEtr2-B1, TaEtr2-D1 and TaEtr2-A1 and OsETR3 with its orthologues TaEtr3-A1, TaEtr3-B1 and TaEtr3-D1 possess no cysteines at these positions.

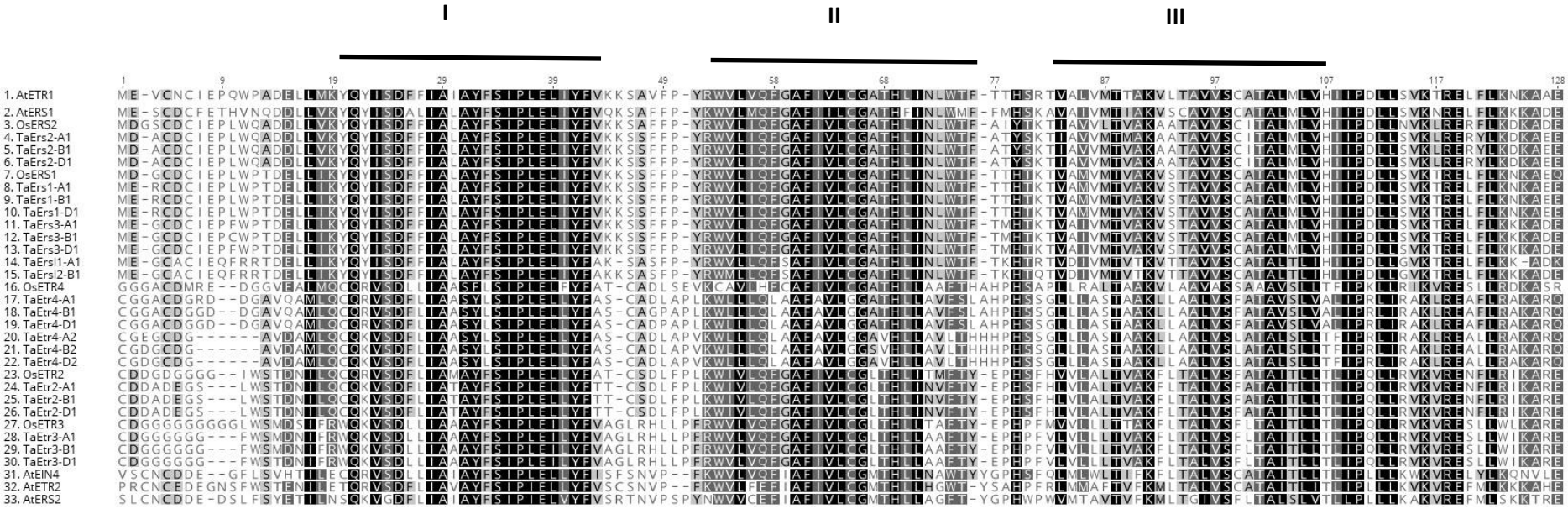

Figure 6.6: *Alignment of transmembrane domain of ethylene receptors.*

Protein alignment of the N-terminal transmembrane domain of AtETR1 with the Arabidopsis, rice and Triticum aestivum ethylene receptors.

Transmembrane α-helices I, II and III are annotated.

The kinase domain of the wheat ethylene receptors in places has high levels of homology and other places low levels of homology compared to Arabidopsis receptors. Figure 6.7 shows the locations of the H box which contains a conserved His residue which is the site of phosphorylation and motifs N, G1, F and G2, which correspond to the nuclear binding pocket of the kinase domain(Robinson *et al.*, 2000). The positions are labelled according to the positions determined by the histidine kinase domain of AtETR1.

The conserved His residue (H353) of the AtETR1 histidine kinase domain is essential for autophosphorylation(Gamble *et al.*, 1998). This residue is absent in Arabidopsis AtERS2 and AtETR2, rice OsETR3 and OsETR2 and wheat TaErs3, TaErs2 and TaErs4 and present in AtEIN4, AtERS1 and AtETR1, OsETR4, as well as OsERS1/2 and their wheat orthologues TaErs2-A1, TaErs2-D1, TaErs2-B1, TaErs3-B1, TaErs3-D1, TaErs3-A1, TaErs1-D1, TaErs1-A1 and TaErs1-B1.

On examination of the N, G1, F and G2 motifs in rice and wheat there is in general lower levels of homology between the different receptors compared to the highly conserved N-motif(Biao Ma, 2015). The red markers correspond to the conserved H353 residue of AtETR1, conserved residues of OsETR2: G487, E489, R491, F493 and G501 and AtETR1 (G545 and G547) (Figure 6.7). Mutants in the OsETR2 residues reveal their role in phosphorylation and therefore are critical for Ser/Thr kinase activity(Biao Ma, 2015). These residues G487, E489, R491, F493 and G501 are highly conserved in most Arabidopsis, wheat and rice ethylene receptors. A major split in function appears to evident in F493. The type of residue appears to correspond with the type of ethylene receptor. AtETR1, AtERS1, OsERS2 and OsERS1 are all members of subfamily I and possess an M residue instead of F at this position. The same appears to be true of their wheat orthologues TaErs1/2/3 (Figure 6.7). This suggests that these proteins possibly lack Ser/Thr kinase activity. Interestingly all these receptors contain the H353 residue of AtETR1, suggesting that instead they either have just histidine kinase activity, as is the case with AtETR1 or both as is the case with AtERS1(Moussatche and Klee, 2004).

Other conserved histidine residues involved in autophosphorylation in the histidine kinase domain of ETR1 were also present in many of the orthologous receptors of

rice and wheat. Both G545 and G547 are phosphorylation sites of the G2 box of AtETR1. Mutants in these residues are predicted to interfere with catalysis via disruption of ATP binding(Gamble *et al.*, 2002). They are both conserved in AtERS1 and AtETR1, OsERS1 and all the homoeologues of TaErs1/2/3.

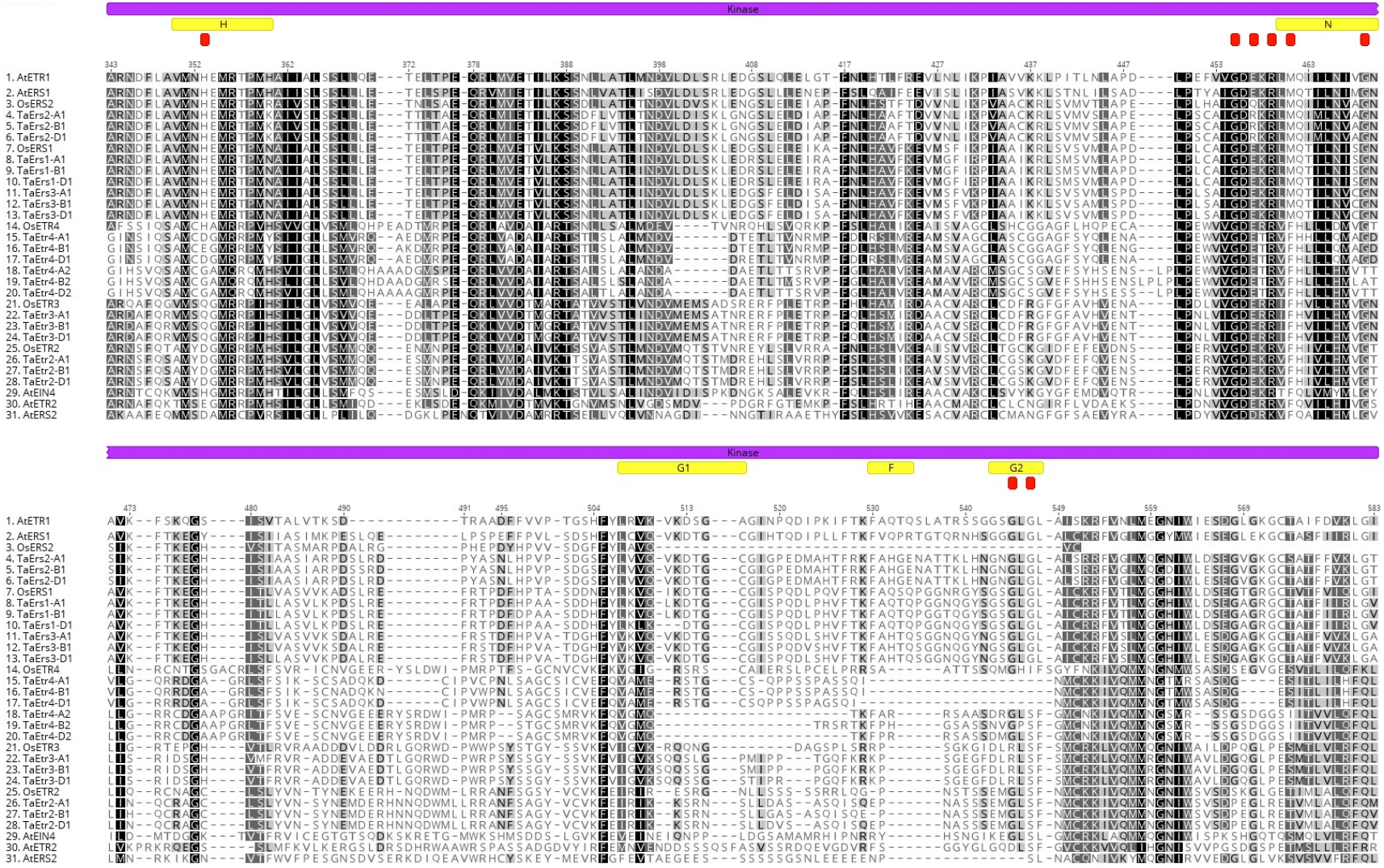
Kinase
H
N
Kinase
G1
F
G2

Figure 6.7*: Alignment of kinase domain of ethylene receptors.*

Protein alignment of the kinase transmembrane domain of Arabidopsis, rice and Triticum aestivum ethylene receptors. The yellow markers indicate the found motifs of N, G1, F and G2 which have been identified from AtETR1, there comprise the nucleotide binding pocket. The red markers indicate conserved amino acids thought to be involved in phosphorylation of the kinase domain in either Arabidopsis or rice. Left to right: AtETR1 position H353 (within the H box), OsETR2 positions G487, E489, R491, F493 and G501 (AtETR1 positions 455, 457, 459 and 469 respectively) (within/near the N box) and finally at the AtETR1 position G545 and G547 in the G2 box.

The expression profiles of these wheat receptor genes was checked by examination of publically available RNAseq data from hexaploid wheat var. Azhurnaya, which covers 22 tissue types from grain, root, leaf and spike at multiple time points (Ramírez-González *et al.*, 2018). There was found to be expression of most wheat ethylene receptor genes throughout the different wheat tissues and development (Figure 6.8). The expression for the most part is also relatively consistent. However, all 6 of the homoeologues of *OsETR4* (*TaEtr4-A2, TaEtr4-B2, TaEtr4-D2, TaEtr4-A1 TaEtr4-B1* and *TaEtr4-D1*), were found to show an absence of expression in most stages of wheat development except some expression in the grain. Interestingly these were also found to not contain the cys-65 in helix II, which is required for copper binding. Therefore, they are unlikely to be able to bind ethylene. *TaEtr4-B2* had a complete absence of expression across all developmental stages and tissues. Overall, the expression of these receptor genes is low, but consistent. When averaged across the different plant tissues and ages none of these genes exceed an expression of greater than 10 tpm in Azhurnaya. The highest levels of expression across the plant are wheat orthologous of *OsERS1*: *TaErs1-A1*, *TaErs1-B1* and *TaErs1-D1* with tpms of 7.79, 6.99 and 7.79 respectively. *TaErsl1-A1* also has surprisingly high levels of expression at 6.39 tpm, despite apparently lacking its kinase and receiver domain. Orthologues of *OsERS2 TaErs2-A1, TaErs2-B1* and *TaErs2-D1* is the second complete group of genes on all three homoeologues with average tpms of 4.66, 6.10 and 5.31 respectively.

In terms of male reproductive development, the expression of rice ethylene receptors was found to occur in the tapetum and pollen at all stages of pollen development(Hirano *et al.*, 2008). In this RNAseq study, only at anthesis were anthers taken and their expression measured(Ramírez-González *et al.*, 2018). The expression values reveal that orthologues of *OsERS2*: *TaErs2-D1* and *TaErs2-A1* had the highest level of expression, followed by the orthologue of *OsERS1*, *TaErs1-D1, TaErsl1-A1, TaErsl2-B1* and the orthologue of *OsERS1* (*TaErs3-D1*) and orthologues of *OsETR4* (*TaEtr4-A2, TaEtr4-A1, TaEtr4-B2, TaEtr4-B1, TaEtr4-D2* and *TaEtr4-D1*) all showed a complete absence of expression at anthesis. The evidence suggests that possibly there is redundancy of function of some of these ethylene receptors due to the hexaploidy of wheat.

Figure 6.8: *Expression profile of wheat ethylene receptors.*

Log2 tpm expression of wheat ethylene receptors of tissue taken across various tissues and developmental stages of hexaploid wheat var. Azhurnaya. n=3. (Ramírez-González *et al.*, 2018). *The figure was constructed using the heat map function on the wheat expression browser website http://www.wheat-expression.com.*

Seedling stage:roots:radicle, Seedling stage:leaves/shoots:coleoptile, Seedling stage:leaves/shoots:stem axis, Seedling stage:leaves/shoots:first leaf sheath, Seedling stage:leaves/shoots:first leaf blade, Seedling stage:roots:roots, Seedling stage:leaves/shoots:shoot apical meristem, three leaf stage:leaves/shoots:third leaf blade, three leaf stage:leaves/shoots:third leaf sheath, three leaf stage:roots:roots, three leaf stage:roots:root apical meristem, three leaf stage:roots:axillary roots, fifth leaf

stage:leaves/shoots:fifth leaf sheath, fifth leaf stage:leaves/shoots:fifth leaf blade, Tillering stage:leaves/shoots:first leaf sheath, Tillering stage:leaves/shoots:first leaf blade, Tillering stage:leaves/shoots:shoot axis, Tillering stage:leaves/shoots:shoot apical meristem, Tillering stage:roots:roots, Tillering stage:roots:root apical meristem, Flag leaf stage:leaves/shoots:flag leaf blade, Flag leaf stage:leaves/shoots:fifth leaf sheath, Flag leaf stage:leaves/shoots:fifth leaf blade, Flag leaf stage:leaves/shoots:shoot axis, Flag leaf stage:roots:roots, Flag leaf stage:leaves/shoots:flag leaf blade night (-0.25h) 06:45, Flag leaf stage:leaves/shoots:fifth leaf blade night (-0.25h) 21:45, Flag leaf stage:leaves/shoots:flag leaf blade night (+0.25h) 07:15, Flag leaf stage:leaves/shoots:fifth leaf blade night (+0.25h) 22:15, Full boot:leaves/shoots:leaf ligule, Full boot:leaves/shoots:flag leaf sheath, Full boot:leaves/shoots:flag leaf blade, Full boot:leaves/shoots:shoot axis, Full boot:spike:spike, 30% spike:roots:roots, 30% spike:leaves/shoots:flag leaf sheath, 30% spike:leaves/shoots:flag leaf blade, 30% spike:leaves/shoots:Internode #2, 30% spike:leaves/shoots:peduncle, 30% spike:spike:spike, 30% spike:spike:spikelets, Ear emergence:leaves/shoots:flag leaf sheath, Ear emergence:leaves/shoots:flag leaf blade, Ear emergence:leaves/shoots:fifth leaf blade, Ear emergence:leaves/shoots:peduncle, Ear emergence:leaves/shoots:Internode #2, Ear emergence:spike:awns, Ear emergence:spike:glumes, Ear emergence:spike:lemma, anthesis:spike:anther, anthesis:spike:stigma & ovary, anthesis:leaves/shoots:flag leaf blade night (-0.25h) 06:45, anthesis:leaves/shoots:fifth leaf blade night (-0.25h) 21:45, milk grain stage:leaves/shoots:flag leaf sheath, milk grain stage:leaves/shoots:flag leaf blade, milk grain stage:leaves/shoots:shoot axis, milk grain stage:leaves/shoots:fifth leaf blade (senescence), milk grain stage:leaves/shoots:peduncle, milk grain stage:leaves/shoots:Internode #2, milk grain stage:spike:awns, milk grain stage:spike:glumes, milk grain stage:spike:lemma, milk grain stage:grain:grain, Dough:leaves/shoots:flag leaf blade (senescence), Soft dough:grain:grain, Hard dough:grain:grain, Dough:grain:endosperm, Dough:grain:embryo proper, Ripening:grain:grain, Ripening:leaves/shoots:flag leaf blade (senescence).

6.3.2 Identification of wheat ethylene receptor mutants using TILLING

The use of wheat TILLING mutants provides a novel reverse genetics approach to investigating the role of ethylene in the development of wheat. TILLING has the advantage of being considered a non-GM approach, therefore interesting phenotypes could be easily brought forward into field trials. Additionally, if agronomically useful traits are identified they could be crossed into the elite wheat varieties without being subjected to the restrictions of GM.

Once a list of the wheat ethylene receptors was obtained, we searched the TILLING population (Section 2.7) for missense mutations within the transmembrane domain at residues which are known to cause gain-of-function ethylene-insensitivity based on previous studies(Sakai *et al.*, 1998; Alonso *et al.*, 1999; Hall *et al.*, 1999; Gamble *et al.*, 2002; Takada *et al.*, 2005, 2006; Binder *et al.*, 2006; Wang *et al.*, 2006; Ishimaru *et al.*, 2006; Kim *et al.*, 2011; Okabe *et al.*, 2011; Shinoyama *et al.*, 2012; Mubarok *et al.*, 2019; Schott-Verdugo *et al.*, 2019). The advantage of these gain-of-function mutants is that only one homoeologue needs to be mutated in order to potentially cause an ethylene insensitive phenotype. A total of 6 mutants were identified in 3 different ethylene receptor genes (Table 6.2).

Table 6.2: *A list of the wheat ethylene receptor TILLING lines, their corresponding IWGSC_ refseqv1.0 scaffold name, abbreviated mutant name and the predicted amino acid substitutions when aligned with ETR1.*

Tilling Line	Gene	IWGSC_ refseqv1.0	Transmembrane domain substitution
Cad1779	*TaErs1-A1b*	*TraesCS4A02G274300*	P36**L**
Cad1445	*TaErs1-A1c*	*TraesCS4A02G274300*	E38**K**
Cad0407	*TaErs1-B1b*	*TraesCS4B02G039300*	P50**S**
Cad1331	*TaErs2-B1b*	*TraesCS1B02G127000*	E38**K**
Cad1865	*TaErs2-B1c*	*TraesCS1B02G127000*	A102**S**

As was previously described when selecting Aux/IAA mutants (Chapter 5), we selected mutants to bring forward based on three criteria. Firstly, whether the missense mutations were in conserved residues of the transmembrane domain which are known to result in an ethylene-insensitive phenotype, whether the gene is an orthologue of a gene known to induce an ethylene-insensitive phenotype and also whether the gene is expressed in wheat, specifically focusing on the anther.

All of the mutations identified in the TILLING population are in transmembrane residues which are known to induce ethylene-insensitivity (Table 6.2). The numbering of the amino acids residues is based on the alignment with the Arabidopsis ETR1 transmembrane protein (Figure 6.5). *TaErs1-A1b* contains the mutation, which results in a P36L substitution. This identical mutation has already been found to induce ethylene insensitivity in Arabidopsis when either AtETR1 or AtETR2 was mutated at this position(Sakai *et al.*, 1998; Wang *et al.*, 2006). Two of the mutants, *TaErs1-A1c* and *TaErs2-B1b*, contain mutations which result in the conversion of glutamic acid(E) on position 38 to a lysine(K). The conversion of this glutamic acid to an alanine was found to result in an ethylene-insensitive phenotype in the ETR1 receptor in Arabidopsis(Wang *et al.*, 2006). We wanted to investigate these mutants as lysine is a positively charged amino acid compared to a glutamic acid which is a negatively charged amino acid, these very different chemical

properties could still impact the function of the receptor. Another mutant, *TaErs1-B1b,* involved converting the proline(p) at position 50 to a serine(s). P50A was found to induce an insensitive phenotype in Arabidopsis(Wang *et al.*, 2006). Serine and alanine have different molecular properties to each other, but also different properties compared to proline, so this might be expected to result in a disruption of receptor function. The final mutant, *TaErs2-B1c*, is a conversion of alanine (A) at position 102 to a serine. At this positions, the conversion of alanine to threonine in the ETR1 gene of Arabidopsis was previously found to induce an ethylene insensitive phenotype(Wang *et al.*, 2006). Both serine and threonine are amino acids with polar uncharged side chains, therefore these amino acids with similar chemical properties could lead to an equivalent disruption of ethylene signalling and an ethylene-insensitive phenotype.

As mentioned previously, we also took into consideration the homologies of the mutated genes. *TaErs1* is an orthologue of Arabidopsis *AtERS1* (Figure 6.4) and clusters closely with *AtETR1*. *TaErs2* is the direct wheat orthologue of *OsERS2* and also clusters closely to *AtETR1*. Mutations in the transmembrane domain of AtETR1 are known to result in an ethylene-insensitive phenotype(Hall *et al.*, 1999; Wang *et al.*, 2006). All three of these genes share key similarities with AtETR1, with a high level of homology in the transmembrane domain and sharing all three of the conserved phosphorylation sites of H353, G545 and G547 (Figure 6.5). However, all these receptors are lacking the receiver domain, although this is thought to not be necessary for receptor function.

The tissue specific expression of these genes was also taken into account. *TaErs1-A1*, *TaErs1-B1*, *TaErs2-B1* are expressed (albeit to a low level) throughout the different tissues of wheat (Figure 6.8). Consequently, disruptions in these gene functions could result in ethylene-insensitivity across a range of different tissues and wheat developmental stages.

Expression of these genes in the anther was also taken into consideration. This is important when considering later experiments of phenotypic characterisation and heat stress tolerance. Chapter 4 details an experiment on Cadenza which investigated changes in the transcription of the anthers across different pollen

development stages and in both control and heat stress conditions. This RNAseq data set provides a valuable resource to investigate the expression of the ethylene receptor genes during anther development in the Cadenza background. Interrogation of this data demonstrated that *TaEtr4-A1*, *TaEtr4-B1*, *TaEtr4-D1*, *TaEtr4-A2*, *TaEtr4-B2* and *TaEtr4-D2* showed very low levels of expression across all stages and treatments with the mean tpm never exceeding 1 (Figure 6.9). On average homoeologues of *TaEtr3* showed the highest average expression level, followed by *TaErs1*, *TaErs2* and *TaErs3*. Greater expression of most ethylene receptor genes tends to be towards the earlier stages of pollen development, with tricellular stage often showing the lower expression levels.

In the anther, in response to heat there was found to be a downregulation of *TaErs1-B1* at unicellular stage, whereas there was an upregulation at tricellular stage (Figure 6.9). *TaErs1-A1* expression appeared to be less impacted by heat treatment with only a small upregulation at heat tricellular stage. For *TaErs2-B1* there was 2.5-fold increase in expression in the heat-treated anthers at bicellular stage. Many ethylene receptors appear to show this preferential expression at the bicellular heat stage. All homoeologues of *TaEtr2*, *TaEtr4*, *TaErs2* and *TaErs3* all show preferential expression at bicellular heat stage compared to bicellular control.

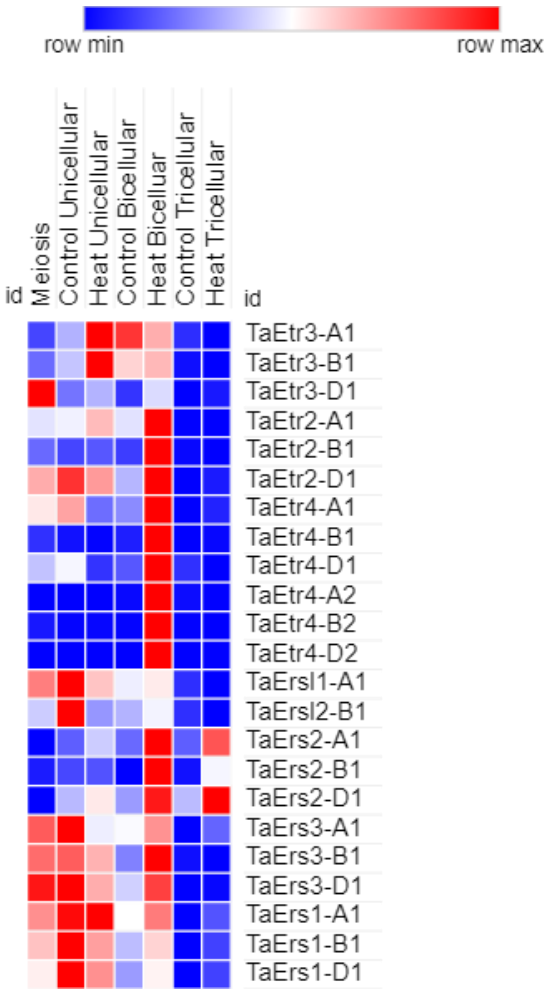

Figure 6.9: *Heat map of the expression of ethylene receptors across 4 main stages of pollen development and in response to heat treatment.*

Anther samples were initially taken at meiosis stage, followed by unicellular, bicellular and tricellular stages in control conditions and after heat stressing for 4 days 33/26°C day/night from meiosis stage. Each colour corresponds to the Z-value. Calculated from the expression of 4 biological replicates. Taken from RNAseq data (chapter 4).

Considering these three factors we deduced that all 5 of the discovered ethylene receptor mutants should be brought forward as it is likely that all could induce an ethylene-insensitive phenotype. The selected TILLING lines were subsequently backcrossed twice to Cadenza to remove approximately 75% of EMS-induced SNPs that are present in the background and which could impact on the phenotype. The ethylene lines were then selfed and the progeny genotyped (section 2.2) to identify

homozygous mutants and null segregants to bring forward for phenotypic characterisation.

6.3.3 Phenotypic characterisation

A complete alanine scanning screen of the transmembrane domain of the ETR1 receptor in *Arabidopsis* revealed that most mutants have a slightly shorter hypocotyl than the WT when grown in air, with few phenotypic differences (Wang *et al.*, 2006). However, when a mutated form of *CmETR1* (H69A/H70A) was constitutively expressed in *Nicotiana tabacum* or *Chrysanthemum morifolium* there was found to be a reduction in male fertility (Takada *et al.*, 2005, 2006; Ishimaru *et al.*, 2006; Shinoyama *et al.*, 2012).

With possibly implications for plant height and fertility, a detailed investigation into the shoot phenotype of the ethylene receptor mutants was conducted by means of a 4-block randomised phenotyping experiment. Plants were grown in glasshouse conditions (Section 2.1) until reaching GS93 (maturity) of the Zadoks scale of wheat development (Figure 3.1). The experiment featured all 5 ethylene receptor mutants, their null segregants (NS) and Cadenza. Each block containing 1 biological replicate of each. Whole plant data was collected on tiller number, and from three of the tallest tillers measurements of internode length and average grain number were taken. Only tillers which produced a spike were counted. Internodes 1-4 (1 being the highest internode of the tiller and 4 being the lowest) were measured individually. ANOVA analysis was performed on the untransformed data. All statistical analysis was performed using statistical handling software Genstat (v20, VSNI, Hemel Hempstead, U.K.).

As was found in *Arabidopsis* ethylene receptor mutants with no overexpression there was very little divergence from a WT Cadenza phenotype (Figure 6.10). There was found to be no impact of mutations in the ETR receptor on grain count ($P=0.738$; 5% LSD=7.408), suggesting no significant impact on fertility (Table 6.3). In contrast, rice mutants which showed reduced sensitivity to ethylene were found to have a reduced seed setting rate, however, these were ETR2 overexpressing lines(Biao Ma, 2015).

Figure 6.10: *Phenotypes of hexaploid wheat (var. Cadenza) ethylene receptor mutants.*

Phenotype of ethylene receptor mutants grown in glasshouse conditions. Cad: Cadenza, NS: Null Segregant and Mut: Mutant. Scale bar = 100mm. Photographs were taken at GS93 of the Zadoks scale.

Ethylene signalling has also been implicated to be involved in tillering of rice. With the *osctr2* mutant, which showed a constitutive ethylene signalling response phenotype, resulted in increased tillering(Wang *et al.*, 2013). Rice mutants overexpressing ETR2, which showed reduced sensitivity to ethylene showed decreased tillering in some lines but not others(Biao Ma, 2015). The rice *mhz5* mutant which shows enhanced sensitivity to ethylene in the coleoptile, was found to show higher levels of tillering than WT(Yin *et al.*, 2015), whereas in *mhz4* (which shows the same ethylene response) there was found to be no difference in tillering(Ma *et al.*, 2014). We would therefore hypothesise that our ethylene-insensitive mutants would show decreased tillering. However, there was also found

to be no significant difference in the level of tillering (P=0.401; 5% LSD=2.171) (Table 6.3).

Ethylene has also been linked to plant height. Rice mutants which show enhanced sensitivity to ethylene were found to have shorter internodes than the WT(Yin *et al.*, 2015). Reduced internode lengths were also observed in rice mutants with reduced sensitivity to ethylene(Biao Ma, 2015). Rice *mhz4* plants were taller than WT, these were found to have enhanced ethylene-sensitivity in the hypocotyl(Ma *et al.*, 2014). In terms of internode length there was some evidence of reduced elongation, which is indicative of ethylene-insensitive mutants. Internode 1 was found to be significantly shorter in the mutant than both the NS and WT Cadenza in *TaErs1-B1b* and just WT Cadenza in *TaErs1-A1b* (Table 6.3). Whereas in *TaErs2-B1b* internode 1 was found to be only significantly shorter than Cadenza and not the NS (P=0.003; 5% LSD=3.009). Internode 3 was also found to be significantly shorter in *TaErs1-B1b* compared to WT Cadenza, but not compared to the NS. Therefore, for *TaErs2-B1b* and *TaErs1-B1b,* this phenotype could be due to other background mutations present. Internodes 2 and 3 were both found to be significantly longer in *TaErs2-B1c* compared to its NS but not Cadenza (P=0.033; 5% LSD=1.712 and P=0.043; 5% LSD=1.46 respectively). This could be due to the presence of a background mutation in the NS of *TaErs2-B1c.* When considering the entire length of the stem only *TaErs1-B1b* was found to be significantly different from both its NS and Cadenza (P<0.001; 5% LSD=5.06).

Table 6.3: *Effect of missense mutations in the transmembrane domain of ethylene receptors on general phenotype.*

A phenotypic comparison of WT Cadenza with the 5 ethylene receptor mutants (Mut) and their null segregant (NS). ANOVA output of grain count/spike, spike length, tiller number, and internode length. Pairwise comparisons were made between each phenotype using 5% LSDs to determine the significance. [a]*= significantly different from NS segregant,* [b]*=significantly different from WT Cadenza.*

Genotype		Grain count/spike	Tiller number	Internode lengths (cm)				Total Stem length (cm)
				1	2	3	4	
Cadenza		48.33	9.25	36.20	18.35	11.51	7.15	75.04
TaErs1-A1a	NS	50.50	8.25	32.95	17.46	10.72	6.83	69.04
TaErs1-A1b	Mut	47.75	9.25	32.61 [b]	18.71	10.11	5.57	67.22 [b]
TaErs1-A1a	NS	50.17	9.00	35.58	19.23	11.24	7.29	74.74
TaErs1-A1c	Mut	47.58	9.50	37.62	18.24	11.62	6.40	75.14
TaErs1-B1a	NS	49.53	8.50	35.43	17.66	10.89	7.03	71.88
TaErs1-B1b	Mut	46.25	7.00	30.93 [a b]	17.18	9.82 [b]	6.56	65.68 [a b]
TaErs2-B1a	NS	51.90	8.10	34.49	18.17	10.52	6.21	70.87
TaErs2-B1b	Mut	44.50	9.50	32.68 [b]	18.97	11.61	6.93	71.62
TaErs2-B1a	NS	48.42	9.00	35.18	16.84	10.07	6.03	69.02
TaErs2-B1c	Mut	47.06	7.94	36.11	19.87 [a]	12.18 [a]	7.65	78.16 [a]
P-value		0.738	0.401	0.003	0.033	0.043	0.525	<.001
SED		3.604	1.058	1.466	0.834	0.711	0.894	2.466
LSD (5%) (d.f)		7.408 (26)	2.171 (27)	3.009 (27)	1.712 (27)	1.460 (27)	1.834 (27)	5.060(27)

6.3.4 Assessing ethylene-insensitivity in wheat ethylene receptor mutants

Following on from the general phenotyping experiment it is necessary to establish whether the mutants displayed ethylene insensitive growth responses. When eudicot seedlings are exposed to ethylene gas, the result is reduced growth of the hypocotyl and root, an exaggerated apical hook and thickening of the hypocotyl, known collectively as the triple response. Measurements of the elongation of the shoot and root of seedlings exposed to ethylene can be used to quantify the level of ethylene sensitivity and identifying ethylene-related mutants(Guzman and Ecker, 1990). Monocots show a variation of this response, a double response. Etiolated maize, wheat, sorghum and *Brachypodium distachyon* seedlings that are treated with ethylene display reduced elongation of roots and coleoptiles(Yang *et al.*, 2015). Applying the same principles as used to identify Arabidopsis ethylene response mutants we screened the ethylene-receptor mutants for evidence of reduced sensitivity to ethylene.

The auxin-insensitive mutants (*TaIaa18-Bb, TaIaa22-Bb, TaIaa22-Bc* and *TaIaa22-Db*) described in chapter 5, were also included to investigate the relationship between auxin and ethylene signalling pathway. There is known to be crosstalk between the auxin and ethylene signalling pathway in terms of hypocotyl elongation(Smalle *et al.*, 1997) and root growth(Pickett *et al.*, 1990; Rahman *et al.*, 2001; Růžička *et al.*, 2007; Lewis *et al.*, 2011). In the root ethylene has been linked to causing increased auxin synthesis and reduced transport, leading to increased accumulation which in turn leads to reduced root elongation(Růžička *et al.*, 2007; Swarup *et al.*, 2007). Conversely, increased levels of auxin in the stem cause increased elongation, due to different physiological roles of auxin in different tissues. We would expect that the auxin-insensitive mutants would not show an ethylene induced reduction of growth in the roots or an elongation in the stem, owing to auxin being an important part of the double/triple response.

A two-cohort ethylene response assay was conducted to quantify the level of ethylene-insensitivity of these mutants (following the methods detailed in section 2.11). Each cohort contained 20 tubes (2 for each genotype) whereby 1 was used in the control and another was used in the ethylene treatment. This led to a total max

of 10 biological replicates for each treatment across the two cohorts. Measurements were taken of the root and shoot length of 5-day old seedlings exposed to either control conditions or 30µl L^{-1} ethylene, to quantify their double response. ANOVA analysis was performed on the untransformed data.

As previously described in wheat, exposure to ethylene causes a reduction of coleoptile height in etiolated seedlings(Yang *et al.*, 2015). There was found to be a significant interaction to genotype and response to ethylene in terms of shoot elongation ($P<0.001$; LSD (5%) = 1.0639 (169 d.f) (Figure 6.11B). Cadenza, *TaErs1-A1b*, *TaErs2-A1c*, *TaErs1-B1b* and *TaErs2-B1c* showing a significant reduction in seedling height compared to the control (Figure 6.11B), showing reductions of 16.4%, 18.3%, 26.5%, 15.7% and 27.5% respectively in response to ethylene treatment. Therefore, suggesting that in the shoot they do not display evidence of ethylene-insensitivity. *TaErs2-B1b* was found to not display the double response when exposed to 30µl/l of ethylene gas, showing no significant difference in shoot length (Figure 6.11B). Therefore, suggesting that it is insensitive to ethylene.

In contrast, the auxin-insensitive mutants *TaIaa18-Bb* and *TaIaa22-Db* showed a 65.6% and 48.4% reduction in shoot length respectively on exposure to ethylene, compared to the more modest reduction of 16.4% in Cadenza. The clear hyper-sensitivity to ethylene of these auxin-insensitive mutants is apparent from the extreme shortness of *TaIaa18-Bb* and the curling of the ethylene treated leaves of *TaIaa22-Db* (Figure 6.11A). This shows that in wheat there is crosstalk between the auxin and ethylene signalling pathway, and that the action of ethylene is probably mediated by auxin accumulation.

Gaseous application of ethylene was found to not show a significant impact on root elongation between different genotypes ($P=0.434$; LSD (5%) = 1.686 (169 d.f) (Figure 6.11C). Even WT Cadenza failed to show a significant reduction in root growth.

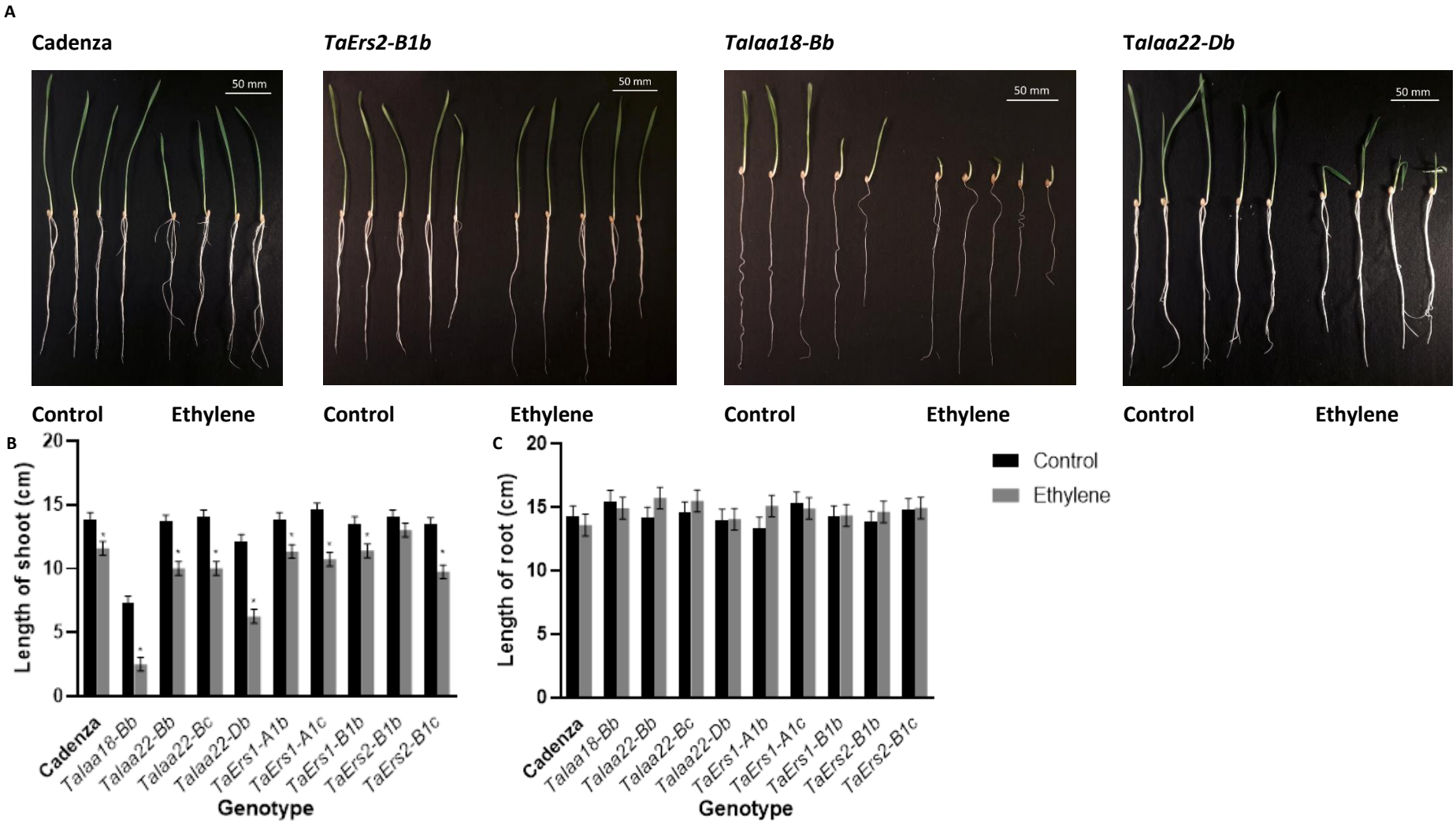
A
Cadenza
TaErs2-B1b
Talaa18-Bb
Talaa22-Db
50 mm
Control
Ethylene
B
Length of shoot (cm)
C
Length of root (cm)
Control
Ethylene
Cadenza
Talaa18-Bb
Talaa22-Bb
Talaa22-Bc
Talaa22-Db
TaErs1-A1b
TaErs1-A1c
TaErs1-B1b
TaErs2-B1b
TaErs2-B1c
Genotype

Figure 6.11: *Sensitivity of Cadenza and 4 auxin insensitive mutants (Taiaa18-Bb, Taiaa22-Bb, Taiaa22-Bc and Taiaa22-Db) and 5 ethylene receptor mutants (TaErs1-A1b, TaErs1-A1c, TaErs1-B, TaErs2-B1b and TaErs2-B1c) to ethylene treatment.*

A: *Photographs of 5-day old seedlings of Cadenza, TaErs2-B1b, Taiaa18-Bb and Taiaa22-Db grown in presence or absence of ethylene gas. Scale bar = 50mm.* **B***: Length of primary shoot of 5-day old seedlings in response to ethylene. Bars are the ANOVA output of the predicted means for 8 biological replicates. Error bars =+/- 1 SED (5%) =* 0.5389*. LSD (5%) =* 1.0639 *(169 d.f). *Significantly different from Cadenza within the same treatment (P<0.001).* **C***: Length of primary root of 5-day old seedlings in response to ethylene. Bars are the ANOVA output of the predicted means for 8 biological replicates. Error bars =+/- 1 SED (5%) =* 0.854*. LSD (5%) =* 1.686 *(169 d.f). P=*0.434*.*

6.3.5 Heat stress tolerance

Many studies implicate the importance of ethylene in heat stress tolerance during anther and pollen development(Qin *et al.*, 2008; Firon *et al.*, 2012; Jegadeesan *et al.*, 2018). Ethylene-insensitive tomato mutants have been found to be more sensitive to heat stress, showing reduced pollen viability(Firon *et al.*, 2012). Utilising the ethylene-insensitive mutant (*TaErs2-B1b*), we sought to investigate whether this insensitivity caused an increased vulnerability to heat stress in hexaploid wheat.

The 4 other ethylene-receptor mutants were still responsive to ethylene in the shoot and therefore were excluded from the experiment (Figure 6.11). *TaErs2-B1b* was subjected to the heat stress assay optimised for Cadenza, as described in chapter 3. An initial experiment focused on grain number was used to ascertain whether it was more vulnerable to heat stress. A 3-cohort experiment was constructed where *TaErs2-B1b* and WT Cadenza were initially grown in glasshouse conditions (Section 2.1). The heat stress assay applied was the same assay that had been already optimised for hexaploid wheat var. Cadenza (see chapter 3; Section 2.8). In summary, tillers were tagged at 9-13cm FLS elongation, as this corresponds to pollen meiosis, the most vulnerable stage. The plants were subsequently heat stressed at 33/26°C day/night for 4 days. Measurements of grain count from the central 6 spikelets either side of the side of the spike and days until anthesis and elongation rate of the FLS was also taken (see chapter 3).

The unbalanced nature of the experiment meant that REML analysis was used to analyse the data. The data for FLS elongation rate and days until anthesis was determined to be normally distributed, therefore no transformation as required. However, grain count data was transformed (logit+1) to ensure normal distribution of data.

There was found to be no significant interaction between genotype and treatment in terms of rate of flag leaf sheath (FLS) elongation, number of days to reach anthesis and grain set (P=0.868**,** 0.316 and 0.990 respectively) (Table 6.4). There was no apparent difference in the heat stress response of *TaErs2-B1b* compared to Cadenza with both genotypes showing a significant reduction in grain set, decreased time to reach anthesis and increased FLS elongation when exposed to heat treatment (P=0.024, <0.001 and 0.041 respectively).

Table 6.4: *Effect heat stress on Cadenza and ethylene-insensitive mutant TaErs2-B1b.*

REML output of FLS elongation, days until anthesis from meiosis and grain set in response to heat treatment. Pairwise comparisons were made between each genotype and treatment using 5% LSDs to determine the significance. **= significantly different from control of same genotype. Statistical analysis was performed on the transformed scale* (*logit+1 transformation*) *for grain set, shown in brackets.*

Genotype	Treatment	FLS elongation (cm)	Days until anthesis	Grain set
Control	Control	5.486	12.16	0.952381 (1.164)
	Heat	6.333	10.17*	0.877976 (0.844)
TaErs2-B1b	Control	5.380	12.99	0.97619 (1.247)
	Heat	6.371	10.17*	0.890625 (0.924)
Genotype		0.818	0.415	0.584
Treatment		0.041	<0.001	0.024
Genotype*Treatment		0.868	0.316	0.990
Max SED		0.6488	0.5884	0.1920
Max LSD (5%) (d.f)		1.366	1.238	0.3995

6.4 Discussion

Ethylene is a gaseous plant hormone which is crucial in regulating development and growth of land plants(Binder, 2020). The production of mutant plants defective in ethylene signalling is a useful tool in identifying the role of ethylene in plant development, as well as identifying key genes involved in the ethylene signalling pathway.

A reverse genetics approach was applied to produce dominant ethylene-insensitive mutants in hexaploid wheat. Using the TILLING resources available missense mutations in the transmembrane domain of wheat ethylene receptors were identified. The remarkable degree of homology of the transmembrane domain with Arabidopsis and rice (Figure 6.5B) suggest homology in the ethylene signalling pathways and shared function of these receptors in wheat. A total of 5 different missense mutations affecting various residues within the transmembrane domain of ethylene receptor genes were identified (Table 6.2). These missense mutations affect amino acid residues known to induce an ethylene-insensitive phenotype(Sakai *et al.*, 1998; Alonso *et al.*, 1999; Hall *et al.*, 1999; Gamble *et al.*, 2002; Takada *et al.*, 2005, 2006; Binder *et al.*, 2006; Wang *et al.*, 2006; Ishimaru *et al.*, 2006; Kim *et al.*, 2011; Okabe *et al.*, 2011; Shinoyama *et al.*, 2012; Mubarok *et al.*, 2019; Schott-Verdugo *et al.*, 2019). Quantifying the phenotype, responsiveness to ethylene and heat stress sensitivity of these mutants gives valuable insights into the role of ethylene signalling in development and abiotic stress tolerance of wheat.

Most of the mutants did not show distinctive phenotypic differences compared to WT Cadenza or the NS. Only one of the mutants (*TaErs2-B1b*) showed an absence of triple response phenotype in the shoot, but not the root, when exposed to ethylene gas. This mutant was exposed to heat treatments to investigate its vulnerability to heat stress and it was found to not show increased sensitivity to heat. This suggests that *TaErs2-B1* is not an essential gene for ensuring successful pollen development and does not appear to play a major role in the heat stress response of wheat.

6.4.1 The ethylene receptor gene family in wheat

In total there were found to be 7 ethylene receptor genes in wheat, compared to 5 genes in Arabidopsis and rice(Gamble *et al.*, 2002; Yau *et al.*, 2004) (Figure 6.4). These 7 ethylene receptor genes have three homoeologues in each of the wheat sub-genomes: A, B and D. The phylogeny of the wheat receptors closely follows that of rice ethylene receptors. However, it appears that wheat has a duplication in the orthologue of rice *OsETR4* and *OsERS1*. In addition, there are two ethylene receptor like genes (*TaErsl1-A1* and *TaErsl2-B1*) which lack the kinase and receiver domain, so their functionality in ethylene signalling is currently unclear (Figure 6.5).

As is expected, there was found to be considerably greater homology between ethylene receptors of rice and wheat, more so than Arabidopsis. An ETR1-type receptor was also found to be absent in wheat, as has previously been found in rice, *B. distachyon*, maize, and sorghum (Yang *et al.*, 2015).

Protein alignments show the remarkable degree of homology of the domain structure of receptors between monocots and dicots (Figure 6.5). Most genes show nearly identical transmembrane domains and highly similar GAF and kinase domains. Most transmembrane domains contained conserved Cys-65 and His-69 which are essential for binding one copper ion per monomer(Rodríguez *et al.*, 1999; Schott-Verdugo *et al.*, 2019) (Figure 6.6). Copper ions are required as a cofactor to allow ethylene binding(Rodríguez *et al.*, 1999). This indicates a shared function of these receptors in binding ethylene and conformational changes which occur leading to signal transduction. Therefore, we can infer a high degree of similarity in the perception of ethylene in both monocots and dicots.

In addition to the similarities in the transmembrane domain, a number of residues of the kinase domain are conserved between Arabidopsis, rice and wheat receptors, indicating a common functionality in autophosphorylation (Figure 6.7). Therefore, the wheat receptors containing a kinase domain are likely to show either His or Ser/Thr kinase activity or both as has previously been found in Arabidopsis ethylene receptors(Gamble *et al.*, 1998; Moussatche and Klee, 2004).

Expression of most of the ethylene receptor genes is relatively low in wheat, but they are expressed throughout most of the plant tissues and throughout development (Figure 6.8). This indicates the importance of ethylene signalling throughout plant development and corresponds with the diversity of functions ethylene is known to be involved in(Binder, 2020). The duplication of genes has potentially led to redundancy of function with some of the genes, as all 6 of the homoeologues of *OsETR4* (*TaEtr4-A2, TaEtr4-B2, TaEtr4-D2, TaEtr4-A1, TaEtr4-B1* and *TaEtr4-D1*), were found to show an absence of expression in most stages of wheat development except in the grain. This also corresponds with the lack of conserved histidine residues in the kinase domain and absence of the conserved Cys-65(Gamble *et al.*, 1998, 2002; Rodríguez *et al.*, 1999; Moussatche and Klee, 2004; Schott-Verdugo *et al.*, 2019). Both of which are required for an effectively functioning receptor.

From the TILLING population a total of 5 different ethylene receptor mutants were found across 3 different genes. Analysis of the phenotypes and ethylene response of these genes gives important insights into the ethylene signalling pathway in hexaploid wheat.

6.4.2 Ethylene-insensitivity of ethylene-receptor mutants

Many studies have exploited the triple response to determine ethylene-sensitivity(Sakai *et al.*, 1998; Hall *et al.*, 1999; Gamble *et al.*, 2002; Wang *et al.*, 2006). Exposing all 5 of these wheat mutants to ethylene treatment showed that only one of them (*TaErs2-B1b*) failed to show inhibited shoot elongation when exposed to ethylene (Figure 6.11A/B). This mutant contains a mutation converting glutamic acid on residue position 38 to lysine (E38K). This substitution led to very little change in the hydrophobicity of the transmembrane domain (Supplementary Figure 2), however this is a conversion of a negatively charged amino acid side chain to a positively charged amino acid side chain. The conversion of this glutamic acid to alanine has been found to result in ethylene-insensitivity in Arabidopsis ETR1, although there was no change in the ethylene binding capacity of the receptor(Wang *et al.*, 2006). *TaErs1-A1c* also showed the same amino acid change as *TaErs2-B1b*, although it did not show an ethylene-insensitive phenotype at the

seedling stage (Figure 6.11). This could be due to differences in expression between *TaERS2-B* and *TaERS1-A* in the seedlings, although there are no strikingly differences in the levels of expression between these two genes at the seedling stage in the shoot (Figure 6.8).

It was surprising that *TaErs1-A1b* does not shown an ethylene-insensitive phenotype as the same missense mutation converting proline at residue 36 to leucine (P36L) led to an ethylene insensitive phenotype in Arabidopsis(Sakai *et al.*, 1998). This mutation disrupts the ability for ethylene to bind to the receptor in Arabidopsis (Wang *et al.*, 2006). *TaErs1-A1* is also widely expressed throughout wheat tissues and developmental stages (Figure 6.8). This suggests that this mutation does not have a similar detrimental effect on receptor function.

TaErs1-B1b also does not show an ethylene-insensitive phenotype (Figure 6.11). The mutation involves the proline on residue number 50, being converted to a serine. The conversion of this proline to alanine in Arabidopsis was found to induce a dominant ethylene-insensitive phenotype, but without having an effect on the ethylene binding activity(Wang *et al.*, 2006), suggesting these residues are involved in turning off the signal transmitter domain of the receptor. It is conceivable that this amino acid change is not sufficient to reduce functionality of the receptor.

TaErs2-B1c also did not show an ethylene-insensitive phenotype (Figure 6.11). The amino acid change involves a conversion of alanine at residue position 102 to a serine. This conversion was predicted to produce a least a partially ethylene insensitive phenotype as in Arabidopsis the A102T mutant in *ETR1* showed partial insensitivity. Given the fact that threonine and serine have similar amino acid side chains with both being polar a similar effect on receptor function is expected (Hall *et al.*, 1999). It was confirmed that A102T in ETR1 results in an ethylene insensitive phenotype, but without having an impact on the ethylene binding activity, suggesting that this residue is involved in turning off the signal transmitter domain(Wang *et al.*, 2006). The mutation, *TaErs2-B1c*, is in the same gene as *TaErs2-B1b*, which has been found to be ethylene insensitive. Potentially the missense mutation of *TaErs2-B1c* was not enough to disrupt the function of the receptor in wheat.

There is known to be crosstalk between the auxin and ethylene signalling pathway in terms of hypocotyl elongation(Smalle *et al.*, 1997) and root growth(Pickett *et al.*, 1990; Rahman *et al.*, 2001; Růžička *et al.*, 2007; Lewis *et al.*, 2011). In the light, ethylene increases levels of IAA responsiveness resulting in elongation of the hypocotyl(Liang *et al.*, 2012). This has been linked to the impact of ethylene on the accumulation of the EIN3, a transcription factor involved in light dependent elongation of the hypocotyl(Chao *et al.*, 1997; Smalle *et al.*, 1997). EIN3 induces expression of *YUCCA1* and *YUCCA5*, resulting in IAA accumulation (Yamamoto *et al.*, 2007).

In Arabidopsis, auxin insensitive mutants were found to show reduced hypocotyl elongation when grown in the light and on ACC(Liang *et al.*, 2012). The same was true for the wheat auxin-insensitive mutants, *TaIaa18-Bb* and *TaIaa22-Db*, which were both found to show a greater inhibition of shoot growth in response to ethylene than WT Cadenza (Figure 6.11B). This is hypothesised to be due to the impact of light in this experiment. The experiment was not completed on etiolated seedlings, but rather the seedlings were exposed to light by the transparent sides of the airtight container, whereas the opaque top was shading. Even at this low level of light, the ethylene could be promoting auxin signalling and inducing some sort of elongation response in the shoots. The auxin-insensitive mutants are not responding to this auxin induced growth and remain smaller. Considering this effect, future studies could aim to establish whether this response occurs in etiolated seedlings.

In terms of root growth none of the wheat genotypes showed an inhibition of root growth (Figure 6.11C) in response to ethylene, therefore suggesting that either the roots are less sensitive to ethylene than the shoots or the glass tubes are saturated with water which is preventing the gas from dissolving and reaching the roots to have an impact on root elongation. Future experiments should aim to repeat the assays described in section 6.3.4, potentially reducing the amount of water the paper was soaked in or using higher concentrations of ethylene. When these assays have been successfully optimised for the controls it will be possible to further investigate the effects of these mutations on root architecture.

6.4.3 General phenotype of ethylene-receptor mutants

In the ethylene receptor mutants of wheat there was found to be no significant difference in grain set between the mutants and their NS and WT Cadenza (Table 6.3). In many studies, male sterility was not described in ethylene receptor mutants (Sakai *et al.*, 1998; Alonso *et al.*, 1999; Hall *et al.*, 1999; Gamble *et al.*, 2002; Wang *et al.*, 2006; Deslauriers *et al.*, 2015). However, when a mutated form of CmETR1 (H69A/H70A) was constitutively expressed in *Nicotiana tabacum* or *Chrysanthemum morifolium* there was found to be a reduction in male fertility due to a combination of lower pollen production, viability and changes in flower morphology that prevent self-fertilisation(Takada *et al.*, 2005, 2006; Ishimaru *et al.*, 2006; Shinoyama *et al.*, 2012). The reduction in pollen viability has been linked to delayed degradation of the tapetum layer(Takada *et al.*, 2005, 2006). Tapetum degradation is essential for ensuring successful pollen development. It is required to release nutrients to nourish the developing pollen and release enzymes which release microspores from their tetrads; it is also required for dehiscence (Goldberg *et al.*, 1993; Wu and Cheung, 2000; Parish and Li, 2010). The lack of male sterility evident in the wheat mutants could be due to the high level of redundancy of the wheat genome, but also the fact that sterility only seems to be achieved when there is an overexpression of the insensitive receptor. ETR2-overexpression lines showed reduced grain sets, whereas knockdown lines were the same as the WT(Biao Ma, 2015).

Various Arabidopsis ethylene receptor mutants (produced from an alanine screen of the transmembrane domain of ETR1) which were not constitutively expressed, were found to have a slightly reduced hypocotyl length compared to the WT when grown in air(Wang *et al.*, 2006). Likewise tomato ethylene receptor mutants, *Sletr1-1* and *Sletr1-2* produced by TILLING, also showed little difference in root or hypocotyl length when grown in air(Okabe *et al.*, 2011). In rice overexpression of *ETR2* resulted in ethylene-insensitivity and shorter seedlings/ 50-day old plants in the field(Biao Ma, 2015). The *MHZ7 (OsEIN2)* overexpressing rice mutants were found to have a constitutive ethylene-signalling response and when grown in the field were shorter than both the WT and *mhz7-1/2* mutant. Both *mhz7-1* and *mhz7-2* are

recessive mutants in *OsEIN2*, which leads to ethylene-insensitivity, but did not appear to have a height phenotype compared to the WT(B. Ma *et al.*, 2013). Likewise, we found no extreme differences in phenotype in our mutants (Figure 6.10; Table 6.3). This suggests in order to get a phenotype the gene needs to be overexpressed.

Ethylene signalling has also been implicated to be involved in tillering of rice. With *osctr2* mutant, which showed a constitutive ethylene signalling response phenotype showed increased tillering(Wang *et al.*, 2013). Rice mutants overexpressing ETR2, which showed reduced sensitivity to ethylene showed decreased tillering in some lines but not others(Biao Ma, 2015). The rice *mhz5* mutant which shows enhanced sensitivity to ethylene in the coleoptile, was found to show higher levels of tillering than WT(Yin *et al.*, 2015), whereas in *mhz4* (which shows the same ethylene response) there was found to be no difference in tillering (Ma *et al.*, 2014). We would therefore hypothesise that our ethylene-insensitive mutants would show decreased tillering. However, there was also found to be no significant difference in the level of tillering (Table 6.3), even in *TaErs2-B1b.*

Ethylene has also been implicated to be involved in flowering time in Arabidopsis and rice with ethylene insensitive mutants showing delayed flowering (Ogawara *et al.*, 2003; Biao Ma, 2015). Future experiments should focus on measuring flowering time in the ethylene-insensitive mutants.

6.4.4 Role of ethylene in the heat stress response during pollen development

TaErs2-B1b did not show any greater reduction in grain set in response to heat treatment compared to WT Cadenza (Table 6.4). These results indicate that ethylene does not play a major role in the reproductive heat stress response and that an insensitivity or deficiency of ethylene should not dramatically impact thermotolerance in wheat. This contrasts with studies on tomato which indicate ethylene is crucial for maintaining ensuring normally pollen development during heat stress. There was found to be a deaccumulation of ethylene after heat treatment in pollen(Jegadeesan *et al.*, 2018) and that ethylene treatment increased pollen viability under heat stress(Firon *et al.*, 2012). Mutant studies show contrasting results. At the seedling stage, ethylene insensitive Arabidopsis mutants

(*etr1-1* and *ein2-1*) were found to be more susceptible to heat (Larkindale and Knight, 2002; Larkindale *et al.*, 2005), whereas another study on the *ein2-1* mutant showed greater thermotolerance(Clarke *et al.*, 2009). Ethylene, however, is thought to relieve heat stress induced oxidative damage by increasing activity of enzymes involved in scavenging ROS (Wu and Yang, 2019). Therefore, it would have been expected that *TaErs2-B1b* would be more sensitive to heat stress than Cadenza.

Future experiments could focus on the impact of heat stress on the seedling stage of this mutant. Measurements of survival rate and levels of oxidative damage of leaf tissue could be implemented. If these results indicate that the ethylene insensitive seedling is more sensitive to heat treatment, then a further investigation could be the exogenous application of ethylene and application of an ethylene inhibitor on the heat stress response. Another possible experiment is to measure the level of ethylene accumulation in the anthers in response to heat stress. Although we did not measure ethylene accumulation (Chapter 4), there are ways to detect ethylene by means of GC detection, electrochemical sensing and optical detection(Cristescu *et al.*, 2013).

6.5 Conclusion

There was found to be a remarkable degree of homology between the ethylene receptors of wheat, Arabidopsis and rice. This is clear evidence of a similarity in ethylene perception in both monocots and dicots. Certain missense mutations in residues affecting ethylene perception led to an ethylene-insensitive seedling as seen in Arabidopsis, however others did not. This could be due to different amino acid changes having fewer impacts on the functionality of the receptor and also the hexaploidy of Cadenza causing redundancy of function. The ethylene insensitive mutant, *TaErs2-B1b*, was not found to show a lower grain set compared to WT Cadenza and its NS, in both control conditions and in response to heat stress, therefore suggesting that ethylene is not as significant a player in anther development and the heat stress response of anthers. Further studies are required to verify this.

Chapter 7: General Discussion

7.1 Project Summary

Extensive research has been completed on understanding the role of hormones and various signalling components in pollen development in model species, such as Arabidopsis and rice. However, little is known about their role in crop plants such as wheat. It is thought that anther development is a conserved pathway in the angiosperms and therefore findings in model species can be applied to wheat(Gomez *et al.*, 2015). We sought to investigate this using hexaploid wheat var. Cadenza. In addition, we investigated the impact heat stress has on this.

The first aim of this project was to optimise an affective heat stress assay for Cadenza. We confirmed that 33/26°C day/night 80% humidity for 4 days was enough to induce a significant loss of grain set when the heat treatment was induced at meiosis and unicellular stages of pollen development (Chapter 3).

The second aim of this project was to investigate the transcriptional and hormone changes that occur during anther development, and changes that occur in response to heat stress. We found a remarkable stage dependent accumulation of hormones JA, IAA and bioactive CKs towards the later stages of pollen development (Chapter 4). This alludes to the importance of these hormones in controlling pollen development in the later stages. In response to heat stress there was a significant accumulation of JA at unicellular stage. This has been speculated to be attributed to an upregulated expression of wheat orthologues of JA biosynthesis genes *AOC* and *AIM1,* and *JAR1*, an enzyme which converts JA to JA-Ile, in the heat-treated plants at unicellular stage. Overall, the results indicate that the JA pathways appears to play a role in the heat stress response of the anthers.

The third aim of this project was to generate wheat hormone signalling mutants from the TILLING population and characterise their phenotype and sensitivity to heat treatment. The auxin-insensitive Aux/IAA mutants showed reduced grain set and partial male sterility, along with being more sensitive to heat stress than WT Cadenza (Chapter 5). However, the ethylene-insensitive mutant, *TaErs2-B1b*, showed no significant reduction in grain set or heat stress tolerance (Chapter 6).

The final aim was to investigate whether exogenous application of hormones could confer heat stress tolerance. We investigated the application of synthetic auxin, NAA, to heat stressed plants, following on from findings that application of auxin restored grain set and pollen viability in heat stressed rice and barley(Sakata *et al.*, 2010; Sharma *et al.*, 2018). However, we found it failed to recover grain set loss in wheat (Chapter 5). Consequently, further studies are required to understand the role of auxin in the heat stress response of wheat.

7.2 Chemical and genetic approaches to mitigate heat stress

Wheat pollen development is sensitive to high temperatures(Saini *et al.*, 1984; Prasad and Djanaguiraman, 2014; Draeger and Moore, 2017). With global temperatures increasing, a greater understanding of the vulnerability of wheat is necessary in order to take measures to mitigate the negative impact of heat stress on yield. For wheat var. Cadenza, meiosis and unicellular stages of pollen development were found to be the most vulnerable to high temperatures (Figure 3.6). This corresponds to previous studies which found that late meiosis to early microspore stage are the most vulnerable stages to heat stress(Saini *et al.*, 1984; Draeger and Moore, 2017).

Recent advances in wheat genome annotation, the most recent being IWGSC published in July 2018, have now allowed a functional genomics approach to wheat research. The spring wheat variety Cadenza was the chosen hexaploid wheat cultivar used in the development of the TILLING population, along with the tetraploid cultivar Kronos, serving as a vital resource of EMS mutants which we can target with genes of interest(Krasileva *et al.*, 2017). One strategy to combat heat stress is to apply a reverse genetics approach. The RNAseq data of the developing anthers, that this study has provided, is a vital resource for investigating the expression of potentially key genes involved in pollen development and the heat stress response. Transcriptional differences between the control and heat-treated samples allow us to delve into the molecular causes of reduced pollen viability. The shear quantity of differentially expressed genes can prove challenging if we are to find genetic targets. However, when compared in conjunction with the hormone data, this will allow us to target key genes which are responsible for the hormonal

changes observed in the anther and investigate their roles in controlling heat stress tolerance.

In this study we found that in response to heat stress there was a greater accumulation of JA and its bioactive conjugate JA-Ile at the unicellular stage (Table 4.2). This could be attributed to increased expression of JA biosynthesis genes, as well as JAR1 which is involved in converting JA to JA-Ile(Staswick *et al.*, 2002)(Figure 4.15). JA signalling is known to play an important role in promoting anther dehiscence, with Arabidopsis JA biosynthesis mutants showing delayed or abolished dehiscence(McConn and Browse, 1996; Sanders *et al.*, 2000; Stintzi and Browse, 2000; Ishiguro *et al.*, 2001; Park *et al.*, 2002; Von Malek *et al.*, 2002; Caldelari *et al.*, 2011). We hypothesise that the increased accumulation of JA, as a result of heat treatment, leads to premature dehiscence and could be responsible for lack of synchrony between male and female reproductive development as the stamen develops faster than the stigma. Further studies should confirm this.

A genetic strategy is to identify mutants which are defective in JA biosynthesis to see if they are less sensitive to heat stress. One clear target which was flagged up by the RNAseq data is to produce a knockout of the wheat orthologues of the *JAR1* gene, as JA-Ile is the bioactive form of JA. A potential negative consequence of disrupting the JA biosynthesis pathway is the possibly of non-specific impacts, with many of the Arabidopsis JA biosynthesis mutants showing defects in male reproductive development(McConn and Browse, 1996; Sanders *et al.*, 2000; Stintzi and Browse, 2000; Ishiguro *et al.*, 2001; Park *et al.*, 2002; Von Malek *et al.*, 2002; Caldelari *et al.*, 2011). Consequently, more specific downstream JA signalling components could be targeted. One downstream signalling component is the transcription factor MYB108. MYB108 is a JA-inducible transcription factor (Figure 7.1). MYB108 expression was linked to the upstream transcription factor MYB21. The *myb108* mutant was found to show delayed dehiscence. MYB108 is thought to interact with MYB24 to promote dehiscence, pollen viability and filament elongation (Mandaokar and Browse, 2009). Producing a triple homoeologue knockout of just the *MYB108* mutant in wheat could be an agronomically beneficial trait in preparation for heat stress induces loss of grain set, however the

Arabidopsis mutant did have the downside of showing a lower grain set compared to WT(Mandaokar and Browse, 2009).

Another alternative target is the promoter of *MYB108*. ARF17 is a transcription factor which was found to directly bind to the promoter of *MYB108* and induce its expression, with the *arf17* mutant showing dramatic down-regulation of *MYB108* expression(Xu *et al.*, 2019). ARF17 is thought to bind to the auxin responsive motif (TGTCTC/ GAGACA). As *MYB108* contains the sequence TGTCTC in its promoter, it is likely that it promotes its expression via this (Figure 7.1)(Yang *et al.*, 2013). By deliberately removing the auxin responsive motif from the promoter, either through TILLING or through Crispr/CAS, this could create a mutant which is more resistant to heat stress, but not so extreme that it compromises male fertility. There is known to be a complex interplay between both the auxin and JA signalling pathway, with auxin being found to repress the expression of *OPR3* and *DAD1* JA biosynthesis genes, thus resulting in reduced accumulation of JA (Figure 7.1) (Cecchetti *et al.*, 2013).

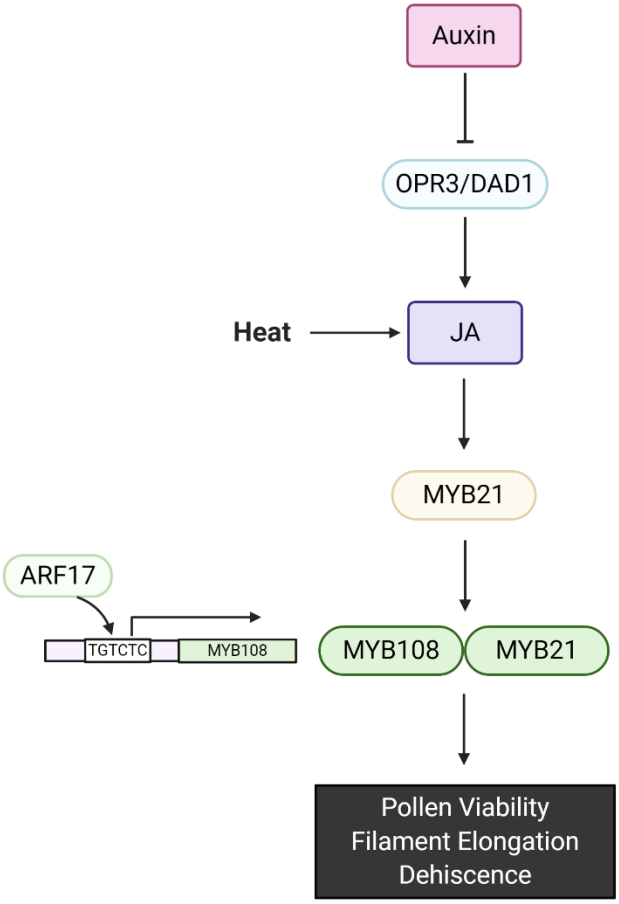

Figure 7.1: *The interaction between JA and auxin signalling in male reproductive development.*

Heat stress was found to induce accumulation of Jasmonic Acid (JA) and Jasmonoyl-Isoleucine (JA-Ile) in the wheat anther. Transcription factors MYB21, MYB24 and MYB108 act downstream of JA to regulate male reproductive development. Auxin appears to regulate the JA pathway in two main ways. It inhibits the expression of OPR3 and DAD1, which are JA biosynthesis genes. It also targets the downstream component of MYB108, by promoting its expression via transcription factor ARF17. Created with BioRender.com.

An alternative approach to enhancing heat stress tolerance is through the chemical application of phytohormones. Exogenous application of IAA/NAA was found to recover grain set and pollen viability in barley and rice(Sakata *et al.*, 2010; Sharma *et al.*, 2018). Auxin is known to slow down dehiscence, by antagonising JA signalling(Cecchetti *et al.*, 2008, 2013). We conclude that the antagonistic nature of IAA/NAA to JA signalling maybe the reason for the rescued pollen viability.

However, in wheat we found that application of NAA did not recover grain set after heat stress, but we found that it did indeed slow down the rate of anther development by around one day (Table 5.8). The loss of grain set as a result of heat stress could also be due to lack of coordination between male and female reproductive development caused by heat stress. The exogenous application of auxin clearly slows down the rate of development, but in this case possibly not enough to match female reproduction. Furthermore, auxin could be inhibiting tapetal breakdown. Premature degradation of the tapetum has been linked to vulnerability to heat stress(Saini *et al.*, 1984; Abiko *et al.*, 2005; Feng *et al.*, 2018). This warrants further investigation into the role of auxin in regulating the timing of pollen development and tapetal PCD in wheat. Future studies could aim to optimise the auxin spray assay for wheat, by completing a dose response experiment of NAA and possibly applying it at different pollen developmental stages.

With global temperatures set to increase, it is vital that further study should focus on finding ways to mitigate the yield losses as a result of heat stress in wheat. This study has provided evidence of the hormonal and genetic changes which are occurring in the anther across normal development and in response to high temperatures.

7.3 The role of hormones in wheat development

In this study we used the reverse genetics approach of TILLING to identify mutants which are defective in auxin and ethylene perception. The phenotype of these mutants is a useful way of investigating which parts of wheat development are affected and therefore inferring the role auxin and ethylene have to play in these processes.

Auxin

The auxin-insensitive Aux/IAA wheat mutants showed reduced grain set and pollen viability (Figure 5.13), as was previously found in Arabidopsis (Yang *et al.*, 2004; Uehara *et al.*, 2008; Rinaldi *et al.*, 2012). This highlights the important role of auxin in ensuring successful pollen development in wheat. Future experiments could investigate the rate of anther development of these mutants. Longitudinal anther

cross sections could be taken to investigate at what stage anther/pollen development is being disrupted and therefore determining what is causing the loss of pollen viability. Auxin is thought to be involved in preventing premature anther dehiscence and pollen maturation(Cecchetti *et al.*, 2008, 2013). Therefore, we would expect the mutants to show accelerated anther development.

The wheat auxin-insensitive mutants *TaIaa22-Bc*, *TaIaa22-Db* and *TaIaa34-Ab* showed greater vulnerability to heat stress based on grain count data (Figure 5.15), therefore indicating that auxin is involved in the heat stress response. There was evidence of reduced pollen number and viability in the auxin-insensitive mutants in response to heat (Table 5.7), however it is likely other factors are also at play. Although not an agronomically useful trait it clearly indicates the importance of auxin in the heat stress response in wheat, therefore confirming the importance of developing sprays which promote auxin signalling to combat heat stress induced loss of yield.

Wheat auxin-insensitive mutants also showed defects in root hair development (Figure 5.9) and lateral root development in both the seminal (Table 5.3/5.4; Figure 5.5) and nodal roots (Table 5.5). The lack of laterals is due to the failure to produce lateral root primordia (Figure 5.6). These root phenotypes are not generally agronomically desirable. The findings indicate the importance of auxin in determining wheat root architecture, as well as male reproductive development.

Promoting the auxin signalling pathway could lead to shallower and denser root networks in wheat which could be beneficial to yield in some types of soil and climate. Shorter roots with numerous laterals have been found to be adventitious in low phosphorus conditions, compared to longer roots with fewer laterals in maize (Zhu and Lynch, 2004; Jia *et al.*, 2018). Root hairs have also been found to be important for water and phosphorus uptake(Miguel *et al.*, 2015; Carminati *et al.*, 2017). Essentially this strategy increases topsoil foraging capabilities, which also has the additional benefit of reducing the metabolic cost of growing deeper roots(Lynch, 2019).

<u>Ethylene</u>

A total of 5 mutants in conserved residues of the transmembrane domain of the ethylene-receptor were identified from the TILLING population. None of the mutants showed a significant difference in grain set when grown in GH conditions (Table 6.3), therefore it can be assumed that there is no difference in male and female reproductive development. This was not unexpected, as male sterility was not described in other studies on ethylene-receptor mutants in Arabidopsis (Sakai *et al.*, 1998; Alonso *et al.*, 1999; Hall *et al.*, 1999; Gamble *et al.*, 2002; Wang *et al.*, 2006; Deslauriers *et al.*, 2015).

Ethylene-sensitivity screens using ethylene gas found that only *TaErs2-B1b* showed ethylene-insensitivity in its shoot. However, none of the mutants, including WT Cadenza, showed ethylene-insensitivity in the root (Figure 6.10). Future studies should repeat these experiments, particularly focusing on the root elongation. We hypothesise that no clear phenotype was observed because the blue-roll columns were potentially too over saturated with water therefore preventing the gaseous ethylene from reaching the roots.

When investigating the heat stress tolerance of the ethylene-insensitive mutant, *TaErs2-B1b*, there was not found to be a greater sensitivity to heat stress in terms of grain set loss (Table 6.4). It would have been expected that these mutants would show a greater sensitivity to heat treatment, following evidence from tomato that ethylene insensitive mutants showed a greater loss of pollen production and viability (Firon *et al.*, 2012). Further investigation into heat stress sensitivity should be ensured using different mutants of different components of the ethylene signalling pathway. Additionally, the application of the ethylene releasing agent, ethephon could be used to investigate the role of ethylene in heat stress tolerance further.

Other hormones

In addition to the described mutants, wheat JA and GA signalling mutants were also investigated. The phenotypes of these mutants were not described in this thesis as they either showed no obvious phenotype or had mostly already been characterised previously.

We sought to produce gain-of-function JA insensitive mutants by targeting the JAZ family of repressors. JA targets the JAZ proteins for degradation via the SCF^{COI1} E3 ubiquitin ligase complex which ubiquitinates the proteins and targets them for degradation by the 26S proteasome (Thines *et al.*, 2007; Chung and Howe, 2009). Certain splice site mutations in the Jas-motif of *JAZ* genes produce JAZ proteins which cannot be targeted for degradation in the presence of JA and consequently continue to repress JA signalling(Chung and Howe, 2009; Chung *et al.*, 2010). In Arabidopsis this has resulted in male sterile mutants due to defects in filament elongation and anther dehiscence(Chung and Howe, 2009). The TILLING population was investigated for analogous mutants in the *JAZ* genes of wheat. Three mutants were found in three homoeologues (TraesCS5A02G204900, TraesCS5B02G203400 and TraesCS2D02G507200). These were brought forward and backcrossed twice to Cadenza. Characterisation of grain set showed no reduction compared to WT Cadenza and the NS. Furthermore, root elongation assays using MeJA showed that non-of the mutants were JA-insensitive in the roots. Consequently, these mutants were not brought forward for further investigation.

GA signalling mutants have been successfully produced in wheat var. Cadenza. Triple knockout mutants in all three of the *GAMYB* homoeologues have been produced by stacking nonsense mutants from separate TILLING lines of Cadenza. This resultant triple mutant (*Tagamyb*) had been determined to be almost completely sterile, showing very low grain set and anthers with failed tapetal PCD (Audley, 2016). This same phenotype was observed in the rice *Osgamyb* mutant(Aya *et al.*, 2009). *Tagamyb* passed onto me by Matt Audley and I conducted two further backcrosses to WT Cadenza in order remove 75% of EMS background mutations. The backcrossed mutant remained sterile, with only a few florets producing grain (possibly the result of outcrossing). A general phenotyping experiment was conducted measuring tiller number, final internode length and grain set of *GAMYB* triple, double and single mutants, along with the NS and WT Cadenza. The findings showed no significant difference in tiller number and final internode length between all the different genotypes. Only the triple mutant showed a significantly

reduced grain set. However, this experiment was severely impacted by an aphid infestation, making interpretation of these results dubious.

7.4 Further applications of our findings

This study has highlighted the valuable resource of the TILLING population as a source of genetic diversity. The benefit of using these EMS induced mutants is that they are not under any regulation and mutants showing agronomically useful traits can become part of the UK breeders' toolkit. The breeders' toolkit is a source of new pre-breeding germplasm which can be crossed into developing varieties of wheat (https://designingfuturewheat.org.uk/breeders-toolkit/). Therefore, future studies should delve more deeply into the TILLING population to uncover traits which could be of potential agronomic benefit. The downside of using TILLING mutants is that it takes a number of backcrosses to remove other unrelated EMS mutations. An alternative approach is gene editing, which would be faster, however as it stands gene edited crops are currently not allowed to be grown commercially in the UK or the EU. If the current regulations were to change, TILLING mutants can inform genetic targets for gene editing.

This study has shown that it is possible to produce gain-of-function dominant mutants in wheat which show a strong phenotype, despite *Triticum aestivum* being hexaploid. Therefore, we are moving away from a time when wheat was considered a difficult plant to work with, owing to the diversity of new resources available. Whereas before in wheat research we relied on QTLs, we can now work on a gene specific level. Using molecular studies of other species, we can now quickly identify orthologous genes and mutants in wheat in the hope to develop equivalent phenotypes which could lead to agronomically useful traits. Examples of agronomically beneficial traits which our mutants could possess are described below:

<u>Stay-Green Trait</u>

An area of agronomic interest is the stay-green trait. A stay-green phenotype is when there is a delayed senescence of the plant foliage after anthesis. In certain conditions this conveys a positive trait in crops as it leads to greater biomass

production. This trait has been particularly sought after in wheat, as it has been found to improve yield following drought conditions after flowering(Christopher *et al.*, 2016).

The stay-green phenotype can be linked to ethylene accumulation, with ethylene promoting earlier senescence. The Arabidopsis *acs* mutant which is defective in ethylene biosynthesis shows a stay green phenotype(Tsuchisaka *et al.*, 2009). The Arabidopsis ethylene-receptor mutant, *etr1-1*, which is analogous to our ethylene receptor mutants, also shows a stay-green phenotype (Grbic and Bleecker, 1995). Consequently, future studies should investigate the senescence of the ethylene-receptor mutants in this study. The ethylene-receptor mutants have the advantage of being gain-of-function ethylene-insensitive mutants, whereby only one homoeologue needs to carry the mutant allele. Therefore, if determined to be agronomically useful, they can quickly be crossed into elite varieties without the need to stack mutant homologous with each cross, as what would be required for loss-of-function mutants.

Increasing soil penetration of roots

Soil compaction is of increased agronomic interest as it is a problem in many of the world's agricultural soils. It is caused by poor farming management processes such as overgrazing, increased use of heavy machinery and short crop rotations. High levels of compaction have been found to restrict root growth by reducing root penetration into the deeper soil layers. This consequently leads to reduced access to water and nutrients, resulting in reduced yields (Hamza and Anderson, 2005; Correa *et al.*, 2019).

Enhanced ethylene accumulation has been found to occur in roots which are mechanically impeded, as what happens in compacted soil(Kays *et al.*, 1974; Sarquis *et al.*, 1991; He *et al.*, 1996). This is thought to be due to reduced ethylene diffusion away from the root, as a result of a reduction in soil pore space in compacted soil (Pandey *et al.*, 2021). Evidence in rice has shown that two rice mutants which are ethylene-insensitive (*osein2* and *oseil1*) resulted in increased penetration of the roots in compacted soil(Pandey *et al.*, 2021). This enhanced soil penetration trait

could be agronomically beneficial in compacted soils, as the roots continue to grow to access water and nutrients. The soil penetration phenotype of our ethylene-insensitive mutants could also be determined. Ones which are determined to be ethylene-insensitive in their roots can then be brought forward for soil penetration studies.

Hybrid wheat

Wheat hormone signalling mutants could be of interest for hybrid wheat production. Hybrid breeding involves crossing two genetically different parents in order to induce heterosis (hybrid vigour). In wheat this was found to increase yields by 3-15%(Longin *et al.*, 2012). However, only 0.2-0.3% of wheat was produced as a result of hybrid breeding, as opposed to 17-20% of rice as of 2012(Longin *et al.*, 2012). Wheat is a highly inbred selfing plant and therefore in order to ensure more efficient hybrid breeding there must be changes to floral architecture to force outcrossing(Whitford *et al.*, 2013). This could be through inducing male sterility, thus creating an effective female parent. It could also be through creating an effective donor male which shows high levels of anther extrusion and dehiscence.

Four of our auxin-insensitive mutants showed partial sterility (*TaIaa18-Bb, TaIaa22-Bb, TaIaa22-Bc* and *TaIaa22-Db*) specifically towards the tip of the spike. This could make them a good candidate for the female parent, as it also has the advantage of being a dominant trait. However, they all lacked complete sterility, which would be preferable.

Delving more deeply into the RNAseq data, many orthologous genes of key regulators of anther and pollen development were found to be highly expressed in the anther in wheat (Figure 4.22). Wheat clearly has a similar molecular pathway controlling male reproductive development as other flowering plants. Therefore, these orthologous genes could also be targeted as another means to induce male sterility for hybrid wheat production. Additionally, as JA, ethylene and GA are involved in promoting anther dehiscence and filament elongation (Section 1.5), future studies could find genetic ways to promote these signalling pathways to produce plants which are more effective pollen donors.

The genetic, hormone and physiological findings of this study have provided evidence for the role of plant hormones in controlling male reproductive development in wheat. Future studies should apply this resource, along with others, to generate an array of TILLING and Crispr/CAS mutants to help paint a more detailed picture of the molecular pathways and hormones involved in the development of wheat.

Appendix: Supplementary Data

Selected Tiller	Position on ear		
	Bottom	Middle	Top
	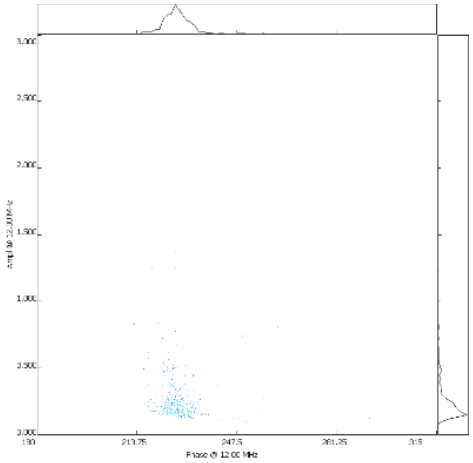	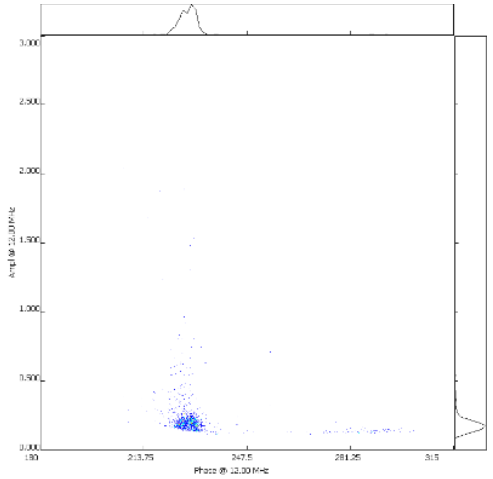	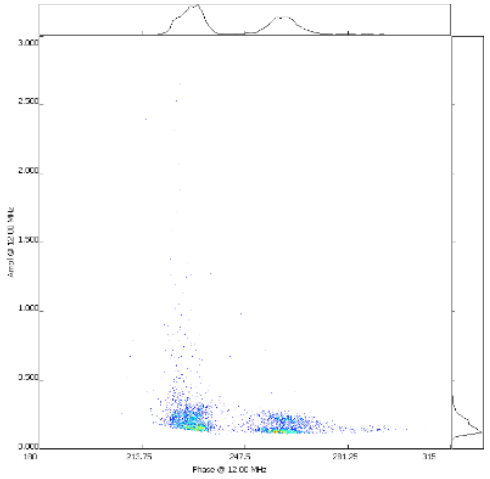

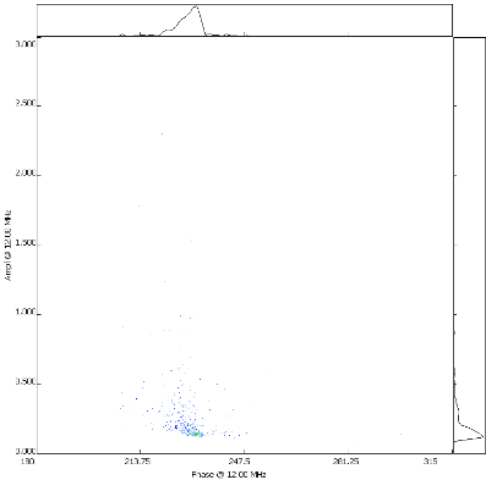

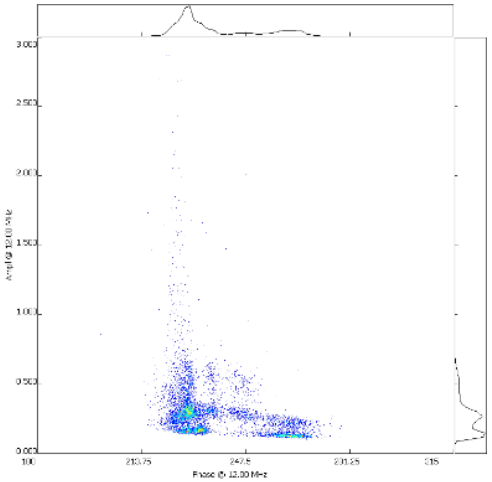

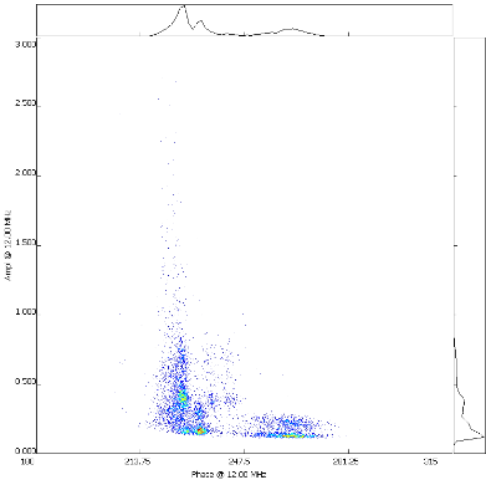

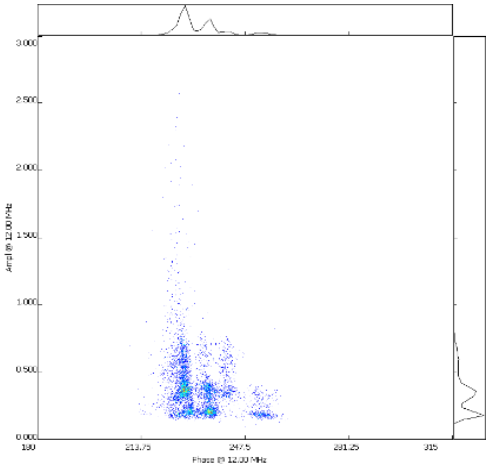

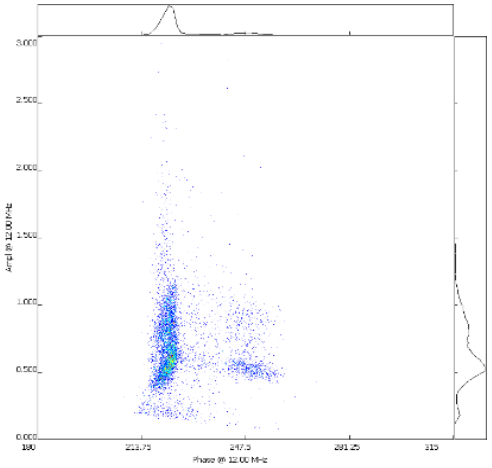

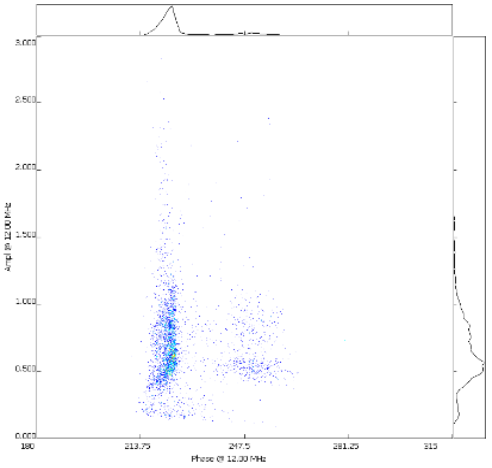

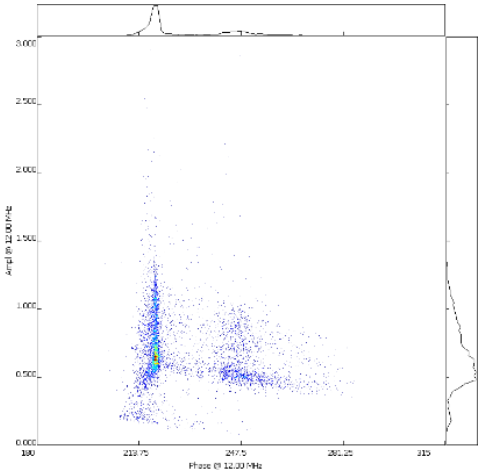

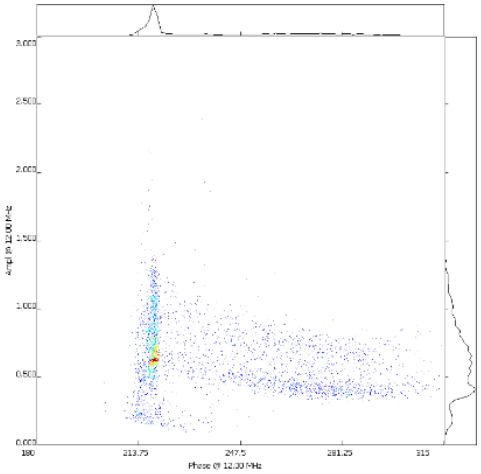

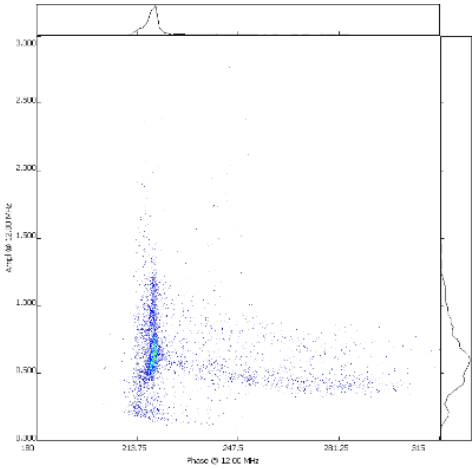

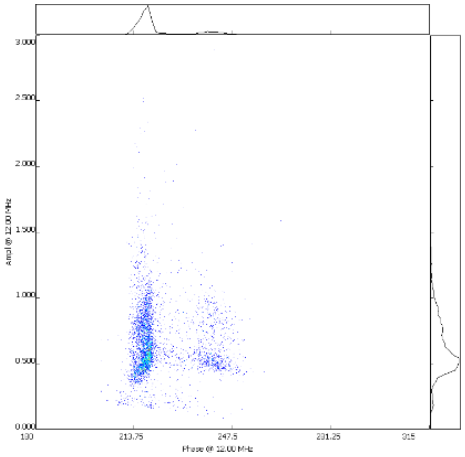

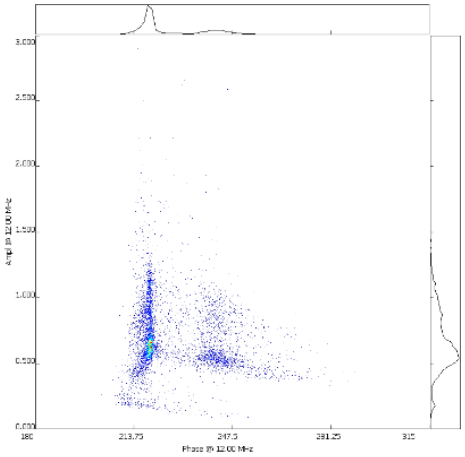

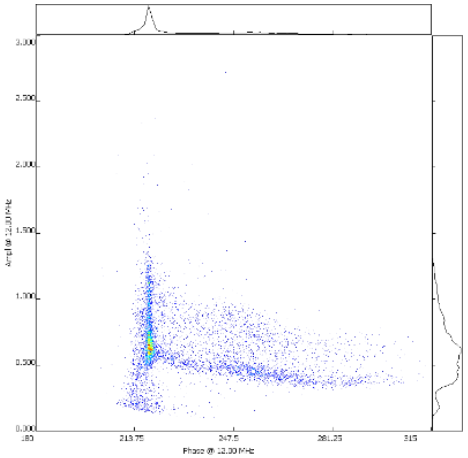

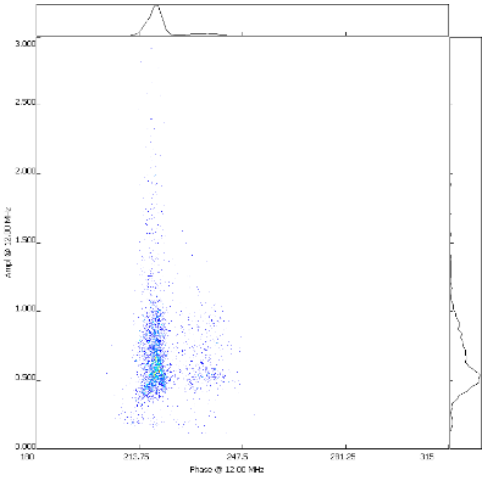

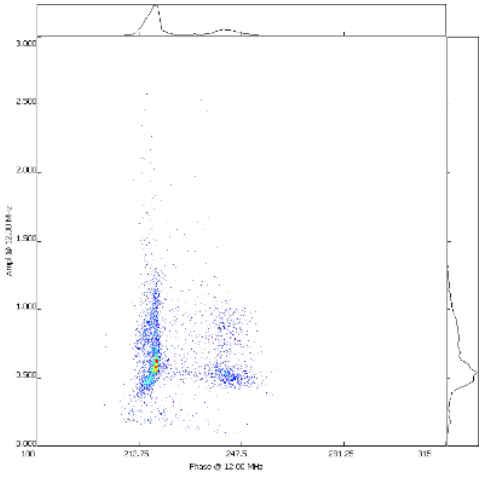

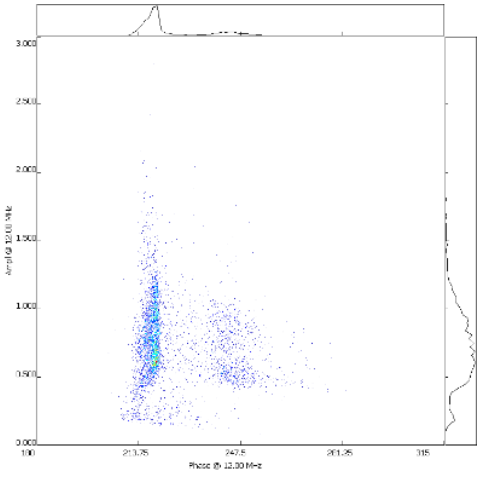

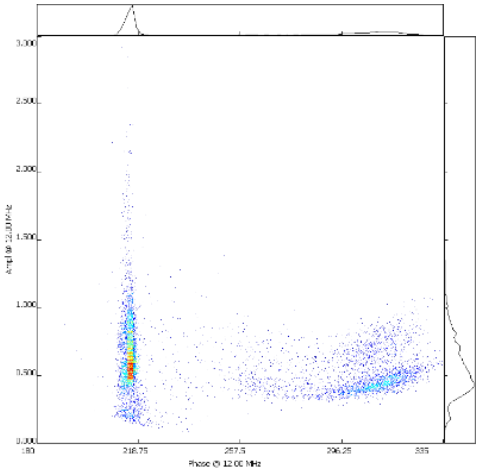

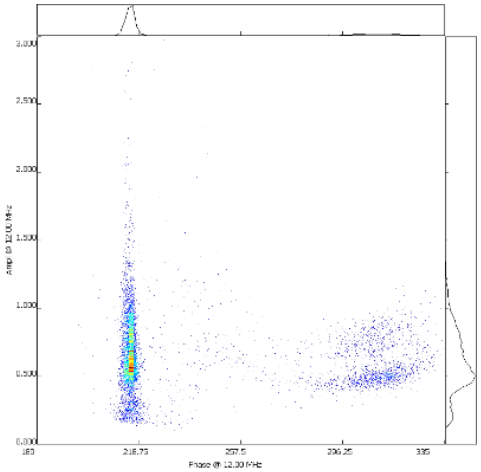

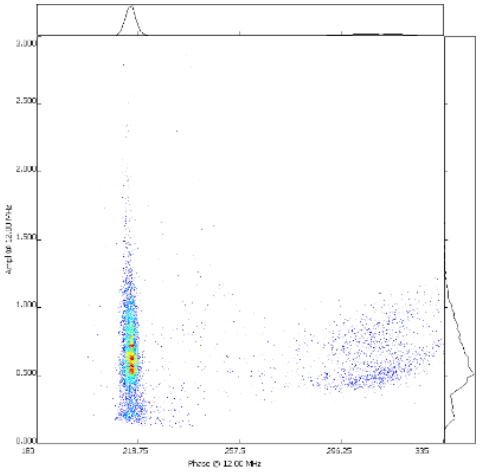

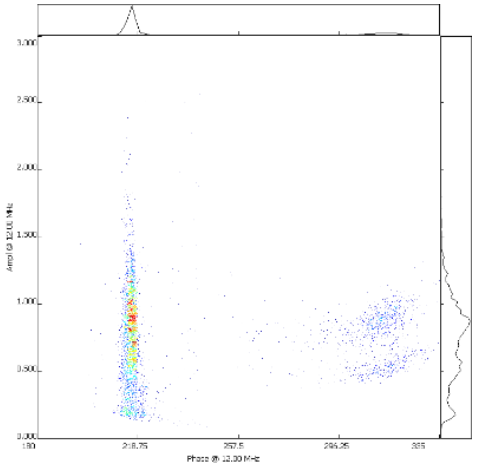

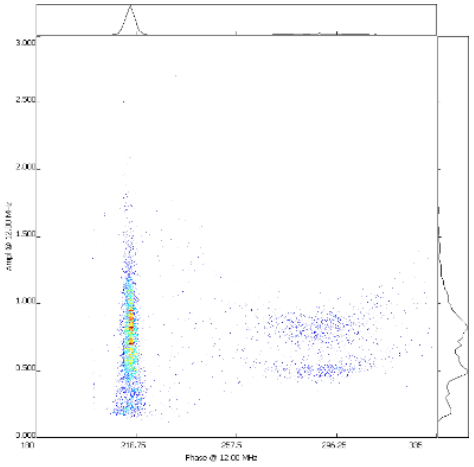

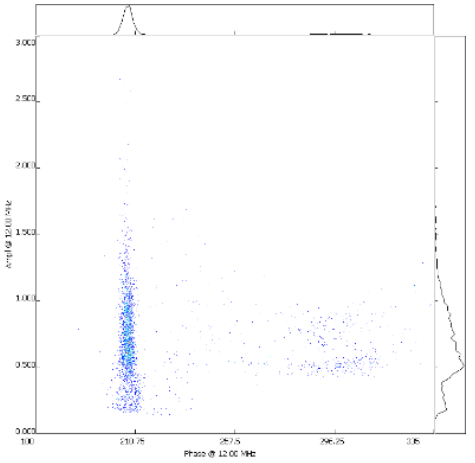

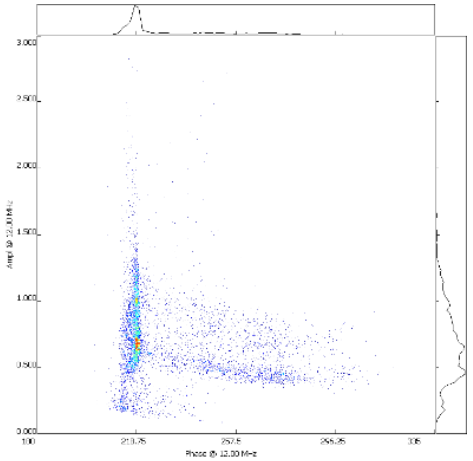

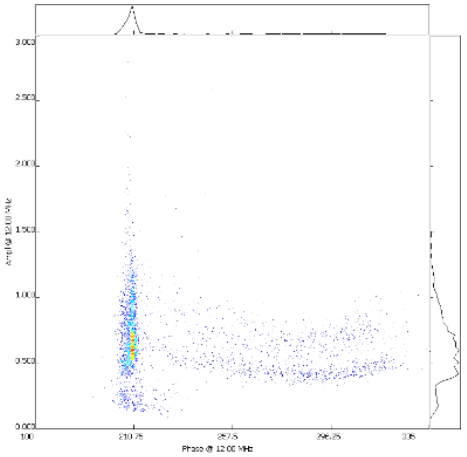

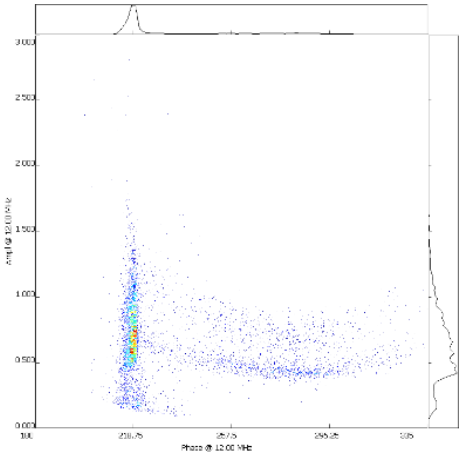

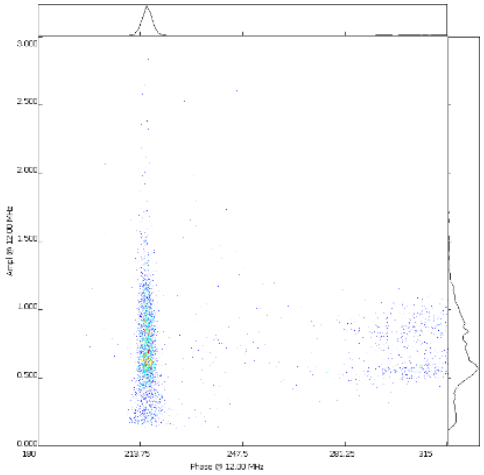

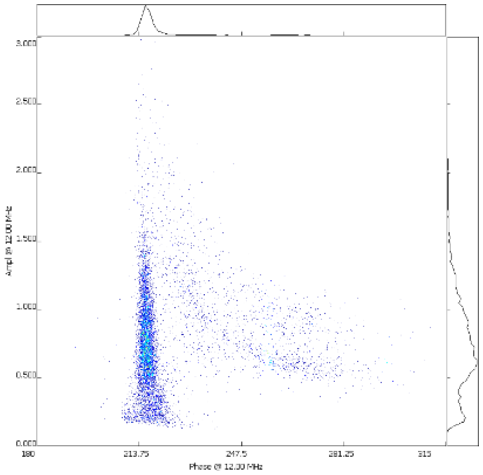

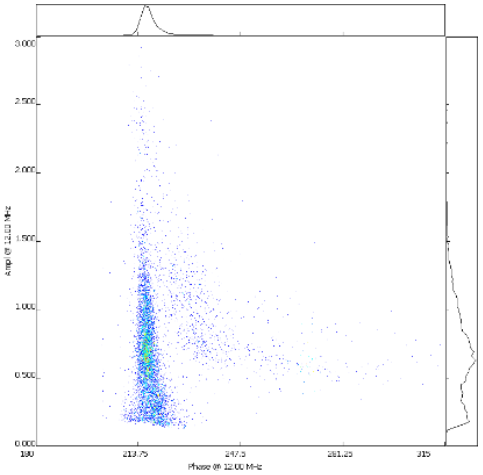

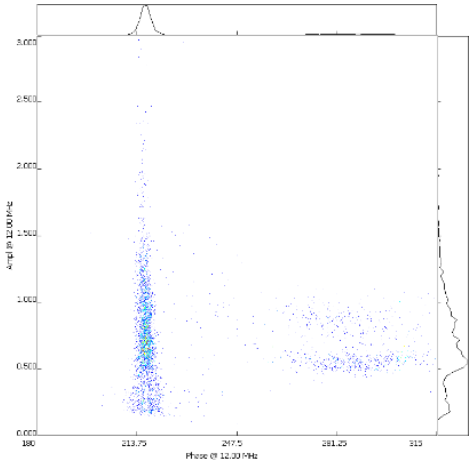

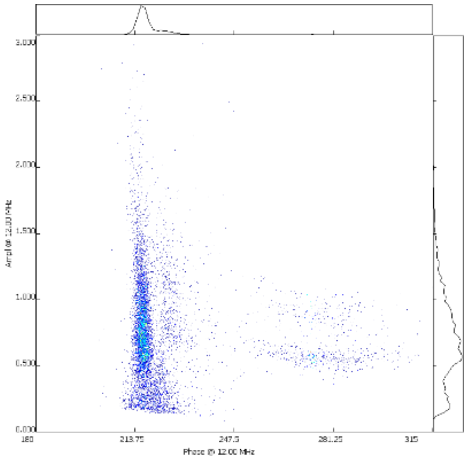

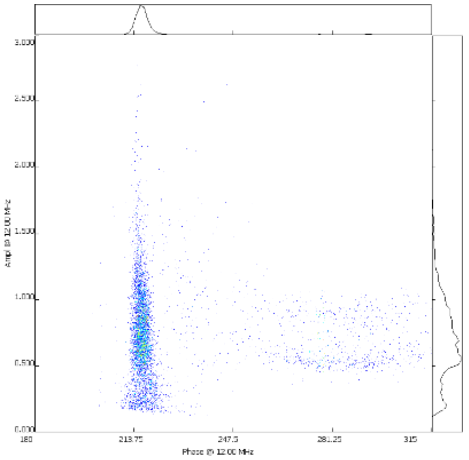

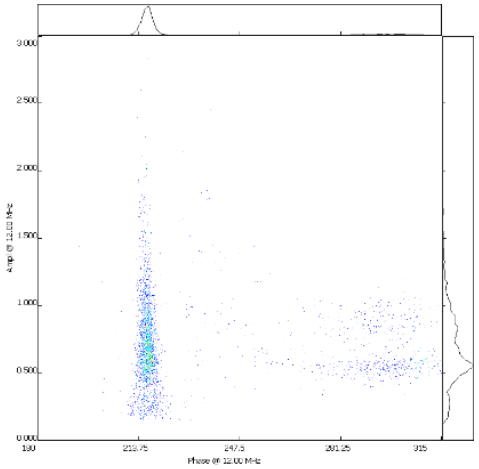

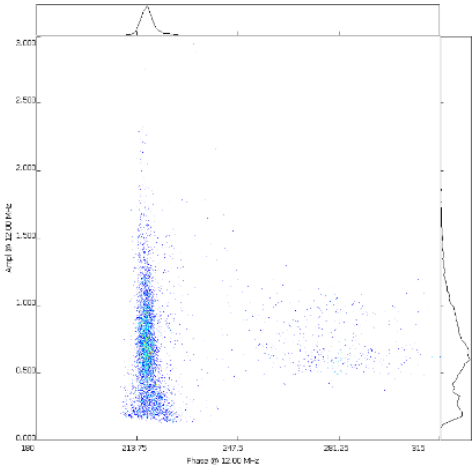

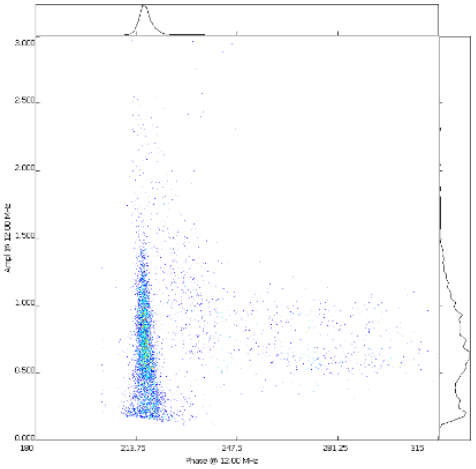

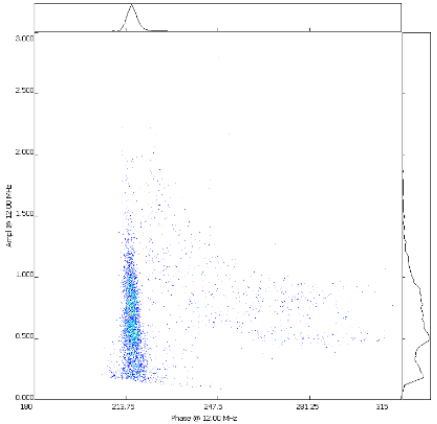

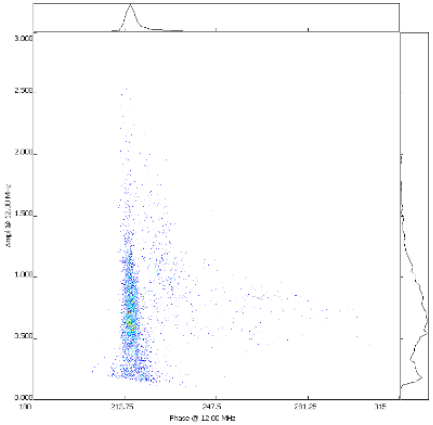

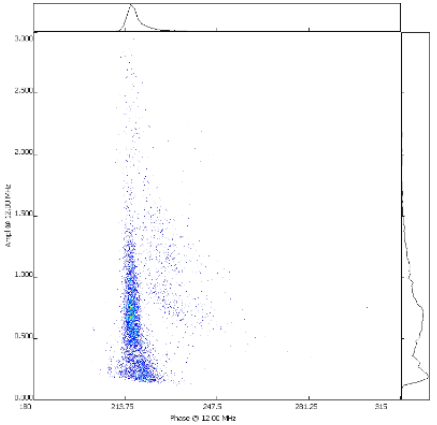

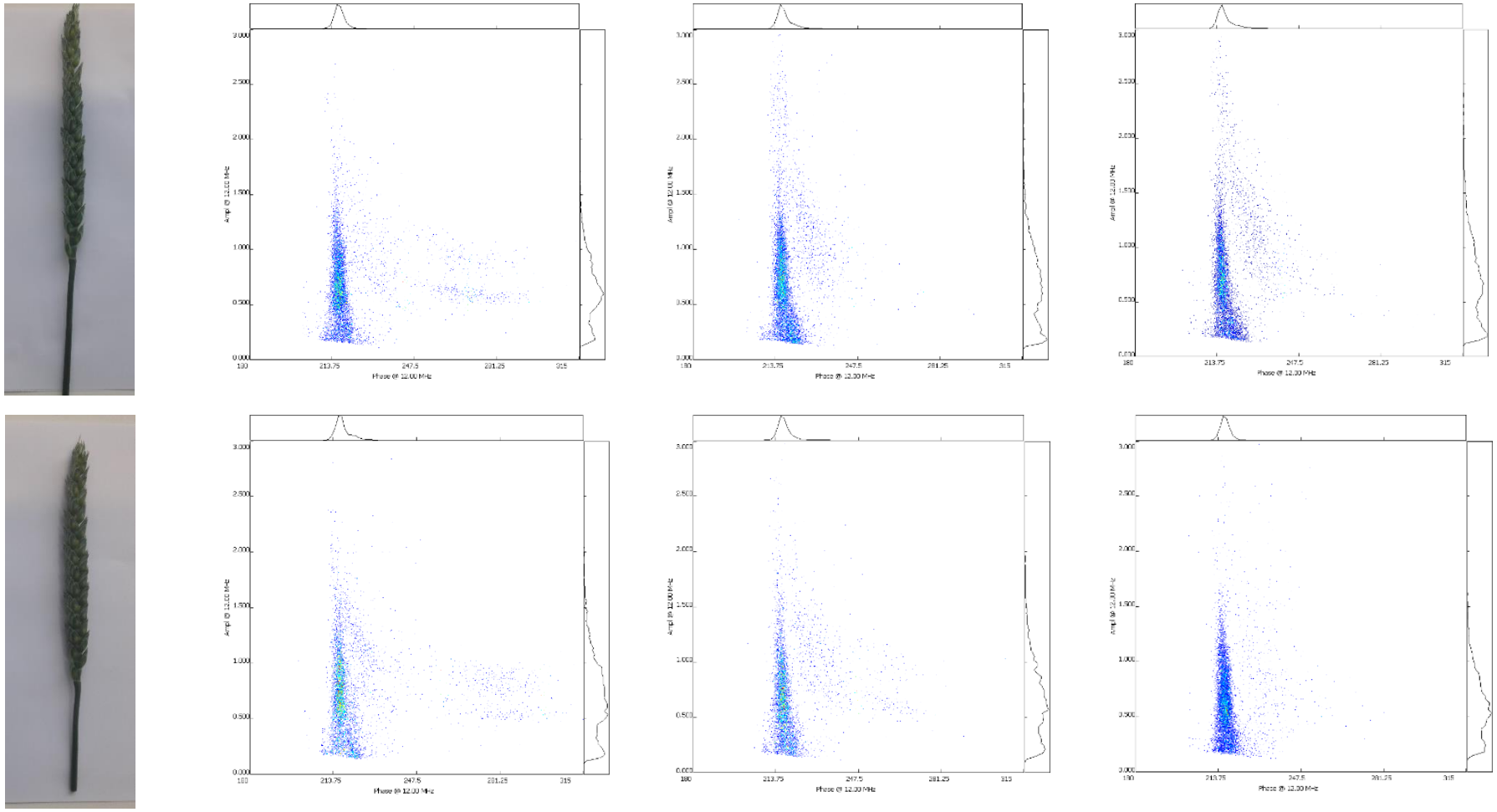

Supplementary Figure 1: *Flow cytometer results of anthers harvested from different positions of spikes at different stages of spike emergence.*

12Mhz triggering frequency was used for determining pollen stage.

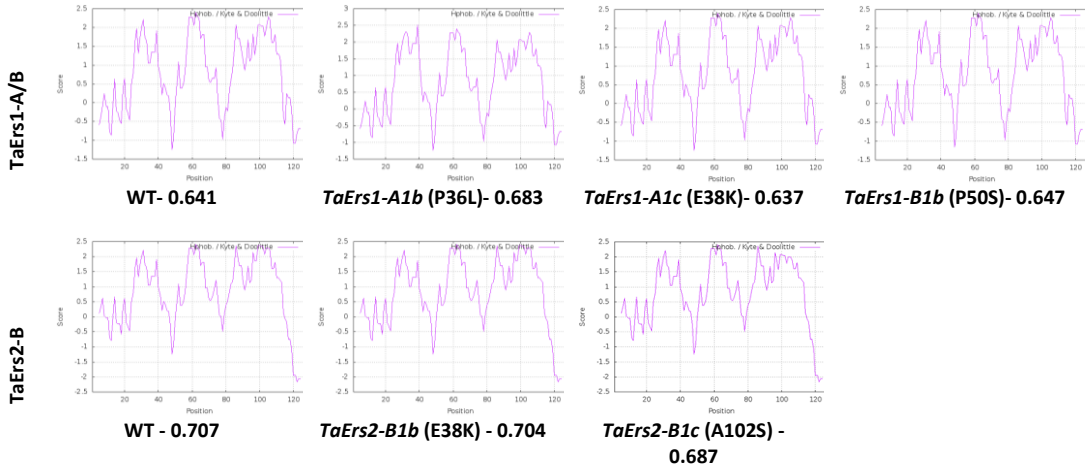

Supplementary Figure 2: *Hydropathicity of the transmembrane domain of wheat ethylene receptors and the effect of missense mutations.*

Hydropathicity is shown across the length of the transmembrane domain and the grand average of hydropathy. Calculated using online resource ProtParam (https://web.expasy.org/protparam/).

Supplementary Table 1: *REML output of logit+1 transformed values of percentage grain set according to different heat treatments at different stages of pollen development.*

Treatment	Pre-meiosis		Meiosis		Unicellular		Bicellular		Tricellular	
	Control	Heat	Control	Heat	Control	Heat	Control	Heat	Control	Heat
32/20	1.329	1.1535	1.3458	1.0044	1.2308	0.9927	1.2673	1.0607	1.3274	1.088
32/26	1.1236	0.2999	1.0262	0.4431	1.1766	0.9105	1.3164	1.159	1.3411	1.0482
33/26	1.336	0.6247	1.3941	0.2337[1]	1.0008	-0.7836[2]	1.1825	1.1499	1.2218	1.0599
35/26	1.3965	0.2449[3]	1.1541	-0.2214[4]	1.3182	-0.7508[5]	1.397	-0.2016[6]	1.3638	-0.2762[7]

5% LSD=[1]1.149, [2]1.043, [3]1.060, [4]1.063, [5]1.023, [6]1.023, [7]1.018
No significant difference between the control treatments. Average SED = 0.7132

Supplementary Table 2: *Orthologous components of hormone biosynthesis and signalling pathways of rice*(Hirano *et al.*, 2008) *and wheat.*

Rice gene name(Hirano *et al.*, 2008)	**Rice gene stable ID**	***Triticum aestivum* gene stable ID**
	Auxin	
OsASA1	*Os03g0826500*	*TraesCS5B02G502700*
OsASA1	*Os03g0826500*	*TraesCS5D02G503800*
OsASA2	*Os03g0264400*	*TraesCS4B02G214500*
OsASA2	*Os03g0264400*	*TraesCS4D02G215100*
OsASA2	*Os03g0264400*	*TraesCS4A02G089800*
OsASB1	*Os04g0463500*	*TraesCS2D02G326400*
OsASB1	*Os04g0463500*	*TraesCS3A02G041400*
OsASB1	*Os04g0463500*	*TraesCS2B02G345400*
OsASB1	*Os04g0463500*	*TraesCS3D02G038900*
OsASB1	*Os04g0463500*	*TraesCS3B02G042300*
OsASB1	*Os04g0463500*	*TraesCS2A02G336500*
OsTAA1;1	*Os01g0169800*	*TraesCS1B02G249600*
OsTAA1;1	*Os01g0169800*	*TraesCS1A02G233800*
OsTAA1;1	*Os01g0169800*	*TraesCS3A02G093000*
OsTAA1;1	*Os01g0169800*	*TraesCS3D02G093300*
OsTAA1;1	*Os01g0169800*	*TraesCS3B02G108200*
OsTAA1;1	*Os01g0169800*	*TraesCS1D02G238100*
OsTAA1;2/3	*Os01g0717400/Os01g0717700*	*TraesCS3B02G275200*
OsTAA1;2/3	*Os01g0717400/Os01g0717700*	*TraesCS3D02G246700*
OsTAA1;2/3	*Os01g0717400/Os01g0717700*	*TraesCS3A02G244700*
OsTAA1;4	*Os05g0169300*	*TraesCS1A02G113400*
OsTAA1;4	*Os05g0169300*	*TraesCS1B02G133500*
OsTAA1;4	*Os05g0169300*	*TraesCS1D02G114800*
OsAAO1/2	*Os10g0138100/Os03g0790900*	*TraesCS5B02G429800*
OsAAO1/2	*Os10g0138100/Os03g0790900*	*TraesCS5D02G435800*
OsAAO1/2	*Os10g0138100/Os03g0790900*	*TraesCS5A02G427800*
OsAAO1/2	*Os10g0138100/Os03g0790900*	*TraesCS5D02G436000*
OsAAO1/2	*Os10g0138100/Os03g0790900*	*TraesCS5D02G435900*
OsAAO1/2	*Os10g0138100/Os03g0790900*	*TraesCS5D02G435700*
OsAAO1/2	*Os10g0138100/Os03g0790900*	*TraesCS5B02G429600*
OsAAO1/2	*Os10g0138100/Os03g0790900*	*TraesCS5B02G429700*
OsAAO1/2	*Os10g0138100/Os03g0790900*	*TraesCS5B02G429900*
OsAAO1/2	*Os10g0138100/Os03g0790900*	*TraesCS5D02G436200*
OsAAO1/2	*Os10g0138100/Os03g0790900*	*TraesCS5A02G427900*
OsAAO1/2	*Os10g0138100/Os03g0790900*	*TraesCS5A02G427700*
OsAAO1/2	*Os10g0138100/Os03g0790900*	*TraesCS5A02G427600*
OsAAO1/2	*Os10g0138100/Os03g0790900*	*TraesCS5B02G430100*
OsAAO1/2	*Os10g0138100/Os03g0790900*	*TraesCS5A02G428200*
OsAAO1/2	*Os10g0138100/Os03g0790900*	*TraesCS5A02G428000*
OsAAO3	*Os07g0281700*	*TraesCS7A02G509300*
OsAAO3	*Os07g0281700*	*TraesCS7D02G498000*
OsNIT1	*Os02g0635200*	*TraesCS6A02G232300*
OsNIT1	*Os02g0635200*	*TraesCS6B02G260700*
OsNIT1	*Os02g0635200*	*TraesCS6D02G215400*
OsNIT1	*Os02g0635200*	*TraesCS6A02G232500*
OsNIT1	*Os02g0635200*	*TraesCS6B02G261000*
OsNIT2	*Os02g0635000*	*TraesCS6D02G215300*
OsNIT2	*Os02g0635000*	*TraesCS6A02G232400*
OsNIT2	*Os02g0635000*	*TraesCS6B02G260800*
OsYUCCA1	*Os01g0645400*	*TraesCS3D02G220500*
OsYUCCA1	*Os01g0645400*	*TraesCS3A02G232600*
OsYUCCA1	*Os01g0645400*	*TraesCS3B02G261900*
OsYUCCA4	*Os01g0224700*	*TraesCS3A02G149500*

OsYUCCA4	*Os01g0224700*	*TraesCS3B02G176800*
OsYUCCA4	*Os01g0224700*	*TraesCS3D02G157600*
OsYUCCA5	*Os12g0512000*	*TraesCS5D02G114500*
OsYUCCA5	*Os12g0512000*	*TraesCS5A02G102700*
OsYUCCA5	*Os12g0512000*	*TraesCS5B02G107000*
OsYUCCA6	*Os07g0437000*	*TraesCS4A02G313200*
OsYUCCA6	*Os07g0437000*	*TraesCS5B02G566700*
OsYUCCA7	*Os04g0128900*	*TraesCS7D02G038500*
OsYUCCA7	*Os04g0128900*	*TraesCS2B02G010100*
OsYUCCA7	*Os04g0128900*	*TraesCS2D02G012100*
OsYUCCA7	*Os04g0128900*	*TraesCS2A02G011500*
OsYUCCA7	*Os04g0128900*	*TraesCSU02G065000*
OsYUCCA7	*Os04g0128900*	*TraesCS2B02G562800*
OsYUCCA7	*Os04g0128900*	*TraesCS2A02G533200*
OsYUCCA7	*Os04g0128900*	*TraesCS2D02G535100*
COW1	*Os03g0162000*	*TraesCS4B02G278300*
COW1	*Os03g0162000*	*TraesCS4D02G276600*
COW1	*Os03g0162000*	*TraesCS4A02G027500*
OsTIR1;1	*Os05g0150500*	*TraesCS1D02G099900*
OsTIR1;1	*Os05g0150500*	*TraesCS1B02G119100*
OsTIR1;1	*Os05g0150500*	*TraesCS1A02G091300*
OsTIR1;2	*Os02g0759700*	*TraesCS6B02G345800*
OsTIR1;2	*Os02g0759700*	*TraesCS6D02G294600*
OsTIR1;2	*Os02g0759700*	*TraesCS6A02G315300*
OsTIR1;3	*Os04g0395600*	*TraesCS2A02G286200*
OsTIR1;3	*Os04g0395600*	*TraesCS2B02G302900*
OsTIR1;3	*Os04g0395600*	*TraesCS2D02G285000*
OsTIR1;5	*Os11g0515500*	*TraesCS5D02G288000*
OsTIR1;5	*Os11g0515500*	*TraesCS5B02G280100*
OsTIR1;5	*Os11g0515500*	*TraesCS5A02G281100*
OsIAA1	*Os01g0178500*	*TraesCS3A02G121300*
OsIAA1	*Os01g0178500*	*TraesCS3B02G140700*
OsIAA1	*Os01g0178500*	*TraesCS3D02G123400*
OsIAA2	*Os01g0190300*	*TraesCS3B02G127400*
OsIAA2	*Os01g0190300*	*TraesCS3D02G110200*
OsIAA2	*Os01g0190300*	*TraesCS3A02G108400*
OsIAA3	*Os01g0231000*	*TraesCS3B02G181500*
OsIAA3	*Os01g0231000*	*TraesCS3A02G155200*
OsIAA3	*Os01g0231000*	*TraesCS3D02G162700*
OsIAA5	*Os01g0675700*	*TraesCS3A02G270000*
OsIAA5	*Os01g0675700*	*TraesCS3B02G303900*
OsIAA5	*Os01g0675700*	*TraesCS3D02G269700*
OsIAA6	*Os01g0741900*	*TraesCS3B02G310500*
OsIAA6	*Os01g0741900*	*TraesCS3D02G276600*
OsIAA6	*Os01g0741900*	*TraesCS3A02G276500*
OsIAA8	*Os02g0723400*	*TraesCS1A02G082700*
OsIAA8	*Os02g0723400*	*TraesCS1B02G100300*
OsIAA8	*Os02g0723400*	*TraesCS1D02G084100*
OsIAA9	*Os02g0805100*	*TraesCS6B02G411000*
OsIAA9	*Os02g0805100*	*TraesCS6A02G373300*
OsIAA9	*Os02g0805100*	*TraesCS6D02G357500*
OsIAA10	*Os02g0817600*	*TraesCS6D02G378300*
OsIAA10	*Os02g0817600*	*TraesCS6B02G432800*
OsIAA10	*Os02g0817600*	*TraesCS6A02G392600*
OsIAA11	*Os03g0633500*	*TraesCS5B02G381900*
OsIAA11	*Os03g0633500*	*TraesCS5A02G378300*
OsIAA11	*Os03g0633500*	*TraesCS5D02G388300*
OsIAA12	*Os03g0633800*	*TraesCS5B02G381800*
OsIAA12	*Os03g0633800*	*TraesCS5A02G378200*
OsIAA12	*Os03g0633800*	*TraesCS5D02G388200*
OsIAA13	*Os03g0742900*	*TraesCS5B02G386800*

OsIAA13	*Os03g0742900*	*TraesCS5D02G392000*
OsIAA13	*Os03g0742900*	*TraesCS5A02G382600*
OsIAA14	*Os03g0797800*	*TraesCS5B02G446100*
OsIAA14	*Os03g0797800*	*TraesCS5D02G449400*
OsIAA15	*Os05g0178600*	*TraesCS1B02G138100*
OsIAA15	*Os05g0178600*	*TraesCS1A02G118400*
OsIAA15	*Os05g0178600*	*TraesCS1D02G119500*
OsIAA18	*Os05g0523300*	*TraesCS1D02G345400*
OsIAA18	*Os05g0523300*	*TraesCS1A02G343300*
OsIAA18	*Os05g0523300*	*TraesCS1B02G356600*
OsIAA19	*Os05g0559400*	*TraesCS1D02G398400*
OsIAA19	*Os05g0559400*	*TraesCS1A02G390200*
OsIAA19	*Os05g0559400*	*TraesCS1B02G418400*
OsIAA20	*Os06g0166500*	*TraesCS7D02G127800*
OsIAA20	*Os06g0166500*	*TraesCS7B02G029000*
OsIAA20	*Os06g0166500*	*TraesCS7D02G128200*
OsIAA20	*Os06g0166500*	*TraesCS7A02G129000*
OsIAA20	*Os06g0166500*	*TraesCS7D02G127900*
OsIAA20	*Os06g0166500*	*TraesCS7B02G029100*
OsIAA20	*Os06g0166500*	*TraesCS7D02G128100*
OsIAA21	*Os06g0335500*	*TraesCS7D02G339300*
OsIAA21	*Os06g0335500*	*TraesCS7A02G331100*
OsIAA21	*Os06g0335500*	*TraesCS7B02G242800*
OsIAA25	*Os08g0109400*	*TraesCS7D02G318900*
OsIAA25	*Os08g0109400*	*TraesCS7A02G322000*
OsIAA25	*Os08g0109400*	*TraesCS7B02G222900*
OsIAA26	*Os09g0527700*	*TraesCS5A02G317200*
OsIAA26	*Os09g0527700*	*TraesCS5B02G317800*
OsIAA26	*Os09g0527700*	*TraesCS5D02G323500*
OsIAA27	*Os11g0221000*	*TraesCS4B02G108600*
OsIAA27	*Os11g0221000*	*TraesCS4A02G204900*
OsIAA27	*Os11g0221000*	*TraesCS4D02G105700*
OsIAA28/29	*Os11g0221200/Os11g0221300*	*TraesCS4A02G205000*
OsIAA28/29	*Os11g0221200/Os11g0221300*	*TraesCS4B02G108700*
OsIAA28/29	*Os11g0221200/Os11g0221300*	*TraesCS4D02G105800*
OsIAA30	*Os12g0601300*	*TraesCS5B02G058500*
OsIAA30	*Os12g0601300*	*TraesCS5A02G058600*
OsIAA30	*Os12g0601300*	*TraesCS5D02G069300*
OsARF1	*Os01g0236300*	*TraesCS3A02G159200*
OsARF1	*Os01g0236300*	*TraesCS3D02G166700*
OsARF1	*Os01g0236300*	*TraesCS3B02G190100*
OsARF2	*Os01g0670800*	*TraesCS3D02G245400*
OsARF2	*Os01g0670800*	*TraesCS3B02G273400*
OsARF2	*Os01g0670800*	*TraesCS3A02G246000*
OsARF3	*Os01g0753500*	*TraesCS3D02G292100*
OsARF3	*Os01g0753500*	*TraesCS3A02G292400*
OsARF3	*Os01g0753500*	*TraesCS3B02G327000*
OsARF4	*Os01g0927600*	*TraesCS3A02G449300*
OsARF4	*Os01g0927600*	*TraesCS3B02G475800*
OsARF4	*Os01g0927600*	*TraesCS3B02G486000*
OsARF4	*Os01g0927600*	*TraesCS3D02G442000*
OsARF4	*Os01g0927600*	*TraesCS3D02G434700*
OsARF4	*Os01g0927600*	*TraesCS3A02G442000*
OsARF6	*Os02g0164900*	*TraesCS6D02G127600*
OsARF6	*Os02g0164900*	*TraesCS6B02G167100*
OsARF6	*Os02g0164900*	*TraesCS6A02G138600*
OsARF9	*Os04g0442000*	*TraesCS2A02G309300*
OsARF9	*Os04g0442000*	*TraesCS2D02G307600*
OsARF9	*Os04g0442000*	*TraesCS2B02G326400*
OsARF10	*Os04g0519700*	*TraesCS2D02G376600*
OsARF10	*Os04g0519700*	*TraesCS2B02G397300*

OsARF10	*Os04g0519700*	*TraesCS2A02G380300*
OsARF11	*Os04g0664400*	*TraesCS2B02G519200*
OsARF11	*Os04g0664400*	*TraesCS2A02G491000*
OsARF11	*Os04g0664400*	*TraesCS2D02G491200*
OsARF12	*Os04g0671900*	*TraesCS2D02G548900*
OsARF12	*Os04g0671900*	*TraesCS2B02G578500*
OsARF12	*Os04g0671900*	*TraesCS2A02G547800*
OsARF13	*Os04g0690600*	*TraesCS2A02G567300*
OsARF13	*Os04g0690600*	*TraesCS2D02G577800*
OsARF14	*Os05g0515400*	*TraesCS1D02G337400*
OsARF14	*Os05g0515400*	*TraesCS1A02G334900*
OsARF14	*Os05g0515400*	*TraesCS1B02G347900*
OsARF15	*Os05g0563400*	*TraesCS1A02G396400*
OsARF15	*Os05g0563400*	*TraesCS1D02G404400*
OsARF15	*Os05g0563400*	*TraesCS1B02G424700*
OsARF16	*Os06g0196700*	*TraesCS7D02G161900*
OsARF16	*Os06g0196700*	*TraesCS7B02G065800*
OsARF16	*Os06g0196700*	*TraesCS7A02G160800*
OsARF17	*Os06g0677800*	*TraesCS7A02G461700*
OsARF17	*Os06g0677800*	*TraesCS7B02G363100*
OsARF17	*Os06g0677800*	*TraesCS7D02G449900*
OsARF18	*Os06g0685700*	*TraesCS7A02G446900*
OsARF18	*Os06g0685700*	*TraesCS7D02G436800*
OsARF18	*Os06g0685700*	*TraesCS7B02G346700*
OsARF21	*Os08g0520500*	*TraesCS7D02G250100*
OsARF21	*Os08g0520500*	*TraesCS7A02G252000*
OsARF21	*Os08g0520500*	*TraesCS7B02G138900*
OsARF25	*Os12g0613700*	*TraesCS5D02G045700*
OsARF25	*Os12g0613700*	*TraesCS5A02G038300*
OsARF25	*Os12g0613700*	*TraesCS5B02G039800*
	Jasmonic Acid	
OsDAD1;2	*Os08g0143600*	*TraesCS7A02G306300*
OsDAD1;2	*Os08g0143600*	*TraesCS7B02G206500*
OsDAD1;2	*Os08g0143600*	*TraesCS7D02G303000*
OsDAD1;3	*Os02g0653900*	*TraesCS6D02G224700*
OsDAD1;3	*Os02g0653900*	*TraesCS6A02G242700*
OsDAD1;3	*Os02g0653900*	*TraesCS6B02G281800*
OsDAD1;4	*Os10g0562200*	*TraesCS1D02G220300*
OsDAD1;4	*Os10g0562200*	*TraesCS1B02G232100*
OsDAD1;4	*Os10g0562200*	*TraesCS1A02G218600*
OsPLA1	*Os07g0520900*	*TraesCS2A02G220900*
OsPLA1	*Os07g0520900*	*TraesCS2D02G226600*
OsPLA1	*Os07g0520900*	*TraesCS2B02G246500*
OsLOX2;1/3	*Os08g0508800/Os08g0509100*	*TraesCS7D02G244800*
OsLOX2;1/3	*Os08g0508800/Os08g0509100*	*TraesCS4D02G347300*
OsLOX2;1/3	*Os08g0508800/Os08g0509100*	*TraesCS7B02G145200*
OsLOX2;1/3	*Os08g0508800/Os08g0509100*	*TraesCS7A02G246200*
OsLOX2;2	*Os12g0559200*	*TraesCS5D02G013400*
OsLOX2;2	*Os12g0559200*	*TraesCS6B02G014400*
OsLOX2;2	*Os12g0559200*	*TraesCS5A02G032800*
OsLOX2;2	*Os12g0559200*	*TraesCS6D02G010100*
OsLOX2;2	*Os12g0559200*	*TraesCS5B02G033000*
OsLOX2;2	*Os12g0559200*	*TraesCS5A02G007900*
OsLOX2;2	*Os12g0559200*	*TraesCS5B02G006500*
OsLOX2;2	*Os12g0559200*	*TraesCS7D02G029400*
OsLOX2;2	*Os12g0559200*	*TraesCS7A02G034900*
OsLOX2;2	*Os12g0559200*	*TraesCS5D02G041100*
OsLOX2;4	*Os02g0194700*	*TraesCS6A02G166000*
OsLOX2;4	*Os02g0194700*	*TraesCS6D02G154600*
OsLOX2;4	*Os02g0194700*	*TraesCS6B02G193400*
OsLOX2;5	*Os03g0179900*	*TraesCS4D02G294100*

OsLOX2;5	*Os03g0179900*	*TraesCS4A02G009400*
OsLOX2;5	*Os03g0179900*	*TraesCS4B02G295200*
OsAOS1	*Os03g0225900*	*TraesCS4B02G237600*
OsAOS1	*Os03g0225900*	*TraesCS4A02G061900*
OsAOS1	*Os03g0225900*	*TraesCS4A02G061800*
OsAOS1	*Os03g0225900*	*TraesCS4D02G238700*
OsAOS1	*Os03g0225900*	*TraesCS4D02G238800*
OsAOS1	*Os03g0225900*	*TraesCS4B02G237500*
OsAOS2	*Os03g0767000*	*TraesCS5D02G413200*
OsAOS2	*Os03g0767000*	*TraesCS5A02G403200*
OsAOS2	*Os03g0767000*	*TraesCS5B02G408000*
OsAOC	*Os03g0438100*	*TraesCS6B02G365200*
OsAOC	*Os03g0438100*	*TraesCS6D02G314300*
OsAOC	*Os03g0438100*	*TraesCS6A02G334800*
OsOPR7	*Os08g0459600*	*TraesCS5B02G487600*
OsOPR7	*Os08g0459600*	*TraesCS7D02G405500*
OsOPR7	*Os08g0459600*	*TraesCS7B02G311600*
OsOPR7	*Os08g0459600*	*TraesCS7A02G412400*
OsOPCL1	*Os03g0132000*	*TraesCS4B02G326800*
OsOPCL1	*Os03g0132000*	*TraesCS5A02G498800*
OsOPCL1	*Os03g0132000*	*TraesCS4D02G323500*
OsACX	*Os06g0103500*	*TraesCS4A02G494700*
OsACX	*Os06g0103500*	*TraesCS7D02G004400*
OsACX	*Os06g0103500*	*TraesCS7A02G003900*
OsAIM1	*Os02g0274100*	*TraesCS6B02G153900*
OsAIM1	*Os02g0274100*	*TraesCS3A02G077000*
OsAIM1	*Os02g0274100*	*TraesCS3B02G091200*
OsAIM1	*Os02g0274100*	*TraesCS6D02G116200*
OsAIM1	*Os02g0274100*	*TraesCS6A02G125800*
OsAIM1	*Os02g0274100*	*TraesCS3D02G077200*
OsJMT1	*Os01g0701700*	*TraesCS3A02G255100*
OsJMT1	*Os01g0701700*	*TraesCS3B02G287100*
OsJMT1	*Os01g0701700*	*TraesCS3D02G256000*
OsJMT2	*Os06g0329900*	*TraesCS7B02G194700*
OsJMT2	*Os06g0329900*	*TraesCS7A02G224900*
OsJMT2	*Os06g0329900*	*TraesCS7D02G229500*
OsJAR1	*Os05g0586200*	*TraesCS1B02G459500*
OsJAR1	*Os05g0586200*	*TraesCS1D02G434100*
OsJAR1	*Os05g0586200*	*TraesCS1A02G425100*
OsCOI1	*Os01g0853400*	*TraesCS3B02G399200*
OsCOI1	*Os01g0853400*	*TraesCS3D02G360400*
OsCOI1	*Os01g0853400*	*TraesCS3A02G367500*
OsJAZ1	*Os03g0180900*	*TraesCS4B02G297000*
OsJAZ1	*Os03g0180900*	*TraesCS4A02G007900*
OsJAZ1	*Os03g0180900*	*TraesCS4D02G295900*
OsJAZ3	*Os07g0615200*	*TraesCS2A02G169300*
OsJAZ3	*Os07g0615200*	*TraesCS2B02G195600*
OsJAZ3	*Os07g0615200*	*TraesCS2D02G176800*
OsJAZ5	*Os03g0181100*	*TraesCS4D02G296000*
OsJAZ5	*Os03g0181100*	*TraesCS4A02G007800*
OsJAZ5	*Os03g0181100*	*TraesCS4B02G297100*
OsJAZ7	*Os09g0439200*	*TraesCS5A02G212800*
OsJAZ7	*Os09g0439200*	*TraesCS5B02G211000*
OsJAZ7	*Os09g0439200*	*TraesCS5D02G219300*
OsJAZ9	*Os04g0395800*	*TraesCS2A02G286700*
OsJAZ9	*Os04g0395800*	*TraesCS2D02G285300*
OsJAZ9	*Os04g0395800*	*TraesCS2B02G303600*
OsMYC2	*Os10g0575000*	*TraesCS1A02G193200*
OsMYC2	*Os10g0575000*	*TraesCS1D02G196900*
OsMYC2	*Os10g0575000*	*TraesCS1B02G208000*
Gibberellin		

CPS	*Os02g0278700*	*TraesCS7A02G552700*
CPS	*Os02g0278700*	*TraesCS1B02G139400*
CPS	*Os02g0278700*	*TraesCS7D02G538600*
CPS	*Os02g0278700*	*TraesCS1D02G120800*
CPS	*Os02g0278700*	*TraesCSU02G099900*
CPS	*Os02g0278700*	*TraesCS7A02G552600*
CPS	*Os02g0278700*	*TraesCS7D02G539200*
CPS	*Os02g0278700*	*TraesCS7B02G476400*
CPS	*Os02g0278700*	*TraesCS1A02G119900*
KO1a/2	*Os06g0570600/Os06g0569900*	*TraesCS7A02G362300*
KO1a/2	*Os06g0570600/Os06g0569900*	*TraesCS2D02G427200*
KO1a/2	*Os06g0570600/Os06g0569900*	*TraesCS2B02G445400*
KO1a/2	*Os06g0570600/Os06g0569900*	*TraesCS2B02G450200*
KO1a/2	*Os06g0570600/Os06g0569900*	*TraesCS7A02G362200*
KO1a/2	*Os06g0570600/Os06g0569900*	*TraesCS7B02G265800*
KO1a/2	*Os06g0570600/Os06g0569900*	*TraesCS2B02G445300*
KO1a/2	*Os06g0570600/Os06g0569900*	*TraesCS7D02G360700*
KO1a/2	*Os06g0570600/Os06g0569900*	*TraesCS2B02G450100*
KO1a/2	*Os06g0570600/Os06g0569900*	*TraesCS2A02G429600*
KAO	*Os06g0110000*	*TraesCS4A02G460100*
KAO	*Os06g0110000*	*TraesCS7A02G029600*
KAO	*Os06g0110000*	*TraesCS7D02G026000*
GA20ox1	*Os03g0856700*	*TraesCS4A02G319100*
GA20ox1	*Os03g0856700*	*TraesCS5D02G566200*
GA20ox1	*Os03g0856700*	*TraesCS5B02G560300*
GA20ox2	*Os01g0883800*	*TraesCS3D02G401400*
GA20ox2	*Os01g0883800*	*TraesCS3B02G439900*
GA20ox2	*Os01g0883800*	*TraesCS3A02G406200*
GA20ox3	*Os07g0169700*	*TraesCS3A02G399800*
GA20ox3	*Os07g0169700*	*TraesCS3D02G393900*
GA20ox3	*Os07g0169700*	*TraesCS3B02G432800*
GA20ox3	*Os07g0169700*	*TraesCS3D02G394000*
GA20ox4	*Os05g0421900*	*TraesCS1D02G263700*
GA20ox4	*Os05g0421900*	*TraesCS1A02G263600*
GA20ox4	*Os05g0421900*	*TraesCS1B02G274200*
GA3ox2	*Os01g0177400*	*TraesCS3B02G141800*
GA3ox2	*Os01g0177400*	*TraesCS3A02G122600*
GA3ox2	*Os01g0177400*	*TraesCS2B02G570800*
GA3ox2	*Os01g0177400*	*TraesCS2D02G542100*
GA3ox2	*Os01g0177400*	*TraesCS2A02G540400*
GA3ox2	*Os01g0177400*	*TraesCS3D02G124500*
GA3ox2	*Os01g0177400*	*TraesCS2B02G570900*
GA2ox1	*Os05g0158600*	*TraesCS1B02G123500*
GA2ox1	*Os05g0158600*	*TraesCS1A02G106200*
GA2ox1	*Os05g0158600*	*TraesCS1D02G108800*
GA2ox3	*Os01g0757200*	*TraesCS3D02G293800*
GA2ox3	*Os01g0757200*	*TraesCS3A02G294000*
GA2ox3	*Os01g0757200*	*TraesCS3B02G328700*
GA2ox6	*Os04g0522500*	*TraesCS5A02G543100*
GA2ox6	*Os04g0522500*	*TraesCS4A02G033200*
GA2ox6	*Os04g0522500*	*TraesCS4B02G272100*
GA2ox6	*Os04g0522500*	*TraesCS4D02G271300*
GA2ox6	*Os04g0522500*	*TraesCS4B02G376100*
GA2ox6	*Os04g0522500*	*TraesCS4B02G376200*
GA2ox6	*Os04g0522500*	*TraesCS2A02G379000*
GA2ox6	*Os04g0522500*	*TraesCS2D02G375300*
GA2ox6	*Os04g0522500*	*TraesCS2B02G396000*
GA2ox7	*Os05g0560900*	*TraesCS1B02G420700*
EUI	*Os05g0482400*	*TraesCS1D02G302500*
EUI	*Os05g0482400*	*TraesCS2B02G230500*
EUI	*Os05g0482400*	*TraesCS1D02G302600*

EUI	*Os05g0482400*	*TraesCS1B02G313400*
EUI	*Os05g0482400*	*TraesCS1A02G303100*
EUIL1	*Os07g0681300*	*TraesCS2B02G121000*
EUIL1	*Os07g0681300*	*TraesCS2D02G103600*
EUIL1	*Os07g0681300*	*TraesCS2A02G103900*
EUIL2	*Os12g0118900*	*TraesCS5B02G144600*
EUIL2	*Os12g0118900*	*TraesCS5A02G145700*
EUIL2	*Os12g0118900*	*TraesCS5D02G146500*
EUIL3	*Os12g0119000*	*TraesCS5D02G146600*
EUIL3	*Os12g0119000*	*TraesCS5B02G144500*
EUIL3	*Os12g0119000*	*TraesCS5A02G145600*
GID1	*Os05g0407500*	*TraesCS1B02G265900*
GID1	*Os05g0407500*	*TraesCS1A02G255100*
GID1	*Os05g0407500*	*TraesCS1D02G254500*
SLRL2	*Os05g0574900*	*TraesCS4D02G338800*
SLRL2	*Os05g0574900*	*TraesCS1D02G421200*
SLRL2	*Os05g0574900*	*TraesCS1B02G443800*
SLRL2	*Os05g0574900*	*TraesCS1A02G413800*
SLRL2	*Os05g0574900*	*TraesCS4B02G342800*
SLRL2	*Os05g0574900*	*TraesCS5A02G511900*
GID2	*Os02g0580300*	*TraesCS3B02G068000*
GID2	*Os02g0580300*	*TraesCS3A02G055600*
GID2	*Os02g0580300*	*TraesCS3D02G055500*
OsSPY	*Os08g0559300*	*TraesCS6A02G107700*
OsSPY	*Os08g0559300*	*TraesCS6D02G095600*
OsSPY	*Os08g0559300*	*TraesCS6B02G136300*
OsGAMYB	*Os01g0812000*	*TraesCS3D02G329400*
OsGAMYB	*Os01g0812000*	*TraesCS3B02G367500*
OsGAMYB	*Os01g0812000*	*TraesCS3A02G336500*
OsGAMYBL1	*Os06g0605600*	*TraesCS7D02G373400*
OsGAMYBL1	*Os06g0605600*	*TraesCS7B02G278400*
OsGAMYBL1	*Os06g0605600*	*TraesCS7A02G377100*
OsGAMYBL2	*Os03g0578900*	*TraesCS7B02G031000*
OsGAMYBL2	*Os03g0578900*	*TraesCS7D02G130100*
OsGAMYBL2	*Os03g0578900*	*TraesCS7A02G130700*
	Ethylene	
OsACS1	*Os03g0727600*	*TraesCS4B02G058200*
OsACS1	*Os03g0727600*	*TraesCS4A02G256500*
OsACS1	*Os03g0727600*	*TraesCS4D02G058200*
OsACS2	*Os04g0578000*	*TraesCS2D02G394200*
OsACS2	*Os04g0578000*	*TraesCS2A02G396400*
OsACS2	*Os04g0578000*	*TraesCS2B02G414800*
OsACS4 /5	*Os05g0319200/Os01g0192900*	*TraesCS3B02G125200*
OsACS4 /5	*Os05g0319200/Os01g0192900*	*TraesCS3D02G108700*
OsACS4 /5	*Os05g0319200/Os01g0192900*	*TraesCS3A02G106600*
OsACS6	*Os06g0130400*	*TraesCS4A02G422900*
OsACS6	*Os06g0130400*	*TraesCS7A02G066400*
OsACS6	*Os06g0130400*	*TraesCS7D02G060600*
OsACO1/3	*Os09g0451400/Os09g0451000*	*TraesCS5B02G232600*
OsACO1/3	*Os09g0451400/Os09g0451000*	*TraesCS5D02G241000*
OsACO1/3	*Os09g0451400/Os09g0451000*	*TraesCS5A02G234200*
OsACO1/3	*Os09g0451400/Os09g0451000*	*TraesCS5B02G232700*
OsACO1/3	*Os09g0451400/Os09g0451000*	*TraesCS5D02G241100*
OsACO1/3	*Os09g0451400/Os09g0451000*	*TraesCS5A02G234300*
OsACO2	*Os02g0771600*	*TraesCS6D02G305200*
OsACO2	*Os02g0771600*	*TraesCS6D02G305400*
OsACO2	*Os02g0771600*	*TraesCS6A02G325400*
OsACO2	*Os02g0771600*	*TraesCS6B02G355800*
OsACO2	*Os02g0771600*	*TraesCS6B02G356200*
OsACO2	*Os02g0771600*	*TraesCS6B02G355700*
OsACO2	*Os02g0771600*	*TraesCS6D02G305100*

OsACO2	*Os02g0771600*	*TraesCS6A02G325700*
OsACO2	*Os02g0771600*	*TraesCS6A02G325600*
OsACO2	*Os02g0771600*	*TraesCS6B02G356000*
OsACO2	*Os02g0771600*	*TraesCS6A02G325500*
OsACO2	*Os02g0771600*	*TraesCS6B02G355900*
OsACO4	*Os11g0186900*	*TraesCSU02G067700*
OsACO4	*Os11g0186900*	*TraesCS4D02G095500*
OsACO4	*Os11g0186900*	*TraesCS4A02G221300*
OsACO5/6	*Os05g0149400/Os05g0149300*	*TraesCS1B02G117500*
OsACO5/6	*Os05g0149400/Os05g0149300*	*TraesCS1B02G117400*
OsACO5/6	*Os05g0149400/Os05g0149300*	*TraesCS1A02G089600*
OsACO5/6	*Os05g0149400/Os05g0149300*	*TraesCS1A02G089500*
OsACO5/6	*Os05g0149400/Os05g0149300*	*TraesCS1D02G098000*
OsACO5/6	*Os05g0149400/Os05g0149300*	*TraesCS1D02G098100*
OsACO7	*Os01g0580500*	*TraesCS7D02G516200*
OsACO7	*Os01g0580500*	*TraesCS7B02G444900*
OsETR1;1	*Os03g0701700*	*TraesCS4B02G039300*
OsETR1;1	*Os03g0701700*	*TraesCS4A02G274300*
OsETR1;1	*Os03g0701700*	*TraesCS4D02G036400*
OsETR1;2	*Os05g0155200*	*TraesCS1D02G105600*
OsETR1;2	*Os05g0155200*	*TraesCS1A02G096600*
OsETR1;2	*Os05g0155200*	*TraesCS1B02G127000*
OsEIN4	*Os04g0169100*	*TraesCS2B02G023800*
OsEIN4	*Os04g0169100*	*TraesCS2D02G000500*
OsEIN4	*Os04g0169100*	*TraesCS2A02G000200*
OsETR2;1	*Os02g0820900*	*TraesCS6D02G383600*
OsETR2;1	*Os02g0820900*	*TraesCS6A02G399400*
OsETR2;1	*Os02g0820900*	*TraesCS6B02G439600*
OsETR2;2	*Os07g0259100*	*TraesCS6A02G329400*
OsETR2;2	*Os07g0259100*	*TraesCS6D02G266200*
OsETR2;2	*Os07g0259100*	*TraesCS6A02G285800*
OsETR2;2	*Os07g0259100*	*TraesCS6B02G360200*
OsETR2;2	*Os07g0259100*	*TraesCS6D02G308300*
OsETR2;2	*Os07g0259100*	*TraesCS6B02G314600*
OsEIN2;2	*Os03g0700800*	*TraesCS5A02G547500*
OsEIN2;2	*Os03g0700800*	*TraesCS4A02G275600*
OsEIN2;2	*Os03g0700800*	*TraesCS4D02G036000*
OsEIN2;2	*Os03g0700800*	*TraesCSU02G131600*
OsEIN2;2	*Os03g0700800*	*TraesCS2B02G133000*
OsEIN2;2	*Os03g0700800*	*TraesCS4B02G381200*
OsEIN2;2	*Os03g0700800*	*TraesCSU02G131800*
OsEIN2;2	*Os03g0700800*	*TraesCS4B02G038100*
OsEIN3;1/2	*Os03g0324200/Os03g0324300*	*TraesCS4A02G129400*
OsEIN3;1/2	*Os03g0324200/Os03g0324300*	*TraesCS4B02G175100*
OsEIN3;1/2	*Os03g0324200/Os03g0324300*	*TraesCS4D02G177000*
OsEIN3;3	*Os07g0685700*	*TraesCS2A02G099900*
OsEIN3;3	*Os07g0685700*	*TraesCS2B02G116900*
OsEIN3;3	*Os07g0685700*	*TraesCS2D02G099400*
OsEIN3;4	*Os09g0490200*	*TraesCS5B02G265400*
OsEIN3;4	*Os09g0490200*	*TraesCS5D02G273600*
OsEIN3;4	*Os09g0490200*	*TraesCS5A02G265700*
OsEIN3;5	*Os08g0508700*	*TraesCS7B02G145400*
OsEIN3;5	*Os08g0508700*	*TraesCS7D02G244600*
OsEIN3;5	*Os08g0508700*	*TraesCS7A02G246100*
OsEIN3;7	*Os04g0456700*	*TraesCS2B02G339800*
OsEIN3;7	*Os04g0456700*	*TraesCS2D02G319800*
OsEIN3;7	*Os04g0456700*	*TraesCS2A02G342100*
	ABA	
OsZEP1	*Os04g0448900*	*TraesCS2A02G317000*
OsZEP1	*Os04g0448900*	*TraesCS2B02G335400*
OsZEP1	*Os04g0448900*	*TraesCS2D02G314900*

OsABA4	*Os01g0128300*	*TraesCS3D02G037000*
OsABA4	*Os01g0128300*	*TraesCS3B02G039800*
OsABA4	*Os01g0128300*	*TraesCS3A02G043800*
OsNCED1	*Os03g0645900*	*TraesCS5D02G383500*
OsNCED1	*Os03g0645900*	*TraesCS5A02G374000*
OsNCED1	*Os03g0645900*	*TraesCS5B02G375900*
OsNCED2	*Os12g0617400*	*TraesCS5D02G038800*
OsNCED2	*Os12g0617400*	*TraesCS5B02G029300*
OsNCED3	*Os07g0154100*	*TraesCS2B02G268400*
OsNCED3	*Os07g0154100*	*TraesCS2D02G251600*
OsNCED3	*Os07g0154100*	*TraesCS2A02G250600*
OsABA2	*Os03g0810800*	*TraesCS5B02G476900*
OsABA2	*Os03g0810800*	*TraesCS1B02G054000*
OsABA2	*Os03g0810800*	*TraesCS5D02G477700*
OsABA2	*Os03g0810800*	*TraesCS5A02G465100*
OsAAO3;1	*Os07g0281700*	*TraesCS7A02G509300*
OsAAO3;1	*Os07g0281700*	*TraesCS7D02G498000*
OsAAO3;3	*Os07g0164900*	*TraesCS2A02G246300*
OsAAO3;3	*Os07g0164900*	*TraesCS2D02G248700*
OsAAO3;3	*Os07g0164900*	*TraesCS2B02G270600*
OsABA3	*Os06g0670000*	*TraesCS7A02G470400*
OsABA3	*Os06g0670000*	*TraesCS7B02G372400*
OsABA3	*Os06g0670000*	*TraesCS7D02G457800*
OsABA8OX1	*Os02g0703600*	*TraesCS6B02G298500*
OsABA8OX1	*Os02g0703600*	*TraesCS6A02G271300*
OsABA8OX1	*Os02g0703600*	*TraesCS6D02G243800*
OsABA8OX3	*Os09g0457100*	*TraesCS5A02G238000*
OsABA8OX3	*Os09g0457100*	*TraesCS5D02G244900*
OsABA8OX3	*Os09g0457100*	*TraesCS5B02G236500*
OsPLDα1	*Os01g0172400*	*TraesCS3D02G130900*
OsPLDα1	*Os01g0172400*	*TraesCS3A02G130000*
OsPLDα1	*Os01g0172400*	*TraesCS3B02G149100*
OsPLDα3	*Os03g0391400*	*TraesCS1B02G393300*
OsPLDα3	*Os03g0391400*	*TraesCS1D02G379900*
OsPLDα3	*Os03g0391400*	*TraesCS1A02G373100*
OsPLDα4	*Os03g0840800*	*TraesCS5D02G524600*
OsPLDα4	*Os03g0840800*	*TraesCS5B02G525600*
OsPLDα4	*Os03g0840800*	*TraesCS4A02G347800*
OsPLDα5	*Os05g0171000*	*TraesCS1B02G135200*
OsPLDα5	*Os05g0171000*	*TraesCS1D02G116700*
OsPLDα5	*Os05g0171000*	*TraesCS1A02G115300*
OsPLDα6/7/8	*Os06g0604200/Os06g0604300/Os06g0604400*	*TraesCS4B02G377600*
OsPLDα6/7/8	*Os06g0604200/Os06g0604300/Os06g0604400*	*TraesCS7B02G277900*
OsPLDα6/7/8	*Os06g0604200/Os06g0604300/Os06g0604400*	*TraesCS7D02G372800*
OsPLDα6/7/8	*Os06g0604200/Os06g0604300/Os06g0604400*	*TraesCS7A02G376500*
OsPLDα6/7/8	*Os06g0604200/Os06g0604300/Os06g0604400*	*TraesCSU02G145400*
OsPLDα9	*Os07g0260400*	*TraesCS5D02G208300*
OsPLDα9	*Os07g0260400*	*TraesCS5B02G200600*
OsPLDα9	*Os07g0260400*	*TraesCS5A02G202000*
OsPLDα11	*Os09g0421300*	*TraesCS5D02G231100*
OsPLDα11	*Os09g0421300*	*TraesCS5B02G222500*
OsPLDα11	*Os09g0421300*	*TraesCS5A02G223500*
OsPLDα12	*Os09g0543100*	*TraesCS5A02G337100*
OsPLDα12	*Os09g0543100*	*TraesCS5B02G336100*
OsPLDα12	*Os09g0543100*	*TraesCS5D02G341800*
OsPLDα13	*Os10g0524400*	*TraesCS1B02G195200*
OsPLDα13	*Os10g0524400*	*TraesCS1A02G187400*
OsPLDα13	*Os10g0524400*	*TraesCS1A02G365100*
OsPLDα13	*Os10g0524400*	*TraesCS1B02G382600*
OsPLDα13	*Os10g0524400*	*TraesCS1D02G189300*
OsPLDα13	*Os10g0524400*	*TraesCS1D02G370600*

OsPP2C1	*Os01g0583100*	*TraesCS3B02G240000*
OsPP2C1	*Os01g0583100*	*TraesCS3A02G209200*
OsPP2C1	*Os01g0583100*	*TraesCS3D02G212100*
OsPP2C2	*Os01g0656200*	*TraesCS3A02G237800*
OsPP2C2	*Os01g0656200*	*TraesCS3B02G266200*
OsPP2C2	*Os01g0656200*	*TraesCS3D02G238000*
OsPP2C3/5	*Os01g0846300/Os05g0457200*	*TraesCS3D02G355900*
OsPP2C3/5	*Os01g0846300/Os05g0457200*	*TraesCS3B02G394600*
OsPP2C3/5	*Os01g0846300/Os05g0457200*	*TraesCS3A02G362200*
OsPP2C4	*Os03g0268600*	*TraesCS4D02G210900*
OsPP2C4	*Os03g0268600*	*TraesCS4B02G210100*
OsPP2C4	*Os03g0268600*	*TraesCS4A02G094300*
OsPP2C6	*Os05g0537400*	*TraesCS1A02G358600*
OsPP2C6	*Os05g0537400*	*TraesCS1B02G375100*
OsPP2C6	*Os05g0537400*	*TraesCS1D02G363500*
OsPP2C7	*Os05g0572700*	*TraesCS1B02G441400*
OsPP2C7	*Os05g0572700*	*TraesCS1D02G419000*
OsPP2C7	*Os05g0572700*	*TraesCS1A02G411200*
OsPP2C8	*Os05g0592800*	*TraesCS1A02G441200*
OsPP2C8	*Os05g0592800*	*TraesCS1D02G449700*
OsPP2C8	*Os05g0592800*	*TraesCS1B02G475700*
OsPP2C9	*Os09g0325700*	*TraesCS5B02G182000*
OsPP2C9	*Os09g0325700*	*TraesCS5D02G188600*
OsPP2C9	*Os09g0325700*	*TraesCS5A02G183600*
SAPK8	*Os03g0764800*	*TraesCS5D02G411900*
SAPK8	*Os03g0764800*	*TraesCS5B02G406400*
SAPK8	*Os03g0764800*	*TraesCS5A02G401700*
SAPK9	*Os12g0586100*	*TraesCS5D02G081700*
SAPK9	*Os12g0586100*	*TraesCS5B02G075800*
SAPK9	*Os12g0586100*	*TraesCS5A02G069500*
SAPK10	*Os03g0610900*	*TraesCS4D02G078100*
SAPK10	*Os03g0610900*	*TraesCS4A02G235600*
SAPK10	*Os03g0610900*	*TraesCS4B02G079300*
OsVP1	*Os01g0911700*	*TraesCS3D02G412800*
OsVP1	*Os01g0911700*	*TraesCS3B02G452200*
OsVP1	*Os01g0911700*	*TraesCS3A02G417300*
OsbZIP9	*Os01g0813100*	*TraesCS3D02G330300*
OsbZIP9	*Os01g0813100*	*TraesCS3A02G337200*
OsbZIP9	*Os01g0813100*	*TraesCS3B02G368300*
OsbZIP12	*Os01g0867300*	*TraesCS3B02G411300*
OsbZIP12	*Os01g0867300*	*TraesCS3A02G378700*
OsbZIP12	*Os01g0867300*	*TraesCS3D02G371900*
OsbZIP23	*Os02g0766700*	*TraesCS6A02G333600*
OsbZIP23	*Os02g0766700*	*TraesCS6B02G364000*
OsbZIP23	*Os02g0766700*	*TraesCS6D02G312800*
OsbZIP24	*Os02g0833600*	*TraesCS2B02G489900*
OsbZIP24	*Os02g0833600*	*TraesCS2A02G467100*
OsbZIP24	*Os02g0833600*	*TraesCS2D02G467100*
OsbZIP29	*Os03g0322700*	*TraesCS4B02G175800*
OsbZIP29	*Os03g0322700*	*TraesCS4A02G128900*
OsbZIP29	*Os03g0322700*	*TraesCS4D02G177700*
OsbZIP40	*Os05g0437700*	*TraesCS1B02G282800*
OsbZIP40	*Os05g0437700*	*TraesCS1D02G273100*
OsbZIP40	*Os05g0437700*	*TraesCS1A02G273000*
OsbZIP42	*Os05g0489700*	*TraesCS1B02G317100*
OsbZIP42	*Os05g0489700*	*TraesCS1A02G306300*
OsbZIP42	*Os05g0489700*	*TraesCS1D02G306000*
OsbZIP46	*Os06g0211200*	*TraesCS7D02G171300*
OsbZIP46	*Os06g0211200*	*TraesCS7A02G170600*
OsbZIP46	*Os06g0211200*	*TraesCS7B02G075600*
OsbZIP62	*Os07g0686100*	*TraesCS2A02G099400*

OsbZIP62	*Os07g0686100*	*TraesCS2B02G115700*
OsbZIP62	*Os07g0686100*	*TraesCS2D02G098700*
OsbZIP72	*Os09g0456200*	*TraesCS5A02G237200*
OsbZIP72	*Os09g0456200*	*TraesCS5B02G235600*
OsbZIP72	*Os09g0456200*	*TraesCS5D02G244500*
OsbZIP77	*Os09g0540800*	*TraesCS5D02G338000*
OsbZIP77	*Os09g0540800*	*TraesCS5A02G332000*
OsbZIP77	*Os09g0540800*	*TraesCS5B02G332300*
	Cytokinin	
OsIPT1/2	*Os03g0358900/Os03g0356900*	*TraesCS1A02G057000*
OsIPT1/2	*Os03g0358900/Os03g0356900*	*TraesCS1B02G074400*
OsIPT4/5	*Os03g0810100/Os07g0211700*	*TraesCS5A02G460000*
OsIPT4/5	*Os03g0810100/Os07g0211700*	*TraesCS5D02G471100*
OsIPT4/5	*Os03g0810100/Os07g0211700*	*TraesCS1B02G323900*
OsIPT4/5	*Os03g0810100/Os07g0211700*	*TraesCS5B02G469600*
OsIPT7	*Os05g0551700*	*TraesCS1A02G376300*
OsIPT7	*Os05g0551700*	*TraesCS1B02G396700*
OsIPT7	*Os05g0551700*	*TraesCS1D02G383600*
OsIPT8	*Os01g0688300*	*TraesCS3A02G263300*
OsIPT8	*Os01g0688300*	*TraesCS3D02G263000*
OsIPT8	*Os01g0688300*	*TraesCS3B02G296500*
OsCYP735A3/4	*Os08g0429800/Os09g0403300*	*TraesCS5B02G203900*
OsCYP735A3/4	*Os08g0429800/Os09g0403300*	*TraesCS5D02G211800*
OsCYP735A3/4	*Os08g0429800/Os09g0403300*	*TraesCS5A02G204300*
LOG	*Os01g0588900*	*TraesCS3D02G213900*
LOG	*Os01g0588900*	*TraesCS3A02G211100*
LOG	*Os01g0588900*	*TraesCS3B02G241600*
OsCKX1	*Os01g0187600*	*TraesCS3B02G128700*
OsCKX1	*Os01g0187600*	*TraesCS3A02G109500*
OsCKX1	*Os01g0187600*	*TraesCS3D02G111300*
OsCKX3	*Os10g0483500*	*TraesCS1B02G176000*
OsCKX3	*Os10g0483500*	*TraesCS1A02G159600*
OsCKX3	*Os10g0483500*	*TraesCS1D02G157000*
OsCKX4	*Os01g0940000*	*TraesCS3D02G475800*
OsCKX4	*Os01g0940000*	*TraesCS3A02G481000*
OsCKX4	*Os01g0940000*	*TraesCS3B02G525300*
OsCKX5	*Os01g0775400*	*TraesCS3A02G321100*
OsCKX5	*Os01g0775400*	*TraesCS3B02G344600*
OsCKX5	*Os01g0775400*	*TraesCS3D02G310200*
OsCKX6/7	*Os02g0220000/Os02g0220100*	*TraesCS6D02G172800*
OsCKX6/7	*Os02g0220000/Os02g0220100*	*TraesCS6B02G214700*
OsCKX6/7	*Os02g0220000/Os02g0220100*	*TraesCS6A02G185800*
OsCKX6/7	*Os02g0220000/Os02g0220100*	*TraesCS6D02G172900*
OsCKX8	*Os04g0523500*	*TraesCS2B02G395200*
OsCKX8	*Os04g0523500*	*TraesCS2D02G374600*
OsCKX8	*Os04g0523500*	*TraesCS2A02G378300*
OsCKX9	*Os05g0374200*	*TraesCS1B02G248700*
OsCKX9	*Os05g0374200*	*TraesCS1A02G234800*
OsCKX9	*Os05g0374200*	*TraesCS1D02G237200*
OsCKX10	*Os06g0572300*	*TraesCS7A02G363400*
OsCKX10	*Os06g0572300*	*TraesCS7B02G264400*
OsCKX10	*Os06g0572300*	*TraesCS7D02G359700*
OsCKX11	*Os08g0460600*	*TraesCS7A02G536900*
OsCKX11	*Os08g0460600*	*TraesCS7B02G455000*
OsCKX11	*Os08g0460600*	*TraesCSU02G106300*
OsHK2	*Os10g0362300*	*TraesCS6A02G041100*
OsHK3	*Os01g0923700*	*TraesCS3D02G426600*
OsHK3	*Os01g0923700*	*TraesCS3A02G433200*
OsHK3	*Os01g0923700*	*TraesCS3B02G469000*
OsHKL1/OsCRL4	*Os12g0454800*	*TraesCS5D02G455600*
OsHKL1/OsCRL4	*Os12g0454800*	*TraesCS5B02G456500*

OsHKL1/OsCRL4	*Os12g0454800*	*TraesCS5B02G351800*
OsHKL1/OsCRL4	*Os12g0454800*	*TraesCS2D02G464000*
OsHKL1/OsCRL4	*Os12g0454800*	*TraesCS2B02G485000*
OsHP1	*Os09g0567400*	*TraesCS4A02G303000*
OsHP1	*Os09g0567400*	*TraesCS4B02G281000*
OsHP1	*Os09g0567400*	*TraesCS4A02G302900*
OsHP1	*Os09g0567400*	*TraesCS1B02G061500*
OsHP1	*Os09g0567400*	*TraesCS4D02G008800*
OsHP1	*Os09g0567400*	*TraesCS4A02G302600*
OsHP1	*Os09g0567400*	*TraesCS4D02G008700*
OsHP1	*Os09g0567400*	*TraesCS1B02G061300*
OsHP1	*Os09g0567400*	*TraesCS4B02G006500*
OsHP1	*Os09g0567400*	*TraesCS4A02G303100*
OsHP1	*Os09g0567400*	*TraesCS4D02G009000*
OsHP1	*Os09g0567400*	*TraesCS4B02G010900*
OsHP1	*Os09g0567400*	*TraesCSU02G241200*
OsHP1	*Os09g0567400*	*TraesCS4B02G011400*
OsHP1	*Os09g0567400*	*TraesCS4A02G303500*
OsHP1	*Os09g0567400*	*TraesCS4D02G009700*
OsHP1	*Os09g0567400*	*TraesCSU02G060000*
OsHP1	*Os09g0567400*	*TraesCS1B02G061400*
OsHP1	*Os09g0567400*	*TraesCS4D02G009500*
OsHP1	*Os09g0567400*	*TraesCS4B02G010800*
OsHP1	*Os09g0567400*	*TraesCS4D02G009800*
OsHP1	*Os09g0567400*	*TraesCS4A02G303200*
OsHP1	*Os09g0567400*	*TraesCS4D02G010000*
OsHP1	*Os09g0567400*	*TraesCS4A02G304200*
OsHP1	*Os09g0567400*	*TraesCS4A02G302400*
OsHP1	*Os09g0567400*	*TraesCS4D02G009300*
OsHP1	*Os09g0567400*	*TraesCS4B02G011500*
OsHP1	*Os09g0567400*	*TraesCS4A02G302300*
OsHP1	*Os09g0567400*	*TraesCSU02G214800*
OsHP1	*Os09g0567400*	*TraesCS4B02G010300*
OsHP1	*Os09g0567400*	*TraesCSU02G059800*
OsHP1	*Os09g0567400*	*TraesCS4B02G011300*
OsHP1	*Os09g0567400*	*TraesCS4B02G011600*
OsHP1	*Os09g0567400*	*TraesCS4D02G008900*
OsHP1	*Os09g0567400*	*TraesCS4D02G009400*
OsHP1	*Os09g0567400*	*TraesCS4A02G302700*
OsHP1	*Os09g0567400*	*TraesCS4D02G009900*
OsHP1	*Os09g0567400*	*TraesCS4B02G011700*
OsHP1	*Os09g0567400*	*TraesCS4A02G302500*
OsHP1	*Os09g0567400*	*TraesCS6A02G364400*
OsHP1	*Os09g0567400*	*TraesCS4B02G010700*
OsHP1	*Os09g0567400*	*TraesCSU02G060100*
OsHP1	*Os09g0567400*	*TraesCSU02G060200*
OsHP1	*Os09g0567400*	*TraesCS4B02G011000*
OsHP1	*Os09g0567400*	*TraesCSU02G059900*
OsHP1	*Os09g0567400*	*TraesCSU02G197100*
OsHP1	*Os09g0567400*	*TraesCSU02G060300*
OsHP1	*Os09g0567400*	*TraesCS4D02G009600*
OsHP1	*Os09g0567400*	*TraesCS4A02G302200*
OsHP1	*Os09g0567400*	*TraesCS4D02G279500*
OsHP1	*Os09g0567400*	*TraesCS4B02G011200*
OsHP1	*Os09g0567400*	*TraesCS4A02G304100*
OsHP1	*Os09g0567400*	*TraesCS4D02G008600*
OsHP1	*Os09g0567400*	*TraesCSU02G157700*
OsHP1	*Os09g0567400*	*TraesCS4A02G302800*
OsHP1	*Os09g0567400*	*TraesCS4B02G011100*
OsHP1	*Os09g0567400*	*TraesCS4A02G022400*
OsHP2	*Os08g0557700*	*TraesCS6A02G020400*

OsHP2	*Os08g0557700*	*TraesCS4A02G480700*
OsHP2	*Os08g0557700*	*TraesCS4A02G480800*
OsHP2	*Os08g0557700*	*TraesCS4A02G479600*
OsHP2	*Os08g0557700*	*TraesCS7D02G012700*
OsHP2	*Os08g0557700*	*TraesCS5B02G378400*
OsHP2	*Os08g0557700*	*TraesCS4A02G480600*
OsHP2	*Os08g0557700*	*TraesCS6D02G067900*
OsHP2	*Os08g0557700*	*TraesCS6D02G021700*
OsHP2	*Os08g0557700*	*TraesCS6D02G023100*
OsHP2	*Os08g0557700*	*TraesCS6B02G027800*
OsHP2	*Os08g0557700*	*TraesCS7A02G016100*
OsHP2	*Os08g0557700*	*TraesCS6D02G021500*
OsHP3	*Os01g0743800*	*TraesCS3A02G275400*
OsHP3	*Os01g0743800*	*TraesCS3D02G275300*
OsHP3	*Os01g0743800*	*TraesCS3B02G309100*
OsHP4	*Os05g0521300*	*TraesCS1D02G343800*
OsHP4	*Os05g0521300*	*TraesCS1A02G341500*
OsHP4	*Os05g0521300*	*TraesCS1B02G354200*
OsHP5	*Os05g0186100*	*TraesCS1B02G141500*
OsHP5	*Os05g0186100*	*TraesCS1A02G122300*
OsHP5	*Os05g0186100*	*TraesCS1D02G123300*
OsRR1	*Os04g0442300*	*TraesCS2A02G309700*
OsRR1	*Os04g0442300*	*TraesCS2B02G326800*
OsRR1	*Os04g0442300*	*TraesCS2D02G308000*
OsRR3	*Os02g0830200*	*TraesCS6A02G416400*
OsRR3	*Os02g0830200*	*TraesCS6D02G401600*
OsRR4	*Os01g0952500*	*TraesCS4B02G178900*
OsRR4	*Os01g0952500*	*TraesCS3B02G548600*
OsRR4	*Os01g0952500*	*TraesCS3D02G494600*
OsRR5	*Os04g0524300*	*TraesCS2A02G377900*
OsRR5	*Os04g0524300*	*TraesCS2B02G394900*
OsRR5	*Os04g0524300*	*TraesCS2D02G374300*
OsRR6	*Os04g0673300*	*TraesCS2A02G551100*
OsRR6	*Os04g0673300*	*TraesCS2D02G552200*
OsRR6	*Os04g0673300*	*TraesCS2B02G582300*
OsRR9/10	*Os11g0143300/Os12g0139400*	*TraesCS5D02G140200*
OsRR9/10	*Os11g0143300/Os12g0139400*	*TraesCS5A02G131600*
OsRR9/10	*Os11g0143300/Os12g0139400*	*TraesCS5B02G132900*
OsRR11	*Os02g0631700*	*TraesCS6B02G259700*
OsRR11	*Os02g0631700*	*TraesCS6A02G221800*
OsRR11	*Os02g0631700*	*TraesCS6D02G213700*
OsRR13	*Os04g0212200*	*TraesCS2B02G086800*
OsRR13	*Os04g0212200*	*TraesCS2A02G072500*
OsRR13	*Os04g0212200*	*TraesCS2D02G071500*
OsRR14	*Os03g0742300*	*TraesCS5B02G385400*
OsRR14	*Os03g0742300*	*TraesCS5A02G381600*
OsRR14	*Os03g0742300*	*TraesCS5D02G391200*
OsRR16	*Os01g0904700*	*TraesCS3D02G384500*
OsRR16	*Os01g0904700*	*TraesCS3B02G423600*
OsRR16	*Os01g0904700*	*TraesCS3A02G391600*
OsRR17	*Os02g0182100*	*TraesCS6A02G146200*
OsRR17	*Os02g0182100*	*TraesCS6D02G135500*
OsRR17	*Os02g0182100*	*TraesCS6B02G174400*
OsRR18	*Os02g0796500*	*TraesCS6D02G342200*
OsRR19	*Os03g0224200*	*TraesCS4A02G063100*
OsRR19	*Os03g0224200*	*TraesCS4B02G240100*
OsRR19	*Os03g0224200*	*TraesCS4D02G239900*
OsRR20	*Os06g0183100*	*TraesCS7A02G146700*
OsRR20	*Os06g0183100*	*TraesCS7D02G148000*
OsRR20	*Os06g0183100*	*TraesCS7B02G049200*
OsRR20	*Os06g0183100*	*TraesCS7B02G049000*

OsRR20	*Os06g0183100*	*TraesCS7D02G148200*
OsRR20	*Os06g0183100*	*TraesCS7A02G146500*
OsRR20	*Os06g0183100*	*TraesCS7A02G146400*
OsRR21	*Os06g0647200*	*TraesCS7B02G420800*
OsRR21	*Os06g0647200*	*TraesCS7B02G421000*
OsRR21	*Os06g0647200*	*TraesCS7D02G499700*
OsRR21	*Os06g0647200*	*TraesCS7B02G408600*
OsRR22/Ehd1	*Os10g0463400*	*TraesCS7D02G499600*
OsRR22/Ehd1	*Os10g0463400*	*TraesCSU02G196300*
OsRR22/Ehd1	*Os10g0463400*	*TraesCS7B02G422100*
OsRR22/Ehd1	*Os10g0463400*	*TraesCS7D02G500600*
OsRR22/Ehd1	*Os10g0463400*	*TraesCS7D02G489600*
OsRR22/Ehd1	*Os10g0463400*	*TraesCS7A02G510300*
OsRR22/Ehd1	*Os10g0463400*	*TraesCSU02G040900*
OsRR22/Ehd1	*Os10g0463400*	*TraesCS7D02G525900*
OsRR22/Ehd1	*Os10g0463400*	*TraesCS7A02G539600*
OsRR22/Ehd1	*Os10g0463400*	*TraesCS7B02G422000*
OsRR22/Ehd1	*Os10g0463400*	*TraesCS7B02G408700*
OsRR22/Ehd1	*Os10g0463400*	*TraesCSU02G105200*
OsRR22/Ehd1	*Os10g0463400*	*TraesCS3A02G473600*
OsRR22/Ehd1	*Os10g0463400*	*TraesCS7A02G511300*
OsRR22/Ehd1	*Os10g0463400*	*TraesCS7B02G420900*
OsRR22/Ehd1	*Os10g0463400*	*TraesCS7A02G511100*
OsRR22/Ehd1	*Os10g0463400*	*TraesCS7B02G461300*
OsRR22/Ehd1	*Os10g0463400*	*TraesCSU02G179800*
OsRR22/Ehd1	*Os10g0463400*	*TraesCS7A02G502300*
OsRR22/Ehd1	*Os10g0463400*	*TraesCS3B02G517000*
OsRR22/Ehd1	*Os10g0463400*	*TraesCS3A02G473800*
	Brassinosteroids	
OsSMT1	*Os07g0206700*	*TraesCS5A02G510200*
OsSMT1	*Os07g0206700*	*TraesCS4D02G336800*
OsSMT1	*Os07g0206700*	*TraesCS4B02G340700*
OsFACKEL1	*Os01g0354200*	*TraesCS1B02G446300*
OsFACKEL1	*Os01g0354200*	*TraesCS1D02G423500*
OsFACKEL1	*Os01g0354200*	*TraesCS1A02G416000*
OsHYD1	*Os01g0103600*	*TraesCS7D02G068300*
OsHYD1	*Os01g0103600*	*TraesCS3A02G079400*
OsHYD1	*Os01g0103600*	*TraesCS3B02G094700*
OsHYD1	*Os01g0103600*	*TraesCS3D02G079800*
OsDWF7	*Os01g0134500*	*TraesCS3D02G041900*
OsDWF7	*Os01g0134500*	*TraesCS3B02G046100*
OsDWF7	*Os01g0134500*	*TraesCS3A02G037600*
OsDWF5	*Os02g0465400*	*TraesCS3B02G536500*
OsDWF5	*Os02g0465400*	*TraesCS3A02G488600*
OsDWF5	*Os02g0465400*	*TraesCS3D02G484700*
OsDIM	*Os10g0397400*	*TraesCS7A02G559400*
OsDIM	*Os10g0397400*	*TraesCS7D02G550700*
OsDIM	*Os10g0397400*	*TraesCS7B02G484200*
OsDET2;1/2	*Os11g0184100/Os01g0851600*	*TraesCS3A02G366000*
OsDET2;1/2	*Os11g0184100/Os01g0851600*	*TraesCS3D02G359100*
OsDET2;1/2	*Os11g0184100/Os01g0851600*	*TraesCS3B02G397800*
OsDWARF4/CYP90B2	*Os03g0227700*	*TraesCS4B02G234100*
OsDWARF4/CYP90B2	*Os03g0227700*	*TraesCS3B02G586500*
OsDWARF4/CYP90B2	*Os03g0227700*	*TraesCS3A02G519000*
OsDWARF4/CYP90B2	*Os03g0227700*	*TraesCS3D02G526400*
OsDWARF4/CYP90B2	*Os03g0227700*	*TraesCS4A02G078000*
OsDWARF4/CYP90B2	*Os03g0227700*	*TraesCS3D02G526300*
OsDWARF4/CYP90B2	*Os03g0227700*	*TraesCS4D02G235200*
D11/CYP724B1	*Os04g0469800*	*TraesCS2A02G331800*
D11/CYP724B1	*Os04g0469800*	*TraesCS2D02G331100*
D11/CYP724B1	*Os04g0469800*	*TraesCS2B02G350400*

D2/CYP90D2	*Os07g0136800*	*TraesCS3A02G103800*
D2/CYP90D2	*Os07g0136800*	*TraesCS3D02G106100*
D2/CYP90D2	*Os07g0136800*	*TraesCS3B02G121200*
OsCPD1/CYP90A3	*Os11g0143200/Os12g0139300*	*TraesCS5D02G139900*
OsCPD1/CYP90A3	*Os11g0143200/Os12g0139300*	*TraesCS5A02G131400*
OsCPD1(2)/CYP90A3(4)	*Os11g0143200/Os12g0139300*	*TraesCS5B02G133400*
OsDWARF/CYP85A1	*Os03g0602300*	*TraesCS2D02G014700*
OsDWARF/CYP85A1	*Os03g0602300*	*TraesCS2A02G013500*
OsDWARF/CYP85A1	*Os03g0602300*	*TraesCS2A02G013200*
OsDWARF/CYP85A1	*Os03g0602300*	*TraesCS2D02G014500*
OsDWARF/CYP85A1	*Os03g0602300*	*TraesCS2B02G004700*
OsDWARF/CYP85A1	*Os03g0602300*	*TraesCS2B02G004500*
OsDWARF/CYP85A1	*Os03g0602300*	*TraesCS2B02G004200*
OsDWARF/CYP85A1	*Os03g0602300*	*TraesCS2A02G013400*
OsDWARF/CYP85A1	*Os03g0602300*	*TraesCS2D02G014200*
OsDWARF/CYP85A1	*Os03g0602300*	*TraesCS2B02G004400*
OsDWARF/CYP85A1	*Os03g0602300*	*TraesCS2B02G004600*
OsDWARF/CYP85A1	*Os03g0602300*	*TraesCS2D02G014600*
OsDWARF/CYP85A1	*Os03g0602300*	*TraesCS2D02G014400*
OsDWARF/CYP85A1	*Os03g0602300*	*TraesCS2A02G013000*
OsBAS1L1/CYP734A4	*Os06g0600400*	*TraesCS7B02G254100*
OsBAS1L1/CYP734A4	*Os06g0600400*	*TraesCS7A02G373100*
OsBAS1L2/CYP734A6	*Os01g0388000*	*TraesCS3D02G128700*
OsBAS1L2/CYP734A6	*Os01g0388000*	*TraesCS3B02G146900*
OsBAS1L2/CYP734A6	*Os01g0388000*	*TraesCS3A02G127700*
OsBAS1L3/CYP734A2	*Os02g0204700*	*TraesCS6D02G166900*
OsBAS1L3/CYP734A2	*Os02g0204700*	*TraesCS6A02G177300*
OsBAS1L3/CYP734A2	*Os02g0204700*	*TraesCS6B02G207300*
OsBRI1	*Os01g0718300*	*TraesCS3B02G275000*
OsBRI1	*Os01g0718300*	*TraesCS3D02G246500*
OsBRI1	*Os01g0718300*	*TraesCS3A02G245000*
OsBRL1	*Os09g0293500*	*TraesCS5B02G174400*
OsBRL1	*Os09g0293500*	*TraesCS5D02G181500*
OsBRL1	*Os09g0293500*	*TraesCS5A02G177300*
OsBRL2	*Os10g0114400*	*TraesCS3B02G115800*
OsBRL2	*Os10g0114400*	*TraesCS3A02G099400*
OsBRL2	*Os10g0114400*	*TraesCS3D02G099700*
OsBAK1;1	*Os08g0174700*	*TraesCS7D02G291200*
OsBAK1;1	*Os08g0174700*	*TraesCS7B02G182300*
OsBAK1;1	*Os08g0174700*	*TraesCS7A02G293300*
OsBAK1;2	*Os04g0457800*	*TraesCS2A02G343100*
OsBAK1;2	*Os04g0457800*	*TraesCS2B02G340700*
OsBAK1;2	*Os04g0457800*	*TraesCS2D02G321400*
OsBIN2;4/OsSKetha	*Os05g0207500*	*TraesCS1D02G129000*
OsBIN2;4/OsSKetha	*Os05g0207500*	*TraesCS1B02G142300*
OsBIN2;4/OsSKetha	*Os05g0207500*	*TraesCS1A02G125000*
OsBSL1	*Os05g0144400*	*TraesCS1B02G107000*
OsBSL1	*Os05g0144400*	*TraesCS1D02G089300*
OsBSL1	*Os05g0144400*	*TraesCS1A02G088000*
OsBSL2	*Os12g0617900*	*TraesCS5A02G030300*
OsBSL2	*Os12g0617900*	*TraesCS5B02G029100*
OsBSL2	*Os12g0617900*	*TraesCS5D02G038500*
OsBZR1/BES1	*Os07g0580500*	*TraesCS2B02G219300*
OsBZR1/BES1	*Os07g0580500*	*TraesCS2D02G199900*
OsBZR1/BES1	*Os07g0580500*	*TraesCS2A02G187800*

References

Abel, S., Nguyen, M. D. and Theologis, A. 1995. The PS-IAA4/5-like Family of Early Auxin-inducible mRNAs in Arabidopsis thaliana. *Journal of Molecular Biology*. 251: 533–549.

Abel, S. and Theologis, A. 1996. Early genes and auxin action. *Plant Physiology*. 111: 9–17.

Abiko, M., Akibayashi, K., Sakata, T., Kimura, M., Kihara, M., Itoh, K., Asamizu, E., Sato, S., Takahashi, H. and Higashitani, A. 2005. High-temperature induction of male sterility during barley (Hordeum vulgare L.) anther development is mediated by transcriptional inhibition. *Sexual Plant Reproduction*. 18: 91–100.

Ahmed, F. E., Hall, A. E. and DeMason, D. A. 1992. Heat Injury During Floral Development in Cowpea (Vigna unguiculata, Fabaceae). *American Journal of Botany*. 79: 784.

Albrecht, C., Russinova, E., Hecht, V., Baaijens, E. and De Vries, S. 2005. The Arabidopsis thaliana SOMATIC EMBRYOGENESIS RECEPTOR-LIKE KINASES1 and 2 control male sporogenesis. *Plant Cell*. 17: 3337–3349.

Alfonso, M., Yruela, I., Almárcegui, S., Torrado, E., Pérez, M. A. and Picorel, R. 2001. Unusual tolerance to high temperatures in a new herbicide-resistant D1 mutant from Glycine max (L.) Merr. cell cultures deficient in fatty acid desaturation. *Planta*. 212: 573–582.

Ali, Z., Raza, Q., Atif, R. M., Aslam, U., Ajmal, M. and Chung, G. 2019. Genetic and molecular control of floral organ identity in cereals. *International Journal of Molecular Sciences*. 20: 1–30.

Alonso, J. M., Hirayama, T., Roman, G., Nourizadeh, S. and Ecker, J. R. 1999. EIN2, a Bifunctional Transducer of Ethylene and Stress Responses in Arabidopsis. *Science*. 284: 2148–2152.

Alonso, J. M., Stepanova, A. N., Solano, R., Wisman, E., Ferrari, S., Ausubel, F. M. and Ecker, J. R. 2003. Five components of the ethylene-response pathway identified in a screen for weak ethylene-insensitive mutants in Arabidopsis. *Proceedings of the*

National Academy of Sciences of the United States of America. 100: 2992–2997.

An, F., Zhao, Q., Ji, Y., Li, W., Jiang, Z., Yu, X., Zhang, C., Han, Y., He, W., Liu, Y., Zhang, S., Ecker, J. R. and Guo, H. 2010. Ethylene-induced stabilization of ETHYLENE INSENSITIVE3 and EIN3-LIKE1 is mediated by proteasomal degradation of EIN3 binding F-box 1 and 2 that requires EIN2 in Arabidopsis. *Plant Cell*. 22: 2384–2401.

Anhthu, M. S., Koen, Q. B., Hsu, K. N. M. Y., Yun, P., Mai, L., Truong, T., Beals, T. P. and Goldberg, R. B. 1999. Anther developmental defects in Arabidopsis thaliana male-sterile mutants. *Sexual Plant Reproduction*. 11: 297–322.

Ariizumi, T., Hatakeyama, K., Hinata, K., Inatsugi, R., Nishida, I., Sato, S., Kato, T., Tabata, S. and Toriyama, K. 2004. Disruption of the novel plant protein NEF1 affects lipid accumulation in the plastids of the tapetum and exine formation of pollen, resulting in male sterility in Arabidopsis thaliana. *Plant Journal*. 39: 170–181.

Ariizumi, T., Kawanabe, T., Hatakeyama, K., Sato, S., Kato, T., Tabata, S. and Toriyama, K. 2008. Ultrastructural characterization of exine development of the transient defective exine 1 mutant suggests the existence of a factor involved in constructing reticulate exine architecture from sporopollenin aggregates. *Plant and Cell Physiology*. 49: 58–67.

Asseng, S., Ewert, F., Martre, P., Rötter, R. P., Lobell, D. B., Cammarano, D., Kimball, B. A., Ottman, M. J., Wall, G. W., White, J. W., Reynolds, M. P., Alderman, P. D., Prasad, P. V. V., Aggarwal, P. K., Anothai, J., Basso, B., Biernath, C., Challinor, A. J., De Sanctis, G., *et al.* 2014. Rising temperatures reduce global wheat production. *Nature Climate Change*. 5: 143–147.

Audley, M. 2016. *UNDERSTANDING THE ROLE OF GIBBERELLIN SIGNALLING IN WHEAT ANTHER DEVELOPMENT DURING HEAT STRESS*. The University of Nottingham.

Aya, K., Ueguchi-Tanaka, M., Kondo, M., Hamada, K., Yano, K., Nishimura, M. and Matsuoka, M. 2009. Gibberellin Modulates Anther Development in Rice via the Transcriptional Regulation of GAMYB. *The Plant Cell*. 21: 1453–1472.

Bai, C., Liang, Y. and Hawkesford, M. J. 2013. Identification of QTLs associated with

seedling root traits and their correlation with plant height in wheat. *Journal of Experimental Botany*. 64: 1745–1753.

Bajguz, A. and Tretyn, A. 2003. The chemical characteristic and distribution of brassinosteroids in plants. *Phytochemistry*. 62: 1027–1046.

Baldwin, K. L., Strohm, A. K. and Masson, P. H. 2013. Gravity sensing and signal transduction in vascular plant primary roots. *American Journal of Botany*. 100: 126–142.

Band, L. R., Fozard, J. A., Godin, C., Jensen, O. E., Pridmore, T., Bennett, M. J. and King, J. R. 2012. Multiscale systems analysis of root growth and development: Modeling beyond the network and cellular scales. *Plant Cell*. 24: 3892–3906.

Bargmann, B. O. R., Vanneste, S., Krouk, G., Nawy, T., Efroni, I., Shani, E., Choe, G., Friml, J., Bergmann, D. C., Estelle, M. and Birnbaum, K. D. 2013. A map of cell type-specific auxin responses. *Molecular Systems Biology*. 9: 1–13.

Barnabás, B., Jäger, K. and Fehér, A. 2008. The effect of drought and heat stress on reproductive processes in cereals. *Plant, Cell and Environment*. 31: 11–38.

Bell, E., Creelman, R. A. and Mullet, J. E. 1995. A chloroplast lipoxygenase is required for wound-induced jasmonic acid accumulation in Arabidopsis. *Proceedings of the National Academy of Sciences of the United States of America*. 92: 8675–8679.

Biao Ma, S.-Y. C. and J.-S. Z. C. Y. X. L. 2015. Ethylene Signaling in Rice and Arabidopsis: Conserved and Diverged Aspects. *Molecular Plant*. 8: 495–505.

Binder, B. M. 2020. Ethylene signaling in plants. *Journal of Biological Chemistry*. 295: 7710–7725.

Binder, B. M., O'Malley, R. C., Wang, W., Zutz, T. C. and Bleecker, A. B. 2006. Ethylene Stimulates Nutations That Are Dependent on the ETR1 Receptor. *Plant Physiology*. 142: 1690–1700.

Binder, B. M., Walker, J. M., Gagne, J. M., Emborg, T. J., Hemmann, G., Bleecker, A. B. and Vierstra, R. D. 2007. The Arabidopsis EIN3 binding F-box proteins EBF1 and EBF2 have distinct but overlapping roles in ethylene signaling. *Plant Cell*. 19: 509–

523.

Bisson, M. M. A. and Groth, G. 2010. New insight in ethylene signaling: Autokinase activity of ETR1 modulates the interaction of receptors and EIN2. *Molecular Plant*. 3: 882–889.

Blilou, I., Xu, J., Wildwater, M., Willemsen, V., Paponov, I., Frimi, J., Heldstra, R., Aida, M., Palme, K. and Scheres, B. 2005. The PIN auxin efflux facilitator network controls growth and patterning in Arabidopsis roots. *Nature*. 433: 39–44.

Bonner, L. J. and Dickinson, H. G. 1989. Anther dehiscence in Lycopersicon esculentum Mill. *New Phytologist*. 113: 97–115.

Boston, R. S., Viitanen, P. V and Vierling, E. 1996. Molecular chaperones and protein folding in plants. *Plant Molecular Biology*. 32: 191–222.

Browne, R. G., Iacuone, S., Li, S. F., Dolferus, R. and Parish, R. W. 2018. Anther morphological development and stage determination in Triticum aestivum. *Frontiers in Plant Science*. 9: 1–13.

Burke, J. J., O'Mahony, P. J. and Oliver, M. J. 2000. Isolation of Arabidopsis mutants lacking components of acquired thermotolerance. *Plant Physiology*. 123: 575–587.

Cai, Q., Yuan, Z., Chen, M., Yin, C., Luo, Z., Zhao, X., Liang, W., Hu, J. and Zhang, D. 2014. Jasmonic acid regulates spikelet development in rice. *Nature communications*. 5: 3476.

Caldelari, D., Wang, G., Farmer, E. E. and Dong, X. 2011. Arabidopsis lox3 lox4 double mutants are male sterile and defective in global proliferative arrest. *Plant Molecular Biology*. 75: 25–33.

Canales, C., Bhatt, A. M., Scott, R. and Dickinson, H. 2002. EXS, a putative LRR receptor kinase, regulates male germline cell number and tapetal identity and promotes seed development in Arabidopsis. *Current Biology*. 12: 1718–1727.

Carminati, A., Passioura, J. B., Zarebanadkouki, M., Ahmed, M. A., Ryan, P. R., Watt, M. and Delhaize, E. 2017. Root hairs enable high transpiration rates in drying soils. *New Phytologist*. : 771–781.

Cecchetti, V., Altamura, M. M., Brunetti, P., Petrocelli, V., Falasca, G., Ljung, K., Costantino, P. and Cardarelli, M. 2013. Auxin controls arabidopsis anther dehiscence by regulating endothecium lignification and jasmonic acid biosynthesis. *Plant Journal*. 74: 411–422.

Cecchetti, V., Altamura, M. M., Falasca, G., Costantino, P. and Cardarelli, M. 2008. Auxin regulates Arabidopsis anther dehiscence, pollen maturation, and filament elongation. *Plant Cell*. 20: 1760–1774.

Chang, C., Kwok, S. F., Bleecker, A. B. and Meyerowitz, E. M. 1993. Arabidopsis ethylene-response gene ETR1: Similarity of product to two-component regulators. *Science*. 262: 539–544.

Chao, Q., Rothenberg, M., Solano, R., Roman, G., Terzaghi, W. and Ecker, J. R. 1997. Activation of the ethylene gas response pathway in arabidopsis by the nuclear protein ETHYLENE-INSENSITIVE3 and related proteins. *Cell*. 89: 1133–1144.

Chaudhury, A. M. 1993. Nuclear Genes Controlling Male Fertility. *The Plant Cell*. 5: 1277–1283.

Chaves, M. M., Costa, J. M., Zarrouk, O., Pinheiro, C., Lopes, C. M. and Pereira, J. S. 2016. Controlling stomatal aperture in semi-arid regions—The dilemma of saving water or being cool? *Plant Science*. 251: 54–64.

Chen, J. F. and Gallie, D. R. 2010. Analysis of the functional conservation of ethylene receptors between maize and Arabidopsis. *Plant Molecular Biology*. 74: 405–421.

Chen, T., Liu, J., Lei, G., Liu, Y. F., Li, Z. G., Tao, J. J., Hao, Y. J., Cao, Y. R., Lin, Q., Zhang, W. K., Ma, B., Chen, S. Y. and Zhang, J. S. 2009. Effects of tobacco ethylene receptor mutations on receptor kinase activity, plant growth and stress responses. *Plant & cell physiology*. 50: 1636–1650.

Chen, Y. F., Gao, Z., Kerris, R. J., Wang, W., Binder, B. M. and Schaller, G. E. 2010. Ethylene receptors function as components of high-molecular-mass protein complexes in Arabidopsis. *PLoS ONE*. 5: 1–10.

Cheng, H., Qin, L., Lee, S., Fu, X., Richards, D., Cao, D., Luo, D., Harberd, N. and J, P.

2004. Gibberellin regulates Arabidopsis floral development via suppression of DELLA protein function. *Development*. 131: 1055–1064.

Cheng, H., Song, S., Xiao, L., Soo, H. M., Cheng, Z., Xie, D. and Peng, J. 2009. Gibberellin acts through jasmonate to control the expression of MYB21, MYB24, and MYB57 to promote stamen filament growth in arabidopsis. *PLoS Genetics*. 5: 20–22.

Cheng, Y., Dai, X. and Zhao, Y. 2006. Auxin biosynthesis by the YUCCA flavin monooxygenases controls the formation of floral organs and vascular tissues in Arabidopsis. *Genes and Development*. 20: 1790–1799.

Chhun, T., Aya, K., Asano, K., Yamamoto, E., Morinaka, Y., Watanabe, M., Kitano, H., Ashikari, M., Matsuoka, M. and Ueguchi-Tanaka, M. 2007. Gibberellin Regulates Pollen Viability and Pollen Tube Growth in Rice. *The Plant Cell*. 19: 3876–3888.

Christopher, J. T., Christopher, M. J., Borrell, A. K., Fletcher, S. and Chenu, K. 2016. Stay-green traits to improve wheat adaptation in well-watered and water-limited environments. *Journal of Experimental Botany*. 67: 5159–5172.

Chung, H. S., Cooke, T. F., Depew, C. L., Patel, L. C., Ogawa, N., Kobayashi, Y. and Howe, G. A. 2010. Alternative splicing expands the repertoire of dominant JAZ repressors of jasmonate signaling. *The Plant Journal*. 63: 613–622.

Chung, H. S. and Howe, G. A. 2009. A critical role for the TIFY motif in repression of jasmonate signaling by a stabilized splice variant of the JASMONATE ZIM-domain protein JAZ10 in Arabidopsis. *The Plant cell*. 21: 131–145.

Clarke, S. M., Cristescu, S. M., Miersch, O., Harren, F. J. M., Wasternack, C. and Mur, L. A. J. 2009. Jasmonates act with salicylic acid to confer basal thermotolerance in Arabidopsis thaliana. *New Phytologist*. 182: 175–187.

Clarke, S. M., Mur, L. A. J., Wood, J. E. and Scott, I. M. 2004. Salicylic acid dependent signaling promotes basal thermotolerance but is not essential for acquired thermotolerance in Arabidopsis thaliana. *Plant Journal*. 38: 432–447.

Coelho Filho, M. A., Colebrook, E. H., Lloyd, D. P. A., Webster, C. P., Mooney, S. J.,

Phillips, A. L., Hedden, P. and Whalley, W. R. 2013. The involvement of gibberellin signalling in the effect of soil resistance to root penetration on leaf elongation and tiller number in wheat. *Plant and Soil*. 371: 81–94.

Colcombet, J., Boisson-Dernier, A., Ros-Palau, R., Vera, C. E. and Schroeder, J. I. 2005. Arabidopsis SOMATIC EMBRYOGENESIS RECEPTOR KINASES1 and 2 are essential for tapetum development and microspore maturation. *Plant Cell*. 17: 3350–3361.

Correa, J., Postma, J. A., Watt, M. and Wojciechowski, T. 2019. Soil compaction and the architectural plasticity of root systems. *Journal of Experimental Botany*. 70: 6019–6034.

Cristescu, S. M., Mandon, J., Arslanov, D., De Pessemier, J., Hermans, C. and Harren, F. J. M. 2013. Current methods for detecting ethylene in plants. *Annals of Botany*. 111: 347–360.

Darwin, C. 1880. *The power of movement in plants*. Edited by J. Murray. London.

Deslauriers, S. D., Alvarez, A. A., Lacey, R. F., Binder, B. M. and Larsen, P. B. 2015. Dominant gain-of-function mutations in transmembrane domain III of ERS1 and ETR1 suggest a novel role for this domain in regulating the magnitude of ethylene response in Arabidopsis. *New Phytologist*. 208: 442–455.

Devoto, A., Nieto-rostro, M., Xie, D., Ellis, C., Harmston, R., Patrick, E., Davis, J., Sherratt, L., Coleman, M. and Turner, J. G. 2002. COI1 links jasmonate signalling and fertility to the SCF ubiquitin–ligase complex in Arabidopsis. *The Plant Journal*. 32: 457–466.

Djanaguiraman, M., Prasad, P. V. V., Boyle, D. L. and Schapaugh, W. T. 2013. Soybean pollen anatomy, viability and pod set under high temperature stress. *Journal of Agronomy and Crop Science*. 199: 171–177.

Draeger, T. and Moore, G. 2017. Short periods of high temperature during meiosis prevent normal meiotic progression and reduce grain number in hexaploid wheat (Triticum aestivum L.). *Theoretical and Applied Genetics*. 130: 1785–1800.

Dreher, K. A. 2006. The Arabidopsis Aux/IAA Protein Family Has Diversified in Degradation and Auxin Responsiveness. *the Plant Cell Online*. 18: 699–714.

Du, H., Liu, H. and Xiong, L. 2013. Endogenous auxin and jasmonic acid levels are differentially modulated by abiotic stresses in rice. *Frontiers in Plant Science*. 4: 1–10.

Duan, X., Wang, X., Fu, Y., Tang, C., Li, X., Cheng, Y., Feng, H., Huang, L. and Kang, Z. 2013. TaEIL1, a wheat homologue of AtEIN3, acts as a negative regulator in the wheat-stripe rust fungus interaction. *Molecular Plant Pathology*. 14: 728–739.

Dubcovsky, J. and Dvorak, J. 2007. Genome Plasticity a Key Factor in the Success of Polyploid Wheat Under Domestication. *Science*. 316: 1862–1866.

Eady, C., Lindsey, K. and Twel, D. 1995. The Significance of Microspore Division and Division Symmetry for Vegetative Cell-Specific Transcription and Generative Cell Differentiation. *The Plant Cell*. 7: 65–74.

El-ghazaly, G. and Huysmans, S. 2001. Re-evaluation of a neglected layer in pollen wall development with comments on its evolution. *Grana*. 40: 3–16.

Ellis, C. M., Nagpal, P., Young, J. C., Hagen, G., Guilfoyle, T. J. and Reed, J. W. 2005. AUXIN RESPONSE FACTOR1 and AUXIN RESPONSE FACTOR2 regulate senescence and floral organ abscission in Arabidopsis thaliana. *Development*. 132: 4563–4574.

Endo, M., Tsuchiya, T., Hamada, K., Kawamura, S., Yano, K., Ohshima, M., Higashitani, A., Watanabe, M. and Kawagishi-Kobayashi, M. 2009. High temperatures cause male sterility in rice plants with transcriptional alterations during pollen development. *Plant and Cell Physiology*. 50: 1911–1922.

Fábián, A., Sáfrán, E., Szabó-Eitel, G., Barnabás, B. and Jäger, K. 2019. Stigma functionality and fertility are reduced by heat and drought co-stress in wheat. *Frontiers in Plant Science*. 10: 1–18.

Fendrych, M., Akhmanova, M., Merrin, J., Glanc, M., Hagihara, S., Takahashi, K., Uchida, N., Torii, K. U. and Friml, J. 2018. Rapid and reversible root growth inhibition by TIR1 auxin signalling. *Nature Plants*. 4: 453–459.

Feng, B., Liu, P., Li, G., Dong, S. T., Wang, F. H., Kong, L. A. and Zhang, J. W. 2014. Effect of Heat Stress on the Photosynthetic Characteristics in Flag Leaves at the Grain-Filling Stage of Different Heat-Resistant Winter Wheat Varieties. *Journal of Agronomy and Crop Science*. 200: 143–155.

Feng, B., Lu, D., Ma, X., Peng, Y., Sun, Y., Ning, G. and Ma, H. 2012. Regulation of the Arabidopsis anther transcriptome by DYT1 for pollen development. *Plant Journal*. 72: 612–624.

Feng, B., Zhang, C., Chen, T., Zhang, X., Tao, L. and Fu, G. 2018. Salicylic acid reverses pollen abortion of rice caused by heat stress. *BMC Plant Biology*. 18: 1–16.

Feng, X. L., Ni, W. M., Elge, S., Mueller-Roeber, B., Xu, Z. H. and Xue, H. W. 2006. Auxin flow in anther filaments is critical for pollen grain development through regulating pollen mitosis. *Plant Molecular Biology*. 61: 215–226.

Ferguson, C., Teeri, T. T., Siika-Aho, M., Read, S. M. and Bacic, A. 1998. Location of cellulose and callose in pollen tubes and grains of Nicotiana tabacum. *Planta*. 206: 452–460.

Fernández-Gómez, J., Talle, B., Tidy, A. C. and Wilson, Z. A. 2020. Accurate staging of reproduction development in Cadenza wheat by non-destructive spike analysis. *Journal of Experimental Botany*. 71: 3475–3484.

Ferrez, J., Davison, A. C. and Rebetez, M. 2011. Extreme temperature analysis under forest cover compared to an open field. *Agricultural and Forest Meteorology*. 151: 992–1001.

Firon, N., Pressman, E., Meir, S., Khoury, R. and Altahan, L. 2012. Ethylene is involved in maintaining tomato (Solanum lycopersicum) pollen quality under heat-stress conditions. *AoB PLANTS*. 2012: 1–9.

Fonseca, S., Chini, A., Hamberg, M., Adie, B., Porzel, A., Kramell, R., Miersch, O., Wasternack, C. and Solano, R. 2009. (+)-7-iso-Jasmonoyl-L-isoleucine is the endogenous bioactive jasmonate. *Nature Chemical Biology*. 5: 344–350.

Friml, J., Benková, E., Blilou, I., Wisniewska, J., Hamann, T., Ljung, K., Woody, S.,

Sandberg, G., Scheres, B., Jürgens, G. and Palme, K. 2002. AtPIN4 mediates sink-driven auxin gradients and root patterning in Arabidopsis. *Cell*. 108: 661–673.

Fu, Z., Yu, J., Cheng, X., Zong, X., Xu, J., Chen, M., Li, Z., Zhang, D. and Liang, W. 2014. The rice basic helix-loop-helix transcription factor TDR interacting protein2 is a central switch in early anther development. *Plant Cell*. 26: 1512–1524.

Fukaki, H., Tameda, S., Masuda, H. and Tasaka, M. 2002. Lateral root formation is blocked by a gain-of-function mutation in the solitary-root/IAA14 gene of Arabidopsis. *Plant Journal*. 29: 153–168.

Gagne, J. M., Smalle, J., Gingerich, D. J., Walker, J. M., Yoo, S. D., Yanagisawa, S. and Vierstra, R. D. 2004. Arabidopsis EIN3-binding F-box 1 and 2 form ubiquitin-protein ligases that repress ethylene action and promote growth by directing EIN3 degradation. *Proceedings of the National Academy of Sciences of the United States of America*. 101: 6803–6808.

Gallie, D. R. 2015. Ethylene receptors in plants - Why so much complexity? *F1000Prime Reports*. 7: 1–12.

Gallie, D. R. and Young, T. E. 2004. The ethylene biosynthetic and perception machinery is differentially expressed during endosperm and embryo development in maize. *Molecular Genetics and Genomics*. 271: 267–281.

Gamble, R. L., Coonfield, M. L. and Schaller, G. E. 1998. Histidine kinase activity of the ETR1 ethylene receptor from Arabidopsis. *Proceedings of the National Academy of Sciences of the United States of America*. 95: 7825–7829.

Gamble, R. L., Qu, X. and Schaller, G. E. 2002. Mutational analysis of the ethylene receptor ETR1. Role of the histidine kinase domain in dominant ethylene insensitivity. *Plant physiology*. 128: 1428–1438.

Gao, T. and Stock, A. M. 2006. Biological Insights from Structures of Two-Component Proteins. *NIH Public Access*. 23: 1–7.

Gawad, S., Schild, L. and Renaud, P. 2001. Micromachined impedance spectroscopy flow cytometer for cell analysis and particle sizing. *Lab on a Chip*. 1: 76–82.

Goldberg, R. B., Beals, T. P. and Sanders, S. M. 1993. Anther development: Basic principles and practical applications. *Plant Cell*. 5: 1217–1229.

Gomez, J. F., Talle, B. and Wilson, Z. A. 2015. Anther and pollen development : A conserved developmental pathway. *Journal of Integrative Plant Biology*. 57: 876–891.

Gomez, J. F. and Wilson, Z. . 2012. Non-destructive staging of barley reproductive development for molecular analysis based upon external morphology. *Journal of Experimental Botany*. 63: 4085–4094.

Gomez, J. F. and Wilson, Z. A. 2014. A barley PHD finger transcription factor that confers male sterility by affecting tapetal development. *Plant Biotechnology Journal*. 12: 765–777.

Goossens, J., Fernández-Calvo, P., Schweizer, F. and Goossens, A. 2016. Jasmonates: signal transduction components and their roles in environmental stress responses. *Plant Molecular Biology*. 91: 673–689.

Gray, W. M., Kepinski, S., Rouse, D., Leyser, O. and Estelle, M. 2001. Auxin regulates SCF TIR1-dependent degradation of AUX / IAA proteins 1. *Nature*. 414: 271–276.

Gray, W. M., Östin, A., Sandberg, G., Romano, C. P. and Estelle, M. 1998. High temperature promotes auxin-mediated hypocotyl elongation in Arabidopsis. *Proceedings of the National Academy of Sciences of the United States of America*. 95: 7197–7202.

Grbic, V. and Bleecker, A. B. 1995. Ethylene regulates the timing of leaf senescence in Arabidopsis. *The Plant Journal*. 8: 595–602.

Gubler, F., Kalla, R., Robert, J. K. and Jacobsen, J. V. 1995. Gibberellin-Regulated Expression of a myb Gene in Barley Aleurone Cells: Evidence for Myb Transactivation of a High-pl a-Amylase Gene Promoter. *The Plant Cell*. 7: 1879–1891.

Guilfoyle, T. J. and Hagen, G. 2012. Getting a grasp on domain III/IV responsible for Auxin Response Factor-IAA protein interactions. *Plant Science*. 190: 82–88.

Guo, H. and Ecker, J. R. 2003. Plant responses to ethylene gas are mediated by SCFEBF1/EBF2- dependent proteolysis of EIN3 transcription factor. *Cell*. 115: 667–677.

Guzman, P. and Ecker, J. . 1990. Exploiting the Triple Response of Arabídopsís To ldentify Ethylene-Related Mutants. *The Plant Cell*. 2: 513–523.

Hagen, G. and Guilfoyle, T. 2002. Auxin-responsive gene expression: Genes, promoters and regulatory factors. *Plant Molecular Biology*. 49: 373–385.

Hall, A. E., Chen, Q. G., Findell, J. L., Schaller, G. E., Bleecker, A. B. and Wisconsin, A. E. H. 1999. The Relationship between Ethylene Binding and Dominant Insensitivity Conferred by Mutant Forms of the ETR1 Ethylene Receptor. *Plant Physiology*. 121: 291–299.

Hall, A. E., Findell, J. L., Schaller, G. E., Sisler, E. C. and Bleecker, A. B. 2000. Ethylene perception by the ERS1 protein in Arabidopsis. *Plant Physiology*. 123: 1449–1457.

Hall, B. P., Shakeel, S. N., Amir, M., Haq, N. U., Qu, X. and Eric Schaller, G. 2012. Histidine kinase activity of the ethylene receptor ETR1 facilitates the ethylene response in Arabidopsis. *Plant Physiology*. 159: 682–695.

Hamann, T., Benkova, E., Bäurle, I., Kientz, M. and Jürgens, G. 2002. The Arabidopsis BODENLOS gene encodes an auxin response protein inhibiting MONOPTEROS-mediated embryo patterning. *Genes and Development*. 16: 1610–1615.

Hamilton, A. J., Lycett, G. W. and Grierson, D. 1990. Antisense gene that inhibits synthesis of the hormone ethylene in transgenic plants. *Nature*. 346: 284–287.

Hamza, M. A. and Anderson, W. K. 2005. Soil compaction in cropping systems: A review of the nature, causes and possible solutions. *Soil and Tillage Research*. 82: 121–145.

Han San Ku , Hiroshi Suge, L. R. and H. K. . P. 1970. Stimulation of Rice Coleoptile Growth by Ethylene. *Planta*. 70: 333–339.

Harberd, N. P., Belfield, E. and Yasumura, Y. 2009. The angiosperm gibberellin-GID1-DELLA growth regulatory mechanism: How an 'inhibitor of an inhibitor' enables

flexible response to fluctuating environments. *Plant Cell*. 21: 1328–1339.

Harrison, J. H. 1979. Pollen-stigma interaction in grasses: A brief review. *New Zealand Journal of Botany*. 17: 537–546.

Harsant, J., Pavlovic, L., Chiu, G., Sultmanis, S. and Sage, T. L. 2013. High temperature stress and its effect on pollen development and morphological components of harvest index in the C3 model grass Brachypodium distachyon. *Journal of Experimental Botany*. 64: 2971–2983.

Hartman, S., Sasidharan, R. and Voesenek, L. A. C. J. 2021. The role of ethylene in metabolic acclimations to low oxygen. *New Phytologist*. 229: 64–70.

Hasegawa, M., Nakajima, M., Takeda, K., Yamaguchi, I. and Murofushi, N. 1995. Endogenous Levels of Gibberellins in Normal and Male Sterile Anthers of Rice (Oryza sativa cv. Nihonmasari). *Bioscience, Biotechnology, and Biochemistry*. 59: 1716–1720.

He, C. J., Finlayson, S. A., Drew, M. C., Jordan, W. R. and Morgan, P. W. 1996. Ethylene biosynthesis during aerenchyma formation in roots of maize subjected to mechanical impedance and hypoxia. *Plant Physiology*. 112: 1679–1685.

Hedden, P. and Phillips, A. L. 2000. Gibberellin metabolism: New insights revealed by the genes. *Trends in Plant Science*. 5: 523–530.

Hedden, P. and Thomas, S. G. 2012. Gibberellin biosynthesis and its regulation. *Biochemical Journal*. 444: 11–25.

Heidmann, I., Schade-Kampmann, G., Lambalk, J., Ottiger, M. and Di Berardino, M. 2016. Impedance flow cytometry: A novel technique in pollen analysis. *PLoS ONE*. 11: 1–15.

Heslop-Harrison, J. 1968. TAPETAL ORIGIN OF POLLEN-COAT SUBSTANCES IN LILIUM. *New Phytologist*. 67: 779–786.

Heslop-Harrison, Y. and Heslop-Harrison, J. S. 1996. Lodicule function and filament extension in the grasses: Potassium ion movement and tissue specialization. *Annals of Botany*. 77: 573–582.

Heun, M., Schäfer-Pregl, R., Klawan, D., Castagna, R., Accerbi, M., Borghi, B. and Salamini, F. 1997. Site of einkorn wheat domestication identified by DNA fingerprinting. *Science*. 278: 1312–1314.

Hirano, K., Aya, K., Hobo, T., Sakakibara, H., Kojima, M., Shim, R. A., Hasegawa, Y., Ueguchi-Tanaka, M. and Matsuoka, M. 2008. Comprehensive transcriptome analysis of phytohormone biosynthesis and signaling genes in microspore/pollen and tapetum of rice. *Plant and Cell Physiology*. 49: 1429–1450.

Hong, S. W., Lee, U. and Vierling, E. 2003. Arabidopsis hot mutants define multiple functions required for acclimation to high temperatures. *Plant Physiology*. 132: 757–767.

Hord, C. L. H., Chen, C., DeYoung, B. J., Clark, S. E. and Ma, H. 2006. The BAM1/BAM2 receptor-like kinases are important regulators of Arabidopsis early anther development. *The Plant Cell*. 18: 1667–1680.

Hord, C. L. H., Sun, Y. J., Pillitteri, L. J., Torii, K. U., Wang, H., Zhang, S. and Ma, H. 2008. Regulation of Arabidopsis early anther development by the mitogen-activated protein kinases, MPK3 and MPK6, and the ERECTA and related receptor-like kinases. *Molecular Plant*. 1: 645–658.

Hori, Y., Kurotani, K. I., Toda, Y., Hattori, T. and Takeda, S. 2014. Overexpression of the JAZ factors with mutated jas domains causes pleiotropic defects in rice spikelet development. *Plant Signaling and Behavior*. 9: 1–7.

Howe, G. A. and Jander, G. 2008. Plant immunity to insect herbivores. *Annual Review of Plant Biology*. 59: 41–66.

Hu, J., Mitchum, M. G., Barnaby, N., Ayele, B. T., Ogawa, M., Nam, E., Lai, W. C., Hanada, A., Alonso, J. M., Ecker, J. R., Swain, S. M., Yamaguchi, S., Kamiya, Y. and Suna, T. P. 2008. Potential sites of bioactive gibberellin production during reproductive growth in Arabidopsis. *Plant Cell*. 20: 320–336.

Hua, J., Chang, C., Sun, Q. and Meyerowitz, E. M. 1995. Ethylene insensitivity conferred by Arabidopsis EPS gene. *Science*. 269: 1712–1714.

Hua, J. and Meyerowitz, E. M. 1998. Ethylene responses are negatively regulated by a receptor gene family in Arabidopsis thaliana. *Cell*. 94: 261–271.

Hua, J., Sakai, H., Nourizadeh, S., Chen, Q. G., Bleecker, A. B., Ecker, J. R. and Meyerowitz, E. M. 1998. EIN4 and ERS2 are members of the putative ethylene receptor gene family in arabidopsis. *Plant Cell*. 10: 1321–1332.

Huang, H., Liu, B., Liu, L. and Song, S. 2017. Jasmonate action in plant growth and development. *Journal of Experimental Botany*. 68: 1349–1359.

Huang, S., Cerny, R. E., Qi, Y., Bhat, D., Aydt, C. M., Hanson, D. D., Malloy, K. P. and Ness, L. A. 2003. Transgenic studies on the involvement of cytokinin and gibberellin in male development. *Plant Physiology*. 131: 1270–1282.

Ikeda, A., Ueguchi-Tanaka, M., Sonoda, Y., Kitano, H., Koshioka, M., Futsuhara, Y., Matsuoka, M. and Yamaguchi, J. 2001. slender Rice, a Constitutive Gibberellin Response Mutant, Is Caused by a Null Mutation of the SLR1 Gene, an Ortholog of the Height-Regulating Gene GAI/RGA/RHT/D8. *The Plant Cell*. 13: 999–1010.

Ishiguro, S., Kawai-Oda, A., Ueda, J., Nishida, I. and Okada, K. 2001. The DEFECTIVE IN ANTHER DEHISCENCE1 Gene Encodes a Novel Phospholipase A1 Catalyzing the Initial Step of Jasmonic Acid Biosynthesis, Which Synchronizes Pollen Maturation, Anther Dehiscence, and Flower Opening in Arabidopsis. *Plant Cell*. 13: 2191–2209.

Ishimaru, K., Takada, K., Watanabe, S., Kamada, H. and Ezura, H. 2006. Stable male sterility induced by the expression of mutated melon ethylene receptor genes in Nicotiana tabacum. *Plant Science*. 171: 355–359.

Ito, T., Nagata, N., Yoshiba, Y., Ohme-Takagi, M., Ma, H. and Shinozakif, K. 2007. Arabidopsis MALE STERILITY1 encodes a PHD-type transcription factor and regulates pollen and tapetum development. *Plant Cell*. 19: 3549–3562.

Ito, Y. and Kurata, N. 2006. Identification and characterization of cytokinin-signalling gene families in rice. *Gene*. 382: 57–65.

Itoh, H., Ueguchi-Tanaka, M., Sato, Y., Ashikari, M. and Matsuoka, M. 2002. The gibberellin signaling pathway is regulated by the appearance and disappearance of

slender rice1 in nuclei. *Plant Cell*. 14: 57–70.

Iwahori, S. 1965. High temperature injuries in tomato. IV. Development of normal flower buds and morphological abnormalities of flower buds treated with high temperature. *Journal of Japanese Society for Horticultural Science*. 34: 33–41.

Jagadish, S. V. K., Raveendran, M., Oane, R., Wheeler, T. R., Heuer, S., Bennett, J. and Craufurd, P. Q. 2010. Physiological and proteomic approaches to address heat tolerance during anthesis in rice (Oryza sativa L.). *Journal of Experimental Botany*. 61: 143–156.

Jain, M., Kaur, N., Garg, R., Thakur, J. K., Tyagi, A. K. and Khurana, J. P. 2006. Structure and expression analysis of early auxin-responsive Aux/IAA gene family in rice (Oryza sativa). *Functional & integrative genomics*. 6: 47–59.

Jaworek, P., Tarkowski, P., Hluska, T., Kouřil, Š., Vrobel, O., Nisler, J. and Kopečný, D. 2020. Characterization of five CHASE-containing histidine kinase receptors from Populus × canadensis cv. Robusta sensing isoprenoid and aromatic cytokinins. *Planta*. 251: 1–15.

Jegadeesan, S., Beery, A., Altahan, L., Meir, S., Pressman, E. and Firon, N. 2018. Ethylene production and signaling in tomato (Solanum lycopersicum) pollen grains is responsive to heat stress conditions. *Plant Reproduction*. 31: 367–383.

Ji, X., Dong, B., Shiran, B., Talbot, M. J., Edlington, J. E., Hughes, T., White, R. G., Gubler, F. and Dolferus, R. 2011. Control of abscisic acid catabolism and abscisic acid homeostasis is important for reproductive stage stress tolerance in cereals. *Plant Physiology*. 156: 647–662.

Ji, X., Shiran, B., Wan, J., Lewis, D. C., Jenkins, C. L. D., Condon, A. G., Richards, R. A. and Dolferus, R. 2010. Importance of pre-anthesis anther sink strength for maintenance of grain number during reproductive stage water stress in wheat. *Plant, Cell and Environment*. 33: 926–942.

Jia, X., Liu, P. and Lynch, J. P. 2018. Greater lateral root branching density in maize improves phosphorus acquisition from low phosphorus soil. *Journal of Experimental Botany*. 69: 4961–14790.

Jung, K. H., Han, M. J., Lee, Y. S., Kim, Y. W. Y. K., Hwang, I., Kim, M. J., Kim, Y. W. Y. K., Nahm, B. H. and An, G. 2005. Rice Undeveloped Tapetum1 is a major regulator of early tapetum development. *Plant Cell*. 17: 2705–2722.

Kaneko, M., Inukai, Y., Ueguchi-tanaka, M., Itoh, H., Izawa, T. and Kobayashi, Y. 2004. Loss-of-Function Mutations of the Rice GAMYB Gene Impair The Plant Cell. *The Plant cell*. 16: 33–44.

Kapoor, M., Sreenivasan, G. M., Goel, N. and Lewis, J. 1990. Development of thermotolerance in Neurospora crassa by heat shock and other stresses eliciting peroxidase induction. *Journal of Bacteriology*. 172: 2798–2801.

Kays, S. J., Nicklow, C. W. and Simons, D. H. 1974. Ethylene in relation to the response of roots to physical impedance. *Plant and Soil*. 40: 565–571.

Keijzer, C. J. 1987. The processes of anther dehiscence and pollen dispersal. *New Phytologist*. : 499–507.

Keijzer, C. J., Hoek, I. H. S. and Willemse, M. T. M. 1987. THE PROCESSES OF ANTHER DEHISCENCE AND POLLEN DISPERSAL III . THE DEHYDRATION OF THE FILAMENT TIP AND THE ANTHER IN THREE MONOCOTYLEDONOUS SPECIES. *New Phytologist*. 106: 281–287.

Kelliher, T. and Walbot, V. 2011. Emergence and patterning of the five cell types of the Zea mays anther locule. *Developmental Biology*. 350: 32–49.

Kieber, J. J., Rothenberg, M., Roman, G., Feldmann, K. A. and Ecker, J. R. 1993. CTR1, a negative regulator of the ethylene response pathway in arabidopsis, encodes a member of the Raf family of protein kinases. *Cell*. 72: 427–441.

Kim, B. 1996. Two dominant photomorphogenic mutations of Arabidopsis thaliana identified as suppressor mutations of hy2. The Plant Journal. : 441–456.

Kim, H., Helmbrecht, E. E., Stalans, M. B., Schmitt, C., Patel, N., Wen, C.-K., Wang, W. and Binder, B. M. 2011. Ethylene Receptor ETHYLENE RECEPTOR1 Domain Requirements for Ethylene Responses in Arabidopsis Seedlings. *Plant Physiology*. 156: 417–429.

Kim, J., Harter, K. and Theologis, A. 1997. Protein-protein interactions among the Aux/IAA proteins. *Proceedings of the National Academy of Sciences of the United States of America*. 94: 11786–91.

Kim, S. Y., Hong, C. B. and Lee, I. 2001. Heat shock stress causes stage-specific male sterility in Arabidopsis thaliana. *Journal of Plant Research*. 114: 301–307.

Kitomi, Y., Inahashi, H., Takehisa, H., Sato, Y. and Inukai, Y. 2012. OsIAA13-mediated auxin signaling is involved in lateral root initiation in rice. *Plant Science*. 190: 116–122.

Kleine-Vehn, J., Ding, Z., Jones, A. R., Tasaka, M., Morita, M. T. and Friml, J. 2010. Gravity-induced PIN transcytosis for polarization of auxin fluxes in gravity-sensing root cells. *Proceedings of the National Academy of Sciences of the United States of America*. 107: 22344–22349.

Knight, L. I. and Crocker, W. 1913. Toxicity of Smoke. *Botanical Gazette*. LV: 337–371.

Kobayashi, M., Sakurai, A., Saka, H. and Takahashi, N. 1989. Quantitative analysis of endogenous gibberellins in normal and dwarf cultivars of rice. *Plant and Cell Physiology*. 30: 963–969.

Kobayashi, M., Yamaguchi, I., Murofushi, N., Ota, Y. and Takahashi, N. 1988. Fluctuation and Localization of Endogenous Gibberellins in Rice. *Agricultural and Biological Chemistry*. 52: 1189–1194.

Korasick, D. A., Enders, T. A. and Strader, L. C. 2013. Auxin biosynthesis and storage forms. *Journal of Experimental Botany*. 64: 2541–2555.

Kosová, K., Vítámvás, P. and Prášil, I. T. 2011. Expression of dehydrins in wheat and barley under different temperatures. *Plant Science*. 180: 46–52.

Krasileva, K. V., Vasquez-Gross, H. A., Howell, T., Bailey, P., Paraiso, F., Clissold, L., Simmonds, J., Ramirez-Gonzalez, R. H., Wang, X., Borrill, P., Fosker, C., Ayling, S., Phillips, A. L., Uauy, C. and Dubcovsky, J. 2017. Uncovering hidden variation in polyploid wheat. *Proceedings of the National Academy of Sciences*. 114: 913–921.

Ku, S., Yoon, H., Suh, H. S. and Chung, Y. Y. 2003. Male-sterility of thermosensitive genic male-sterile rice is associated with premature programmed cell death of the tapetum. *Planta*. 217: 559–565.

Kuderová, A., Gallová, L., Kuricová, K., Nejedlá, E., Čurdová, A., Micenková, L., Plíhal, O., Šmajs, D., Spíchal, L. and Hejátko, J. 2015. Identification of AHK2- and AHK3-like cytokinin receptors in Brassica napus reveals two subfamilies of AHK2 orthologues. *Journal of Experimental Botany*. 66: 339–353.

Lanahan, M. B. and Ho, T. H. D. 1988. Slender barley: A constitutive gibberellin-response mutant. *Planta*. 175: 107–114.

Larkindale, J., Hall, J. D., Knight, M. R. and Vierling, E. 2005. Heat Stress Phenotypes of Arabidopsis Mutants Implicate Multiple Signaling Pathways in the Acquisition of Thermotolerance. *Plant Physiology*. 138: 882–897.

Larkindale, J. and Knight, M. R. 2002. Protection against heat stress-induced oxidative damage in Arabidopsis involves calcium, abscisic acid, ethylene, and salicylic acid. *Plant Physiology*. 128: 682–695.

Laskowski, M. J., Williams, M. E., Nusbaum, H. C. and Sussex, I. M. 1995. Formation of lateral root meristems is a two-stage process. *Development*. 121: 3303–3310.

Leitz, G., Kang, B. H. and Schoenwaelder, M. E. A. 2009. Statolith sedimentation kinetics and force transduction to the cortical endoplasmic reticulum in gravity-sensing Arabidopsis columella cells. *Plant Cell*. 21: 843–860.

Lewis, D. R., Negi, S., Sukumar, P. and Muday, G. K. 2011. Ethylene inhibits lateral root development, increases IAA transport and expression of PIN3 and PIN7 auxin efflux carriers. *Development*. 138: 3485–3495.

Leyser, O. 2018. Auxin signaling. *Plant Physiology*. 176: 465–479.

Li, H., Yuan, Z., Vizcay-Barrena, G., Yang, C., Liang, W., Zong, J., Wilson, Z. A. and Zhang, D. 2011. PERSISTENT TAPETAL CELL1 encodes a PHD-finger protein that is required for tapetal cell death and pollen development in rice. *Plant Physiology*. 156: 615–630.

Li, N., Zhang, D. S., Liu, H. S., Yin, C. S., Li, X. X., Liang, W. Q., Yuan, Z., Xu, B., Chu, H. W., Wang, J., Wen, T. Q., Huang, H., Luo, D., Hong, M. and Zhang, D. B. 2006. The rice tapetum degeneration retardation gene is required for tapetum degradation and anther development. *Plant Cell*. 18: 2999–3014.

Li, W., Ma, M., Feng, Y., Li, H., Wang, Y., Ma, Y., Li, M., An, F. and Guo, H. 2015. EIN2-Directed Translational Regulation of Ethylene Signaling in Arabidopsis. *Cell*. 163: 670–683.

Li, Y., Dai, X., Cheng, Y. and Zhao, Y. 2011. NPY genes play an essential role in root gravitropic responses in Arabidopsis. *Molecular Plant*. 4: 171–179.

Liang, X., Wang, H., Mao, L., Hu, Y., Dong, T., Zhang, Y., Wang, X. and Bi, Y. 2012. Involvement of COP1 in ethylene- and light-regulated hypocotyl elongation. *Planta*. 236: 1791–1802.

Lin, H., Yu, J., Pearce, S. P., Zhang, D. and Wilson, Z. A. 2017. RiceAntherNet: a gene co-expression network for identifying anther and pollen development genes. *Plant Journal*. 92: 1076–1091.

Liu, J. X., Liao, D. Q., Oane, R., Estenor, L., Yang, X. E., Li, Z. C. and Bennett, J. 2006. Genetic variation in the sensitivity of anther dehiscence to drought stress in rice. *Field Crops Research*. 97: 87–100.

Liu, Y., Song, Q., Li, Daxing, Yang, X. and Li, Dequan 2017. Multifunctional roles of plant dehydrins in response to environmental stresses. *Frontiers in Plant Science*. 8: 2015–2018.

Liu, Z., Bao, W., Liang, W., Yin, J. and Zhang, D. 2010. Identification of gamyb-4 and Analysis of the Regulatory Role of GAMYB in Rice Anther Development. *Journal of Integrative Plant Biology*. 52: 670–678.

Lobell, D. B. and Field, C. B. 2007. Global scale climate–crop yield relationships and the impacts of recent warming. *Environmental Research Letters*. 2: 1–7.

Lomin, S. N., Yonekura-Sakakibara, K., Romanov, G. A. and Sakakibara, H. 2011. Ligand-binding properties and subcellular localization of maize cytokinin receptors.

Journal of Experimental Botany. 62: 5149–5159.

Longin, C. F. H., Mühleisen, J., Maurer, H. P., Zhang, H., Gowda, M. and Reif, J. C. 2012. Hybrid breeding in autogamous cereals. *Theoretical and Applied Genetics*. 125: 1087–1096.

Luo, J., Zhou, J. J. and Zhang, J. Z. 2018. Aux/IAA gene family in plants: Molecular structure, regulation, and function. *International Journal of Molecular Sciences*. 19: 1–17.

Luo, S., Li, Q., Liu, S., Pinas, N. M., Tian, H. and Wang, S. 2015. Constitutive expression of OsIAA9 affects starch granules accumulation and root gravitropic response in arabidopsis. *Frontiers in Plant Science*. 6: 1–10.

Lynch, J. P. 2019. Root phenotypes for improved nutrient capture: an underexploited opportunity for global agriculture. *New Phytologist*. 223: 548–564.

Ma, B., He, S. J., Duan, K. X., Yin, C. C., Chen, H. W. H., Yang, C., Xiong, Q., Song, Q. X., Lu, X., Chen, H. W. H., Zhang, W. K., Lu, T. G., Chen, S. Y. and Zhang, J. S. 2013. Identification of rice ethylene-response mutants and characterization of MHZ7/OsEIN2 in distinct ethylene response and yield trait regulation. *Molecular Plant*. 6: 1830–1848.

Ma, B., Yin, C. C., He, S. J., Lu, X., Zhang, W. K., Lu, T. G., Chen, S. Y. and Zhang, J. S. 2014. Ethylene-Induced Inhibition of Root Growth Requires Abscisic Acid Function in Rice (Oryza sativa L.) Seedlings. *PLoS Genetics*. 10.

Ma, H. 2005. Molecular genetic analyses of microsporogenesis and microgametogenesis in flowering plants. *Annual Review of Plant Biology*. 56: 393–434.

Ma, L. J., Yang, Z. N. and Zhang, S. 2013. DEX1, a plasma membrane-localized protein, functions in microspore development by affecting CalS5 expression in Arabidopsis thaliana. *Chinese Science Bulletin*. 58: 2855–2861.

Ma, Q. H. and Wang, X. M. 2003. Characterization of an ethylene receptor homologue from wheat and its expression during leaf senescence. *Journal of*

Experimental Botany. 54: 1489–1490.

Magneschi, L. and Perata, P. 2009. Rice germination and seedling growth in the absence of oxygen. *Annals of Botany*. 103: 181–196.

Von Malek, B., Van Der Graaff, E., Schneitz, K. and Keller, B. 2002. The Arabidopsis male-sterile mutant dde2-2 is defective in the ALLENE OXIDE SYNTHASE gene encoding one of the key enzymes of the jasmonic acid biosynthesis pathway. *Planta*. 216: 187–192.

Mandaokar, A. and Browse, J. 2009. MYB108 acts together with MYB24 to regulate jasmonate-mediated stamen maturation in Arabidopsis. *Plant Physiology*. 149: 851–862.

Mao, C., Wang, S., Jia, Q. and Wu, P. 2006. OsEIL1, a rice homolog of the Arabidopsis EIN3 regulates the ethylene response as a positive component. *Plant Molecular Biology*. 61: 141–152.

Matsui, T., Omasa, K. and Horie, T. 1997. High Temperature-Induced Spikelet Sterility of Japonica Rice at Flowering in Relation to Air Temperature, Humidity and Wind Velocity Conditions. *Chemical Pharmaceutical Bulletin*. 66: 449–455.

Matsui, T., Omasa, K. and Horie, T. 2000. High temperature at flowering inhibits swelling of pollen grains, a driving force for thecae dehiscence in rice (Oryza sativa L.). *Plant Production Science*. 3: 430–434.

Matsui, T., Omasa, K. and Horie, T. 2001. Comparison between anthers of two rice (Oryza sativa L.) Cultivars with tolerance to high temperatures at flowering or susceptibility. *Plant Production Science*. 4: 36–40.

Maucher, H., Hause, B., Feussner, I., Ziegler, J. and Wasternack, C. 2000. Allene oxide synthases of barley (Hordeum vulgare cv. Salome): Tissue specific regulation in seedling development. *The Plant journal : for cell and molecular biology*. 21: 199–213.

Mayerhofer, H., Panneerselvam, S., Kaljunen, H., Tuukkanen, A., Mertens, H. D. T. and Mueller-Dieckmann, J. 2015. Structural model of the cytosolic domain of the

plant ethylene receptor 1 (ETR1). *Journal of Biological Chemistry*. 290: 2644–2658.

McConn, M. and Browse, J. 1996. The Critical Requirement of Linolenic Acid is Pollen Development, Not Photosynthesis in an Arabidopsis Mutant. *The Plant Cell*. 8: 403–416.

Mcfadden, E. S. and Sears, E. R. 1946. The origin of triticum spelta and its free-threshing hexaploid relatives. *Journal of Heredity*. 37: 81–89.

Merchante, C., Brumos, J., Yun, J., Hu, Q., Spencer, K. R., Enríquez, P., Binder, B. M., Heber, S., Stepanova, A. N. and Alonso, J. M. 2015. Gene-Specific Translation Regulation Mediated by the Hormone-Signaling Molecule EIN2. *Cell*. 163: 684–697.

Miguel, M. A., Postma, J. A. and Lynch, J. P. 2015. Phene synergism between root hair length and basal root growth angle for phosphorus Acquisition. *Plant Physiology*. 167: 1430–1439.

Millar, A. A. and Gubler, F. 2005. The Arabidopsis GAMYB-like Genes, MYB33 and MYB65, are microRNA-regulated genes that redundantly facilitate anther development. *Plant Cell*. 17: 705–721.

Mironova, V. V., Omelyanchuk, N. A., Wiebe, D. S. and Levitsky, V. G. 2014. Computational analysis of auxin responsive elements in the Arabidopsis thaliana L. genome. *BMC Genomics*. 15: 1–14.

Mitchum, M. G., Yamaguchi, S., Hanada, A., Kuwahara, A., Yoshioka, Y., Kato, T., Tabata, S., Kamiya, Y. and Sun, T. P. 2006. Distinct and overlapping roles of two gibberellin 3-oxidases in Arabidopsis development. *Plant Journal*. 45: 804–818.

Mizelle, M. B., Sethi, R., Ashton, M. E. and Jensen, W. A. 1989. Sexual Plant Reproduction Development of the pollen grain and tapetum of wheat (Triticum aestirum) in untreated plants and plants treated with chemical hybridizing agent RH0007. *Sexual Plant Reproduction*. 2: 231–232.

Mockaitis, K. and Estelle, M. 2008. Auxin receptors and plant development: a new signaling paradigm. *Annual review of cell and developmental biology*. 24: 55–80.

Morita, M. T. and Tasaka, M. 2004. Gravity sensing and signaling. *Current Opinion in*

Plant Biology. 7: 712–718.

Moussatche, P. and Klee, H. J. 2004. Autophosphorylation activity of the Arabidopsis ethylene receptor multigene family. *Journal of Biological Chemistry*. 279: 48734–48741.

Mubarok, S., Hoshikawa, K., Okabe, Y., Yano, R., Tri, M. D., Ariizumi, T. and Ezura, H. 2019. Evidence of the functional role of the ethylene receptor genes SlETR4 and SlETR5 in ethylene signal transduction in tomato. *Molecular Genetics and Genomics*. 294: 301–313.

Müller-Dieckmann, H. J., Grantz, A. A. and Kim, S. H. 1999. The structure of the signal receiver domain of the Arabidopsis thaliana ethylene receptor ETR1. *Structure*. 7: 1547–1556.

Murray, F., Kalla, R., Jacobsen, J. and Gubler, F. 2003. A role for HvGAMYB in anther development. *Plant Journal*. 33: 481–491.

Nagpal, P., Ellis, C. M., Weber, H., Ploense, S. E., Barkawi, L. S., Guilfoyle, T. J., Hagen, G., Alonso, J. M., Cohen, J. D., Farmer, E. E., Ecker, J. R. and Reed, J. W. 2005. Auxin response factors ARF6 and ARF8 promote jasmonic acid production and flower maturation. *Development*. 132: 4107–4118.

Nakajima, M., Yamaguchi, I. and Kizawa, S. 1991. Semi-Quantification of GA. 32: 511–513.

Niu, N., Liang, W., Yang, X., Jin, W., Wilson, Z. A., Hu, J. and Zhang, D. 2013. EAT1 promotes tapetal cell death by regulating aspartic proteases during male reproductive development in rice. *Nature Communications*. 4: 1–11.

Nonomura, K., Miyoshi, K., Eiguchi, M., Suzuki, T., Miyao, A., Hirochika, H. and Kurata, N. 2003. The MSP1 Gene Is Necessary to Restrict the Number of Cells Entering into Male and Female Sporogenesis and to Initiate Anther Wall Formation in Rice. *The Plant Cell*. 15: 1728–1739.

Normanly, J., Grisafi, P., Fink, G. R. and Bartel, B. 1997. Arabidopsis mutants resistant to the auxin effects of indole-3-acetonitrile are defective in the nitrilase

encoded by the NIT1 gene. *Plant Cell*. 9: 1781–1790.

Ogawara, T., Higashi, K., Kamada, H. and Ezura, H. 2003. Ethylene advances the transition from vegetative growth to flowering in Arabidopsis thaliana. *Journal of Plant Physiology*. 160: 1335–1340.

Okabe, Y., Asamizu, E., Saito, T., Matsukura, C., Ariizumi, T., Brs, C., Rothan, C., Mizoguchi, T. and Ezura, H. 2011. Tomato TILLING technology: Development of a reverse genetics tool for the efficient isolation of mutants from micro-tom mutant libraries. *Plant and Cell Physiology*. 52: 1994–2005.

Okada, A., Arndell, T., Borisjuk, N., Sharma, N., Watson-Haigh, N. S., Tucker, E. J., Baumann, U., Langridge, P. and Whitford, R. 2019. CRISPR/Cas9-mediated knockout of Ms1 enables the rapid generation of male-sterile hexaploid wheat lines for use in hybrid seed production. *Plant Biotechnology Journal*. 17: 1905–1913.

Oliver, S. N., Dennis, E. S. and Dolferus, R. 2007. ABA regulates apoplastic sugar transport and is a potential signal for cold-induced pollen sterility in rice. *Plant and Cell Physiology*. 48: 1319–1330.

Oliver, S. N., Van Dongen, J. T., Alfred, S. C., Mamun, E. A., Zhao, X., Saini, H. S., Fernandes, S. F., Blanchard, C. L., Sutton, B. G., Geigenberger, P., Dennis, E. S. and Dolferus, R. 2005. Cold-induced repression of the rice anther-specific cell wall invertase gene OSINV4 is correlated with sucrose accumulation and pollen sterility. *Plant, Cell and Environment*. 28: 1534–1551.

Olmedo, G., Guo, H., Gregory, B. D., Nourizadeh, S. D., Aguilar-Henonin, L., Li, H., An, F., Guzman, P. and Ecker, J. R. 2006. ETHYLENE-INSENSITIVE5 encodes a 5’→3’ exoribonuclease required for regulation of the EIN3-targeting F-box proteins EBF1/2. *Proceedings of the National Academy of Sciences of the United States of America*. 103: 13286–13293.

Oshino, T., Abiko, M., Saito, R., Ichiishi, E., Endo, M., Kawagishi-Kobayashi, M. and Higashitani, A. 2007. Premature progression of anther early developmental programs accompanied by comprehensive alterations in transcription during high-temperature injury in barley plants. *Molecular Genetics and Genomics*. 278: 31–42.

Oshino, T., Miura, S., Kikuchi, S., Hamada, K., Yano, K., Watanabe, M. and Higashitani, A. 2011. Auxin depletion in barley plants under high-temperature conditions represses DNA proliferation in organelles and nuclei via transcriptional alterations. *Plant, Cell and Environment*. 34: 284–290.

Ouellet, F., Overvoorde, P. J. and Theologis, A. 2001. IAA17/AXR3: biochemical insight into an auxin mutant phenotype. *The Plant cell*. 13: 829–41.

Overvoorde, P. J., Okushima, Y., Alonso, J. M., Chan, A., Chang, C., Ecker, J. R., Hughes, B., Liu, A., Onodera, C., Quach, H., Smith, A., Yu, G. and Theologis, A. 2005. Functional genomic analysis of the AUXIN/INDOLE-3-ACETIC ACID gene family members in Arabidopsis thaliana. *Plant Cell*. 17: 3282–3300.

Owen, H. A. and Makaroff, C. A. 1995. Ultrastructure of microsporogenesis and microgametogenesis in Arabidopsis thaliana (L .) Heynh . ecotype Wassilewskija (Brassicaceae). *Protoplasma*. 185: 7–21.

Ozga, J. A., Kaur, H., Savada, R. P. and Reinecke, D. M. 2017. Hormonal regulation of reproductive growth under normal and heat-stress conditions in legume and other model crop species. *Journal of Experimental Botany*. 68: 1885–1894.

Pandey, B., Huang, G., Bhosale, R., Hartman, S., Jose, L., Sturrock, C. J., Martin, O. C., Karady, M., Voesenek, L., Ljung, K., Lynch, J., Brown, K. M., Whalley, W. R., Mooney, S. J., Zhang, D. and Bennett, M. J. 2021. Plant roots sense soil compaction through restricted ethylene diffusion. *Science*. 371: 276–280.

Papini, A., Mosti, S. and Brighigna, L. 1999. Programmed-cell-death events during tapetum development of angiosperms. *Protoplasma*. 207: 213–221.

Pareek, A., Singh, A., Kumar, M., Kushwaha, H. R., Lynn, A. M. and Singla-Pareek, S. L. 2006. Whole-genome analysis of Oryza sativa reveals similar architecture of two-component signaling machinery with Arabidopsis. *Plant Physiology*. 142: 380–397.

Parish, R. W. and Li, S. F. 2010. Death of a tapetum: A programme of developmental altruism. *Plant Science*. 178: 73–89.

Park, Halitschke, R., Kim, H. B., Baldwin, I. T., Feldmann, K. A. and Feyereisen, R.

2002. A knock-out mutation in allene oxide synthase results in male sterility and defective wound signal transduction in Arabidopsis due to a block in jasmonic acid biosynthesis. *The Plant Journal*. 31: 1–12.

Park, J. Y., Kim, H. J. and Kim, J. 2002. Mutation in domain II of IAA1 confers diverse auxin-related phenotypes and represses auxin-activated expression of Aux/IAA genes in steroid regulator-inducible system. *Plant Journal*. 32: 669–683.

Pearce, S., Ferguson, A., King, J. and Wilson, Z. A. 2015. FlowerNet : A Gene Expression Correlation Network for Anther and Pollen Development. *Plant Physiology*. 167: 1717–1730.

Peet, M. M., Sato, S. and Gardner, R. G. 1998. Comparing heat stress effects on male-fertile and male-sterile tomatoes. *Plant, Cell and Environment*. 21: 225–231.

Pickett, F. B., Wilson, A. K. and Estelle, M. 1990. The aux 1 mutation of Arabidopsis confers both auxin and ethylene resistance. *Plant Physiology*. 94: 1462–1466.

Plackett, A. R. G., Ferguson, A. C., Powers, S. J., Wanchoo-Kohli, A., Phillips, A. L., Wilson, Z. A., Hedden, P. and Thomas, S. G. 2014. DELLA activity is required for successful pollen development in the Columbia ecotype of Arabidopsis. *New Phytologist*. 201: 825–836.

Plackett, A. R. G., Powers, S. J., Fernandez-Garcia, N., Urbanova, T., Takebayashi, Y., Seo, M., Jikumaru, Y., Benlloch, R., Nilsson, O., Ruiz-Rivero, O., Phillips, A. L., Wilson, Z. A., Thomas, S. G. and Hedden, P. 2012. Analysis of the developmental roles of the arabidopsis gibberellin 20-oxidases demonstrates that GA20ox1, -2, and -3 are the dominant paralogs. *Plant Cell*. 24: 941–960.

Polit, J. T., Maszewski, J. and Kaźmierczak, A. 2003. Effect of BAP and IAA on the expression of G1 and G2 control points and G1-S and G2-M transitions in root meristem cells of Vicia faba. *Cell Biology International*. 27: 559–566.

Potuschak, T., Lechner, E., Parmentier, Y., Yanagisawa, S., Grava, S., Koncz, C. and Genschik, P. 2003. EIN3-dependent regulation of plant ethylene hormone signaling by two Arabidopsis F box proteins: EBF1 and EBF2. *Cell*. 115: 679–689.

Potuschak, T., Vansiri, A., Binder, B. M., Lechner, E., Vierstra, R. D. and Genschik, P. 2006. The exoribonuclease XRN4 is a component of the ethylene response pathway in Arabidopsis. *Plant Cell*. 18: 3047–3057.

Prasad, P. V. V., Boote, K. J., Allen, L. H., Sheehy, J. E. and Thomas, J. M. G. 2006. Species, ecotype and cultivar differences in spikelet fertility and harvest index of rice in response to high temperature stress. *Field Crops Research*. 95: 398–411.

Prasad, P. V. V. and Djanaguiraman, M. 2014. Response of floret fertility and individual grain weight of wheat to high temperature stress: Sensitive stages and thresholds for temperature and duration. *Functional Plant Biology*. 41: 1261–1269.

Pucciariello, C., Banti, V. and Perata, P. 2012. ROS signaling as common element in low oxygen and heat stresses. *Plant Physiology and Biochemistry*. 59: 3–10.

Qi, P. F., Jiang, Y. F., Guo, Z. R., Chen, Q., Ouellet, T., Zong, L. J., Wei, Z. Z., Wang, Y., Zhang, Y. Z., Xu, B. J., Kong, L., Deng, M., Wang, J. R., Chen, G. Y., Jiang, Q. T., Lan, X. J., Li, W., Wei, Y. M. and Zheng, Y. L. 2019. Transcriptional reference map of hormone responses in wheat spikes. *BMC Genomics*. 20: 1–13.

Qi, T., Huang, H., Song, S. and Xie, D. 2015. Regulation of jasmonate-mediated stamen development and seed production by a bHLH-MYB complex in Arabidopsis. *Plant Cell*. 27: 1620–1633.

Qiao, H., Chang, K. N., Yazaki, J. and Ecker, J. R. 2009. Interplay between ethylene, ETP1/ETP2 F-box proteins, and degradation of EIN2 triggers ethylene responses in Arabidopsis. *Genes and Development*. 23: 512–521.

Qiao, L., Zhang, X., Han, X., Zhang, L., Li, X., Zhan, H., Ma, J., Luo, P., Zhang, W., Cui, L., Li, X. and Chang, Z. 2015. A genome-wide analysis of the auxin/indole-3-acetic acid gene family in hexaploid bread wheat (Triticum aestivum L.). *Plant Science*. 30: 1–14.

Qin, D., Wu, H., Peng, H., Yao, Y., Ni, Z., Li, Z., Zhou, C. and Sun, Q. 2008. Heat stress-responsive transcriptome analysis in heat susceptible and tolerant wheat (Triticum aestivum L.) by using Wheat Genome Array. *BMC genomics*. 9: 1–19.

Qu, X. and Schaller, G. E. 2004. Requirement of the histidine kinase domain for signal transduction by the ethylene receptor ETR1. *Plant Physiology*. 136: 2961–2970.

Quilichini, T. D., Grienenberger, E. and Douglas, C. J. 2015. Phytochemistry The biosynthesis , composition and assembly of the outer pollen wall : A tough case to crack. *Phytochemistry*. 113: 170–182.

Rademacher, E. H., Lokerse, A. S., Schlereth, A., Llavata-Peris, C. I., Bayer, M., Kientz, M., FreireRios, A., Borst, J. W., Lukowitz, W., Jürgens, G. and Weijers, D. 2012. Different Auxin Response Machineries Control Distinct Cell Fates in the Early Plant Embryo. *Developmental Cell*. 22: 211–222.

Rahman, A., Amakawa, T., Goto, N. and Tsurumi, S. 2001. Auxin is a positive regulator for ethylene-mediated response in the growth of arabidopsis roots. *Plant and Cell Physiology*. 42: 301–307.

Ramírez-González, R. H., Borrill, P., Lang, D., Harrington, S. A., Brinton, J., Venturini, L., Davey, M., Jacobs, J., Van Ex, F., Pasha, A., Khedikar, Y., Robinson, S. J., Cory, A. T., Florio, T., Concia, L., Juery, C., Schoonbeek, H., Steuernagel, B., Xiang, D., *et al.* 2018. The transcriptional landscape of polyploid wheat. *Science*. 361.

Ramos, J. A., Zenser, N., Leyser, O. and Callis, J. 2001. Rapid degradation of auxin/indoleacetic acid proteins requires conserved amino acids of domain II and is proteasome dependent. *Plant Cell*. 13: 2349–2360.

Ray, D. K., Mueller, N. D., West, P. C. and Foley, J. A. 2013. Yield Trends Are Insufficient to Double Global Crop Production by 2050. *PLoS ONE*. 8: 1–8.

Reed, J. W. 2001. Roles and activities of Aux/IAA proteins in Arabidopsis. *Trends in Plant Science*. 6: 420–425.

Reed, J. W., Elumalai, R. P. and Chory, J. 1998. Suppressors of an Arabidopsis thaliana phyB mutation identify genes that control light signaling and hypocotyl elongation. *Genetics*. 148: 1295–1310.

Reyes, J. L. and Chua, N. H. 2007. ABA induction of miR159 controls transcript levels

of two MYB factors during Arabidopsis seed germination. *Plant Journal*. 49: 592–606.

Richards, D. E., King, K. E., Ait-ali, T. and Harberd, N. P. 2001. How gibberellin regulates plant growth and development: A molecular genetic analysis of gibberellin signaling. *Annual Review of Plant Biology*. 52: 67–88.

Richmond, T. A. and Bleecker, A. B. 1999. A defect in β-oxidation causes abnormal inflorescence development in Arabidopsis. *Plant Cell*. 11: 1911–1923.

Riemann, M., Haga, K., Shimizu, T., Okada, K., Ando, S., Mochizuki, S., Nishizawa, Y., Yamanouchi, U., Nick, P., Yano, M., Minami, E., Takano, M., Yamane, H. and Iino, M. 2013. Identification of rice Allene Oxide Cyclase mutants and the function of jasmonate for defence against Magnaporthe oryzae. *Plant Journal*. 74: 226–238.

Rieu, I., Ruiz-Rivero, O., Fernandez-Garcia, N., Griffiths, J., Powers, S. J., Gong, F., Linhartova, T., Eriksson, S., Nilsson, O., Thomas, S. G., Phillips, A. L. and Hedden, P. 2008. The gibberellin biosynthetic genes AtGA20ox1 and AtGA20ox2 act, partially redundantly, to promote growth and development throughout the Arabidopsis life cycle. *Plant Journal*. 53: 488–504.

Rieu, I., Wolters-Arts, M., Derksen, J., Mariani, C. and Weterings, K. 2003. Ethylene regulates the timing of anther dehiscence in tobacco. *Planta*. 217: 131–137.

Rinaldi, M. A., Liu, J., Enders, T. A., Bartel, B. and Strader, L. C. 2012. A gain-of-function mutation in IAA16 confers reduced responses to auxin and abscisic acid and impedes plant growth and fertility. *Plant Molecular Biology*. 79: 359–373.

Robinson, V. L., Buckler, D. R. and Stock, A. M. 2000. A tale of two components: A novel kinase and a regulatory switch. *Nature Structural Biology*. 7: 626–633.

Rodríguez, F. I., Esch, J. J., Hall, A. E., Binder, B. M., Eric Schaller, G. and Bleecker, A. B. 1999. A copper cofactor for the ethylene receptor ETR1 from Arabidopsis. *Science*. 283: 996–998.

Rouse, D., Mackay, P., Stirnberg, P., Estelle, M. and Leyser, O. 1998. Changes in auxin response from mutations in an AUX/IAA gene. *Science*. 279: 1371–1373.

Ruiz-Vera, U. M., Siebers, M. H., Jaiswal, D., Ort, D. R. and Bernacchi, C. J. 2018. Canopy warming accelerates development in soybean and maize, offsetting the delay in soybean reproductive development by elevated CO2 concentrations. *Plant Cell and Environment*. 41: 2806–2820.

Růžička, K., Ljung, K., Vanneste, S., Podhorská, R., Beeckman, T., Friml, J. and Benková, E. 2007. Ethylene regulates root growth through effects on auxin biosynthesis and transport-dependent auxin distribution. *Plant Cell*. 19: 2197–2212.

Rzewuski, G. and Sauter, M. 2008. Ethylene biosynthesis and signaling in rice. *Plant Science*. 175: 32–42.

Saini, H. S. and Aspinall, D. 1982. Abnormal Sporogenesis In Wheat (Triticum-Aestivum L) Induced By Short Periods Of High-Temperature. *Annals of Botany*. 49: 835–846.

Saini, H. S., Sedgley, M. and Aspinall, D. 1983. Effect of Heat Stress during Floral Development on Pollen Tube Growth and Ovary Anatomy in Wheat (Triticum aestivum L .). *Australian Journal of Physiology*. 10: 137–144.

Saini, H. S., Sedgley, M. and Aspinall, D. 1984. Developmental Anatomy in Wheat of Male Sterility Induced by Heat Stress, Water Deficit or Abscisic Acid. *Aust. J. Plant Physiol*. 11: 243–253.

Sakai, H., Hua, J., Chen, Q. G., Chang, C., Medrano, L. J., Bleecker, a B. and Meyerowitz, E. M. 1998. ETR2 is an ETR1-like gene involved in ethylene signaling in Arabidopsis. *Proceedings of the National Academy of Sciences of the United States of America*. 95: 5812–7.

Sakai, H., Mizuno, H., Kawahara, Y., Wakimoto, H., Ikawa, H., Kawahigashi, H., Kanamori, H., Matsumoto, T., Itoh, T. and Gaut, B. S. 2011. Retrogenes in rice (Oryza sativa L. ssp. japonica) exhibit correlated expression with their source genes. *Genome Biology and Evolution*. 3: 1357–1368.

Sakakibara, H. 2006. Cytokinins: Activity, biosynthesis, and translocation. *Annual Review of Plant Biology*. 57: 431–449.

Sakata, T., Oshino, T., Miura, S., Tomabechi, M., Tsunaga, Y., Higashitani, N., Miyazawa, Y., Takahashi, H., Watanabe, M. and Higashitani, A. 2010. Auxins reverse plant male sterility caused by high temperatures. *Proceedings of the National Academy of Sciences*. 107: 8569–8574.

Sakata, T., Takahashi, H., Nishiyama, I. and Higashitani, A. 2000. Effects of high temperature on the development of pollen mother cells and microspores in Barley Hordeum vulgare L. *Journal of Plant Research*. 113: 395–402.

Sanders, P. M., Lee, P. Y., Biesgen, C., Boone, J. D., Beals, T. P., Weiler, E. W., Goldberg, R. B. and Goldberg, R. B. 2000. The Arabidopsis DELAYED DEHISCENCE1 Gene Encodes an Enzyme in the Jasmonic Acid Synthesis Pathway. *The Plant Cell*. 12: 1041–1061.

Dos Santos Maraschin, F., Memelink, J. and Offringa, R. 2009. Auxin-induced, SCFTIR1-mediated poly-ubiquitination marks AUX/IAA proteins for degradation. *Plant Journal*. 59: 100–109.

Sarquis, J. I., Jordan, W. R. and Morgan, P. W. 1991. Ethylene evolution from maize (Zea mays L.) Seedling roots and shoots in response to mechanical impedance. *Plant Physiology*. 96: 1171–1177.

Sasaki, A., Itoh, H., Gomi, K., Ueguchi-Tanaka, M., Ishiyama, K., Kobayashi, M., Jeong, D. H., An, G., Kitano, H., Ashikari, M. and Matsuoka, M. 2003. Accumulation of phosphorylated repressor for Gibberellin signaling in an F-box mutant. *Science*. 299: 1896–1898.

Satake, T. and Harase, H. 1974. Male Sterility Caused by Cooling Treatment at the Young Microspore Stage in Rice Plants. *Proc Crop Science*. 43: 36–39.

Satler, S. and Kende, H. 1985. Growth of Rice. *Growth Lakeland*. 79: 194–198.

Sato, E. M., Hijazi, H., Bennett, M. J., Vissenberg, K. and Swarup, R. 2015. New insights into root gravitropic signalling. *Journal of Experimental Botany*. 66: 2155–2165.

Sato, S., Peet, M. M. and Thomas, J. F. 2002. Determining critical pre- and post-

anthesis periods and physiological processes in Lycopersicon esculentum Mill. exposed to moderately elevated temperatures. *Journal of Experimental Botany*. 53: 1187–1195.

Schaller, G. E., Ladd, A. N., Lanahan, M. B., Spanbauer, J. M. and Bleecker, A. B. 1995. The Ethylene Response Mediator ETR1 from Arabidopsis Forms a Disulfide-linked Dimer. *The Journal of Biological Chemistry*. 270: 12526–12530.

Schiefthaler, U., Balasubramanian, S., Sieber, P., Chevalier, D., Wisman, E. and Schneitz, K. 1999. Molecular analysis of NOZZLE, a gene involved in pattern formation and early sporogenesis during sex organ development in Arabidopsis thaliana. *Proceedings of the National Academy of Sciences of the United States of America*. 96: 11664–11669.

Schmülling, T., Werner, T., Riefler, M., Krupková, E. and Bartrina Y Manns, I. 2003. Structure and function of cytokinin oxidase/dehydrogenase genes of maize, rice, Arabidopsis and other species. *Journal of Plant Research*. 116: 241–252.

Schott-Verdugo, S., Müller, L., Classen, E., Gohlke, H. and Groth, G. 2019. Structural Model of the ETR1 Ethylene Receptor Transmembrane Sensor Domain. *Scientific Reports*. 9: 1–14.

Schwartz, S. H., Tan, B. C., Gage, D. A., Zeevaart, J. A. D. and McCarty, D. R. 1997. Specific oxidative cleavage of carotenoids by VP14 of maize. *Science*. 276: 1872–1874.

Scott, R. J., Spielman, M. and Dickinson, H. G. 2004. Stamen Structure and Function. *The Plant Cell*. 16: 46–60.

Sharma, L., Dalal, M., Verma, R. K., Kumar, S. V. V., Yadav, S. K., Pushkar, S., Kushwaha, S. R., Bhowmik, A. and Chinnusamy, V. 2018. Auxin protects spikelet fertility and grain yield under drought and heat stresses in rice. *Environmental and Experimental Botany*. 150: 9–24.

Shewry, P. R. 2009. Wheat. *Journal of Experimental Botany*. 60: 1537–1553.

Shi, Q., Zhang, Y., To, V. T., Shi, J., Zhang, D. and Cai, W. 2020. Genome-wide

characterization and expression analyses of the auxin/indole-3-acetic acid (Aux/IAA) gene family in barley (Hordeum vulgare L.). *Scientific Reports*. 10: 1–14.

Shi, W., Li, X., Schmidt, R. C., Struik, P. C., Yin, X. and Jagadish, S. V. K. 2018. Pollen germination and in vivo fertilization in response to high-temperature during flowering in hybrid and inbred rice. *Plant Cell and Environment*. 41: 1287–1297.

Shinoyama, H., Sano, T., Saito, M., Ezura, H., Aida, R., Nomura, Y. and Kamada, H. 2012. Induction of male sterility in transgenic chrysanthemums (Chrysanthemum morifolium Ramat.) by expression of a mutated ethylene receptor gene, Cm-ETR1/H69A, and the stability of this sterility at varying growth temperatures. *Molecular Breeding*. 29: 285–295.

Šimura, J., Antoniadi, I., Široká, J., Tarkowská, D., Strnad, M., Ljung, K. and Novák, O. 2018. Plant Hormonomics: Multiple Phytohormone Profiling by Targeted Metabolomics. *Plant Physiology*. 177: 476–489.

Smalle, J., Haegman, M., Kurepa, J., Van Montagu, M. and Van Der Straeten, D. 1997. Ethylene can stimulate Arabidopsis hypocotyl elongation in the light. *Proceedings of the National Academy of Sciences of the United States of America*. 94: 2756–2761.

Smalle, J. and Vierstra, R. D. 2004. The Ubiquitin 26S Proteasome Proteolytic Pathway. *Annual Review of Plant Biology*. 55: 555–590.

De Smet, I., Tetsumura, T., De Rybel, B., dit Frey, N. F., Laplaze, L., Casimiro, I., Swarup, R., Naudts, M., Vanneste, S., Audenaert, D., Inzé, D., Bennett, M. J. and Beeckman, T. 2007. Auxin-dependent regulation of lateral root positioning in the basal meristem of Arabidopsis. *Development*. 134: 681–690.

Solano, R., Stepanova, A., Chao, Q. and Ecker, J. R. 1998. Nuclear events in ethylene signaling: A transcriptional cascade mediated by ETHYLENE-INSENSITIVE3 and ETHYLENE-RESPONSE-FACTOR1. *Genes and Development*. 12: 3703–3714.

Song, S., Qi, T., Huang, H., Ren, Q., Wu, D., Chang, C., Peng, W., Liu, Y., Peng, J. and Xie, D. 2011. The jasmonate-ZIM domain proteins interact with the R2R3-MYB transcription factors MYB21 and MYB24 to affect jasmonate-regulated stamen

development in Arabidopsis. *Plant Cell*. 23: 1000–1013.

Sorensen, A. M., Kröber, S., Unte, U. S., Huijser, P., Dekker, K. and Saedler, H. 2003. The Arabidopsis aborted microspores (ams) gene encodes a MYC class transcription factor. *Plant Journal*. 33: 413–423.

Spíchal, L., Rakova, N. Y., Riefler, M., Mizuno, T., Romanov, G. A., Strnad, M. and Schmülling, T. 2004. Two cytokinin receptors of Arabidopsis thaliana, CRE1/AHK4 and AHK3, differ in their ligand specificity in a bacterial assay. *Plant and Cell Physiology*. 45: 1299–1305.

Stadler, R., Truernit, E., Gahrtz, M. and Sauer, N. 1999. The AtSUC1 sucrose carrier may represent the osmotic driving force for anther dehiscence and pollen tube growth in Arabidopsis. *Plant Journal*. 19: 269–278.

Staswick, P. E., Tiryaki, I. and Rowe, M. L. 2002. Jasmonate Response Locus JAR1 and Several Related Arabidopsis Genes Encode Enzymes of the Firefly Luciferase Superfamily That Show Activity on Jasmonic, Salicylic, and Indole-3-Acetic Acids in an Assay for Adenylation. *The Plant Cell*. 14: 1405–1415.

Stintzi, A. and Browse, J. 2000. The Arabidopsis male-sterile mutant, opr3, lacks the 12-oxophytodienoic acid reductase required for jasmonate synthesis. *Proceedings of the National Academy of Sciences of the United States of America*. 97: 10625–10630.

Suza, W. P. and Staswick, P. E. 2008. The role of JAR1 in Jasmonoyl-l-isoleucine production during Arabidopsis wound response. *Planta*. 227: 1221–1232.

Suzuki, K., Takeda, H., Tsukaguchi, T. and Egawa, Y. 2001. Ultrastructural study on degeneration of tapetum in anther of snap bean (Phaseolus vulgaris L.) under heat stress. *Sexual Plant Reproduction*. 13: 293–299.

Swarup, R., Perry, P., Hagenbeek, D., Van Der Straeten, D., Beemster, G. T. S., Sandberg, G., Bhalerao, R., Ljung, K. and Bennett, M. J. 2007. Ethylene upregulates auxin biosynthesis in Arabidopsis seedlings to enhance inhibition of root cell elongation. *Plant Cell*. 19: 2186–2196.

Szemenyei, H., Hannon, M. and Long, J. A. 2008. TOPLESS mediates auxin-dependent transcriptional repression during Arabidopsis embryogenesis. *Science*. 319: 1384–1386.

Takada, K., Ishimaru, K., Kamada, H. and Ezura, H. 2006. Anther-specific expression of mutated melon ethylene receptor gene Cm-ERS1/H70A affected tapetum degeneration and pollen grain production in transgenic tobacco plants. *Plant Cell Reports*. 25: 936–941.

Takada, K., Ishimaru, K., Minamisawa, K., Kamada, H. and Ezura, H. 2005. Expression of a mutated melon ethylene receptor gene Cm-ETR1/H69A affects stamen development in Nicotiana tabacum. *Plant Science*. 169: 935–942.

Talukder, A. S. M. H. M., McDonald, G. K. and Gill, G. S. 2014. Effect of short-term heat stress prior to flowering and early grain set on the grain yield of wheat. *Field Crops Research*. 160: 54–63.

Tan, X., Calderon-Villalobos, L. I. A., Sharon, M., Zheng, C., Robinson, C. V., Estelle, M. and Zheng, N. 2007. Mechanism of auxin perception by the TIR1 ubiquitin ligase. *Nature*. 446: 640–645.

Tang, R. S., Zheng, J. C., Jin, Z. Q., Zhang, D. D., Huang, Y. H. and Chen, L. G. 2008. Possible correlation between high temperature-induced floret sterility and endogenous levels of IAA, GAs and ABA in rice (Oryza sativa L.). *Plant Growth Regulation*. 54: 37–43.

Tatematsu, K., Kumagai, S., Muto, H., Sato, A., Watahiki, M. K., Liscum, E. and Yamamoto, K. T. 2004. MASSUGU2 Encodes Aux/IAA19, an Auxin-Regulated Protein That Functions Together with the Transcriptional Activator NPH4/ARF7 to RegulateDifferential Growth Responses of Hypocotyl and Formation of Lateral Roots in Arabidopsis thaliana. *The Plant Cell*. 16: 379–393.

Thines, B., Katsir, L., Melotto, M., Niu, Y., Mandaokar, A., Liu, G., Nomura, K., He, S. Y., Howe, G. A. and Browse, J. 2007. JAZ repressor proteins are targets of the SCF(COI1) complex during jasmonate signalling. *Nature*. 448: 661–665.

Tian, G. W., Chen, M. H., Zaltsman, A. and Citovsky, V. 2006. Pollen-specific pectin

methylesterase involved in pollen tube growth. *Developmental Biology*. 294: 83–91.

Tian, Q. and Reed, J. W. 1999. Control of auxin-regulated root development by the Arabidopsis thaliana SHY2/IAA3 gene. *Development*. 126: 711–21.

Tilman, D., Balzer, C., Hill, J. and Befort, B. L. 2011. Global food demand and the sustainable intensification of agriculture. *Proceedings of the National Academy of Sciences*. 108: 20260–20264.

Timpte, C., Wilson, A. K. and Estelle, M. 1994. The axr2-1 mutation of Arabidopsis thaliana is a gain-of-function mutation that disrupts an early step in auxin response. *Genetics*. 138: 1239–1249.

Tiryaki, I. and Staswick, P. E. 2002. An Arabidopsis mutant defective in jasmonate response is allelic to the auxin-signaling mutant axr1. *Plant Physiology*. 130: 887–894.

Tiwari, S. B., Hagen, G. and Guilfoyle, T. J. 2004. Aux/IAA Proteins Contain a Potent Transcriptional Repression Domain. *Plant Cell*. 16: 533–543.

Tsuchisaka, A., Yu, G., Jin, H., Alonso, J. M., Ecker, J. R., Zhang, X., Gao, S. and Theologis, A. 2009. A combinatorial interplay among the 1-aminocyclopropane-1-carboxylate isoforms regulates ethylene biosynthesis in Arabidopsis thaliana. *Genetics*. 183: 979–1003.

Tucker, E. J., Baumann, U., Kouidri, A., Suchecki, R., Baes, M., Garcia, M., Okada, T., Dong, C., Wu, Y., Sandhu, A., Singh, M., Langridge, P., Wolters, P., Albertsen, M. C., Cigan, A. M. and Whitford, R. 2017. Molecular identification of the wheat male fertility gene Ms1 and its prospects for hybrid breeding. *Nature Communications*. 8.

Tyler, L., Thomas, S. G., Hu, J., Dill, A., Alonso, J. M., Ecker, J. R. and Sun, T. P. 2004. Della proteins and gibberellin-regulated seed germination and floral development in Arabidopsis. *Plant Physiology*. 135: 1008–1019.

Ueguchi-Tanaka, M., Ashikari, M., Nakajima, M., Itoh, H., Katoh, E., Kobayashi, M., Chow, T. Y., Hsing, Y. I. C., Kitano, H., Yamaguchi, I. and Matsuoka, M. 2005. GIBBERELLIN INSENSITIVE DWARF1 encodes a soluble receptor for gibberellin.

Nature. 437: 693–698.

Uehara, T., Okushima, Y., Mimura, T., Tasaka, M. and Fukaki, H. 2008. Domain II mutations in CRANE/IAA18 suppress lateral root formation and affect shoot development in Arabidopsis thaliana. *Plant and Cell Physiology*. 49: 1025–1038.

Ulmasov, T., Murfett, J., Hagen, G. and Guilfoyle, T. J. 1997. Creation of a Highly Active Synthetic AuxRE. *Society*. 9: 1963–1971.

Urbanová, T., Tarkowská, D., Novák, O., Hedden, P. and Strnad, M. 2013. Analysis of gibberellins as free acids by ultra performance liquid chromatography-tandem mass spectrometry. *Talanta*. 112: 85–94.

Varnier, A.-L., Mazeyrat-Gourbeyre, F., Sangwan, R. S. and Clément, C. 2005. Programmed cell death progressively models the development of anther sporophytic tissues from the tapetum and is triggered in pollen grains during maturation. *Journal of Structural Biology*. 152: 118–128.

Vizcay-Barrena, G. and Wilson, Z. A. 2006. Altered tapetal PCD and pollen wall development in the Arabidopsis ms1 mutant. *Journal of Experimental Botany*. 57: 2709–2717.

Voet-Van-Vormizeele, J. and Groth, G. 2008. Ethylene controls autophosphorylation of the histidine kinase domain in ethylene receptor ETR1. *Molecular Plant*. 1: 380–387.

De Vries, A. P. 1971. Flowering biology of wheat, particularly in view of hybrid seed production - A review. *Euphytica*. 20: 152–170.

Wang, A., Xia, Q., Xie, W., Datla, R. and Selvaraj, G. 2003. The classical Ubisch bodies carry a sporophytically produced structural protein (RAFTIN) that is essential for pollen development. *Proceedings of the National Academy of Sciences of the United States of America*. 100: 14487–14492.

Wang, B., Xue, J. S., Yu, Y. H., Liu, S. Q., Zhang, J. X., Yao, X. Z., Liu, Z. X., Xu, X. F. and Yang, Z. N. 2017. Fine regulation of ARF17 for anther development and pollen formation. *BMC Plant Biology*. 17: 1–12.

Wang, J.-W., Wang, L.-J., Mao, Y.-B., Cai, W.-J., Xue, H.-W. and Chen, X.-Y. 2005. Control of Root Cap Formation by MicroRNA-Targeted Auxin Response Factors in Arabidopsis. *The Plant Cell*. 17: 2204–2216.

Wang, M., Yan, W., Peng, X., Chen, Z., Xu, C., Wu, J., Deng, X. W. and Tang, X. 2020. Identification of late-stage pollen-specific promoters for construction of pollen-inactivation system in rice. *Journal of Integrative Plant Biology*. 62: 1246–1263.

Wang, Q., Zhang, W., Yin, Z. and Wen, C. K. 2013. Rice constitutive triple-Response2 is involved in the ethylene-Receptor signalling and regulation of various aspects of rice growth and development. *Journal of Experimental Botany*. 64: 4863–4875.

Wang, S., Bai, Y., Shen, C., Wu, Y., Zhang, S., Jiang, D., Guilfoyle, T. J., Chen, M. and Qi, Y. 2010. Auxin-related gene families in abiotic stress response in Sorghum bicolor. *Functional and Integrative Genomics*. 10: 533–546.

Wang, W., Esch, J. J., Shiu, S.-H., Agula, H., Binder, B. M., Chang, C., Patterson, S. E. and Bleecker, A. B. 2006. Identification of important regions for ethylene binding and signaling in the transmembrane domain of the ETR1 ethylene receptor of Arabidopsis. *The Plant cell*. 18: 3429–3442.

Wang, Y., Deng, D., Bian, Y., Lv, Y. and Xie, Q. 2010. Genome-wide analysis of primary auxin-responsive Aux/IAA gene family in maize (Zea mays. L.). *Molecular Biology Reports*. 37: 3991–4001.

Wang, Y. and Kumar, P. P. 2007. Characterization of two ethylene receptors PhERS1 and PhETR2 from petunia: PhETR2 regulates timing of anther dehiscence. *Journal of Experimental Botany*. 58: 533–544.

Wang, Y., Sun, F., Cao, H., Peng, H., Ni, Z., Sun, Q. and Yao, Y. 2012. TamiR159 Directed Wheat TaGAMYB Cleavage and Its Involvement in Anther Development and Heat Response. *PLoS ONE*. 7: 1–10.

Wasternack, C. and Hause, B. 2013. Jasmonates: Biosynthesis, perception, signal transduction and action in plant stress response, growth and development. An update to the 2007 review in Annals of Botany. *Annals of Botany*. 111: 1021–1058.

Watanabe, H., Saigusa, M., Hase, S., Hayakawa, T. and Satoh, S. 2004. Cloning of a cDNA encoding an ETR2-like protein (Os-ERL1) from deep water rice (Oryza sativa L.) and increase in its mRNA level by submergence, ethylene, and gibberellin treatments. *Journal of Experimental Botany*. 55: 1145–1148.

Wen, X., Zhang, C., Ji, Y., Zhao, Q., He, W., An, F., Jiang, L. and Guo, H. 2012. Activation of ethylene signaling is mediated by nuclear translocation of the cleaved EIN2 carboxyl terminus. *Cell Research*. 22: 1613–1616.

Whitford, R., Fleury, D., Reif, J. C., Garcia, M., Okada, T., Korzun, V. and Langridge, P. 2013. Hybrid breeding in wheat: Technologies to improve hybrid wheat seed production. *Journal of Experimental Botany*. 64: 5411–5428.

Wilson, Z. A., Song, J., Taylor, B. and Yang, C. 2011. The final split: The regulation of anther dehiscence. *Journal of Experimental Botany*. 62: 1633–1649.

Worley, C. K., Zenser, N., Ramos, J., Rouse, D., Leyser, O., Theologis, A. and Callis, J. 2000. Degradation of Aux/IAA proteins is essential for normal auxin signalling. *Plant Journal*. 21: 553–562.

Wu, H. and Cheung, A. Y. 2000. Programmed cell death in plant reproduction. *Plant Molecular Biology*. 44: 267–281.

Wu, J., Peng, Z., Liu, S., He, Y., Cheng, L., Kong, F., Wang, J. and Lu, G. 2012. Genome-wide analysis of Aux/IAA gene family in Solanaceae species using tomato as a model. *Molecular Genetics and Genomics*. 287: 295–311.

Wu, M. F., Yamaguchi, N., Xiao, J., Bargmann, B., Estelle, M., Sang, Y. and Wagner, D. 2015. Auxin-regulated chromatin switch directs acquisition of flower primordium founder fate. *eLife*. 4: 1–20.

Wu, Y. S. and Yang, C. Y. 2019. Ethylene-mediated signaling confers thermotolerance and regulates transcript levels of heat shock factors in rice seedlings under heat stress. *Botanical Studies*. 60: 1–12.

Xiao, Y., Chen, Y., Charnikhova, T., Mulder, P. P. J., Heijmans, J., Hoogenboom, A., Agalou, A., Michel, C., Morel, J. B., Dreni, L., Kater, M. M., Bouwmeester, H., Wang,

M., Zhu, Z. and Ouwerkerk, P. B. F. 2014. OsJAR1 is required for JA-regulated floret opening and anther dehiscence in rice. *Plant Molecular Biology*. 86: 19–33.

Xie, F., Liu, Q. and Wen, C. K. 2006. Receptor signal output mediated by the ETR1 N terminus is primarily subfamily I receptor dependent. *Plant Physiology*. 142: 492–508.

Xin, M., Wang, Y., Yao, Y., Xie, C., Peng, H., Ni, Z. and Sun, Q. 2010. Diverse set of microRNAs are responsive to powdery mildew infection and heat stress in wheat (Triticum aestivum L.). *BMC Plant Biology*. 10.

Xu, J., Ding, Z., Vizcay-Barrena, G., Shi, J., Liang, W., Yuan, Z., Werck-Reichhart, D., Schreiber, L., Wilson, Z. A. and Zhang, D. 2014. Aborted microspores acts as a master regulator of pollen wall formation in Arabidopsis. *Plant Cell*. 26: 1544–1556.

Xu, J., Wolters-Arts, M., Mariani, C., Huber, H. and Rieu, I. 2017. Heat stress affects vegetative and reproductive performance and trait correlations in tomato (Solanum lycopersicum). *Euphytica*. 213: 1–12.

Xu, J., Yang, C., Yuan, Z., Zhang, Dasheng, Gondwe, M. Y., Ding, Z., Liang, W., Zhang, Dabing and Wilson, Z. A. 2010. The ABORTED MICROSPORES regulatory network is required for postmeiotic male reproductive development in Arabidopsis thaliana. *Plant Cell*. 22: 91–107.

Xu, L., Zhao, H., Ruan, W., Deng, M., Wang, F., Peng, J., Luo, J., Chen, Z. and Yi, K. 2017. ABNORMAL INFLORESCENCE MERISTEM1 functions in salicylic acid biosynthesis to maintain proper reactive oxygen species levels for root meristem activity in rice. *Plant Cell*. 29: 560–574.

Xu, Wang, B., Feng, Y. F., Xue, J. S., Qian, X. X., Liu, S. Q., Zhou, J., Yu, Y. H., Yang, N. Y., Xu, P. and Yang, Z. N. 2019. AUXIN RESPONSE FACTOR17 Directly Regulates MYB108 for Anther Dehiscence. *Plant Physiology*. 181: 645–655.

Yamamoto, Y., Kamiya, N., Morinaka, Y., Matsuoka, M. and Sazuka, T. 2007. Auxin biosynthesis by the YUCCA genes in rice. *Plant Physiology*. 143: 1362–1371.

Yang, C., Lu, X., Ma, B., Chen, S. Y. and Zhang, J. S. 2015. Ethylene signaling in rice

and arabidopsis: Conserved and diverged aspects. *Molecular Plant*. 8: 495–505.

Yang, C., Vizcay-Barrena, G., Conner, K. and Wilson, Z. A. 2007. Male Sterility1 is required for tapetal development and pollen wall biosynthesis. *Plant Cell*. 19: 3530–3548.

Yang, C., Xu, Z., Song, J., Conner, K., Barrena, G. V. and Wilson, Z. A. 2007. Arabidopsis MYB26/MALE STERILE35 regulates secondary thickening in the endothecium and is essential for anther dehiscence. *Plant Cell*. 19: 534–548.

Yang, J., Tian, L., Sun, M. X., Huang, X. Y., Zhu, J., Guan, Y. F., Jia, Q. S. and Yang, Z. N. 2013. AUXIN RESPONSE FACTOR17 is essential for pollen wall pattern formation in Arabidopsis. *Plant Physiology*. 162: 720–731.

Yang, S., Xie, L., Mao, H., Puah, C. S., Yang, W., Jiang, L., Sundaresan, V. and Ye, D. 2003. Tapetum determinant1 Is Required for Cell Specialization in the Arabidopsis Anther. *The Plant cell*. 15: 2792–2804.

Yang, W. C., Ye, D., Xu, J. and Sundaresan, V. 1999. The SPOROCYTELESS gene of Arabidopsis is required for initiation of sporogenesis and encodes a novel nuclear protein. *Genes and Development*. 13: 2108–2117.

Yang, X., Lee, S., So, J. H., Dharmasiri, S., Dharmasiri, N., Ge, L., Jensen, C., Hangarter, R., Hobbie, L. and Estelle, M. 2004. The IAA1 protein is encoded by AXR5 and is a substrate of SCF TIR1. *Plant Journal*. 40: 772–782.

Yau, C. P., Wang, L., Yu, M., Zee, S. Y. and Yip, W. K. 2004. Differential expression of three genes encoding an ethylene receptor in rice during development, and in response to indole-3-acetic acid and silver ions. *Journal of Experimental Botany*. 55: 547–556.

Yin, C. C., Ma, B., Collinge, D. P., Pogson, B. J., He, S. J., Xiong, Q., Duan, K. X., Chen, H., Yang, C., Lu, X., Wang, Y. Q., Zhang, W. K., Chu, C. C., Sun, X. H., Fang, S., Chu, J. F., Lu, T. G., Chen, S. Y. and Zhang, J. S. 2015. Ethylene responses in rice roots and coleoptiles are differentially regulated by a carotenoid isomerase-mediated abscisic acid pathway. *Plant Cell*. 27: 1061–1081.

Zadoks, J., Chang, T. and Konzak, C. 1974. A decimal growth code for the growth stages of cereals. *Weed Research*. 14: 415–421.

Zenser, N., Ellsmore, A., Leasure, C. and Callis, J. 2001. Auxin modulates the degradation rate of Aux/IAA proteins. *Proc Natl Acad Sci U S A*. 98: 11795–11800.

Zhang, D., Luo, X. and Zhu, L. 2011. Cytological analysis and genetic control of rice anther development. *Journal of genetics and genomics*. 38: 379–390.

Zhang, F., Wang, L., Qi, B., Zhao, B., Ko, E. E., Riggan, N. D., Chin, K. and Qiao, H. 2017. EIN2 mediates direct regulation of histone acetylation in the ethylene response. *Proceedings of the National Academy of Sciences of the United States of America*. 114: 10274–10279.

Zhang, G. Y., Feng, J., Wu, J. and Wang, X. W. 2010. BoPMEI1, a pollen-specific pectin methylesterase inhibitor, has an essential role in pollen tube growth. *Planta*. 231: 1323–1334.

Zhang, Y., He, P., Ma, X., Yang, Z., Pang, C., Yu, J., Wang, G., Friml, J. and Xiao, G. 2019. Auxin-mediated statolith production for root gravitropism. *New Phytologist*. 224: 761–774.

Zhang, Z. B., Zhu, J., Gao, J. F., Wang, C., Li, Hui, Li, Hong, Zhang, H. Q., Zhang, S., Wang, D. M., Wang, Q. X., Huang, H., Xia, H. J. and Yang, Z. N. 2007. Transcription factor AtMYB103 is required for anther development by regulating tapetum development, callose dissolution and exine formation in Arabidopsis. *Plant Journal*. 52: 528–538.

Zhao, D.-Z., Wang, G.-F., Speal, B. and Ma, H. 2002. The EXCESS MICROSPOROCYTES1 that controls somatic and reproductive repeat receptor protein kinase gene encodes a putative leucine-rich cell fates in the Arabidopsis anther. *Genes & Development*. 16: 2021–2031.

Zhao, X., De Palma, J., Oane, R., Gamuyao, R., Luo, M., Chaudhury, A., Hervé, P., Xue, Q. and Bennett, J. 2008. OsTDL1A binds to the LRR domain of rice receptor kinase MSP1, and is required to limit sporocyte numbers. *Plant Journal*. 54: 375–387.

Zhao, Y., Christensen, S. K., Fankhauser, C., Cashman, J. R., Cohen, J. D., Weigel, D. and Chory, J. 2001. A role for flavin monooxygenase-like enzymes in auxin biosynthesis. *Science*. 291: 306–309.

Zhao, Y., Dong, W., Zhang, N., Ai, X., Wang, M., Huang, Z., Xiao, L. and Xia, G. 2014. A wheat allene oxide cyclase gene enhances salinity tolerance via jasmonate signaling. *Plant Physiology*. 164: 1068–1076.

Zhu, J., Chen, H., Li, H., Gao, J. F., Jiang, H., Wang, C., Guan, Y. F. and Yang, Z. N. 2008. Defective in Tapetal Development and Function 1 is essential for anther development and tapetal function for microspore maturation in Arabidopsis. *Plant Journal*. 55: 266–277.

Zhu, J., Kaeppler, S. M. and Lynch, J. P. 2005. Mapping of QTLs for lateral root branching and length in maize (Zea mays L.) under differential phosphorus supply. *Theoretical and Applied Genetics*. 111: 688–695.

Zhu, J. and Lynch, J. P. 2004. The contribution of lateral rooting to phosphorus acquisition efficiency in maize (Zea mays) seedlings. *Functional Plant Biology*. 31: 949–958.

Zhu, Y., Nomura, T., Xu, Y., Zhang, Y., Peng, Y., Mao, B., Hanada, A., Zhou, H., Wang, R., Li, P., Zhu, X., Mander, L. N., Kamiya, Y., Yamaguchi, S. and He, Z. 2006. ELONGATED UPPERMOST INTERNODE encodes a cytochrome P450 monooxygenase that epoxidizes gibberellins in a novel deactivation reaction in rice. *Plant Cell*. 18: 442–456.

Zhu, Z. X., Liu, Y., Liu, S. J., Mao, C. Z., Wu, Y. R. and Wu, P. 2012. A gain-of-function mutation in OsIAA11 affects lateral root development in rice. *Molecular Plant*. 5: 154–161.

Ziegler, J., Hamberg, M., Miersch, O. and Parthier, B. 1997. Purification and Characterization of Allene Oxide Cyclase from Dry Corn Seeds. *Plant Physiology*. 114: 565–573.

Ziegler, J., Stenzel, I., Hause, B., Maucher, H., Hamberg, M., Grimm, R., Ganal, M. and Wasternack, C. 2000. Molecular cloning of allene oxide cyclase: The enzyme

establishing the stereochemistry of octadecanoids and jasmonates. *Journal of Biological Chemistry*. 275: 19132–19138.